GENETIC INVESTIGATIONS OF CENTRAL CORNEAL THICKNESS IN RELATION TO OPEN-ANGLE GLAUCOMA

DAVID PAUL DIMASI

Bachelor of Biotechnology (Honours)

Thesis submitted for the degree of

Doctor of Philosophy

February 2011

Faculty of Health Sciences

School of Medicine

Flinders University of South Australia

Adelaide, Australia

TABLE OF CONTENTS

SUMMARY

Open-angle glaucoma (OAG) is a leading cause of permanent blindness in Australia, affecting 2-3% of the population over 40. Death of neurons in the retina causes a progressive loss of vision that can lead to total blindness if left untreated. OAG has a strong genetic component, yet the genetic architecture of this condition is poorly characterised.

The cornea is the transparent tissue located at the front of the eye and lower central corneal thickness (CCT) values are a major risk-factor for OAG. CCT varies between individuals, exhibiting a normal distribution in the population. Differences in CCT are evident between ethnic groups and there is evidence suggesting that skin pigmentation may also influence this trait. Several studies have indicated that CCT is highly heritable, yet the genes that account for normal CCT variation are unknown.

Given the strong correlation between a reduced CCT and OAG and the fact that both of these traits are highly heritable, this thesis was undertaken to investigate the hypothesis that genes involved in the determination of normal CCT variation are also susceptibility loci for OAG. In order to test this hypothesis, the initial goal was to identify genes associated with CCT, followed by investigation of these genes in an OAG cohort. The role of mammalian pigmentation in influencing CCT was also assessed. The aims of the work described in this thesis were:

i. To investigate the association between pigmentation and CCT.

ii. To identify novel genetic determinants of CCT.

iii. To determine if any identified CCT genes are associated with OAG.

Both human and rodent studies were used to assess if pigmentation is associated with CCT. A meta-analysis of published CCT data in different human ethnic groups was conducted, along with measurement of CCT in 13 different inbred strains of mice with various pigmentation phenotypes. Findings from the meta-analysis ($p < 0.001$) and mouse studies ($p = 0.008$) indicated that pigmentation does influence CCT, thus recognising pigment-related genes as candidates for influencing CCT.

In order to identify novel genetic determinants of CCT, two approaches were employed, a candidate gene study and a genome-wide association study. The candidate gene study involved selecting 17 genes that were hypothesised to be involved in CCT determination based on their functional properties. Two of these genes, *COL1A1* and *COL1A2*, were found to have a significant association with CCT. A genome-wide association study is a technique that interrogates the entire genome in order to find genetic loci associated with a particular trait, which in this case is CCT. The results of the genome-wide association study identified *FOXO1* and *ZNF469* as novel CCT genes. The four identified CCT genes were then screened in an OAG cohort, with *FOXO1* found to increase susceptibility to the development of OAG.

Data from this thesis has significantly improved knowledge of the factors involved in CCT variation. Along with confirmation that pigmentation influences CCT, *COL1A1*, *COL1A2, FOXO1* and *ZNF469* provided the first evidence of any genes involved in the determination of this trait. The identification of *FOXO1* as a potential OAG gene is also a finding of significance which may have implications for future research into the disease.

DECLARATION BY STUDENT

I certify that this thesis does not incorporate without acknowledgment any material previously submitted for a degree or diploma in any university; and that to the best of my knowledge and belief it does not contain any material previously published or written by another person except where due reference is made in the text.

David P Dimasi

ACKNOWLEDGEMENTS

First and foremost, I wish to acknowledge the two people that made this whole project possible, Jamie Craig and Kathryn Burdon. I don't think it is possible to have two more dedicated, talented and hard-working supervisors than Jamie and Kathryn. To Jamie, your encouragement, support and guidance over the journey has been invaluable and not just during my PhD tenure, but in the years before as well. There have been many times when I have become disillusioned with the project or with research as a whole, yet your enthusiasm and thirst for new ideas always manages to get me motivated again! To Kathryn, I think your patience and willingness to help are just incredible. I always marvel at the way you manage to find the time and energy to help when you have a lab full of students and research assistants demanding your time. It is also safe to say that Kathryn has taught me pretty much everything I know about genetics and her ability to make me understand such a difficult topic is a credit to her teaching skills. I think I could on for pages about how much I appreciate all the work that Jamie and Kathryn have put into this project, but in summary, I would just like to thank them both for believing in me as a student and for above all else, being kind, supportive people who I consider friends. While I am on the topic of supervisors, I would also like to thank David Mackey for his help and input, particularly with his critiquing of manuscripts and the thesis.

Along with my supervisors, there are several other people I would like to thank for their guidance over the years. To Shiwani Sharma, who offered me my first job out of university and has been there ever since, I thank you immensely for all your support during this time, your knowledge of laboratory techniques is a great asset to the department and I owe many of my current skills to your teaching. Many thanks also to Keryn Williams, whose encouragement gave me the confidence to take on the responsibility of a PhD in the first place. The general assistance that Keryn has offered in so many ways is also much appreciated, particularly with her knowledge of everything NHMRC! Finally, I would like to thank Doug Coster for giving me the opportunity to undertake a PhD in the department. I feel truly fortunate to have been involved with Ophthalmology over the years and I think Doug must take a lot of the credit for turning the department into what it is today. Doug's stories always have a way of brightening my day and I hope to hear many more in the future.

Perhaps the major reason I have enjoyed my time in Ophthalmology so much has been the people I have met along the way. The task of coming to work every day is made a great deal easier when you know you get to spend your time amongst friends. There are so many Ophthalmology people, both past and present, I would like to acknowledge but I can't do everyone, so here's hoping I don't forget anyone important! A big thank you to members of the lab, including Margaret, Abraham, Alpana, Helen, Sarah M, Mona, Peter, Doug P, Bastien, Rhys, Gemma, Iman, Greta, Shari and Beverley. A special mention must go to Kirsty for help with animal and fishing techniques, to my fellow suffering PhD students Mel, Alison, Sue and Sarah B, to my fellow Entourage buddy Lauren, to Yazad for endless discussions on cricket and sport, to Paul for his help and scrutiny of footy tipping and to Amy and Kate for being long time compatriots on the bench in level 4. I would also like to acknowledge all the staff in my new home, the office, including Lyn, Anne, Bronwyn, Lynda, Emmanuelle, Marie, Miriam and Richard. In particular, I would

like to thank Deb for all her help sorting out my endless contract problems and for providing the daily paper.

There are also several people I wish to acknowledge for the technical assistance they provided to this project. Thank you to the members of the anatomical pathology department at Flinders, including Sonja, Richard and John for their help with EM imaging. I am also grateful to the assistance provided by Stu in the animal house and Oliver in the DNA sequencing facility. Finally, a big thank you to Stuart Macgregor and Yi Lu from the QIMR for their analysis of the genome-wide association data. In particular, I am especially thankful to Yi for responding to my barrage of my emails and running extra analyses in her own time for the benefit of my project.

Finally, a big thank you must go to my family and friends, who all played a part in helping me complete this thesis. To my parents, who must have got sick of hearing me say 'I'm almost finished', I thank you for your support and patience over the last 4 years. I would also like to thank my friends for not giving too much of a hard time when I couldn't commit to as many social outings as I would have liked over the last few months. Lastly, I am especially grateful to my girlfriend Claire for her help during the course of this PhD, particularly during the months when I was stuck at home writing. I cannot thank Claire enough for the encouragement she has given me and I am so grateful for the patience she has shown while our relationship has effectively been put on hold. The fact that Claire also found the time to read and critique my thesis speaks volumes of the person she is. I look forward to spending some quality time together now that this thesis is complete.

CHAPTER 1

INTRODUCTION

Publications arising from this chapter:

Dimasi DP, Burdon KP, Craig JE. The genetics of central corneal thickness. *Br J Ophthalmol*. 2010 Aug; 94(8):971-6

1.1 ANATOMY OF THE HUMAN EYE

The eye is one of the most complex organs in the human body and is responsible for receiving input for the visual sensory system. The normal adult eyeball is shaped like a slightly irregular sphere, with its outer segment comprised of several tissue layers and an internal cavity that is essentially hollow (Figure 1.1). The external part of the eye consists of two visibly different structures, the sclera and cornea. The sclera is commonly known as the 'white of the eye' and helps to protect and maintain the shape of the eyeball, whilst the transparent cornea acts as a 'window' at the anterior surface of the eye to permit the entry of light. Lying below the sclera are the choroid, ciliary body and iris. The choroid is a highly vascular, pigmented membrane responsible for delivering oxygen and nutrients to the ocular tissues. The ciliary body consists chiefly of smooth muscle fibres that are important for controlling the shape of the lens, a transparent, avascular structure whose primary function is to focus light onto the retina. The iris regulates the amount of light passing through to the lens by adjusting the size of its central opening, the pupil. The retina is the innermost layer of the eye and contains the neurons that are responsible for processing light into a visual image. Light is detected by the photoreceptor cells, which relay the electrical signal to the brain via the retinal ganglion cell axons that converge to form the optic nerve. The retinal ganglion cells comprise what is commonly referred to as the retinal nerve fibre layer. The fovea is an area of the retina that is densely packed with a type of photoreceptor known as a cone cell, with this region largely responsible for colour vision and high visual acuity.

The internal cavities of the eye are divided into the posterior and anterior segments, which are separated by the lens. The larger posterior segment is filled with a

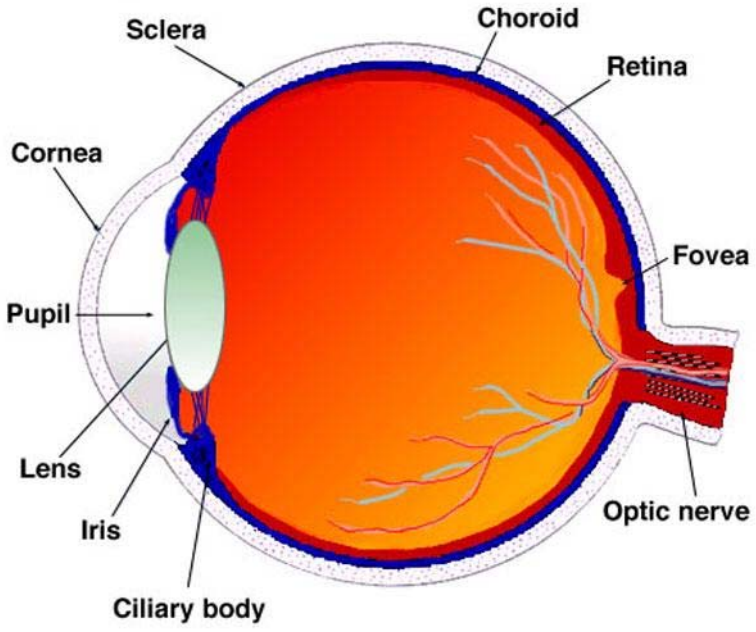

Figure 1.1: Schematic of a cross-section of human eye. The location of the main anatomical features of the eye are indicated by the arrows. Sourced from: http://webvision.med.utah.edu/anatomy.html

gelatinous fluid called the vitreous humor, which allows the transmission of light as well as supporting the internal structures of the eye. The anterior segment is filled with aqueous humor, a clear fluid that helps retain the eye's shape as well as supplying nutrients and oxygen to various tissues. The pressure of this aqueous humor is referred to as the intraocular pressure (IOP).[1, 2]

1.2 THE CORNEA

The cornea is a curved, avascular, transparent tissue found on the anterior outer surface of the eye. It is a unique and highly specialised tissue that must meet a variety of demands. The cornea must be transparent, refract light onto the retina, contain the IOP and provide a protective interface with the environment. Each of these functions is provided by several different cell layers with a distinctive substructural organisation.

Whilst it serves a number of purposes, the major role of the cornea is optical. It forms the principal refractive surface, accounting for approximately 70% of the total refractive power of the eye, with the remainder provided by the lens.[3, 4] The ability of the cornea to refract light efficiently is due its transparency, the curvature of the anterior surface and the optical qualities of the overlying tear film. Along with its ability to refract light, the cornea also forms a protective barrier against environmental insults, including ultraviolet light, pollutants, abrasion and infections.

1.2.1 Structure

The adult cornea consists of five distinct layers (from anterior to posterior): the epithelium, Bowman's layer, the stroma, Descemet's membrane and the endothelium (Figure 1.2).

1.2.1.1 Epithelium

The epithelium is the outermost layer of the cornea and provides an interface between the cornea and the tear film. It consists of a 5-7 cells thick layer of stratified squamous epithelium supported by a basal lamina. The primary function of the corneal epithelium, along with the tear film, is to provide a smooth refractive surface at the front of the eye. The epithelium is relatively impermeable to water soluble agents from the tear film and to bacterial and fungal infections, although it is susceptible to viral infections.[5] It is also important in maintaining proper corneal hydration by resisting absorption of fluid from the tears and preventing evaporation.

1.2.1.2 Bowman's layer

Bowman's layer is a strong, acellular layer of collagen fibres located between the basal lamina of the epithelium and the stroma. Its role is to help maintain the shape of the cornea and protect the deeper tissue layers from both trauma and invasion by microorganisms. Bowman's layer does not regenerate following injury and may become opacified by scar tissue.

1.2.1.3 Stroma

The stroma is the most prominent layer of the cornea, comprising up to 90% of the total corneal thickness. It is integral in giving the cornea its strength, shape and

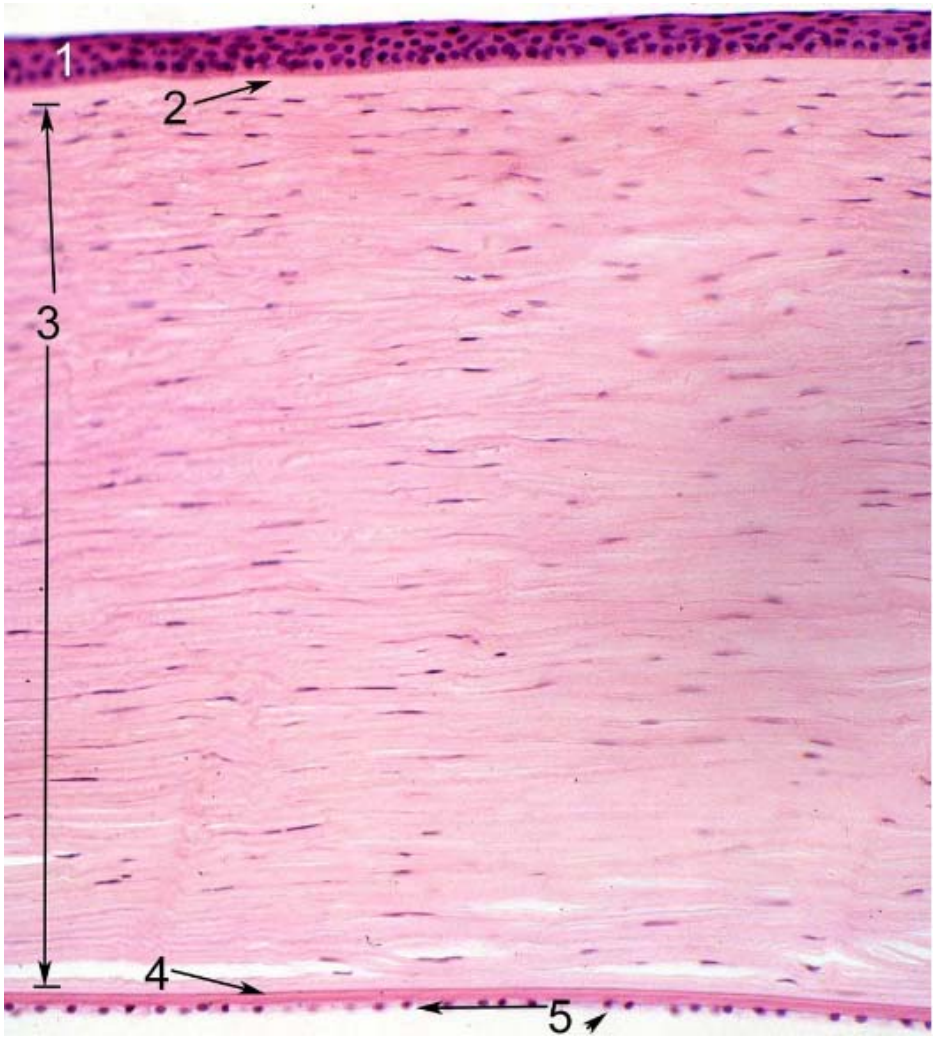

Figure 1.2: Histological cross-section of a human cornea stained with hematoxylin and eosin. The numbers and arrows indicate the different layers of the cornea. **(1)** Epithelium. **(2)** Bowman's layer. **(3)** Stroma. **(4)** Descemet's membrane. **(5)** Endothelium. Sourced from: http://www.images.missionforvisionusa.org/anatomy/uploaded_images/KnumbMfV-731936.jpg

transparency. The most abundant protein found in the corneal stroma is type I collagen, which forms lamellae of 1 μm wide heterotypic fibrils with type V collagen.[6] These specialised collagen fibrils are found in a parallel orientation and possess remarkably uniform diameter and spacing, a unique physical property that gives the cornea its transparent qualities. Another group of extracellular proteins known as the proteoglycans constitute the majority of the support material that surrounds the collagen fibrils. Proteoglycans play an important role in modifying the structure and function of these collagen fibrils, thus maintaining their transparent properties. Many of the proteoglycans found in the cornea are tissue specific and include proteins such as decorin, keratocan, lumican and mimecan.[6] The stroma also consists of a population of cells known as keratocytes that synthesize stromal proteins and play an important role in wound healing and inflammation.

1.2.1.4 Descemet's membrane

Descemet's membrane is a clear elastic tissue layer of between 8 μm and 12 μm thickness that forms the basement membrane for the corneal endothelium. The major protein of Descemet's membrane is type IV collagen which, along with associated glycoproteins and proteoglycans, is secreted from the endothelial cells. Descemet's membrane thickens with age and in degenerative conditions of the corneal endothelium, such as congenital endothelial dystrophy or posterior polymorphous dystrophy.[3] It is also easily detached from the stroma as a result of trauma and does not regenerate following injury, but rather forms scar tissue.

1.2.1.5 Endothelium

The corneal endothelium is the most posterior cellular layer of the cornea and thus lines the corneal surface of the anterior chamber. It contains a monolayer of cells that rarely undergo mitosis, and as a consequence, adult human corneas contain a relatively fixed population of approximately 500,000 endothelial cells, although this number does decrease with age.[3] The corneal endothelium is highly metabolically active as it is responsible for regulating the movement of fluid out of the stroma, which is essential for maintaining corneal clarity. Major increases in hydration can cause corneal edema and a loss of transparency, along with scarring if the effect is prolonged. Due to their inability to regenerate, endothelial cells that are lost to injury or disease in the adult eye are not replaced, but this is somewhat compensated for by the thinning and spreading of surrounding cells.[3]

1.2.2 Central corneal thickness

As the name suggests, central corneal thickness (CCT) is a measurement of the thickness of the central part of the cornea (Figure 1.3A). The clinical significance of CCT has been discussed widely in the recent literature, as its importance to several ocular and non-ocular conditions becomes more widely recognized. Interest in corneal thickness has been ongoing for over a century, with the first documented measurement in a living human eye occurring in 1880.[7] Since this time, significant advancements have been made in not only measurement techniques, but also in our understanding of the clinical relevance of this trait.

1.2.2.1 Measurement techniques

Several methods are available to obtain reliable and reproducible measurements of CCT. At present, the most commonly used approach is ultrasonic pachymetry, a method that utilises sound waves to measure the thickness of the cornea. Ultrasound pachymeters are typically small, portable devices that must be placed on the corneal surface to make a reading, thus requiring the use of topical anaesthesia (Figure 1.3B). Ultrasonic pachymetry is an efficient and affordable means of measuring CCT that gives highly reproducible readings,[8-10] although it can suffer from greater inter-observer variability than other measurement techniques. This is largely due to the placement of the probe on the corneal surface, as it is difficult to accurately locate the same point of measurement in serial examinations or between different observers.[9, 11]

Whilst not as widely employed as ultrasonic pachymetry, numerous other techniques are available to measure CCT. These include optical pachymetry, optical coherence tomography, optical low-coherence reflectometry, scanning-slit topography (Orbscan®), Scheimpflug camera and specular microscopy. All these methodologies offer their own advantages and disadvantages, but in general no two techniques will yield precisely the same measurement. Some of the more recent technology includes instruments such as the Orbscan®(Bausch and Lomb), which is a non-contact, computerised device that can measure CCT as well as generating topographical maps of both the anterior and posterior surface of the cornea. It is widely used in clinics that perform laser corrective eye surgery and in the diagnosis of keratoconus, a condition caused by irregular thinning of the cornea that results in a distortion of corneal shape. Studies have shown that CCT measurements taken with the Orbscan® are highly reproducible.[10, 12-14]

A

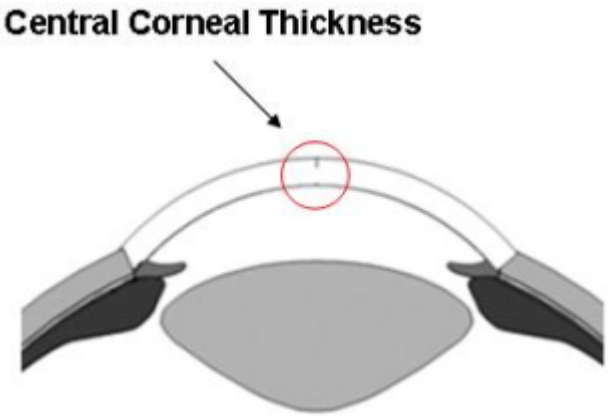

B

Figure 1.3: Measurement of CCT. (A) Schematic depicting location of CCT measurement. **(B)** An ultrasound pachymeter used to measure CCT.

Figure A adapted from:

http://www.agingeye.net/mainnews/glaucomapachymetry.php

Figure B sourced from discontinued website:

http://www.focuseyehealth.com/focus/technology/ultrasound_pachymetry/images/pach.jpg

1.2.2.2 Population characteristics

Within the general population, CCT is a normally distributed quantitative trait. A large meta-analysis conducted by Doughty and Zaman concluded that the mean CCT of 230 different datasets involving measurements of over 14,000 individuals was 536 ± 31 μm, with 95% of values ranging between 473 μm to 595 μm.[15] There are conflicting data on whether age and sex influence CCT, with Doughty and Zaman concluding there was inconsistent evidence that either variable was associated with CCT.[15] Numerous studies have shown that CCT decreases with age,[16-22] whilst others show no association.[23-27] The situation is similar for sex, with several studies indicating that males have slightly thicker corneas than females,[16, 18, 20, 24, 26, 28] whilst other studies show no gender bias.[17, 21-23, 27] Both ethnicity and familial inheritance play a significant role in determining CCT and these will be discussed in more detail later. Numerous disease states can also alter corneal thickness, although these alterations are not considered to be part of the normal trait distribution.

1.2.2.3 Application of central corneal thickness measurements

Measurement of CCT has become routine for the diagnosis or monitoring of several corneal diseases, such as keratoconus, bullous keratopathy, Fuchs' endothelial dystrophy and macular corneal dystrophy. Patients wishing to undergo laser refractive eye surgery also require CCT measurements to determine their eligibility for the procedure, as do corneal graft recipients to monitor the health of the donor cornea. There are also several systemic disorders where measurement of CCT may be utilised to aid in diagnosis, including Ehlers-Danlos syndrome,[29-31] Marfan syndrome[32, 33] and osteogenesis imperfecta. [34, 35] However, perhaps the most widely employed application for measuring CCT is in the diagnosis and management of the

ocular disorder open-angle glaucoma (OAG). (Jamie Craig, personal communication)

1.3 OPEN-ANGLE GLAUCOMA

The glaucomas are a group of optic neuropathies characterised by a slow and progressive degeneration of retinal ganglion cells and their axons that ultimately results in a permanent loss of vision.[36] A feature of all glaucomas is the distinct appearance of the optic nerve head, also known as the optic disc, that results from death of these retinal ganglion cells. There are numerous glaucoma sub-types, the most common of which is OAG.[37] Open-angle refers to the appearance of the anterior chamber, or iridocorneal, angle. In OAG, this angle is normal in appearance and is thus described as 'open'. When glaucoma is associated with a narrowing of the anterior chamber angle, it is termed angle-closure glaucoma. The condition of the angle can influence the level of IOP, which is often elevated in glaucoma. Whilst an elevated IOP is not always associated with OAG, it is a strong risk factor and lowering of IOP is the only proven method of treatment.[38-42] OAG is generally an adult-onset condition that occurs in patients over 40 years of age, although a juvenile form of the disease does exist.[43] The disease is a major health concern in both the developed and developing world and by the year 2020 it is estimated that 58 million people worldwide will be affected, making it one of the leading causes of blindness after cataract.[37]

1.3.1 Visual field defects

OAG results in distinctive visual field defects, with the pattern of field loss, the nature of its progression and the correlation of damage to the optic disc and retinal nerve fibre layer all characteristics of the disease.[44-46] In the majority of cases, OAG is a bilateral condition, although the progression of visual loss often varies in each eye. The onset of visual field defects in OAG is usually subtle and asymptomatic, with patients often unaware they have lost vision even though damage to retinal nerve fibre layer may have already occurred.[47] This is due to the first signs of visual dysfunction generally manifesting in the mid-peripheral field of vision.[44] Enlargement of the blind spot is also commonly experienced as one of the earliest indications of damage. Progression may involve the development of a nasal scotoma, an area of visual loss surrounded by normal vision on the nasal (medial) side of the retina. Defects in peripheral vision then develop as nerve fibre layer bundles in both the inferior and superior regions of the retina degenerate. Further constriction of the visual field in advanced OAG results in the loss of all peripheral vision, with only an island of central vision remaining, with further progression leading to total blindness (Figure 1.4).[2, 4]

1.3.2 Quality of life

Loss of vision associated with OAG can have a severe impact on a patient's quality of life, particularly in the later stages of the disease. A broad range of lifestyle activities may become affected and this can have detrimental consequences on an individual's overall health. Many of these problems are exacerbated by the fact that a large proportion of people with OAG are elderly. Studies have shown that OAG patients suffer from decreased mobility and have an increased risk of falls, which

A

B

Figure 1.4: Typical pattern of visual field loss seen in OAG. (A) Vision in a normal eye. **(B)** Vision in an eye with advanced OAG. The peripheral and mid-peripheral field of view have been lost and only central vision remains.

Source: http://www.nei.nih.gov/

have the potential to cause serious injury in the elderly.[48-54] Driving ability can also be severely affected, with OAG patients more likely to either cease driving or be involved in motor vehicle accidents than non-vision impaired drivers.[52, 55-57] Other daily tasks such as reading may also become more difficult.[50, 58] Surveys have shown that OAG patients suffer from a reduction in their overall quality of life, which can include a loss of confidence in social environments and a decline in general physical and mental health.[50, 59-61]

1.3.3 Anatomy and physiology

1.3.3.1 Aqueous production and outflow

Given that elevated IOP is a strong risk factor for OAG and lowering of IOP is the only effective treatment, it is important to understand aqueous humor dynamics in the context of glaucoma physiology. The aqueous humor that fills the anterior segment of the eye is secreted by the ciliary body and is ultimately drained via one of two pathways, known as the trabecular and uveoscleral routes (Figure 1.5). The trabecular route involves passage of the aqueous humor through the trabecular meshwork and into Schlemm's canal, where it then travels into the episcleral venous system. In uveoscleral drainage, the aqueous humor leaves the anterior chamber via the face of the ciliary body. Evidence suggests the trabecular route is the major pathway for aqueous outflow, accounting for approximately 50-90% of total drainage, although this appears to be dependent on age.[62] In a normal eye, the aqueous humor is produced and drained at the same rate, thus maintaining a constant IOP, although slight variations are evident as a result of circadian flux. However, in a glaucomatous eye that has an elevated IOP, defects in aqueous outflow through the trabecular and uveoscleral routes result in an increase in

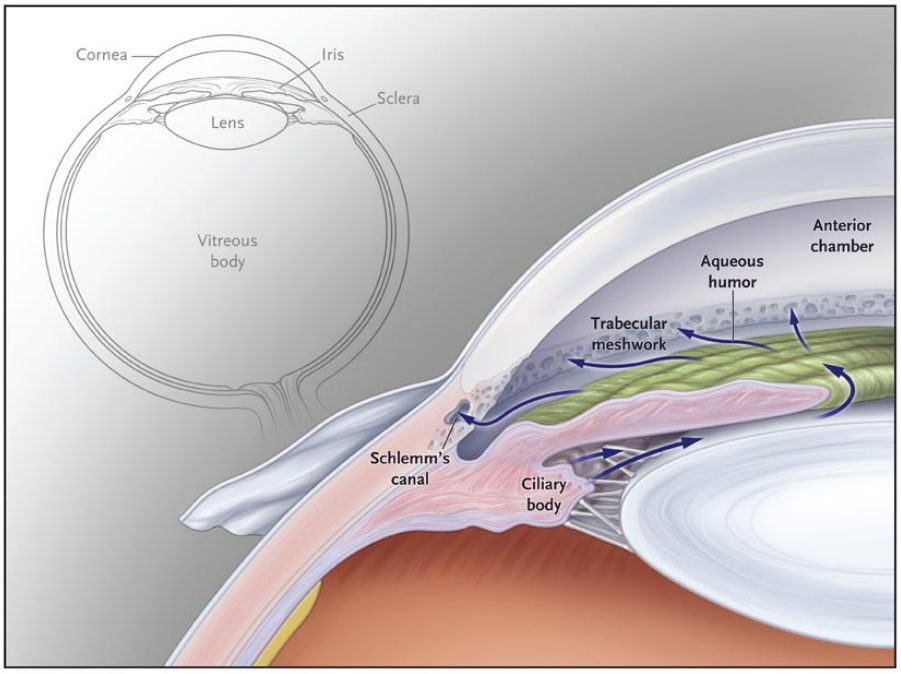

Figure 1.5: Schematic of aqueous humor circulation in the anterior segment of the eye. Arrows depict secretion of aqueous humor from the ciliary body and passage through the pupil into the anterior chamber. The majority of aqueous humor drainage occurs via the trabecular meshwork and into Schlemm's canal. A smaller amount of aqueous humor leaves the eye through the face of the ciliary body, just below the trabecular meshwork (uveoscleral route). Sourced from Kwon *et al* 2009.[63]

pressure, although the mechanisms responsible for this dysfunction of the drainage pathways are unknown.[64]

1.3.3.2 The retina

To interpret the damage that occurs in OAG, a thorough understanding of the anatomy of the retina and optic nerve is necessary. Of particular relevance are the retinal ganglion cells, as these are the neurons that die in glaucomatous eyes.[63] The retinal ganglion cells are found at the innermost layer of the retina and are responsible for transmitting the visual signal produced in the photoreceptors to the brain. The human eye contains approximately one million retinal ganglion cells, the axons of which form the retinal nerve fibre layer. These axons traverse the inner surface of the retina and converge on the optic disc, where they leave the posterior cavity of the eye as the optic nerve (Figure 1.6A). Ultimately, the optic nerve mainly, but not exclusively, synapses with the lateral geniculate nucleus of the brain.

1.3.3.3 The optic disc

The optic disc, or optic nerve head, is a circular region in the posterior segment of the eyeball where the optic nerve exits the eye. It is commonly called the blind spot because it lacks photoreceptors and light focused on it cannot be seen. Apart from the optic nerve, the central retinal artery and central retinal vein, which provide blood flow to the retina, also pass through the surface of the optic disc. Both the optic nerve and central retinal blood vessels pass through pores in the lamina cribrosa, a sieve-like structure made from collagen fibres that is a continuation of the sclera (Figure 1.6B). The role of lamina cribrosa is to support the optic nerve fibres and blood vessels as they pass through the optic disc.

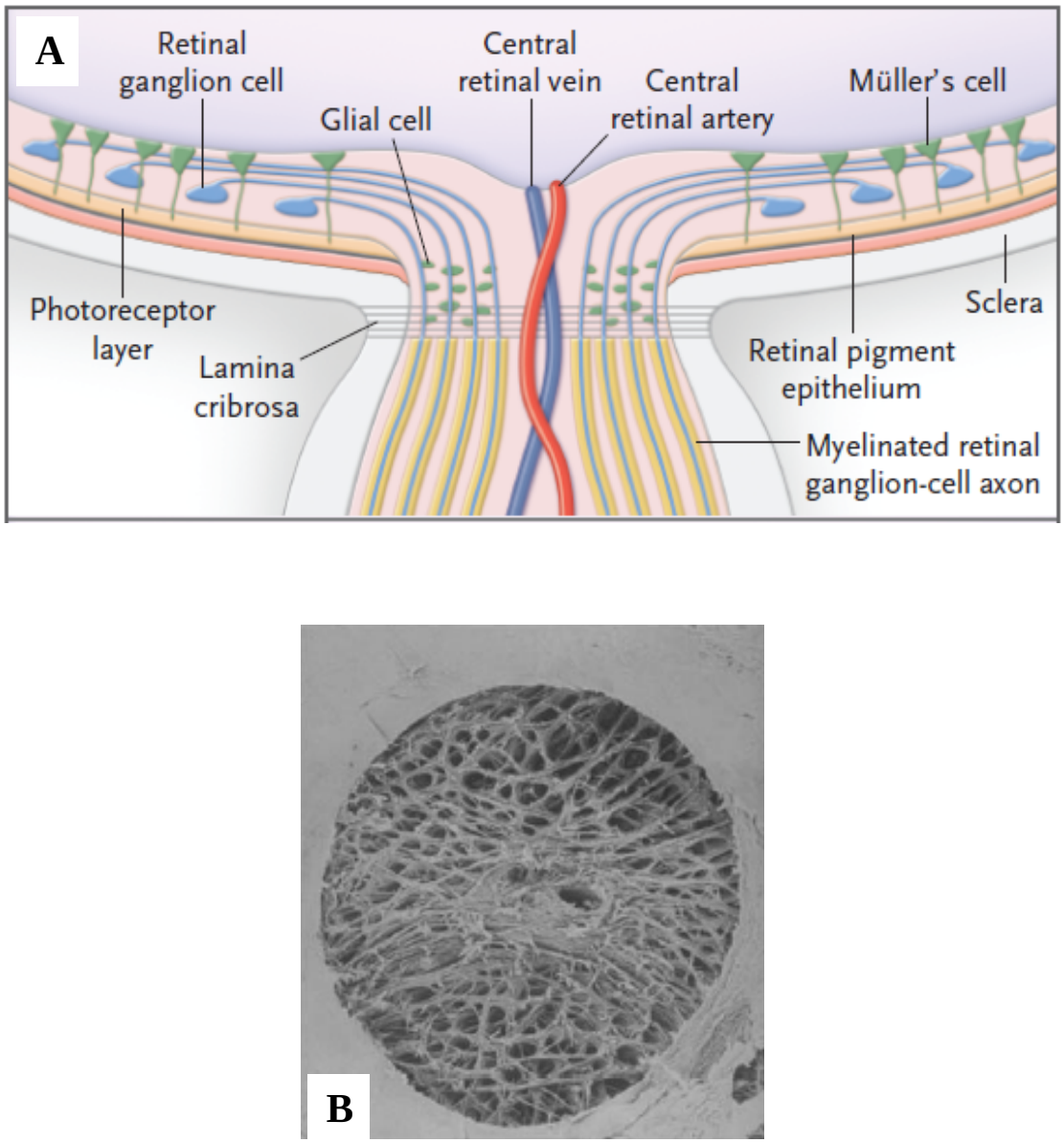

Figure 1.6: Structures of the retina and optic disc important in OAG pathogenesis. (A) Schematic representation depicting the retinal ganglion cells (blue) traversing the retina and exiting the eye through the lamina cribrosa. The scleral region adjacent to the lamina cribrosa is also known as the peripapillary sclera. **(B)** Electron microscopy of the laminar cribrosa revealing the pores through which the retinal gannglion cell axons pass. Figures sourced from Kwon *et al* 2009[63] and Burgoyne *et al* 2005.[65]

1.3.4 Pathophysiology of the retinal ganglion cells

Whilst OAG is a complex disorder with a multifactorial etiology, elevated IOP is a significant risk factor that is unquestionably associated with the death of retinal ganglion cells and their axons.[63, 65, 66] However, the mechanism by which IOP induced stress causes degeneration of these cells is unclear. In addition, not all OAG patients express an elevated IOP; a subset of individuals exhibit normal-tension glaucoma (NTG). In many cases NTG patients show similar pathology to high-tension OAG patients[67, 68] and respond to lowering of IOP,[39] suggesting they a have lower threshold to IOP induced damage.

Evidence shows that the lamina cribrosa, where axon bundles that pass through the lamina pores are potentially vulnerable to damage, is the initial site of glaucoma injury.[69-72] The peripapillary sclera, which adjoins the lamina cribrosa, is postulated to be another site of early glaucomatous damage.[73] It is believed that elevated IOP exerts a force on the sclera that is distributed towards the weakest point, the lamina cribrosa, where its composite tissues and structures are placed under stress.[70] As a consequence, damage to the ganglion cell axons results and although the precise mechanism is unknown, it has been proposed that direct mechanical stress to the axons or interruption of the blood supply to the optic nerve are potential causes.[74] Non-IOP mediated damage to ganglion cells is also believed to play a role in OAG, as evidenced by progression of the disease in patients who have had IOP lowering treatments.[39, 41, 75-77] Irrespective of the early pathways involved in the disease progression and whether or not they are related to elevated IOP, the ultimate result is loss of ganglion cell neurons due to apoptosis, a cellular suicide mechanism employed by cells in response to damage or stress.[78]

1.3.5 Clinical features of the optic disc and retinal nerve fibre layer

OAG results in characteristic signs of damage to the retinal nerve fibre layer and the optic disc. The nature of this damage helps to distinguish the glaucomas from other optic neuropathies.[79] One predominant feature of glaucomatous damage is cupping, or excavation, of the optic disc. The optic cup is a pale depression in the centre of the optic disc that is not occupied by neural tissue. As degeneration of ganglion cell axons in the optic nerve progresses, the size of the cup within the optic disc begins to enlarge due to the death of the neural tissue, leading to an increase in the cup-to-disc ratio (Figure 1.7). Most normal eyes have a cup-to-disc ratio of around 0.3,[80] while those with a cup-to-disc ratio of 0.55 or more are at an increased risk of developing any form of glaucoma.[47] This makes the cup-to-disc ratio a useful diagnostic parameter, although there is a strong overlap between normal and glaucomatous individuals. If left to progress to end-stage disease, complete cupping of the optic nerve occurs whereby all the neural disc tissue is destroyed.[2] Cupping of the disc may also be accompanied by thinning of the neuroretinal rim, the tissue found between the outer edge of the cup and the disc margin. Haemorrhaging of the blood vessels at the disc margin is often seen in glaucoma, particularly in NTG,[81] and is considered a significant risk factor for progression of visual field loss.[82, 83] The retinal nerve fibre layer also begins to thin as ganglion cells undergo apoptosis.[46]

1.3.6 Treatment

The primary goal of OAG treatment is to prevent further loss of functional vision by slowing the rate of ganglion cell death. Currently, the only method of treatment that has been proven to slow disease progression is by inducing a reduction in IOP.[38-42] Whilst the visual damage associated with OAG is irreversible, early therapeutic

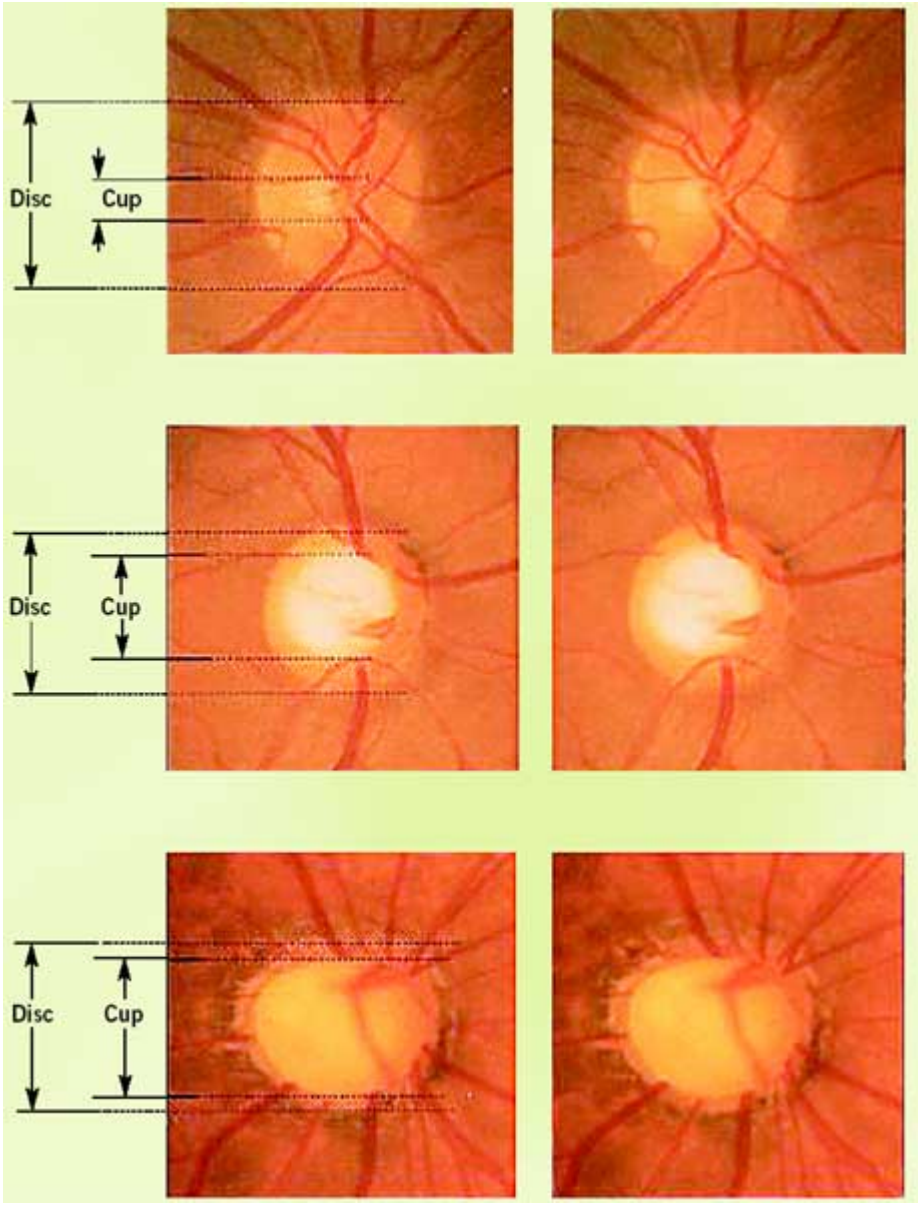

Figure 1.7: Stages of glaucomatous cupping of the optic disc. The arrows indicate the dimensions of the optic cup and optic disc, which yields the cup-to-disc ratio (Note that the left and right images are the same optic disc). **(A and B)** Normal optic disc with small cup; cup-to-disc ratio is 0.2. **(C and D)** Low level glaucoma suspicion with moderate cupping; cup-to-disc ratio is 0.7. **(E and F)** High level glaucoma suspicion with advanced cupping; cup-to-disc ratio is 0.9. Sourced from: http://www.revoptom.com/index.asp?ArticleType=SiteSpec&page=osc/3146/lesson.htm

intervention is essential for limiting the total amount of visual loss.[41] The most widely-employed treatment for OAG involves the use of topical eye drops and this is generally the first method utilised when therapy is initiated.[84, 85] Whilst there are several classes of topical eye drop medication, the most commonly used and effective form are the prostaglandin analogues.[85, 86] In addition to topical eye drops, other forms of treatment can involve the use of a laser or surgery to improve aqueous outflow and subsequently lower IOP. Ultimately, each form of treatment has its own advantages and disadvantages and therapy must be tailored to suit the individual.

1.3.7 Risk factors

In a recent review, Boland and Quigley identified 34 separate risk factors for OAG that have been described in the literature.[87] Whilst some of the risk factors mentioned in the review are well accepted and supported by significant clinical evidence, others are controversial and the available data are inconclusive. For the purpose of this thesis, only a selection of the established OAG risk factors will be discussed.

1.3.7.1 Age

Older age is a well-established risk factor for OAG, being consistently associated with disease across a range of studies. Most cases present over the age of 65 and it is unusual for a diagnosis to be made before the age of 40.[43] In a recently conducted meta-analysis, disease prevalence rose steadily with age and more steeply in Europeans than in other populations. For each decade increase in age over the age of 40 in European-derived populations, there was a doubling in OAG prevalence.[88]

1.3.7.2 Ethnicity

Several large population-based studies have shown that people of African descent are disproportionately affected with OAG. The Baltimore Eye Study, which assessed both black and white communities, found that African Americans were four to five times more likely to have OAG than their white counterparts.[89] The Barbados Eye Study, published in 1994, revealed an even higher prevalence of OAG in the same age group, finding the rate amongst people of African descent to be 7.0%.[90] These data most likely reflect an underlying genetic susceptibility to the disease in these communities. OAG also develops earlier and is more severe in Africans than in Caucasians.[89, 90] A study conducted on a Latino population of Los Angeles also found this population was at a higher risk of developing OAG when compared to Caucasians.[91]

1.3.7.3 Family history

Having a family history of affected relatives is another important risk factor for the development of OAG. The Glaucoma Inheritance Study in Tasmania revealed that a positive family history of OAG is found in almost 60% of cases when family members of an affected individual are examined.[92] The Baltimore Eye survey concluded that first-degree relatives of patients with OAG had a 2.9 times greater odds of developing the disease than non-relatives.[93] In the Rotterdam Study, where all available family members of OAG patients were also examined, the lifetime risk of developing glaucoma was approximately 10 times higher in siblings and offspring of OAG sufferers than in siblings and offspring of controls.[94] Whilst OAG clearly aggregates in families, it is a complex trait and definitive inheritance patterns are generally not evident. Nevertheless, the strong association with family history points to a significant genetic component to the disease.

1.3.7.4 Intraocular pressure

Perhaps one of the strongest risk factors associated with OAG is the level of IOP. It is well established that the risk of developing OAG increases with higher levels of IOP, as does the risk of disease progression.[87] The mean IOP within the general population is approximately 16 mmHg, with a normal distribution of values ranging from 9 to 21 mmHg and a long tail of higher measurements above 21 mmHg.[95] Although there is no absolute upper limit, IOP readings over 21 mmHg are considered high and predispose an individual to an increased risk of OAG. The relationship between IOP and OAG incidence is well illustrated by a 9-year follow-up of participants conducted as part of the Barbados Eye Study.[96] The study showed that the incidence of OAG steadily increased from 1.8% for persons with an IOP of less than or equal to 17 mmHg, to 22.3% for those with an IOP over 25 mmHg. Overall, OAG risk increased in the cohort by 12% with each 1 mmHg increase in IOP. Further support for the association between OAG and IOP comes from the study of patients with asymmetric damage to the optic nerve, with higher pressures generally found in the eye with the greater amount of damage.[97]

A significant proportion of OAG cases have an IOP in the normal range, which is termed NTG. The prevalence of NTG varies between different ethnic communities, with a large Japanese study finding that 92% of identified OAG patients had an IOP under 21 mmHg.[98] Whilst this rate is higher than that found in most studies, it is consistent with observations from around the world that show NTG comprises up to 50% of OAG cases.[99] Alternatively, not all people exhibit signs of glaucomatous damage with IOP readings over 21 mmHg and are thus termed ocular hypertensive. It is therefore important to consider IOP as a continuous variable and although those with an IOP under 21 mmHg are termed as having NTG, this is a rather arbitrary

definition. The diverse relationship between IOP and OAG may reflect individual differences in the susceptibility to glaucomatous damage at different IOP levels.

1.3.7.5 Central corneal thickness

The importance of CCT in the management of OAG, particularly in those with ocular hypertension, was brought to the forefront by the Ocular Hypertension Treatment Study (OHTS).[100] The OHTS was a large-scale clinical trial designed to evaluate whether reducing IOP in people with ocular hypertension could prevent or delay the onset of OAG. The study also analysed which demographic and clinical factors could predict the progression from ocular hypertension to OAG. Amongst its many findings, the OHTS determined that CCT was a powerful predictor for the development of OAG, whereby participants with the thinnest CCT measurements had a 3-fold greater risk of developing OAG than those with the thickest corneas.[100] Another large-scale clinical trial, the European Glaucoma Prevention Study, also found that a thinner CCT was a strong risk factor for the development of OAG in ocular hypertensive patients.[101] Several smaller studies have verified these findings.[102-105] In a recent review for the American Academy of Ophthalmology, Dueker *et al* confirmed that there is reliable evidence that CCT is a risk factor for progression from ocular hypertension to OAG and stated that 'CCT measurement should be included in the examination of all patients with ocular hypertension.'[106]

Apart from being an important risk factor in patients with ocular hypertension, there is also evidence that CCT is associated with other OAG parameters, including incidence of disease and progression of established field loss. The Barbados Eye Study found that as CCT decreased, the incidence of OAG increased significantly,

with a 40% higher risk of OAG per 40 μm reduction in CCT.[107] Numerous other studies have shown an association between the prevalence or incidence of OAG and a thinner CCT.[108-112] However, several large population-based investigations have not verified these findings.[98, 113] A thinner CCT has also been associated with more rapid progression of established field loss, as evidenced by the most recent analysis of the Early Manifest Glaucoma Trial data.[114] After a median follow-up of 8 years, the Early Manifest Glaucoma Trial found that enrolled patients with a high baseline IOP had an approximately 50% greater risk of OAG progression per 40 μm reduction of CCT. Data presented by Medeiros *et al* [115] and Kim *et al* [116] demonstrated that progression of visual field loss is associated with a thinner cornea, although these results have not been consistently replicated.[110, 117] Several studies have also revealed that a thinner CCT is a risk factor for greater severity of visual field damage in OAG.[118-120] The inconsistency of some of these findings indicates that further research is required to confirm or refute the association of CCT with OAG incidence, progression or severity.

1.3.7.5.1 The impact of tonometry artefact

Whilst there is substantial evidence supporting a thinner CCT as a risk factor for OAG, the mechanism responsible for this relationship is unclear. It is likely however, that a phenomenon known as tonometry artefact, caused by the influence of CCT on IOP measurements, is a component of this association. Measurement of IOP is crucial for determining an individual's risk of developing OAG and is also necessary for assessing the effectiveness of IOP lowering treatment strategies. The measurement of IOP is known as tonometry and is based on the principle that the force required to flatten the cornea is dependent on the pressure of the aqueous

humor within the anterior chamber (Figure 1.8A). Whilst a range of tonometry devices currently exist, the Goldmann Applanation Tonometer (GAT) is the most widely used and has been regarded as the gold standard instrument for measuring IOP over the past 50 years (Figure 1.8B).[121] Developed by Professor Hans Goldmann and first introduced in 1957, GAT is based on the Imbert-Fick principle which states that for an ideal, dry, thin-walled sphere, the pressure inside the sphere equals the force necessary to flatten its surface divided by the area of flattening. However, the human cornea is not an ideal sphere, thus limiting the accuracy of GAT. In particular, the thickness of the cornea can influence the accuracy of GAT readings, a point acknowledged by Goldmann himself, who stated that the design of his instrument was based on a CCT of 500 μm.[122] In 1975, a study performed by Ehlers *et al* demonstrated that the GAT most accurately reflected the true IOP when the cornea has a thickness of 520 μm, thus contrasting with Goldmann's initial assumption.[123]

A major limitation of GAT and other applanation tonometers is that CCT varies considerably in the general population, thus ensuring that the accuracy of the tonometer is regularly compromised. An extensive review presented by Doughty and Zaman in 2000, investigated the impact of human corneal thickness on tonometry readings.[15] In a meta-analysis of 52 reports performed on normal corneas, they found a significant association between CCT and IOP readings using GAT, with thicker corneas generally yielding higher IOP values and thinner corneas lower IOP readings. They calculated that each 10 μm change in CCT induced a 0.2 mmHg change in IOP reading. Subsequent reports have published similar findings, with Kniestedt *et al* showing a 0.25 mmHg adjustment in IOP per 10 μm measurement of CCT,[124] whilst Tonnu *et al* found it to be 0.28 mmHg per 10 μm.[125]

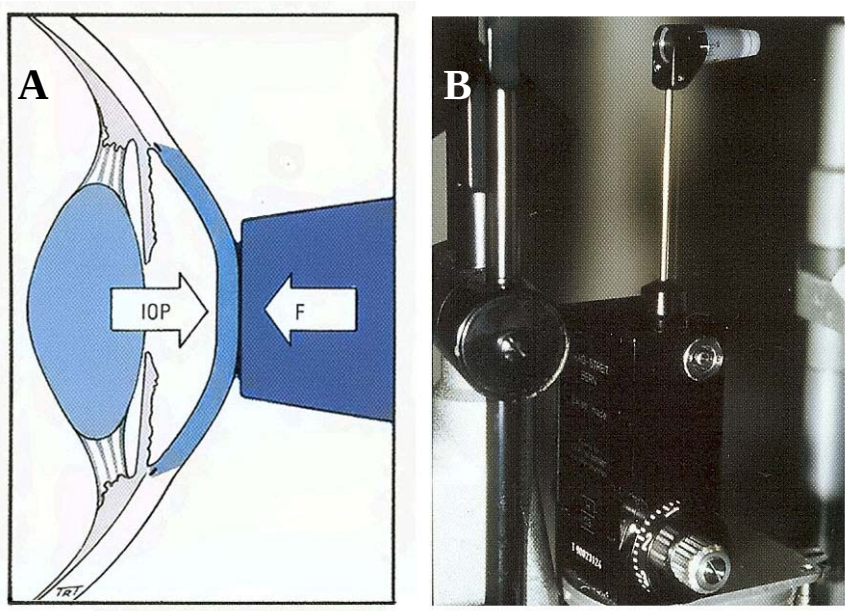

Figure 1.8: Goldmann applanation tonometry. (A) The Imbert-Fick principle states that for an ideal, dry, thin-walled sphere, the pressure inside the sphere (IOP) equals the force necessary to flatten its surface (F) divided by the area of flattening. **(B)** A Goldmann applanation tonometer. Figures adapted from Kanski 2003.[43]

The inaccuracy of applanation tonometers induced by CCT is the result of the different resistance levels of thick and thin corneas. A thick cornea requires more force to flatten, thus resulting in the tonometer overestimating the actual pressure within the eye. Conversely, thinner corneas require less force to flatten and a consequent underestimation of IOP. This can have implications for OAG diagnosis and treatment, as individuals with thin corneas may have higher IOP than those recorded by the tonometer. This could lead to individuals being misclassified in terms of their risk of developing OAG by the assumption that the measured IOP is within the normal range. Problems could also arise during treatment, whereby IOP may not be lowered to a level low enough to prevent visual loss. In an attempt to counter the influence of corneal thickness, several studies have described adjustment algorithms that give corrected IOP measurements from the GAT readings.[123, 126] However, these algorithms have not been demonstrated to improve the accuracy of GAT measurements,[108, 127] which has led to several authors questioning the clinical relevance of such practices.[128, 129] Whilst it is acknowledged that inaccuracies do exist with the use of GAT, it remains a reliable, simple instrument that gives results with excellent repeatability.[130]

1.3.7.5.2 The impact of open-angle glaucoma medication

The degree to which tonometry artefact can explain the correlation between CCT and OAG is uncertain, although reports such as those from the American Academy of Ophthalmology suggest it as the sole cause.[106] Another mechanism that could contribute to the association between CCT and OAG is the effect of glaucoma medication on the cornea. Prolonged use of prostaglandin analogue eye drops has been demonstrated to cause a reduction in CCT of 5-15 μm over a two-year

period.[131-137] However, the impact of prostaglandin treatment on corneal thickness is irrelevant in some studies that demonstrate CCT as a risk factor for OAG. For example, the OHTS,[100] the Barbados Eye Study[107] and the Los Angeles Latino Eye Study[112] were able to show an association between CCT and OAG in patients that had not undergone any prostaglandin treatment.

1.3.7.5.3 Central corneal thickness as an independent risk factor

There is evidence to suggest that the association between CCT and OAG is more than just tonometry artefact and represents an independent mechanism based on the biological properties of ocular tissues. Using multivariate analysis, the OHTS showed that CCT was the strongest predictive risk factor for progression from ocular hypertension to OAG independent of the influence of IOP.[100] The European Glaucoma Prevention Study also had similar findings, with CCT found to be a powerful predictor for the development of OAG independent of IOP.[101] Further supporting data comes from the Early Manifest Glaucoma Trial, which found that thinner CCT significantly predicted progression of visual loss in patients with OAG.[114] An important distinction with the Early Manifest Glaucoma Trial is that patients were recruited based on their level of visual field loss and IOP was not a factor in diagnosis, thus ensuring that tonometry artefact had no real opportunity to influence the outcome of the study. These data imply that a biological link may exist between aspects of the cornea that regulate its thickness and the physical and structural properties of tissues involved in glaucoma pathogenesis. Regardless of the mechanism responsible, measurement of CCT is now an important component of OAG diagnosis and management and is recommended in order to guide effective therapy.[36]

1.3.8 Epidemiology

1.3.8.1 Australia

The prevalence of OAG in Australia has been investigated in the last decade or so by two separate population-based studies, the Blue Mountains Eye Study (BMES) and the Melbourne Visual Impairment Project. The BMES found an OAG prevalence rate of 2.4% in people aged over 49,[138] whilst the Melbourne Visual Impairment Project found the rate to be 1.7% in people aged over 40.[139] As the Australian population continues to age, it is estimated that by the year 2030, the number of Australians with OAG will double from its current levels to between 307,000 and 337,000 people.[140] This will place substantial pressure on the health-care system and a report commissioned by the Centre for Eye Research Australia and Access Economics has calculated that by the year 2025, the total annual cost of OAG to the Australian economy will be $4.3 billion.[141] Of concern is the finding from both the Melbourne Visual Impairment Project and the BMES that approximately 50% of those with OAG were unaware they had the condition.[138, 139] This figure is of particular importance as it suggests that the prevalence of OAG within the population is significantly higher than has been estimated.

1.3.8.2 Global prevalence rates

Numerous population-based studies have described the prevalence rates of OAG in a range of countries and ethnic communities, although it is often difficult to compare some of these results due to differences in the relevant protocols (Table 1.1). As discussed previously, the prevalence of OAG varies between ethnic groups, with people of African descent tending to have the highest rates of disease. By and large, studies conducted in Asian populations have shown that the prevalence of OAG is similar in these groups to that seen in Caucasians. Conflicting data have been

Table 1.1: Global prevalence rates of open-angle glaucoma

Study Location	Ethnicity	Age (years)	N	Prevalence (%)	Reference
Blue Mountains, Australia	Caucasian	49 +	3654	2.4	Mitchell *et al* [138]
Melbourne, Australia	Caucasian	40 +	3271	1.7	Wensor *et al* [139]
Beaver Dam, USA	Caucasian	43-84	4926	2.1	Klein *et al* [142]
Roscommon, Ireland	Caucasian	50 +	2186	1.9	Coffey *et al* [143]
Rotterdam, Netherlands	Caucasian	55 +	3062	1.1	Dielmans *et al* [144]
Baltimore, USA	Caucasian	40 +	2913	1.3	Tielsch *et al* [145]
Baltimore, USA	African	40 +	2395	4.7	Tielsch *et al* [145]
Barbados	African	40-84	4314	7.0	Leske *et al* [90]
Arizona, USA	Hispanic	40 +	4774	1.9	Quigley *et al* [146]
Los Angeles, USA	Hispanic	40 +	6142	4.7	Varma *et al* [91]
Japan	Japanese	40 +	8126	2.6	Shiose *et al* [147]
Guangzhou, China	Chinese	50 +	1504	2.1	He *et al* [148]
Tamil Nadu, India	Indian	40 +	5150	1.7	Ramakrishnan *et al* [149]
Bangkok, Thailand	Thai	50 +	701	2.3	Bourne *et al* [150]
Dhaka, Bangladesh	Bangladeshi	40 +	2347	2.1	Rahman *et al* [151]

Table depicts the prevalence rates of OAG from various studies conducted around the world. The 'Age' column indicates the recruitment age of each study. N = number of participants.

presented from two major studies of OAG in Hispanic communities from the United States, with rates of 1.97% and 4.7% from populations in Arizona and Los Angeles respectively.[91, 146] Racial differences in OAG are of particular interest as they allude to a genetic predisposition to the disease.

1.3.9 Genetics

Evidence from familial and ethnic studies demonstrates that there is a strong genetic contribution to the pathogenesis of OAG. Furthermore, data from twin studies have shown concordance rates amongst monozygotic twins with OAG of up to 98%.[152-154] Even though OAG exhibits a strong genetic component, it is a complex disease that possesses an equally complex genetic aetiology. Familial studies have shown that OAG does not always display a clear Mendelian inheritance pattern, suggesting that multiple inherited and environmental risk factors are required to induce onset of the condition. The complex nature of OAG has made the search for causative genes difficult, where much of the focus has been on investigating the genetics of large pedigrees using genome-wide linkage analysis. Pedigree analysis is further complicated by the late age of onset of OAG, ensuring that the parents of affected individuals will often be deceased, whilst children will be too young to manifest disease. Despite these difficulties, up to 20 different genetic loci have been linked with OAG, although many have not been replicated in later studies.[155] Among them, 14 chromosomal loci have been designated *GLC1A* to *GLC1N* by the HUGO Genome Nomenclature Committee. Of these 14 loci, only three, *GLC1A* (*myocilin*), *GLC1E* (*optinuerin*) and *GLC1G* (*WDR36*), have had the relevant gene identified.

1.3.9.1 Myocilin

MYOC was the first identified OAG gene, when in 1997 it was mapped to chromosome 1q where the locus for the juvenile form of OAG (*GLC1A*) had previously been located.[156, 157] Mutations in *MYOC* are the most common identified genetic cause of OAG, accounting for approximately 3% of cases, although this rate varies slightly according to ethnicity.[158] To date, there have been more than 60 different published missense mutations,[159] with the nonsense change Gln368STOP accounting for almost half of all mutations associated with OAG.[158] Although the precise function of the MYOC protein is unknown, homology modelling suggests it is a secreted protein that functions in the extracellular matrix.[160, 161] It is postulated that mutations in *MYOC* lead to intracellular accumulation of the aberrant protein in trabecular meshwork cells, a process that ultimately results in impaired aqueous outflow and an increase in IOP.[162]

1.3.9.2 Optineurin

The second identified OAG gene, *optineurin* (*OPTN*), was discovered in 2002 after screening of candidate genes from the *GLC1E* locus.[163, 164] Subsequent research has largely determined that variants within *OPTN* are not a *common* cause of normal or high-tension OAG. The Glu50Lys (E50K) mutation has been confirmed as a rare cause of severe NTG,[164-168] while a recent meta-analysis found that the polymorphism Met98Lys (M98K) may predispose to an increased risk of developing disease.[169] Given its proposed role in apoptotic signalling pathways,[170-172] and the fact that mutations in *OPTN* have been associated with other neurodegenerative conditions,[173] it has been postulated that OPTN is involved in the apoptotic pathways leading to retinal ganglion cell death in OAG.[174, 175]

1.3.9.3 WD repeat-containing protein 36

The most recent gene to be associated with familial OAG is *WD repeat-containing protein 36* (*WDR36*), located within the *GLC1G* locus.[176] The original study by Monemi *et al* found *WDR36* mutations in 6.92% of the OAG families screened, with the Asp658Gly (D658G) variant the most prevalent.[176] Subsequent studies have largely failed to replicate these initial findings,[177, 178] although mutations in *WDR36* may be a rare cause of OAG in German and Japanese patients.[179-181] Although the function of WDR36 and its role in normal ocular physiology and OAG is unclear, overexpression of mutant *WDR36* in a transgenic mouse model leads to degeneration of retinal ganglion cells, thus substantiating the potential role of this protein in OAG.[182]

1.3.9.4 Other candidate genes

Numerous studies have assessed selected candidate genes for an association with OAG, with mostly conflicting data that has been difficult to replicate. A recent review found that up to 25 different genes, including *TNFα*, *p53* and *OPA1*, have been investigated for association with OAG in the published literature, although none of these has been conclusively shown to be causative for disease.[183] An inherent problem with candidate gene studies is a limited understanding of the complex nature of OAG pathogenesis, which makes selection of potential susceptibility genes a difficult and almost random process.

1.3.10 Why study open-angle glaucoma genetics?

As OAG is a major cause of permanent blindness in both the developed and developing world, reducing the burden of this disease is of great importance.

Improving the knowledge of genetic mechanisms that underlie OAG is crucial in achieving this aim, given that the currently identified genes only account for small percentage of disease.[184] The benefits of understanding the genetic determinants of OAG are immense and offer the potential for improved methods of diagnosis and treatment. By identifying causative genes, a greater understanding of the mechanisms and pathways involved in the development of OAG can be achieved, which is vital for discovering new therapeutic targets. Another goal of disease gene discovery is the development of predictive diagnostic tests. This can be of particular benefit for a disease such as OAG, where many individuals remain undiagnosed and early treatment can limit visual loss.

Strategies to reduce the impact of visual loss caused by OAG must be aimed at identifying at-risk individuals. Genetic profiling offers a promising approach to this problem as it can theoretically predict the onset of disease before any damage to the visual field has occurred. This is particularly applicable with OAG, where current diagnostic methods can only detect the disease once damage to the retinal ganglion cells has occurred.[47, 185, 186] Genetic profiling can be applied at a family level where a known mutation is segregating with the disease, or could potentially be used as a tool for population-based screening, where a panel of susceptibility alleles is assessed in order to determine an individual's risk of developing OAG. In a recent report, Burr *et al* concluded that population screening for OAG using current diagnostic methods is not cost effective and there are presently no countries where a screening programme has been adopted.[187] Whilst genetic profiling could in the future offer an effective and cost-efficient means of undertaking population screening, our current knowledge of OAG genetics is insufficient to adopt such a programme, particularly given the

complex nature of the disease. Multiple susceptibility genes are likely to be involved in OAG pathogenesis and factors such as incomplete penetrance, additive effects of other variants and the impact of environmental variables all complicate the analysis. Any identified variant must also be rigorously verified in multiple cohorts before it can be applied to a population screening methodology.

Whilst population screening for OAG using genetic testing is not currently feasible, cascade screening within families carrying *MYOC* mutations has been successfully applied.[188-190] When an OAG patient is identified as having a pathogenic mutation, all of their first degree relatives can be tested for the same mutation. If any of these individuals carry the mutation, their first-degree relatives are also screened until all the distal family members of the index case have been assessed for their mutation status. This process is known as cascade screening and within families that carry a *MYOC* mutation, it can be a highly beneficial means of assessing an individual's risk of developing OAG. This is particularly relevant when genotype-phenotype correlations are well understood and the penetrance of the mutation is known. Investigation of several *MYOC* variants has demonstrated that there are strong correlations with specific mutations and the age of onset, peak IOP and the proportion requiring surgery.[188-191] Identification of family members who carry a pathogenic mutation can ensure these individuals undergo increased surveillance and early treatment if necessary, which will greatly improve their chances of minimising visual loss. In addition, monitoring can be reduced in individuals who don't carry the mutation, thus reducing clinical costs. A study by Healey *et al* has also found that families involved in *MYOC* screening have a generally positive perception of the

genetic testing protocol, which is an important factor in assessing the suitability of this approach.[192]

1.3.11 The future of open-angle glaucoma genetics

Despite the genes discussed earlier, approximately 90% of the genetic architecture of OAG remains unknown.[193] Although considerable progress has been made through the use of genome-wide linkage analysis in large pedigrees, this approach has only limited power to detect the small gene effects often seen in complex disorders such as OAG.[194] Another approach that offers great potential to discover novel genetic determinants of OAG is the genome-wide association study (GWAS). GWA studies employ the use of population-based cohorts, rather than family pedigrees, and can assess the frequencies of up to 2.5 million genetic markers from across the whole genome in order to find an association with the disease or trait of interest. They have shown recent success in unravelling the genetics of several common complex diseases, including age-related macular degeneration,[195, 196] type 2 diabetes,[197, 198] Crohn's disease[197, 199] and rheumatoid arthritis.[197, 200]

Along with the use of the GWAS, several other methods could be utilised to identify genetic loci associated with OAG. Analysis of gene expression changes in tissues important for OAG pathogenesis is one such approach. For instance, microarray analysis has been used to examine the molecular pathways involved in the response of trabecular meshwork cells to elevated IOP.[201, 202] Similarly, proteomics offers the ability to look at differential protein levels in specific tissues.[203] Animal models present another potential avenue for dissecting OAG genetics, with well established glaucoma models existing in monkeys, rats and mice.[204] Another approach is to

investigate the genetic determinants of quantitative biomarkers, known as endophenotypes, that comprise part of the overall disease phenotype. This technique has been successfully applied in the field of psychiatric genetics.[205] Traits such as IOP, cup-to-disc ratio and CCT offer potential endophenotypes that could be used to help dissect the genetics of OAG.

1.4 CENTRAL CORNEAL THICKNESS AS AN ENDOPHENOTYPE FOR OPEN-ANGLE GLAUCOMA

The complex nature of OAG ensures that understanding its genetic component is problematic. There is a broad spectrum of phenotypic heterogeneity found with OAG, which includes differences in the appearance of the optic nerve head, variation in the damage to visual fields, large discrepancies in IOP and asymmetrical loss of vision. Age of onset and response to treatment can also differ greatly amongst individuals. This has led some authors to suggest that OAG is not a single disease but rather a group of disorders that are yet to be systematically defined.[206] Crucial to the success of a genetic study designed to find susceptibility genes is a rigid definition of the disease phenotype, a criteria that is difficult to adhere to with a study involving OAG. This is particularly relevant for association-based studies that involve cohorts of unrelated participants who may be diagnosed with OAG but will undoubtedly have varying underlying causes. Further complicating the issue is that susceptibility to late-onset complex disorders is the result of a combined interaction between genes and environmental factors. A potential solution to this problem is to analyse the genetic architecture of individual and quantifiable components of the OAG phenotype, also known as endophenotypes.

Endophenotypes are essentially biomarkers or traits that comprise part of the overall phenotype of the disease. To be classified as an endophenotype, the biomarker or trait in question must fulfil certain criteria.[205] The endophenotype must be associated with the disease in the population, it must be heritable, it needs to be state-independent (manifest in an individual whether or not the disease is active) and within families, the endophenotype and disease should co-segregate. Analysis of endophenotypes has recently been used to identify susceptibility genes for hypertension,[207] alcoholism[208] and numerous behavioural and psychiatric disorders.[209-212] Among the established risk factors for OAG, optic nerve cupping as measured by cup-to-disc ratio, IOP and CCT all represent plausible endophenotypes. In the case of CCT, it is state-independent and heritable and as it is a quantitative variable, it allows individuals to be ranked along a continuum of risk, thus providing substantially more information than a dichotomous trait. To be classified as an endophenotype however, it must be demonstrated that there is a genetic correlation between CCT and OAG and this is where studying the genetics of this trait may provide some answers.

1.4.1 Genetics of central corneal thickness

Despite a wealth of knowledge on the structure and function of the cornea, little is known about the mechanisms underlying individual variation in CCT. It is likely that differences in the composition of the corneal stroma, the predominant layer of the cornea, are in some way responsible for CCT variability. No environmental factors have been associated with these changes, although outdoor lifestyle and socioeconomic status have been cited as possible influences.[213, 214] Similarly, no genes have been identified that contribute to the variation in CCT seen in the normal

population. However, there is evidence supporting a genetic component for CCT determination, including data from heritability studies, comparison of CCT between different ethnic populations and the characteristic CCT associations found in several rare genetic diseases.

1.4.1.1 Heritability

There are currently five studies that have investigated the heritability of CCT. The first to report familial correlation with CCT was published by Alsbirk in 1978.[213] Conducted on 86 Eskimo families from Greenland, the study found heritability estimates of 0.6-0.7 for CCT and concluded that there was 'a major genetic influence on CT (corneal thickness)'. Environmental factors, such as occupation and place of residence, were proposed as accounting for some of the remaining variation. Almost 30 years later, Toh *et al* published findings of a CCT heritability study conducted on monozygotic and dizygotic twins from Australia and the United Kingdom.[215] A total of 256 sets of twin pairs were investigated and CCT heritability was calculated to be 0.95. The authors suggested that unique environmental factors, including measurement error, contributed to the remaining variance. Another twin study, this time conducted on 449 sets of both monozygotic and dizygotic twins from China, found heritability estimates for CCT amongst males to be 0.88 and females 0.91.[216] Recently, two large familial based studies have investigated CCT heritability with similar outcomes. Landers *et al* examined 33 families from Australia and found a parent-child heritability estimate for CCT of 0.68,[217] whilst Charlesworth *et al* assessed 22 pedigrees comprising 1181 individuals from Australia and the United States and determined CCT heritability to be 0.72.[206]

The similarity of the twin study results, which were carried out on ethnically distinct populations, implies that CCT is one of the most highly heritable traits identified. Heritability estimates from the twins are comparable to those obtained for other highly heritable traits such as finger ridge count.[218-220] Furthermore, the consistency in the findings of the three familial-based studies support the strong hereditary component of this trait. The lower heritability estimates obtained from the familial studies when compared to the twin results could be due to a number of factors, but the higher degree of a shared environment encountered in twin studies could account for some of this variation. Regardless of the varying outcomes of the five studies, it is clear that the determination of CCT has a strong hereditary component.

1.4.1.2 Differences between ethnic groups

A considerable amount of research has been committed to investigating the mean CCT values of various ethnic communities and populations from across the world. Whilst there are limitations to making direct comparisons between studies due to methodological differences, there is clear evidence of ethnic-dependent differences in CCT. A multitude of factors can influence the results obtained from cohort-based CCT studies, including subject ascertainment, inclusion or exclusion of OAG or ocular hypertensive patients, recruitment age, contact lens wear, inter-observer measurement variability and importantly, the type of measurement instrument used. For example, OAG patients can present with thinner than average CCT measurements whilst ocular hypertensive patients have thicker corneas, [109, 221-223] thus making inclusion or exclusion of these participants integral to the final cohort mean. As such, it is important to compare data obtained from studies using similar methodologies in order to draw meaningful conclusions.

There have been several population-based studies investigating CCT as either a primary outcome or as an adjunct to a glaucoma or diabetes study (Table 1.2). There is a broad distribution of mean CCT values amongst the various ethnic groups surveyed, with the Mongolian population having the thinnest (504.5 μm)[16] and the Chinese the thickest (556.2 μm).[26] One of the major issues encountered when comparing these studies is the choice of instrument used to measure CCT, as notable discrepancies have been documented between different methods. Ultrasound is the most widely employed method as it is ideal for large population studies, particularly where field work is required. As seen in Table 1.2, results from ultrasound pachymetry show apparent differences between ethnic groups, with values ranging from 520.7 μm in the Indian population[214] to 546.9 μm in a Hispanic cohort from the United States.[18] Even amongst Asian ethnic groups, variations in mean CCT are apparent amongst the Indian[214] and Burmese[27] studies compared to the Singaporean population.[224] Whilst other factors such as the inclusion or exclusion of glaucoma patients and user variability must be considered, comparison of the population studies conducted using ultrasound pachymetry reveals evident differences in mean CCT between several ethnic groups.

Several other methods for measuring CCT were employed in the studies shown in Table 1.2. Optical pachymetry can give similar measurement readings to ultrasound[225, 226] but suffers from poor reproducibility and high inter-observer variability.[12, 227] Optical coherence tomography,[228-231] Scheimpflug camera[10, 11, 232] and specular microscopy[9, 13, 233, 234] have all been shown to yield different CCT measurements when compared to ultrasound pachymetry, although the magnitude of the difference varies. In order to illustrate how the choice of instrument can affect

Table 1.2: Population studies that have investigated CCT

Ethiniciy	Country	Number of Participants	Age Range (years)	Mean CCT (µm)	OAG Included	Measurement Technique	Reference
African	Barbados	1064	40-84	529.8	Yes	Ultrasound	Nemesure *et al* [17]
Asian	Burma	1909	40+	521.9	No	Ultrasound	Casson *et al* [27]
	China	3100	40-101	556.2	Yes	OCT	Zhang *et al* [26]
	India	2532	40-103	520.7	No	Ultrasound	Vijaya *et al* [214]
	Japan	7313	40+	517.5	No	Specular	Suzuki *et al* [20]
	Mongolia	1129	10-60	504.5	Yes	Optical	Foster *et al* [16]
	Singapore	3239	40-80	541.2	Yes	Ultrasound	Su *et al* [224]
Caucasian	Australia	1343	49+	539.5	Yes	Ultrasound	Healey *et al* [235]
	Iceland	925	50-85	529	No	Scheimpflug	Eysteinsson *et al* [23]
	Netherlands	352	55+	537.4	No*	Ultrasound	Wolfs *et al* [109]
Eskimo	Greenland	839	7-89	523.7	Yes	Optical	Alsbirk *et al* [236]
Hispanic	USA	1699	40+	546.9	Yes**	Ultrasound	Hahn *et al* [18]

OCT = optical coherence tomography. * ocular hypertensive patients included. ** only untreated OAG patients included.

comparisons between ethnic groups, the specular microscope offers a good example. Specular microscopy, such as that used by Suzuki *et al*,[20] consistently underestimates CCT by 14-32 μm when compared to ultrasound.[9, 13, 233, 234] In a study performed on 224 Japanese control participants, Wu *et al* found a mean CCT of 548.2 μm using ultrasound pachymetry,[237] which is significantly more than the 517.5 μm stated by Suzuki *et al* from the same population.[20] It is possible that this difference can be accounted for by the use of the two distinct measurement methods.

Ethnic-dependent variation in CCT has also been demonstrated by cross-sectional studies that have investigated two or more ethnic groups as part of their study design (Table 1.3). In many ways, these analyses offer a more accurate representation of the differences in CCT between ethnic groups as they have the same selection criteria for each participant, use the same measurement method and limit the number of instrument operators, thus significantly reducing variability. Data from numerous studies has demonstrated that participants of African descent have thinner corneas than their Caucasian counterparts.[17, 19, 24, 238-240] This observation is supported by the population data in Table 1.2. Several of the ethnic groups shown in Table 1.3 have not been investigated in population cohorts. Two papers from Australia by Landers *et al* and Durkin *et al* both indicate that the indigenous Australian Aboriginals of central and southern Australia have significantly thinner CCT values than Caucasians.[22, 241] In a study by Lifshitz *et al*, people of North African descent were found to have significantly thinner CCT values than a cohort of mixed ethnicities from Israel.[242] Research by Torres *et al* has also demonstrated that the American Indian and Alaskan Native populations have significantly thicker CCT values than

Table 1.3: Studies investigating CCT in two or more ethnic groups

Country	Ethnicity	N	Mean Age (years)	Mean CCT ± SD (μm)	OAG Included	Reference
Australia	Aboriginal	91	51	511 ± 34	No	Landers *et al* [22]
	Caucasian	84	56	541 ± 31		
Australia	Aboriginal	74	44.8	514.9 ± 30.5	No	Durkin *et al* [241]
	Caucasian	115	47.1	544.7 ± 31.9		
Barbados	African	1064	64.3*	529.8 ± 37.7	Yes	Nemesure *et al* [17]
	Caucasian	25	64.3*	545.2 ± 45.7		
Canada	Asian	24	45.2*	532.8 ± 7.0**		
	Black	32	45.2*	529.7 ± 5.3**		
	Native	5	45.2*	527.8 ± 12.0**	Yes	Dohadwala *et al*[238]
	Other	19	45.2*	539.1 + 9.9**		
	White	227	45.2*	552.5 ± 2.3**		
Israel	Mixed Origin	83	32.4	545.4 ± 30.4	No	Lifshitz *et al* [242]
	North African	121	35.9	518.9 ± 31.5		
USA	African	26	63.1	533.8 ± 33.9	No	LaRosa *et al* [239]
	Caucasian	51	65.2	555.9 ± 33.2		
USA	African	116	37.2	535.8 ± 33.4		
	Asian	170	34.8	549.8 ± 32.3	No	Shimmyo *et al* [24]
	Caucasian	1466	38.1	552.6 ± 34.5		
	Hispanic	203	34.2	551.1 ± 35.4		
USA	African	26	62.6	524.8 ± 38.4		
	Caucasian	36	69.1	562.8 ± 31.1		
	Chinese	41	65.9	569.5 ± 31.8	No	Aghaian *et al* [19]
	Filipino	33	67.6	559 ± 24.9		
	Hispanic	27	67.5	563.6 ± 29.1		
	Japanese	38	70.2	538.5 ± 29.6		
USA	AI/AN	429	55.7	554.8 ± 33.9	Yes	
	African	33	53	528.5 ± 33.2	No	Torres *et al* [240]
	Caucasian	46	54.7	551.9 ± 28.3	No	

All the studies listed in this table utilised ultrasound pachymetry. AI = American Indian. AN = Alaskan native. N = number of participants. SD = standard deviation. * Mean age of entire cohort not individual ethnic groups. ** Standard error.

both African American and Caucasian participants from the same geographical area of the United States.[240]

Taken collectively, the findings from the population and cross-sectional studies conclusively demonstrate the ethnic-dependent differences in CCT. People of African and Australian Aboriginal descent tend to have a lower mean CCT than other populations. Curiously, the data from these groups suggest that darker skin pigmentation is associated with a thinner CCT. Both the Hispanic and Caucasian populations appear to have similar CCT measurements, while amongst the various Asian ethnic groups there is a broad diversity in mean CCT values, with the Chinese appearing to have the highest readings.[19, 26] Whilst environmental factors unique to certain cultures or geographical areas may account for some of the variation between populations, these are likely to be negligible in studies conducted from the same clinics or geographical regions. It is probable that specific genetic variants have become enriched in certain populations and that these play a major role in determining CCT.

1.4.1.3 Abnormal central corneal thickness measurements associated with disease

The association of abnormal CCT measurements with several genetic diseases provides further evidence to support the genetic nature of this trait (Table 1.4). Abnormal CCT is an important clinical finding, particularly for patients with extremely thin measurements due to the higher risk of globe rupture or injury. These diseases are also caused by mutations in known genes, thus identifying these genes as candidates for determining normal CCT variation, albeit as a result of less pathogenic sequence variants. Importantly, apart from the abnormal CCT

Table 1.4: Abnormal CCT measurements associated with various disorders

Disease	Gene	Disease Participants	Mean Disease CCT (µm)	Control Participants	Mean Control CCT (µm)	Reference
Aniridia	*PAX6*	17	631.6	-	-	Brandt *et al* [243]
Aniridia	*PAX6*	10	691.8	10	548.2	Whitson *et al* [244]
Anterior Segment Dysgenesis	*FOXC1*	27	600	20	532	Lehmann *et al* [245]
Axenfeld-Reiger Syndrome	*PITX2*	8	484	5	582	Asai-Coakwell *et al* [246]
Behcet's Disease	*?*	19	589	20	553	Everekliogl*u et al* [247]
Down's Syndrome	*Trisomy chromosome 21*	28	488.4	20	536.3	Everekliogl*u et al* [248]
EDS (Type I/II)	*COL5A1/COL5A2*	7	435.8	8	568.9	Segev *et al* [31]
Marfan Syndrome	*FBN1*	31	502	17	552.4	Sultan *et al* [32]
Marfan Syndrome	*FBN1*	62	543.5	98	564.2	Heur *et al* [33]
Osteogenesis Imperfecta	*COL1A1/COL1A2*	53	443	35	522	Pedersen *et al* [34]
Osteogenesis Imperfecta	*COL1A1/COL1A2*	23	459.5	15	543.6	Everekliogl*u et al* [35]
Weill-Marchesani Syndrome	*FBN1/ADAMTS10*	6	631.5	20	535.8	Razeghinejad [249]

measurements, the cornea generally appears healthy in these conditions, which is in contrast to diseases such as keratoconus and Fuchs endothelial dystrophy. The majority of conditions associated with abnormal CCT are connective tissue disorders such as Ehlers-Danlos syndrome, Marfan syndrome, osteogenesis imperfecta and Weill-Marchesani syndrome, as well as developmental abnormalities of the anterior segment, including aniridia, anterior segment dysgenesis and Axenfeld-Rieger syndrome.

The connective tissue disorders associated with abnormal CCT measurements result from mutations in extracellular matrix proteins that are important components of the corneal stroma, the predominately acellular layer that comprises 90% of the total corneal thickness. Osteogenesis imperfecta and Ehlers-Danlos syndrome are, in the majority of cases, caused by mutations in the genes that encode type I and type V collagen respectively.[250-253] Both of these disorders result in a significant reduction in CCT, consistent with the integral role that collagens play in the structure of the cornea.[29-31, 34, 35] Type 1 and type V collagen are abundant in the corneal stroma where they interact to form a highly ordered and intricate array of heterotypic type I/V collagen fibrils.[254] Studies in human osteogenesis imperfecta patients and a mouse model of Ehlers-Danlos syndrome have demonstrated that mutations in the type I and type V collagen genes respectively, lead to alterations in the diameter and density of corneal stromal collagen fibrils, which in turn is the likely cause of the reduced corneal thickness.[31, 255] It has also been postulated that altered metabolism of type VI collagen, another collagen prominent in the cornea, may be responsible for the reduced CCT seen in Down syndrome patients.[248] Another extracellular matrix protein, fibrillin 1, is mutated in Marfan syndrome[256-259] and autosomal dominant

forms of Weill-Marchesani syndrome.[260] As with osteogenesis imperfecta and Ehlers-Danlos syndrome, patients with Marfan syndrome have reduced CCT, although the magnitude of the difference in Marfan patients is smaller.[32, 33] Interestingly, the cohort of Weill-Marchesani participants investigated by Razeghinejad *et al* had a markedly increased CCT, although it is not known which gene was mutated in these patients.[249] It is unknown how mutations in fibrillin influence CCT, but expression of the protein has been demonstrated in the cornea.[261, 262]

Abnormal ocular development, such as that caused by the anterior segment dysgenesis disorders aniridia and Axenfeld-Rieger syndrome, can have a detrimental impact on corneal structure. Aniridia is caused by mutations in the paired box transcription factor *PAX6* and amongst its many ocular manifestations, patients have been shown to present with substantially increased CCT.[243, 244] It has been postulated that mutations in *PAX6* may disrupt the normal proliferative or apoptotic homeostasis of corneal stromal keratocytes, which ultimately results in increased stromal extracellular matrix synthesis.[244] Chromosomal duplications of the Forkhead Box transcription factor *FOXC1* can cause a range of anterior segment dysgenesis phenotypes, including iris hypoplasia and Axenfeld-Rieger syndrome, and have also been associated with abnormally thick CCT measurements, most likely due to cellular hyperplasia or increased recruitment of cells to the developing cornea.[245] In contrast, mutations in the paired-like homeodomain transcription factor *PITX2* result in a significantly thinner CCT associated with Axenfeld-Rieger syndrome.[246] This could be a consequence of the vital role *PITX2* plays in corneal development, as

murine neural crest cells that ultimately form the endothelium and stroma express *Pitx2* upon reaching the anterior segment.[263]

1.4.2 Why study the genetics of central corneal thickness?

Along with potentially offering an improved understanding of corneal disorders such as keratoconus, studying the genetics of CCT is also clinically relevant due to the association of this trait with OAG. Despite presenting compelling evidence, studies such as the OHTS are still unable to completely separate tonometry artefact from underlying biological risk. The resolution to this problem may lie with uncovering the genes that determine CCT. By developing an understanding of the genetic basis of CCT variation, the mechanisms underlying the association of this trait with OAG should become more apparent. If a genuine biological link exists between the two, then improving our knowledge of CCT genetics offers the opportunity of identifying novel OAG genes. Whilst OAG is known to exhibit a strong genetic component, it is poorly characterised and methodologies used to identify susceptibility loci have been largely unsuccessful. The loci identified to-date represent simple Mendelian forms of the disorder and mutations in the genes are relatively rare. Novel approaches are required to discover new OAG genes, such as studying the genetics of risk factors like CCT.

1.4.3 Central corneal thickness as a biological risk factor for open-angle glaucoma

With several studies indicating that a thinner CCT is a risk factor for OAG independent of IOP, it is conceivable that genes involved in controlling the thickness of the cornea may also be associated with the development of OAG. The cornea is

structurally continuous with tissues important in glaucoma pathogenesis, such as the lamina cribrosa and peripapillary sclera and similarities are evident in the protein compositions of these tissues. Type I collagen, for example, is the major extracellular protein found within the corneal stroma[6] and is also strongly expressed in the sclera and lamina cribrosa.[264] Numerous other extracellular proteins, such as collagen types V and VI and the proteoglycans decorin and biglycan, are also expressed in these tissues.[6, 265] The strength and elasticity of connective tissues like the sclera and lamina cribrosa is reliant on extracellular proteins such as collagens and proteoglycans and these biomechanical properties are essential for resisting IOP-related stress.[65] Failure to withstand the chronic mechanical stress inflicted by an elevated IOP can result in glaucomatous damage. It is plausible therefore, that proteins important for maintaining the structural integrity of the peripapillary sclera and lamina cribrosa are also expressed in the cornea, where they could potentially play a role in the determination of CCT.

Scleral thickness has been suggested as a potential factor in the development of OAG, particularly the posterior region near the optic nerve. The thickness of the sclera influences its ability to withstand IOP-induced mechanical stress and modelling has established that the biomechanical properties of the peripapillary sclera are important in the OAG pathogenesis.[266] An association between scleral thickness and OAG has been found in enucleated human eyes[267] and in an induced glaucoma non-human primate model.[268] Several studies have also demonstrated a correlation between CCT and the thickness of the anterior sclera.[269-271] Given the structural continuity of cornea and sclera, there is potential that genes may be common to the developmental pathways of both tissues. Accurate measurement of

the posterior sclera *in vivo* is technically challenging using modern imaging equipment and it is unclear what relationship exists between the thickness of the anterior and posterior sclera. Given the correlation between CCT and the anterior sclera, it is possible that corneal thickness could be related to posterior scleral thickness, although several reports have shown there is no association between CCT and the thickness of peripapillary sclera and lamina cribrosa using histological analysis.[272-274] Future research utilising *in vivo* measurements of the cornea and posterior sclera is likely to provide a definitive analysis of any similarites in the structural properties of these tissues.

The relationship between CCT and various physical parameters of the optic disc, such as optic disc area and depth of the optic cup, has also been widely investigated. The structure of the optic disc is of fundamental importance in OAG pathogenesis and any association between CCT and a component of the optic disc would support the hypothesis that CCT is a biological risk factor for OAG. Additionally, features of the optic disc such as the cup-to-disc ratio are known to exhibit high heritability,[275-277] which supports the possibility that genes may be common to the developmental pathways of both the cornea and optic disc. Several studies have demonstrated a negative correlation with CCT and optic disc area, whereby participants with thinner corneas had larger optic discs.[278-281] The population-based BMES found that OAG participants had larger optic discs than controls[282] and it has been postulated that larger optic discs are more susceptible to glaucomatous damage due to a reduced ability of the lamina cribrosa to withstand mechanical stress and support the optic nerve axons.[71, 283] However, there are conflicting data on the association between CCT and optic disc area, with some studies reporting no correlation,[284-286] whilst

others have found a positive correlation.[26, 110] In addition, Lesk *et al* have shown that a thinner CCT correlates with a shallower optic cup and reduced neuroretinal rim blood flow.[287] Lesk *et al* propose that a shallow optic cup is a surrogate marker for lamina cribrosa compliance (mobility), which is important in the development of OAG. Again, these findings have not always been replicated and further research is required to confirm any association between CCT and physical parameters of the optic disc.[288, 289]

1.4.4 The future of central corneal thickness genetics

The evidence presented in this introduction, strongly implicates CCT as a genetically determined trait, yet no genes have been identified that contribute to normal CCT variation seen within the general population. As with any quantitative trait, CCT is likely to be determined by a number of genes of varying effect sizes. Various methodologies could be utilised in order to discover these genes, including a candidate gene approach, familial linkage analysis or a GWAS. Indeed, candidate gene analysis has recently identified the *COL8A2* gene as a possible modifier of CCT in some OAG patients.[290] Given the current prominence of the GWAS methodology, it would appear that CCT would be a model trait to uncover quantitative trait loci utilising this approach. Recent GWA studies have uncovered loci associated with traits such as height,[291, 292] body mass index,[293, 294] bone mineral density[295, 296] and lipid and cholesterol levels,[297] illustrating the power of this approach in identifying genes for quantitative traits. With available data suggesting that CCT has a strong genetic component, a well designed GWAS would provide an ideal opportunity to identify genes associated with this trait and progress this field.

1.5 SUMMARY AND AIMS

As the Australian population continues to age, the burden of OAG on the health system and economy will increase. The development of new diagnostic and treatment methods is vital in limiting the impact of this disease over the coming decades. One of the most promising approaches for improving our understanding of OAG is to study the genetic mechanisms that underlie its pathogenesis. Although mutations in genes such as *MYOC* have been associated with OAG, these variants only account for a small percentage of cases and further susceptibility loci remain to be identified.

Due to the complex nature of the OAG phenotype, genetic studies are inherently difficult and have often yielded limited success. An approach that may improve the viability of a genetic study on a complex disease is to investigate the genetic architecture of an endophenotype. As several studies have demonstrated, CCT is a significant risk factor associated with OAG and is a good candidate for an endophenotype based genetic study. Due to its high heritability and ease and accuracy of measurement, CCT offers a model trait for genetic dissection. The discovery of genes that govern normal CCT variation can offer an insight into the developmental mechanisms of the cornea, whilst also potentially identifying new genes associated with the development of OAG.

The work undertaken in this thesis investigated the hypothesis that genes involved in the determination of normal CCT variation are also susceptibility loci for OAG. This initially required the identification of genes associated with CCT, as there was no prior knowledge in this area. In addition, the relationship between pigmentation and

CCT was also examined, based on the observation from the human ethnic studies that there may be a correlation between the two traits. The rationale behind this investigation was to ascertain if genes involved in the regulation of pigmentation are also candidates for influencing CCT. The final part of this thesis involved determining if any identified CCT genes also increased susceptibility to OAG.

The general aims addressed in this thesis were:

1. To determine if CCT is associated with human and rodent pigmentation and whether pigmentation genes can directly influence CCT.
2. To identify novel genes associated with normal CCT variation through the use of a candidate gene study and a GWAS.
3. To investigate if any identified CCT genes are also associated with OAG.

CHAPTER 2

ETHNIC AND MOUSE STRAIN DIFFERENCES IN CENTRAL CORNEAL THICKNESS AND ASSOCIATION WITH PIGMENT PHENOTYPE

Publications arising from this chapter:

Dimasi DP, Hewitt AW, Kagame K, Ruvama S, Tindyebwa L, Llamas B, Kirk KA, Mitchell P, Burdon KP, Craig JE. Ethnic and Mouse Strain Differences in Central Corneal Thickness and Association with Pigmentation Phenotype. *PLoS One* (*in press*)

2.1 HYPOTHESIS AND AIMS

Variations in CCT between different human ethnic groups are well established jn the literature. A further observation is that darker skin pigmentation appears to be correlated with a thinner CCT. Based on this evidence, the hypothesis investigated in this chapter is that mammalian pigmentation is correlated with CCT. In order to test this hypothesis, a series of analyses were conducted in both a rodent model and humans.

The specific aims investigated in this chapter were:

1. To verify that CCT is correlated with human skin pigmentation.
2. To determine if CCT varies in different inbred mouse strains and whether it is influenced by coat colour.
3. To assess whether mutations in mouse pigment genes can alter CCT.

2.2 OVERVIEW

2.2.1 Skin pigmentation and central corneal thickness

As previously discussed, there is substantial evidence that CCT is correlated with ethnicity. However, a further observation from data collected in human ethnic groups is that skin pigmentation appears to influence CCT. Numerous studies that have concomitantly investigated the CCT of Caucasian groups and people of African descent have found that Caucasians consistently have a thicker CCT than the darker skinned ethnic groups.[17, 19, 24, 238, 239, 298] Additional support for this hypothesis comes from data obtained in Australian Aboriginals, who have significantly thinner CCT measurements than Australian Caucasians.[22, 241] Other ethnic groups with dark skin pigmentation, such as Asian Indians and Burmese, also have thinner CCT when

compared to Caucasian populations.[27, 214, 299] The suggestion that molecular pathways involved in the determination of skin pigmentation could also be involved in the development of a clear tissue such as the cornea is extremely novel and warrants further investigation.

2.2.1.1 Regulation of mammalian pigmentation

The colour of mammalian skin, hair and eyes is predominately the result of a pigmented molecule known as melanin. Melanin is a complex biopolymer that is synthesised from the amino acid tyrosine through a process known as melanogenesis. The production of melanin takes place in a specialised population of cells known as melanocytes and is largely confined to a lysosomal-like organelle termed the melanosome. In humans and mice, there are two major types of melanin, both of which have different pigmentation characteristics: eumelanin, which is brown or black in colour and pheomelanin, which is red or yellow. Variations in skin, hair and eye pigmentation are largely determined by the amount and type of melanin pigment produced by the melanocytes.[300-303]

The process of melanogenesis begins within the melanosome, where the tyrosinase (TYR) enzyme performs the critical rate-limiting activity of hydroxylating tyrosine to L-3,4-dihydroxyphenylalanine (DOPA), which is rapidly converted to DOPAquinone (Figure 2.1). This first step of the biosynthetic pathway is common to both eumelanin and pheomelanin production. If the amino acid cysteine is available, the melanogenesis pathway will be driven towards the production of pheomelanin. As the levels of intramelanosomal cysteine become depleted, the formation of eumelanin is favoured.[304] Tyrosinase-related protein 1 (TYRP1) and dopachrome

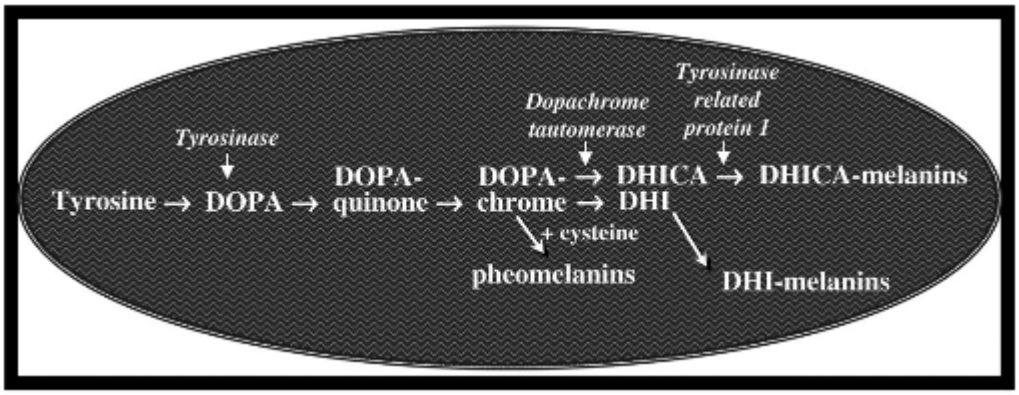

Figure 2.1: Melanin biosynthesis pathway. The synthesis of melanin takes place within the melanosome and begins with the conversion of tyrosine to DOPA by the enzyme *tyrosinase*. The incorporation of cysteine leads to the production of the pheomelanins, whilst the enzymes *dopachrome tautomerase* and *tyrosinase-related proteins 1 are* crucial for the production of the eumelanins (DHI- and DHICA-melanins). Figure sourced from Costin *et al* 2007.[305]

tautomerase (DCT), both of which share 40-45% homology with TYR, are crucial to eumelanin synthesis.[306] Not only do TYRP1 and DCT catalyse the formation of an intermediate in the eumelanin synthesis pathway, they also interact with and stabilise TYR.[307-309] Individual melanocytes typically synthesize both eumelanin and pheomelanin, with the ratio of the two being determined by a balance of variables, including pigment enzyme expression and the availability of tyrosine and sulphydryl-containing reducing agents in the cell.[304, 310]

Following melanogenesis, the process that regulates both skin and hair pigmentation is similar. In the case of skin pigmentation, epidermal melanocytes, located in the basal layer of the epidermis, secrete the melanin-containing melanosomes into adjacent keratinocytes. This melanin remains within the keratinocytes as they differentiate and migrate into the upper epidermal layers. Similarly, for hair pigmentation, melanosomes are secreted into the keratinocytes that will later constitute the shaft of the hair fibre. In order to secrete the mature melanosomes into neighbouring cells, the melanocytes develop multiple dendritic extensions that act as channels to transport the melanosomes into the keratinocytes.[311] Studies in the mouse have shown that a protein complex consisting of myosin VA, Rab27a and melanophilin is crucial for the intracellular trafficking of the melanosomes into the dendrites of the melanocytes, where they can associate with the plasma membrane prior to secretion.[312, 313] However, the mechanism responsible for the transfer of the melanosome into the keratinocyte remains poorly understood. In terms of eye pigmentation, the colour of the iris is regulated slightly differently, whereby pigmented melanosomes are not secreted but rather retained within the melanocytes.

2.2.1.2 Human skin pigmentation

Skin colour in humans ranges from extremely fair/light to extremely dark, depending on the ethnic background, yet the density of melanocytes within a given area of the body is virtually identical in all types of skin.[314] Differences in skin pigmentation are largely the result of the amount and type of melanin synthesised, as well as the structure and packaging of melanin. The type of melanin produced is an important factor in the determination of skin colour. A phenotype of fair or light skin is associated with a large amount of pheomelanin and small amounts of eumelanin, whilst the melanin ratios are switched for darker skin.[315] However, the total amount of melanin produced is more important than the ratio of melanin types. Lighter skin tends to have less melanin and what is produced is typically found arranged in clusters of melanosomes within the keratinocytes, whereas darker skin has more melanin and the melanosomes are larger and dispersed more widely throughout the keratinocytes.[316] Thus the regulation of skin pigmentation is controlled by factors both inside and outside the melanocyte.

Melanocortin 1 receptor (MC1R), a seven-transmembrane G protein-coupled receptor that regulates the quantity and quality of melanin production, is a major determinant of skin and hair pigmentation.[306, 317] The MC1R protein is located on the plasma membrane of melanocytes and has a role in modulating the melanogenic cell signalling pathways. MC1R function is primarily regulated by two agonists, α-melanocyte-stimulating hormone (αMSH) and adrenocorticotropic hormone (ACTH) and an antagonist, agouti signalling protein (ASIP). Binding of MC1R to αMSH or ACTH induces cyclic AMP production, which ultimately leads to the phosphorylation of the cAMP responsive-element-binding protein (CREB)

transcription family members.[318-320] In turn, CREB proteins activate expression of various genes, including microphthalmia transcription factor (*MITF*), the transcription factor that is pivotal to the expression of numerous pigment enzymes including TYR, TYRP1 and DCT (Figure 2.2).[321] Activation of this pathway stimulates production of eumelanin, whereas binding of the antagonist ASIP to MC1R down-regulates cAMP signalling and leads to increased synthesis of pheomelanin.[322, 323] MC1R function is therefore able to control the switch that favours production of eu- or pheomelanin.

2.2.1.3 Genetics of human skin colour determination

Regulation of human skin pigmentation is under the control of both genetic and environmental factors. Skin pigmentation is strongly correlated with ethnicity and a study in Caucasian twins has demonstrated that differences in skin tone are highly heritable, illustrating the significant genetic contribution to this trait.[324] Exposure to ultraviolet (UV) radiation, which occurs primarily through sunlight, is the major environmental factor responsible for influencing skin pigmentation through a process termed the 'tanning reaction'.[325, 326] The ability of human skin to respond to UV radiation and the degree to which tanning occurs however, is tightly linked to an individual's underlying genetic profile. Determination of skin colour is a polygenic trait and in the mouse, for example, some 368 loci associated with skin and coat colour have been identified.[327] Characterisation of genes associated with human skin colour is not as extensive as in the mouse, although a recent review by Sturm *et al* discussed 11 genes that influence hair and eye pigmentation.[328]

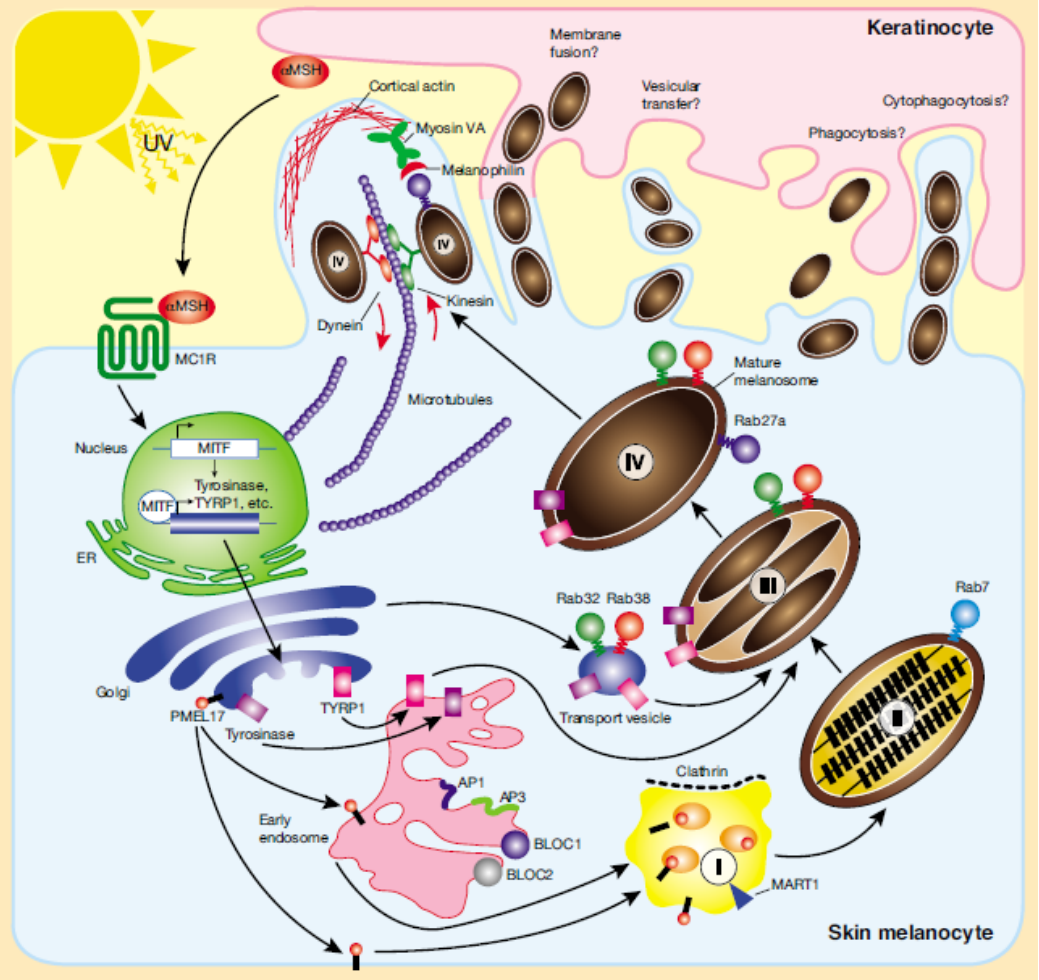

Figure 2.2: Molecular pathways involved in the regulation of skin pigmentation. The synthesis of melanin is primarily stimulated by ultraviolet radiation (UV), which leads to the secretion of α-MSH by keratinocytes. Activation of MC1R ultimately leads to expression of a host of genes, including *TYR* and *TYRP1*, the protein products of which are trafficked to the melanosome. Melanosomes are believed to derive from endosomes and undergo four stages of maturation before they are transported to dendrites of the melanocyte. From here, the mature melanosomes are transported into the keratinocytes by an as yet underdetermined mechanism. Sourced from Wasmeier *et al* 2008.[329]

Some of the initial discoveries in the field of skin pigmentation genetics were made from studying pigmentation disorders such as oculocutaneous albinism (OCA). OCA is a condition characterised by a congenital hypopigmentation of the skin, hair and eyes. Four different forms of OCA have been described, each presenting with varying degrees of skin and hair pigmentation. The underlying genetic defect is also unique to each form of OCA, with mutations in *TYR, oculocutaneous albinism II* (*OCA2*)*, TYRP1* and *solute carrier family 45, member 2* (*SLC45A2*) associated with OCA types 1-4 respectively.[330, 331] Both TYR and TYRP1 are enzymes involved in melanogenesis and their functions have been discussed previously, whereas *OCA2* and *SLC45A2* are transmembrane proteins that appear to be important for proper melanosomal function. The *OCA2* gene encodes the human homologue of the mouse *p* (pink-eyed dilution) gene, which has been extensively described in mouse pigmentation studies.[332] Whilst the complete function of *OCA2* is yet to be determined, there is evidence that it is involved in the transport of TYR and TYRP1 into the melanosome as well as regulating melanosomal pH.[332-335] As with *OCA2*, the function of *SLC45A2* is not completely understood, although it is also believed to be involved in the trafficking of TYR and TYRP1 into the melansome.[336] Mutations in any of these four genes cause significant disruption to melanin synthesis, with the most severe forms presenting with a complete absence of melanin production throughout life. There is also evidence that polymorphisms in *TYR, OCA2, TYRP1* and *SLC45A2* are associated with normal skin and eye colour variation seen within and between different ethnic groups.[303, 328]

Several other genes have been associated with alterations in normal pigmentation. Genetic variants within *MC1R* have been extensively linked to the phenotype of red

hair and fair skin, with over 70 different polymorphisms and mutations identified to date.[320, 337] An increased risk of skin cancer has also been correlated with several *MC1R* variants.[338, 339] Polymorphisms in the MC1R antagonist *ASIP* have been associated with skin and eye colour variation.[340-343] Another major human pigmentation gene is the recently identified *solute carrier family 24, member 5* (*SLC24A5*), the homologue of which is responsible for the zebrafish *golden* phenotype.[344] The *SLC24A5* gene encodes the NCKX5 protein, which is a member of the potassium-dependent sodium calcium exchanger family that regulates the transport of calcium.[344] It has been postulated that NCKX5 is involved in the maturation of TYR in the trans-golgi network or in melanosome biogenesis.[345] A specific polymorphism within *SLC24A5*, the non-synonymous variant Ala111Thr, shows extreme differences in frequency between populations of African and European ancestry and the threonine allele has been associated with the evolution of lighter skin in Europeans.[343, 344, 346] The remaining genes that have been demonstrated to influence human skin, hair and eye colour include *KITLG*, *IRF4*, *SLC24A4* and *TPCN2*.[328]

2.2.2 Other factors that influence central corneal thickness

If there is a genuine correlation between pigmentation and CCT, it is likely that there will be genetic factors common to the determination of both traits. As previously discussed, there is a strong genetic contribution to both pigmentation and CCT. However, whilst UV radiation has been definitively shown to influence skin pigmentation, the impact of environmental factors on CCT is difficult to ascertain. Both Alsbirk *et al* and Vijaya *et al* have demonstrated that individuals from rural communities have lower CCT measurements than those from urban communities

within the same geographical area.[213, 214] The authors suggest that outdoor lifestyle and socioeconomic status could potentially explain these differences. Whilst there is no doubt that genetic factors contribute to the differences in CCT observed between ethnic groups, it is unknown what impact environmental factors have on this variation.

The use of animal models, in particular inbred rodent species such as the mouse, provides a powerful tool to examine the role genetic and environmental factors play in CCT variation. Foremost, the ability to utilise inbred mouse strains offers immense genetic power.[347] Mice within an inbred strain are genetically homogenous and their phenotypes can be treated as replicate samples, thus enabling better estimates of genetic effects when mice from different strains are raised in a common environment. The ability to control environmental conditions is another advantage of using animal models, as it helps to eliminate any phenotypic variability that may arise due to different environmental exposures. In regards to this study, the use of a mouse model also allows CCT to be measured with the same instrument and operator for the entire protocol. This significantly reduces the variability that is evident in human studies when different instruments and operators are used.

2.3 METHODS

2.3.1 Ethics statement

Ethics approval for the research conducted on human participants was obtained from the human research ethics committees of the following institutions (cohort in parentheses): Flinders University and the Southern Adelaide Health Service (OCA); Westmead Millennium Institute at the University of Sydney (Blue Mountains Eye

Study); Mbarara University of Science and Technology (Ugandan). Ethics approvals for work conducted on the mice used in this study were granted by the Animal Welfare Committee of Flinders University. This research adhered to the tenets of the Declaration of Helsinki and informed consent was obtained from all participants.

2.3.2 Participant recruitment

2.3.2.1 Blue Mountains Eye Study

The Blue Mountains Eye Study (BMES) is a population-based survey of vision and common eye diseases in the Blue Mountains region, west of Sydney, Australia. The 956 participants recruited for this study were predominately Caucasian and the population and full recruitment methodology has been described in detail previously.[348] Recruitment age ranged from 60 to 95 years. As part of the ocular examination, CCT was measured using contact ultrasound pachymetry with prior topical anaesthetic drops (either 0.4% oxybuprocaine or 0.5% proxymetacaine) administered to both eyes 1 minute before measurement. An average of twenty-five consecutive measurements were recorded in each eye, such that each recording had a standard deviation < 5μm. An individual's CCT was calculated as mean of both eye measurements. A detailed ocular history and ocular examination was performed on all participants and people who had anterior segment disease or previous refractive surgery were excluded from the study. There were 62 (6.5%) confirmed cases of OAG within the 956 BMES samples.

2.3.2.2 Oculocutaneous albinism cohort

Recruitment of patients with OCA was undertaken by Associate Professor Jamie Craig, Dr. Alex Hewitt and Dr. Sue Abhary during the National Albinism Fellowship

Conference held in 2008 in Adelaide, Australia. The cohort included a total of 22 patients with OCA, with 15 confirmed cases of OCA 1A, one case of OCA 1B, whilst the clinical diagnosis was inconclusive on the remaining subjects. All OCA patients were of Australian-Caucasian descent. Recruitment age ranged from 5 to 65 years. CCT was measured with a contact ultrasound pachymeter (Pachmate DGH55, DGH-KOI, Inc., PA, USA) or by using non-contact slit-lamp mounted optical low-coherence reflectometry (OLCR) (Haag-Streit, Switzerland). Topical anaesthesia was administered as described earlier. An average of 25 consecutive measurements were recorded in each eye, such that each recording had a standard deviation < 5µm. An individual's CCT was calculated as mean of both eye measurements. Ultrasound and OLCR have been shown to have good correlation.[232, 349] A detailed ocular history and ocular examination was performed on all participants and people who had anterior segment disease or previous refractive surgery were excluded from the study.

2.3.2.3 Ugandan cohort

A total of 297 Ugandan participants were recruited from the Ruharo Eye Centre located in the Mbarara Municipality, Uganda. Recruitment age ranged from 5 to 90 years. CCT was measured using a Pachmate DGH55 ultrasound pachymeter. Topical anaesthesia was administered as described earlier. An average of 25 consecutive measurements were recorded in each eye, such that each recording had a standard deviation < 5µm. An individuals CCT was calculated as the mean of both eye measurements. A detailed ocular history and ocular examination was performed on all subjects and people who had anterior segment disease or previous refractive surgery were excluded from the study. The following personnel were involved in the recruitment of the Ugandan participants: Dr. Kenneth Kagame; Dr. Sam Ruvama;

Dr. Ludovica Tindyebwa; Dr. Alex Hewitt; Professor Paul Mitchell; Associate Professor Jamie Craig.

2.3.3 Study design

2.3.3.1 Analysis of central corneal thickness data from human populations

The human studies involved two separate analyses. Further examination of the relationship between CCT and skin pigmentation was carried out by assessing CCT in a group of individuals with OCA and a cohort from Uganda. The rationale for the inclusion of these two groups was that they possess distinct skin pigmentation phenotypes and their involvement in the study would add further data to test the hypothesis. A meta-analysis of published CCT measurements taken from different ethnic groups was also undertaken. The meta-analysis involved collating data from different populations with the aim of calculating a mean CCT value for a range of ethnic groups from across the globe. Given the diverse range of skin colour phenotypes amongst different ethnic groups, the meta-analysis will allow for a comprehensive assessment of whether skin pigmentation and CCT are correlated in humans.

2.3.3.2 Measurement of central corneal thickness in a mouse model

In order to verify the observations from humans and to determine what impact genetic, environmental and pigmentation factors have on CCT, measurement of CCT in a range of inbred mouse strains was performed. The initial investigation involved determining if inter-strain variation in CCT is evident in a mouse model, which was achieved by measuring CCT in 13 different inbred strains. There was a variety of coat colours amongst the 13 different strains with seven albino, two black, two agouti

and two dilute brown strains. This permitted a direct examination of whether the pigmentation phenotype is correlated with CCT. Finally, to directly test the impact of pigment in CCT determination and to potentially identify candidate genes, measurements were taken from mouse strains with mutations in the pigment genes *Tyr*, *Oca2* and *Slc45a2*.

2.3.4 Protocols for human studies

2.3.4.1 Statistical analysis for comparison of cohorts

All statistical analyses were conducted using SPSS v18.0. Differences in age and sex distribution between the BMES, OCA and Ugandan cohorts were assessed using the one-way ANOVA and chi-square procedures respectively. A two-way analysis of covariance (ANCOVA) was used to assess if significant differences in mean CCT were evident between the BMES, OCA and Ugandan cohorts. The two-way ANCOVA procedure allows for control of covariates such as age and sex. Statistical significance was accepted as $p < 0.05$.

2.3.4.2 Meta-analysis

A systematic literature search was performed to identify all published studies that investigated CCT in human populations. The PubMed database (National Center for Biotechnology Information; NCBI) was explored in August 2010 by using the following keyword string: 'central corneal thickness'. A total of 1,956 articles were identified in the PubMed database. Only articles in English were reviewed. Several criteria had to be met for an article to be included in the meta-analysis. To ensure consistency of data, CCT had to be measured by ultrasound pachymetry, as variation in CCT measurements has been demonstrated between different instruments.[11, 13, 231]

As there is evidence to suggest that CCT decreases slightly with age,[17-20] only studies involving adult populations (mean age or recruitment > 18 years) were included. The study group had to comprise individuals with normal, healthy corneas and be predominately made up of normal eyes, although cohorts that contained a proportion of glaucomatous or ocular hypertensive eyes at normal population rates were permitted. An implicit statement regarding the ethnicity of the population being investigated had to be included in the article and the study group had to be ethnically homogeneous. Reporting of all necessary data such as cohort size, mean CCT values and variance was also required. No limit was applied with regards to publication date of the study. Fifty-three studies, including the Caucasian and Ugandan data from this study, qualified for inclusion in the meta-analysis. A flow chart of the study selection process, including the number of papers excluded at each phase, can be seen in Figure 2.3.

Studies that met the inclusion criteria stated above are shown in Table 2.1. The BMES and Ugandan data from this study were also included in the meta-analysis. Each study population was assigned to an ethnic group based on the reported ethnicity and geographical location of the recruitment. Geographical regions were based on definitions used by the United Nations Population Division (http://www.un.org/esa/population/). African and Caucasian ethnic groups that were recruited outside of Africa and Europe, respectively, were designated ‘African Migrant’ and ‘Caucasian Migrant’.

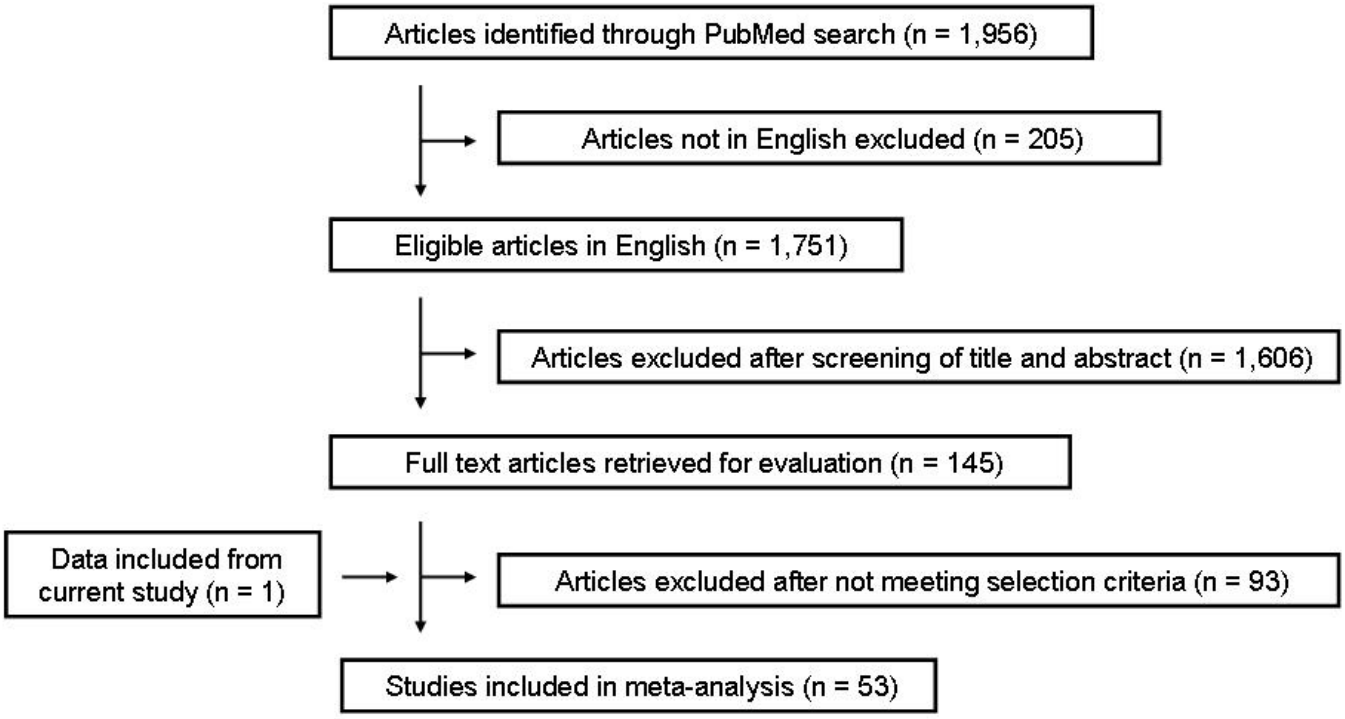

Figure 2.3: Flow chart of articles accepted and rejected during the selection process.

Table 2.1: Studies included in meta-analysis of human CCT measurements

Ethnic Group	Country of Study	Number of Participants	Mean CCT ± SD (µm)	Glaucoma Included	Reference
Australian Aboriginal	Australia	189	514.9 ± 30.5	No	Durkin *et al* [241]
Australian Aboriginal	Australia	91	509 ± 33.5	No	Landers *et al* [22]
African Migrant	Barbados	1064	529.8 ± 37.7	Yes	Nemesure *et al* [17]
African Migrant	Canada	32	529.7 ± 30**	No	Dohadwala *et al* [238]
African Migrant	Israel	121	518.9 ± 31.5	No	Lifshitz *et al* [242]
African Migrant	Puerto Rico	98	542 ± 32	Yes	Graeber *et al* [350]
African Migrant	USA	26	524.8 ± 38.4	No	Aghaian *et al* [19]
African Migrant	USA	26	533.8 ± 33.9	No	La Rosa *et al* [239]
African Migrant	USA	393	533.8 ± 33.7	No	Racette *et al* [298]
African Migrant	USA	18	533 ± 37.8	No	Semes *et al* [351]
African Migrant	USA	58*	535.8 ± 33.4	No	Shimmyo *et al* [24]
African Migrant	USA	33	528.5 ± 33.2	No	Torres *et al* [240]
African Migrant	USA	36	530 ± 34.2	?	Yo *et al* [352]
African Native	Cameroon	485	528.7 ± 35.9	No	Eballe *et al* [353]
African Native	Ethiopia	300	518.7 ± 32.9	No	Gelaw *et al* [354]
African Native	Ghana	155	525.3 ± 33.5	?	Kim *et al* [355]
African Native	Nigeria	49	551.6 ± 44.5	No	Iyamu *et al* [356]
African Native	Nigeria	34	535 ± 38	No	Mercieca *et al* [357]
African Native	Uganda	297	517.3 ± 37	?	This Study
Caucasian European	Austria	30	552 ± 31.7	?	Lackner *et al* [11]
Caucasian European	Croatia (Korcula)	849	555.6 ± 36	?	Vitart *et al* [358]
Caucasian European	Croatia (Split)	349	561 ± 36.3	?	Vitart *et al* [359]
Caucasian European	Croatia (Vis)	596	561.2 ± 34.6	?	Vitart *et al* [358]
Caucasian European	Greece	57	547.4 ± 33.1	No	Kitsos *et al* [360]
Caucasian European	Hungary	20	559 ± 30.7	No	Schneider *et al* [361]

* Study originally quoted total number of eyes measured.

** Standard deviation calculated from standard error.

Table 2.1: ***continued***

Ethnic Group	Country of Study	Number of Participants	Mean CCT ± SD (µm)	Glaucoma Included	Reference
Caucasian European	Netherlands	352	537.4 ± 33.8**	No	Wolfs *et al* [109]
Caucasian European	Scotland	475	536 ± 33.4	?	Vitart *et al* [359]
Caucasian European	Spain	100	557.5 ± 15	?	Sanchis-Gimeno *et al* [362]
Caucasian European	Switzerland	18	552 ± 35	No	Copt *et al* [222]
Caucasian European	England	983	544.1 ± 36.5	No	Hawker *et al* [284]
Caucasian European	England	1759	545.8 ± 34	Yes	Lu *et al* [363]
Caucasian Migrant	Australia	115	544.7 ± 31.9	No	Durkin *et al* [241]
Caucasian Migrant	Australia	84	542 ± 32	No	Landers *et al* [22]
Caucasian Migrant	Australia	1714	544.3 ± 35	?	Lu *et al* [363]
Caucasian Migrant	Australia	956	539.7 ± 32.8	Yes	This Study
Caucasian Migrant	Barbados	25	545.2 ± 45.7	Yes	Nemesure *et al* [17]
Caucasian Migrant	Canada	227	552.5 ± 34.7**	No	Dohadwala *et al* [238]
Caucasian Migrant	Puerto Rico	361	542 ± 32	Yes	Graeber *et al* [350]
Caucasian Migrant	USA	36	562.8 ± 31.1	No	Aghaian *et al* [19]
Caucasian Migrant	USA	51	555.9 ± 33.2	No	La Rosa *et al* [239]
Caucasian Migrant	USA	101	554 ± 34	?	Phillips *et al* [364]
Caucasian Migrant	USA	367	551.9 ± 36.8	No	Racette *et al* [298]
Caucasian Migrant	USA	38	562 ± 31	No	Realini *et al* [365]
Caucasian Migrant	USA	48	556.1 ± 38.8	No	Semes *et al* [351]
Caucasian Migrant	USA	733*	552.6 ± 34.5	No	Shimmyo *et al* [24]
Caucasian Migrant	USA	46	551.9 ± 28.3	No	Torres *et al* [240]
Caucasian Migrant	USA	138	545 ± 33.9	?	Yo *et al* [352]
East Asian	China	1669	548.6 ± 34.3	No	Li *et al* [366]
East Asian	Hong Kong	151	575 ± 32	No	Cho *et al* [367]
East Asian	Hong Kong	240	551.7 ± 30.6	No	Lam *et al* [368]
East Asian	Hong Kong	125	560.3 ± 22.7	No	Lam *et al* [369]

* Study originally quoted total number of eyes measured.

** Standard deviation calculated from standard error.

Table 2.1: *continued*

Ethnic Group	Country of Study	Number of Participants	Mean CCT ± SD (μm)	Glaucoma Included	Reference
East Asian	Hong Kong	50	543 ± 33	No	Leung *et al* [230]
East Asian	Hong Kong	39	555.1 ± 35.3	No	Wong *et al* [229]
East Asian	Japan	50	552 ± 36	No	Wu *et al* [237]
East Asian	Korea	205	535.8 ± 36	No	Kim *et al* [370]
East Asian	Korea	224	553.6 ± 39.6	No	Lee *et al* [371]
East Asian	Taiwan	500	554 ± 29	No	Chen *et al* [372]
East Asian	Taiwan	56	567 ± 43	No	Ko *et al* [373]
East Asian (Chinese)	USA	41	569.5 ± 31.8	No	Aghaian *et al* [19]
East Asian (Japanese)	USA	38	538.5 ± 29.6	No	Aghaian *et al* [19]
East Asian (Japanese)	USA	136	554.8 ± 38.8	No	Pekmezci *et al* [374]
Hispanic	USA	27	563.6 ± 29.1	No	Aghaian *et al* [19]
Hispanic	USA	104	541.8 ± 34.5	No	Erickson *et al* [375]
Hispanic	USA	1699	546.9 ± 33.5	Yes	Hahn *et al* [18]
Hispanic	USA	102*	551.1 ± 35.5	No	Shimmyo *et al* [24]
Hispanic	USA	139	542 ± 34.6	?	Yo *et al* [352]
South Asian	India	2532	520.7 ± 33.4	No	Vijaya *et al* [214]
South Asian	India	532	532.2 ± 34	No	Kohli *et al* [376]
South Asian	India	615	519.9 ± 33.4	?	Kunert *et al* [377]
South Asian	India	46	541.8 ± 30.6	No	Ladi *et al* [378]
South Asian	India	4612	514 ± 33	?	Nangia *et al* [299]
South Asian	Pakistan	100	531.1 ± 33.4	No	Channa *et al* [379]
South East Asian	Burma	1909	521.9 ± 33.3	No	Casson *et al* [27]
South East Asian	Thailand	50	554.4 ± 27.5	?	Chaidaroon *et al* [380]
South East Asian	Thailand	467	535.2 ± 29.9	?	Lekskul *et al* [21]
South East Asian (Filipino)	USA	33	559 ± 24.9	No	Aghaian *et al* [19]

* Study originally quoted total number of eyes measured.

Each ethnic group was assigned to the 'Light Skin' or 'Dark Skin' cohorts based on the map of native skin colour distributions compiled by Biasutti in 1941 (Figure 2.4).[381] The data in this map are based on the 36-tone chromatic scale devised by Austrian anthropologist Felix von Luschan to assess the unexposed skin of human populations. In general, pinkish-white skin corresponds to 1-12 on the scale; white 12-14; white-light brown 15-17; light brown 18-23; brown 24-26; dark brown 27 or above. It was decided that the 'Light Skin' cohort would consist of ethnic groups that had a skin tone between 1-17 on the von Luschan scale and the 'Dark Skin' cohort would consist of ethnic groups that were 18 or above. Therefore, the groups were assigned as follows: Light Skin; Caucasian European, Caucasian Migrant, East Asian. Dark Skin; Australian Aboriginal, African Native, African Migrant, Hispanic, South Asian, South East Asian. Although the American Hispanic population can be quite heterogeneous in terms of ancestry, a large proportion are descendants of Central and Southern America and thus were designated as having a skin colour of 18 or above.

The calculation of mean CCT and standard deviation values for each ethnic group was performed by compiling data from each study and weighting it according to the number of participants. These data were used in the calculation of mean CCT and standard deviation values for the 'Light Skin' and 'Dark Skin' groups, which was also weighted according to the number of participants. Comparison of the mean CCT values of the 'Light Skin' and 'Dark Skin' groups was undertaken using Student's *t* test in Microsoft Excel 2003 and statistical significance was accepted as $p < 0.05$. As complete data on age and sex were not available from all studies, correction for these variables was not performed.

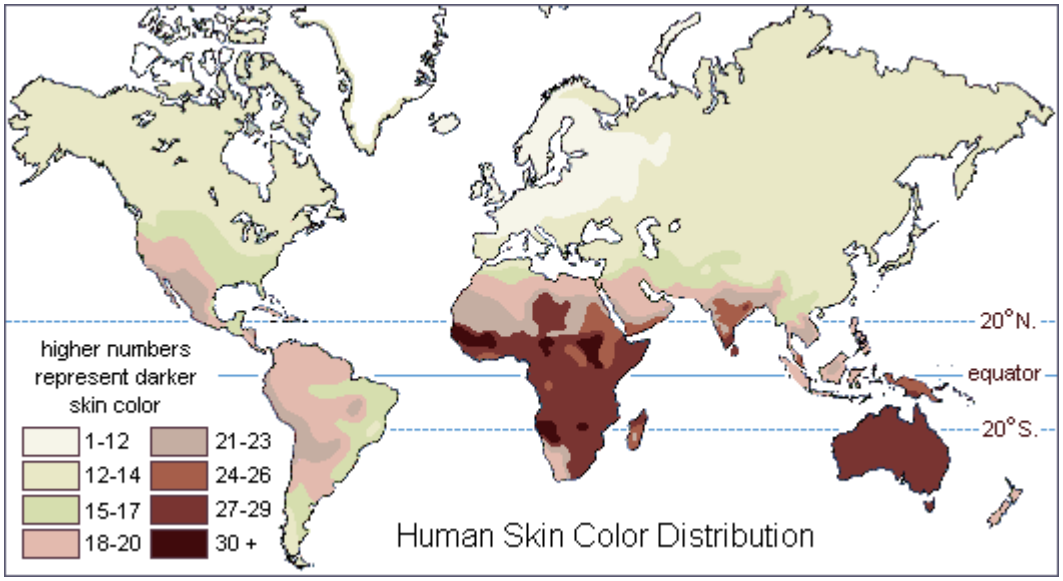

Figure 2.4: Global skin colour distribution of native populations. The colours on the map are based on the 36-tone chromatic scale devised by Austrian anthropologist Felix von Luschan to assess the unexposed skin of human populations. The higher numbers represent darker skin colour. Original data compiled by Biasutti 1941.[381]

2.3.5 Protocols for mouse studies

2.3.5.1 Measurement of central corneal thickness

For all inbred mouse strains, CCT was measured in adult female mice between 6-10 weeks of age as this minimised the potential effect sex and age may have on measurements. Both female and male mice were measured in two of the mutant strains. Mice were weighed then sedated with inhaled isoflurane before being anaesthetised by intraperitoneal injection of 75 mg/kg ketamine and 30 μg/kg metatomidine. Pupils of both eyes were dilated using tropicamide drops. Animals were placed on an improvised support structure mounted on the slit lamp to enable correct height adjustment with the OLCR (Haag-Streit, USA) (Figure 2.5). This method for CCT measurement in animals has been verified previously.[382] Right eye measurements were taken unless there was an existing problem, such as corneal scarring, in which case the left eye was measured. In order to prevent the corneal surface from drying out, a 2 μl drop of saline solution was administered 30 seconds prior to taking the first measurement. Each reading consisted of 10 measurements with the highest and lowest measurements excluded. The instrument then presented the mean of 8 measurements with a standard deviation. At least 2 readings with a standard deviation of less than 2 μm taken within 3 minutes of the administration of the saline were required for inclusion. An overall mean measure was then calculated for each animal. In order to reduce the potential for day-to-day variation in readings, all mutant animals were measured with their appropriate control strains on the same day.

A

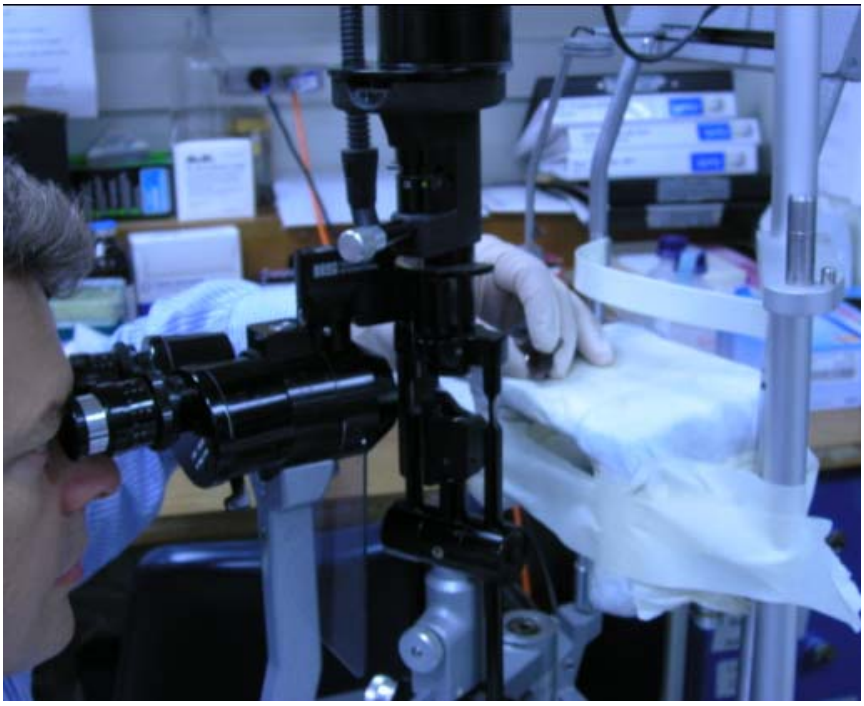

B

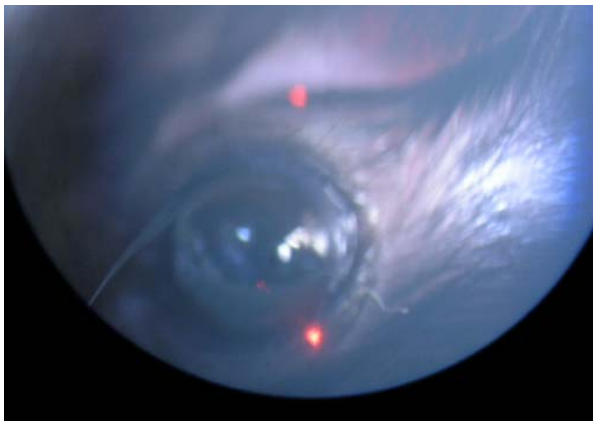

Figure 2.5: Measurement of CCT in the mouse using the OLCR. (A) The OLCR is mounted on a slit-lamp, which also houses a make-shift platform to position the mouse at the correct height for measurement. **(B)** Close-up image of the mouse eye taken through the eyepiece of the slit lamp. The red light from the laser of the OLCR can be seen in the photo.

2.3.5.2 Mouse strains

Inbred mouse strains for this study were obtained from the following institutes: Adelaide University, Adelaide, Australia (AU); Animal Resource Centre, Perth, Australia (PARC); Canberra Hospital, Canberra, Australia (CH); Gilles Plains Animal Resource Centre, Adelaide, Australia (GPARC); The Jackson Laboratory, Bar Harbor, USA (JAX); Walter and Eliza Hall Institute, Melbourne, Australia (WEHI). The following strains of mice were included in this study (source of strain in parentheses): 129X1/SvJ (WEHI); A/J (JAX); AKR (PARC); BALB/c (GPARC); C3H/HeJ (JAX); CBA/CaH (AU); C57B1/KALWRIJ (PARC); C57BL/6J (JAX); DBA/1J (JAX); DBA/2J (JAX); FVB/NJ (PARC); NOD/ Lt (CH); SJL/J (PARC). All animals were on the same diet and housed under identical conditions that included a room temperature of 21ºC, 50% humidity and a 12/12 hour light/dark cycle in the Flinders Medical Centre Animal House. The 13 strains were classified as either pigmented or albino as follows: Albino; 129X1/SvJ, A/J, AKR, BALB/c, FVB/NJ, NOD/Lt, SJL/J. Pigmented; C3H/HeJ, CBA/CaH, C57B1/KALWRIJ, C57BL/6J, DBA/1J, DBA/2J. The genotype of each strain (excluding C57B1/KALWRIJ, as no genotype information was available) at five known mouse coat colour genes was determined from information in the mouse genome database (http://www.jax.org/). The five genes selected were the mouse homologue of *ASIP* known as nonagouti (*a*), myosin VA (*Myo5a*), *Oca2* (also known as the *p* gene), tyrosinase (*Tyr*) and tyrosinase-related protein (*Tyrp1*). The genotype of each mouse strain at each gene is given in Table 2.2. All the mutations investigated are recessive and the observed phenotype is dependent on the combination with other alleles. In general each mutation results in the following pigment phenotypes; *a* - black coat, A^w - light-bellied agouti[383]; $Myo5a^d$ - dilution of hair pigmentation[384]; *Oca2* - reduction in coat and eye pigmentation[332]; Tyr^c - albino[385]; $Tyrp1^b$ - brown coat.[386]

Table 2.2: Genotype of each mouse strain for five pigment-associated genes

		Allele at coat colour loci				
Strain	**Coat Colour**	***a***	***Myo5a***	***Oca2***	***Tyr***	***Tyrp1***
129X1/SvJ	Albino	A^w	+	$Oca2^P$	Tyr^c	+
A/J	Albino	a	+	+	Tyr^c	$Tyrp1^b$
AKR	Albino	a	+	+	Tyr^c	+
BALB/c	Albino	+	+	+	Tyr^c	$Tyrp1^b$
C3H/HeJ	Agouti	+	+	+	+	+
CBA/CaH	Agouti	+	+	+	+	+
C57BL/6J	Black	a	+	+	+	+
DBA/1J	Dilute Brown	a	$Myo5a^d$	+	+	$Tyrp1^b$
DBA/2J	Dilute Brown	a	$Myo5a^d$	+	+	$Tyrp1^b$
FVB/NJ	Albino	+	+	+	Tyr^c	+
NOD/Lt	Albino	+	+	NA	Tyr^c	+
SJL/J	Albino	+	+	$Oca2^P$	Tyr^c	+

For each gene, the wild-type allele is designated by the '+' symbol. The 'A^w' allele of the *a* gene carried by the 129X1/SvJ strain is a distinct variant that has been classified as wild-type for this study. No genotype information was available for the C57BL/KALWRIJ strain. NA indicates an unavailable genotype.

Three strains with spontaneous mutations in the known pigment genes *Tyr*, *Oca2* and *Slc45a2* were also assessed. The strains were as follows; *Tyr*, B6(Cg)-*Tyr*$^{c-2J}$/J; *Oca2*, C3H/HeJ-*Oca2*$^{p-J}$/J; *Slc45a2*, C57BL/6J-Slc45a2uw/J. All were obtained from the Jackson Laboratory (Bar Harbor, ME, USA). In order to simplify the names for the remainder of the chapter, the *Tyr* mutant will be designated B6.Tyr, the *Oca2* mutant will be C3H/p and the *Slc45a2* mutant will be C57/Slc45a2. Both the B6.Tyr and C57/Slc45a2 strains carry the mutation on a C57BL/6J background whilst the C3H/p strain is on a C3H/HeJ background. The B6.Tyr mice carry a single base mutation in *Tyr* that causes an almost complete absence of the protein when in the homozygous state, resulting in an albino phenotype with no pigment in the skin, eyes or coat. The C3H/p mice carry a partial deletion of the *Oca2* gene that ablates the protein function and homozygous carriers exhibit a diluted agouti appearance with pink eyes. The C57/Slc45a2 mice carry a 7 bp deletion in exon 3 of *Slc45a2*, with the resultant protein lacking the C terminal 6 transmembrane domains. Mice homozygous for this mutation exhibit abnormal eye and coat pigmentation with very white underfur. All genotypic and phenotypic information for these strains was obtained from the Jackson Laboratory website (http://www.jax.org/index.html). CCT was measured in both male and female mice from the B6.Tyr and C57/Slc45a2 strains, whilst only female mice were measured in the C3H/p strain. For the B6.Tyr, C3H/p and C57/Slc45a2 strains, measurement of CCT was only undertaken in the homozygous mutants, which were all phenotypically discernable from the heterozygotes due to their altered pigmentation state.

2.3.5.3 Statistical analysis

All statistical analyses were conducted using SPSS v18.0. Correlation between weight, age and CCT was assessed using the Pearson correlation coefficient. General strain differences were tested using a Kruskal-Wallis test. The mean CCT of pigmented animals was compared to that of albino animals using a Mann-Whitney U test and the CCT of mutant strains compared to that of wild-type controls. Mutant strains were only compared to wild-type animals that were measured on the same day. Statistical significance was defined as $p < 0.05$.

2.4 RESULTS

2.4.1 Measurement of central corneal thickness in human cohorts and meta-analysis to assess influence of skin pigmentation

Data from the BMES, OCA and Ugandan cohorts are shown in Table 2.3. There was a 46 μm (8.2%) difference in mean CCT between the thickest (OCA) and thinnest (Ugandan) groups. After adjusting for age and gender, there was a significant difference in the mean CCT between each of the three cohorts ($p < 0.001$). Results from the meta-analysis of human CCT are shown in Table 2.4 (also see Figure 2.6A). In all, 53 studies were included in the meta-analysis with data from 76 different ethnic groups. Across all ethnic groups there was a broad range of measurements, with a 38.4 μm (6.9%) difference in mean CCT between the thinnest (Australian Aboriginals) and thickest (East Asian) groups. Following segregation of the ethnic groups into two cohorts based on skin pigmentation, the mean CCT measurements were as follows: Light Skin = 548.4 ± 34.1 (n = 14,152); Dark Skin = 524.6 ± 33.6 μm (n = 16,472) ($p < 0.001$) (Figure 2.6B).

Table 2.3: Characteristics of human cohorts

	BMES	**OCA**	**Ugandan**	***p* value**
N	956	22	297	
Mean Age (years)	73.8	35.4	40.8	< **0.001**
Gender (% Female)	59.9	72.7	46.5	< **0.001**
Mean CCT ± SD (μm)	539.7 ± 32.8	563.3 ± 37.2	517.3 ± 37	< **0.001**

Age, gender and mean CCT were compared in each cohort using a chi-square or one-way ANOVA procedure, with the *p* value shown. Values in bold were considered significant at the $p < 0.05$ threshold. N = number of participants; SD = standard deviation.

Table 2.4: Mean CCT for each ethnic group assessed in meta-analysis

Ethnicity	Number of Studies	Number of Participants	Mean CCT ± SD (µm)
Australian Aboriginal	2	280	513 ± 31.5
South Asian	6	8437	517.9 ± 33.2
Native African	6	1320	524.5 ± 35.6
South East Asian	4	2459	525.6 ± 32.4
African Migrant	11	1905	530.8 ± 35.8
Caucasian Migrant	16	5040	546.2 ± 34.2
Hispanic	5	2071	546.7 ± 33.7
European Caucasian	9	5588	548.6 ± 34.5
East Asian	13	3524	551.4 ± 33.5

The cumulative number of studies and total number of participants from these studies in each ethnic group is given. A mean CCT and standard deviation (SD) was calculated for each ethnic group with each study weighted according to size.

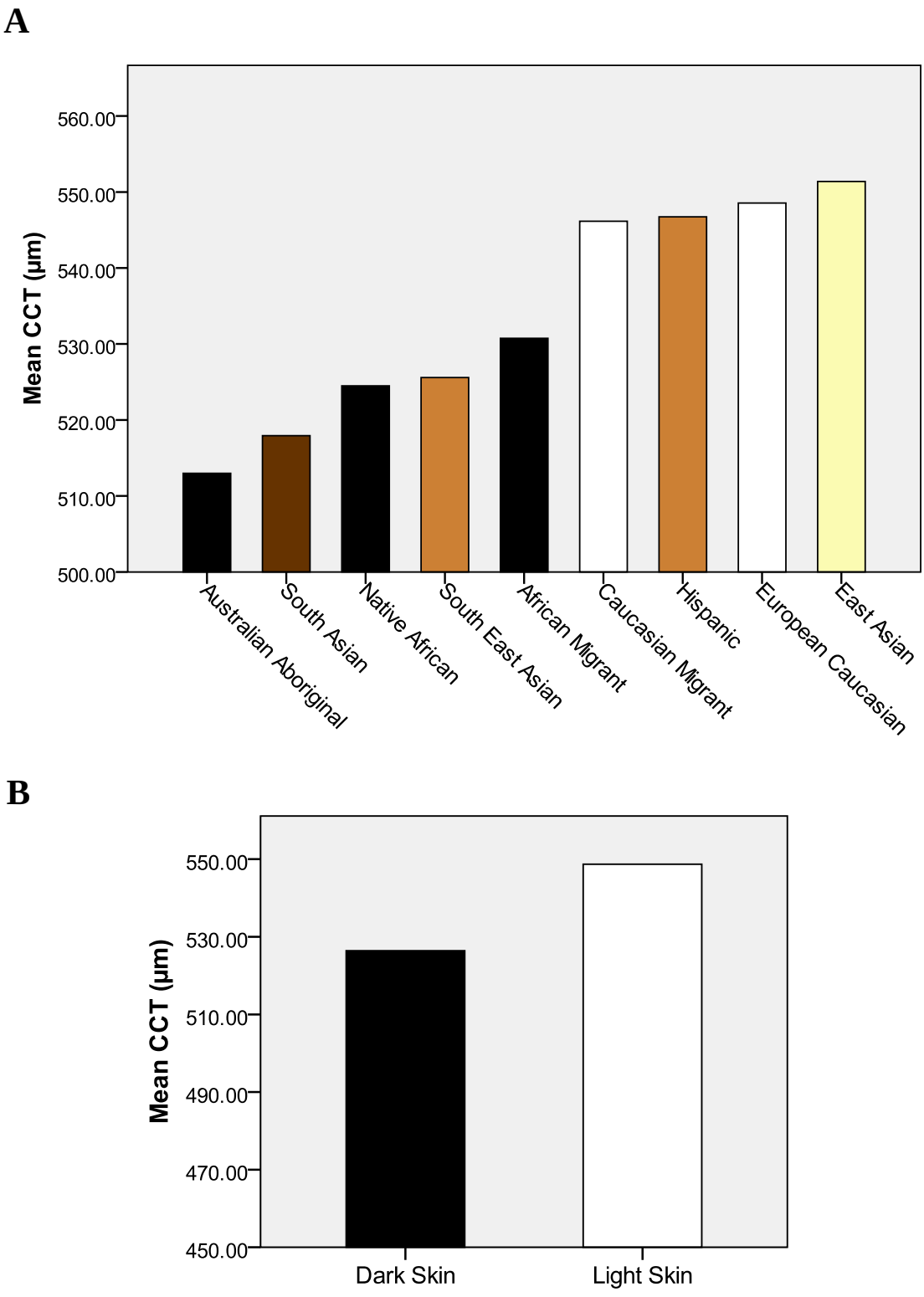

Figure 2.6: Graphical representation of the human CCT meta-analysis results.

(see next page for legend)

Figure 2.6: Graphical representation of the human CCT meta-analysis results. **(A)** Mean CCT of each ethnic group. Colours indicate tone of skin pigmentation according to the chart devised by Biasutti, 1941 (see Figure 2.4). **(B)** Mean CCT of the Dark Skin (524.6 ± 33.6 μm, n = 16,472) and Light Skin (548.4 ± 34.1 μm, n = 14,152) groups, which was based on the skin colour of the ethnic groups shown in Figure 2.6A. There was a significant difference between the groups ($p < 0.001$).

2.4.2 Measurement of central corneal thickness in the mouse

2.4.2.1 Results from inbred mouse strains and analysis based on coat colour

Mean CCT readings from the 13 inbred mouse strains are given in Table 2.5 (also see Figure 2.7A). There was a broad range of measurements, with a 24.9 μm (26.1%) difference in mean CCT between the thinnest (DBA/1J) and thickest (AKR) strains. There was a significant difference between the CCT measurements across all strains ($p < 0.001$). There was no correlation between weight ($p = 0.297$) or age ($p = 0.426$) of the mice and CCT. Following segregation of the mice into two groups based on coat pigmentation, the mean CCT measurements were as follows: Albino = 83.5 ± 11.1 μm (n = 79); Pigmented = 78.3 ± 8.8 μm (n = 53) ($p = 0.008$) (Figure 2.7B). Data were also analysed based on the genotype status of five pigment associated mouse genes; *a*, *Tyrp1, Oca2*, *Tyr* and *Myo5a.* Mice were divided into groups based on whether they were mutant or wild-type at the particular locus and then assessed for any differences in mean CCT (Table 2.6). Significant differences were seen between mice carrying the wild-type and mutant alleles of *a*, *Tyrp1, Tyr* and *Myo5a.* There was no significant difference in CCT in mice carrying the wild-type and mutant alleles of *Oca2*.

2.4.2.2 Results from mutant mouse strains

Further analysis of the association between coat pigmentation and CCT was undertaken by comparing the B6.Tyr, C3H/p and C57/Slc45a2 mutant strains to their appropriate control animals to determine if the specific pigment gene has an effect on CCT. The following mean CCT values were observed: B6.Tyr = 77.9 ± 4.9 μm (n = 19); C57/Slc45a2 = 68.8 ± 8.9 μm (n = 11); C3H/p = 88.7 + 4.2 μm (n = 10). Both the B6.Tyr ($p = 0.013$) (Figure 2.8A) and C57/Slc45a2 ($p < 0.001$) (Figure 2.8B)

Table 2.5: Coat colour and mean CCT of each inbred mouse strain

Strain	Coat Colour	Number	Mean CCT ± SD (μm)
DBA/1J	Dilute Brown	6	70.6 ± 6.9
DBA/2J	Dilute Brown	5	71.1 ± 2.6
C57B1/KALWRIJ	Black	5	73.6 ± 4.6
A/J	Albino	28	74.4 ± 5.8
CBA/CaH	Agouti	6	79.3 ± 7.4
C3H/HeJ	Agouti	12	79.9 ± 12.3
C57BL/6J	Black	19	82.8 ± 5.6
SJL/J	Albino	5	86.8 ± 24.2
FVB/NJ	Albino	6	87.4 ± 13.9
BALB/c	Albino	24	87.6 ± 6.3
NOD/Lt	Albino	6	87.9 ± 6.6
129X1/SvJ	Albino	4	88.6 ± 6.1
AKR	Albino	6	95.5 ± 4.6

SD = standard deviation.

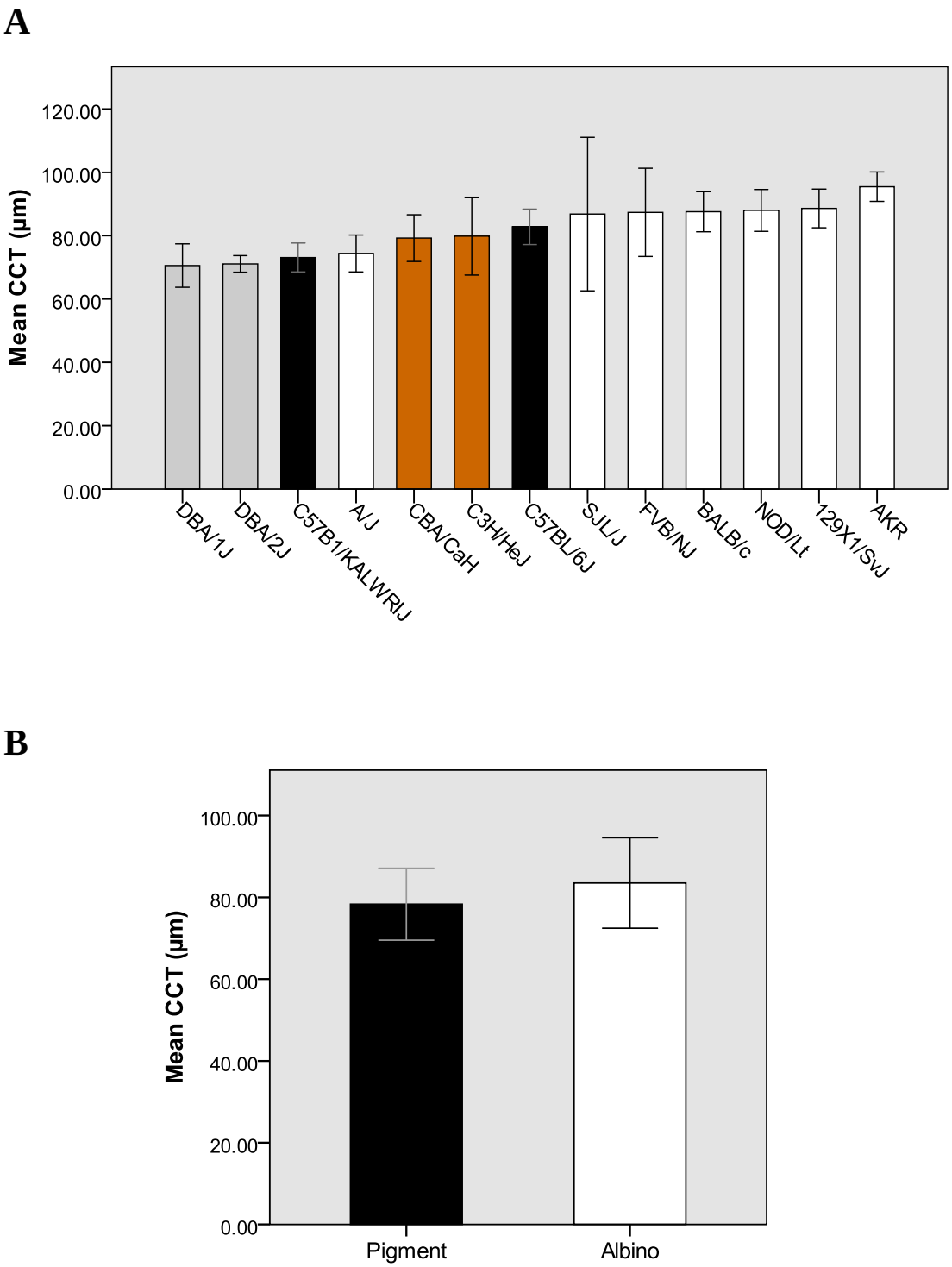

Figure 2.7: Graphical representation of CCT measurements conducted on the 13 inbred mouse strains assessed in this study. (see next page for legend)

Figure 2.7: Graphical representation of CCT measurements conducted on the 13 inbred mouse strains. (A) Mean CCT and coat colour of each individual strain. There was a significant difference in mean CCT of each strain ($p < 0.001$). The colours of the bars represent the coat pigmentation of the animals. Error bars indicate standard deviation. **(B)** Mean CCT of the pigmented (n = 53 animals) and albino (n = 79 animals) groups based on the coat colour of the animals in Figure 2.7A. Error bars indicate standard deviation. There was a significant difference between the groups ($p = 0.008$).

Table 2.6: Mean CCT values for each genotype of the five pigment associated genes

Gene	Wild-type Number	Wild-type Mean CCT ± SD (µm)	Mutant Number	Mutant Mean CCT ± SD (µm)	*p* value
a	63	85.3 ± 10.9	64	78.2 ± 9.0	**< 0.001**
Myo5a	116	82.8 ± 10.3	11	70.8 ± 5.1	**< 0.001**
Oca2	112	81.0 ± 9.8	9	87.6 ± 17.6	0.121
Tyr	48	78.9 ± 9.0	79	83.5 ± 11.1	**0.025**
Tyrp1	64	84.7 ± 11.0	63	78.8 ± 9.2	0.078

The number of animals and mean CCT for each genotype of the five pigment-associated genes is shown in the table. A Mann-Whitney U test was used to compare the CCT values of the wild-type and mutant animals, with the *p* values shown. Values in bold were considered significant at the $p < 0.05$ level. SD = standard deviation.

strains had significantly different mean CCT values from the C57BL/6J (82.8 ± 5.6 μm) control. The mean CCT of the C3H/p strain was not significantly different from its C3H/HeJ control (79.9 ± 12.3) (p = 0.08) (Figure 2.8C).

2.5 DISCUSSION AND SUMMARY

2.5.1 Association of central corneal thickness with human skin pigmentation

Studies in human populations have consistently demonstrated that ethnicity influences CCT. Furthermore, data from African American, Australian Aboriginal and Indian populations suggest that people with darker skin tend to have thinner CCT measurements than fairer skinned Caucasians.[17, 19, 22, 24, 214, 238, 239, 241, 298, 299] Results from this chapter verify these observations, with the description for the first time of CCT measurements in an OCA and Ugandan cohort and the presentation of findings from the meta-analysis of studies investigating CCT in various ethnic groups. The findings from the Ugandan cohort are in accordance with those of other African and dark skin populations, with a mean CCT that is significantly lower than the Australian-Caucasian cohort. With a mean CCT of 517.3 μm, the Ugandan cohort also had the lowest measurement of any African population included in the meta-analysis (see Table 2.1). Only three studies from the meta-analysis observed a lower CCT than that found in the Ugandans, with two of these from Australian Aboriginal cohorts and the other from an Indian population.[22, 241, 299]

The meta-analysis revealed that Australian Aboriginals have the lowest CCT measurements of any ethnic group, although the smaller number of participants assessed in this population suggests that further studies are required to confirm this

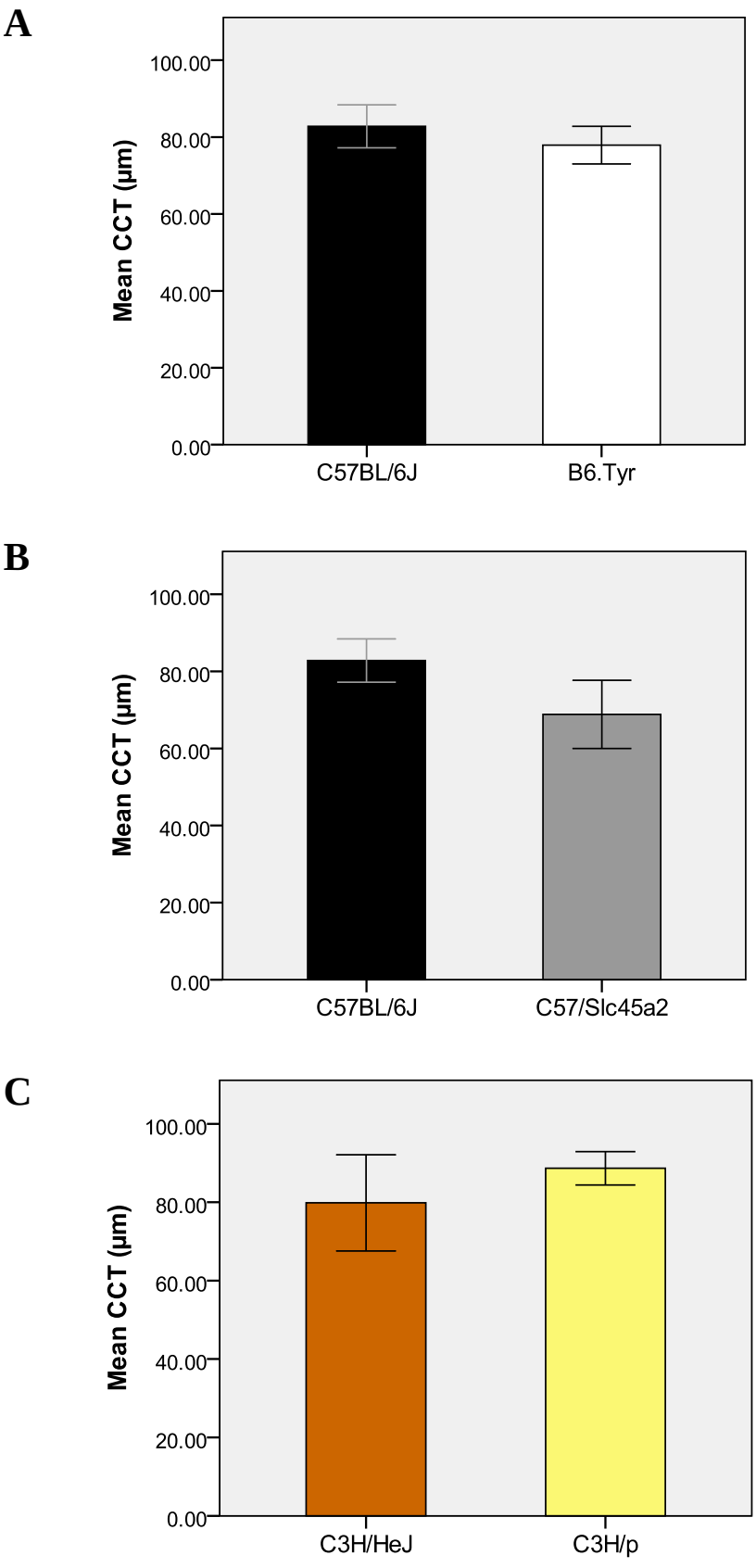

Figure 2.8: Comparison of mean CCT measurements between mutant mouse strains and their relevant controls. (see next page for legend)

Figure 2.8: Comparison of mean CCT measurements between mutant mouse strains and their relevant controls. (A) The B6.Tyr strain (77.9 ± 4.9 μm, n = 19) had a significantly thinner CCT than the C57BL/6J controls (82.8 ± 5.6 μm, n = 19) (p = 0.013). **(B)** The C57/Slc45a2 strain (68.8 ± 8.9 μm, n = 11) had a significantly thinner CCT than the C57BL/6J controls ($p < 0.001$). **(C)** There was no significant difference in the mean CCT of the C3H/p (88.7 + 4.2 μm, n = 10) and C3H/HeJ stains (79.9 ± 12.3 μm, n = 12) (p = 0.08). The colours of the bars represent the coat pigmentation of the animals. Error bars indicate standard deviation.

finding. What is intriguing about this result is that despite the fact Australian Aboriginals have some of the thinnest documented CCT readings of any ethnic group, they also experience very low rates of OAG.[387] Given the correlation between CCT and OAG and the fact that African Americans have thinner than average CCT measurements but a higher risk of OAG,[89, 90] this is a particularly interesting occurrence. Further investigation of this phenomenon in Aboriginal populations could provide insight into the mechanisms of the relationship between CCT and OAG. Along with the Australian Aboriginals, other ethnicities with darker skin pigmentation also had thinner CCT measurements, including the South Asians, African natives, South East Asians and African migrants. Even though groups with lighter skin pigmentation, such as Caucasians and East Asians, had relatively thick CCT values, the Hispanic population showed a thicker CCT than the Caucasian migrant population despite their darker skin tone. However, when all the ethnic groups were segregated into 'Light Skin' and 'Dark Skin' and cohorts, the 'Dark Skin' group had a significantly thinner CCT. This result is in support of the hypothesis that darker skin pigmentation is associated with a thinner CCT.

The data from the OCA patients, who were collectively found to have a significantly thicker CCT than the Australian-Caucasian population, are particularly interesting. OCA is a group of disorders characterised by a congenital hypopigmentation of the skin, hair and eyes. Ocular abnormalities are also a major clinical sign of OCA and include nystagmus, foveal hypoplasia, colour vision impairment, reduced visual acuity and misrouting of the optic nerve fibres.[331] Despite some genetic and phenotypic variability, all forms of OCA present with similar ocular abnormalities. Whilst not a distinct ethnic group, the OCA patients made an interesting comparator.

OCA patients have little or no skin pigmentation and thus sit at the opposite end of the spectrum to African or Australian Aboriginal groups. The CCT measurements in the OCA group are significantly thicker than all races of people with darker skin, including other Caucasians, confirming the pigmentation hypothesis. These data from the OCA cohort may also offer insights into the genetic mechanisms that influence CCT in humans. The majority of patients in this study presented with OCA1, which is caused by mutations in *TYR*.[331, 388] Whilst the exact mutation is unknown in these patients, the results do identify *TYR* as a candidate gene for future studies of CCT genetics.

2.5.2 Analysis of mouse data

2.5.2.1 Strain-dependent variation in central corneal thickness

Measurements from the 13 inbred mouse strains used in this study definitively showed that differences in CCT are evident between strains ($p < 0.001$) and as there was no correlation with weight or age, these were eliminated as potential causes. Given the ability to control for variables such as the type of pachymeter, pachymeter operator and environmental conditions, it is highly likely that the genetic diversity between the strains is responsible for the differences in CCT. These data are consistent with the study conducted by Lively *et al*, which showed a significant difference in CCT across 17 strains of mice.[389] A smaller study conducted by Henriksson *et al* also demonstrated variation in CCT across three inbred mouse strains.[390] Methodological differences make it difficult to compare the measurements across these studies, with Lively *et al* employing ultrasound pachymetry, Henriksson *et al* utilising histology and this study employing OLCR. For example, in this study the mean CCT measurement for BALB/c mice was 87.6 ± 6.3µm, whilst Henriksson

et al found a mean of 134.2 ± 12.9μm for the same strain. Whilst the small size of the mouse eye makes accurate measurement problematic, a previous study has confirmed the validity of using OLCR for this purpose.[382] Further evidence that strain differences in CCT are genetically determined comes from a recent linkage study that identified a quantitative trait locus for CCT on mouse chromosome 7.[391] If the data from mouse studies are extrapolated to humans, then it would suggest that genetic factors play a large role in the CCT variation seen between ethnic groups. The genes responsible however, remain largely unknown, although our data from the pigment analysis may offer some clues.

2.5.2.2 Association of central corneal thickness with mouse coat pigmentation

Upon segregating the mouse strains into either albino or pigmented groups, the albino animals were found to have a significantly thicker CCT. Of the seven albino strains measured, six had greater mean CCT measurements than the C57BL/6J mouse, which was the pigmented strain with the thickest CCT. This result was consistent with the human data and supported the hypothesis that darker skin or coat pigmentation is associated with a thinner CCT. The use of a murine model alleviates many of the problems faced in human studies and can potentially offer a more accurate representation of the influence that pigmentation has on CCT. The experimental design allowed for control of variables that may influence data from human studies, including type of pachymeter, pachymeter operator, sex and age. The impact of environmental factors was also limited, with the mice kept in the same living conditions and on the same diet. The use of inbred mice also reduced any intra-strain variation that could result from genetic differences. If the association between CCT and coat pigmentation is a genuine biological interaction, then it is

plausible that genes involved in pigment biosynthesis are also involved in the development of the cornea. To date, some 368 mouse colour loci have been identified, of which 159 are cloned genes, ensuring there are numerous candidate genes that could be involved in CCT determination.[327]

To identify which genes may be responsible for this variability in CCT, genotype information was obtained for specific mutations within five known mouse pigment genes (http://www.jax.org/). The goal of this analysis was to ascertain if the melanin biosynthesis pathway was potentially linked to CCT determination. The genes investigated were *a*, *Myo5a*, *Oca2*, *Tyr* and *Tyrp1*. Mutations in these genes have varying effects on pigment expression, whilst the combination of alleles is also important to the final phenotype of the mouse. Results indicated that the *a*, $Myo5a^{d}$, Tyr^{c} and $Tyrp1^{b}$ alleles were all significantly associated with a difference in CCT when compared to the wild-type alleles. In particular, the *a*, $Myo5a^{d}$ and $Tyrp1^{b}$ alleles all showed a significant association with a thinner CCT. The potential role of these genes in the determination of CCT however, is unclear. The functions of these proteins have been discussed previously and none appear to have any obvious involvement in corneal development, although this probably reflects the novelty of the association between pigmentation and CCT. It is also unclear as to whether these genes are acting independently or whether there is a combined effect on overall pigmentation levels. Other pigment-related genes in addition to the five investigated in this study may also be contributing to the association with CCT. Further work is needed to verify the relationship between *a*, $Myo5a^{d}$, Tyr^{c} and $Tyrp1^{b}$ and CCT, including measurement in additional mouse strains, expression and functional analysis and potentially, examination of these genes in human cohorts.

2.5.2.3 Measurement of central corneal thickness in mutant mouse strains

In order to directly test specific pigment genes for an association with CCT, mice carrying mutations in *Tyr*, *Oca2* and *Slc45a2* were analysed. As is the case with humans, mutations in these genes can significantly alter the pigmentation phenotype of the mouse. Whilst the function of TYR is well characterised, the role of the OCA2 and SLC45A2 proteins is not well understood. Both the B6.Tyr and C57/Slc45a2 strains had significantly thinner CCT measurements than the control mice, although the magnitude of this difference was greater in the C57/Slc45a2 animals. However, there was no significant difference between the C3H/p strain and its control. This result correlates somewhat with the findings of Semes *et al*, who showed no association between CCT and eye colour in a Caucasian cohort.[351] As polymorphisms in *OCA2* have been demonstrated to influence human eye colour,[341, 392-395] the findings by Semes *et al* suggest this gene may not be involved in CCT determination. As the only difference genetically between the mutant and control strains is the pigment gene mutation and there are common environmental conditions, it is probable that the significant results seen in the B6.Tyr and C57/Slc45a2 animals reveal a direct relationship between CCT and the pigment phenotype of the mouse.

As previously stated, how alterations in the protein function of TYR can impact CCT determination is unclear and the situation is similar for SLC45A2. However, it is plausible that the mutations in *Tyr* and *Slc45a2* are not directly involved with the change in CCT and that alterations in expression of other genes involved in related pathways could be responsible. It is interesting to note that the correlation between a thinner CCT and darker coat pigmentation seen in the comparison of the albino and pigmented mouse strains is opposite to the results obtained for the B6.Tyr and

C57/Slc45a2 mice. The complex nature of the pigmentation process and the myriad of different genes involved could provide a possible explanation for this observation. A similar situation is evident in the human OCA1 patients and B6.Tyr mice, where mutations in the respective *tyrosinase* genes have opposing impacts on CCT. Differences in genetic background and the complexity of the pigmentation process in humans and mice could account for this discrepancy. Further work is needed to verify the association of these genes with CCT, including expression analysis, functional assays and examination of genetic variants in human cohorts. Given that the quantity and type of melanin may be important in determining CCT, experiments designed to assess the melanin profile of specific tissues could be beneficial. This could include studying mice with a variety of pigmentation phenotypes and determining melanin distribution during embryonic development. Further experiments could involve assays that assess what impact melanin has on cultured corneal cells.

2.5.3 Pigmentation and corneal development

The concept that genes associated with pigment regulation are also involved in the development of a transparent tissue such as the cornea is extremely novel. Previous data from human studies have confirmed the presence of melanocytes and their product melanin at the corneo-scleral junction of adult eyes, although the function of a pigmented limbus remains unknown.[396] Similar findings have been found in an avian model, where melanocytes are present in the corneal limbus of day 13 embryos, indicating that expression of pigment genes is evident in the tissue directly adjacent to the developing cornea.[397] Mutations in *TYR, P, TYRP1* and *SLC45A2* are also known to be associated with the significant ocular abnormalities seen in OCA

patients.[331] In addition, a study by Libby *et al* found that *Tyr* modifies ocular development of the iridocorneal angle in mice, leading the authors to hypothesise that DOPA synthesised by TYR may escape melanocytes and act as a signalling molecule.[398] These observations clearly demonstrate that genes associated with pigmentation pathways are intimately involved in the development of ocular structures and this may include the cornea. Given that a healthy adult cornea is transparent, regulation of its growth by pigment- associated genes would suggest that these genes play a more significant role in mammalian development than what is currently understood.

2.5.4 Summary

One of the primary goals of the experiments and analyses described in this chapter was to investigate the hypothesis that mammalian pigmentation is associated with CCT and in particular, whether darker skin and coat pigmentation are associated with CCT measurements. The human data compiled from the OCA and Ugandan cohorts, coupled with the meta-analysis, were consistent with this hypothesis. Importantly, the findings from the mouse model largely supported the human data, although there were some inconsistencies amongst the mutant strains. Another important finding from this chapter was that significant strain differences in CCT are evident in the mouse, which is again consistent with the ethnic variation observed in humans. Given the evidence for a correlation with skin and coat pigmentation, it is plausible that genes involved in pigment pathways are candidate CCT genes. The benefits of characterising these genes lie beyond the mere identification of quantitative trait loci, as they may offer insights into other developmental pathways that are associated with pigmentation.

CHAPTER 3

CANDIDATE GENE STUDY TO INVESTIGATE THE GENETIC DETERMINANTS OF NORMAL CENTRAL CORNEAL THICKNESS VARIATION

Publications arising from this chapter:

David P Dimasi, Kathryn P Burdon, Alex W Hewitt, Ravi Savarirayan, Paul R Healey, Paul Mitchell, David A Mackey, Jamie E Craig. Candidate Gene Study to Investigate the Genetic Determinants of Normal Variation in Central Corneal Thickness. *Mol Vis.* 2010 Mar; 16:562-9.

Dimasi DP, Chen JY, Hewitt AW, Klebe S, Davey R, Stirling J, Thompson E, Forbes R, Tan TY, Savarirayan R, Mackey DA, Healey PR, Mitchell P, Burdon KP, Craig JE. Novel quantitative trait loci for central corneal thickness identified by candidate gene analysis of osteogenesis imperfecta genes. *Hum Genet.* 2010 Jan; 127(1):33-44.

3.1 HYPOTHESIS AND AIMS

Despite evidence indicating that normal CCT variation is governed by a strong genetic component, the genes involved in the determination of this trait have not been identified. However, given its high heritability and the ease and accuracy of measurement, CCT is a model trait for genetics research. This chapter will focus on a candidate gene study that was undertaken with the aim of finding novel genetic determinants of CCT in humans. The hypothesis was that common polymorphisms within the selected genes contribute to normal variation in CCT.

3.2 OVERVIEW

3.2.1 Candidate gene studies

Several methodologies exist for identifying quantitative trait loci, including linkage analysis and association studies. All methodologies offer their own advantages and disadvantages. Linkage analysis relies on studying the inheritance of genetic markers within families, whereas association techniques such as GWA and candidate gene studies involve recruiting individuals from the general population. In regards to candidate gene studies, this recruitment is based on the phenotype of interest and may involve case and control cohorts for a disease study or a normal population cohort for the study of a quantitative trait. The aim of a candidate gene study is to identify markers, generally SNPs, within selected genes that are associated with the disease or trait of interest. These genes are selected for analysis based on the hypothesis that they have a functional involvement in the development of the particular disease or trait. The evidence for selecting genes can come from numerous sources but is often based on the structure or function of the nominated protein and its relationship to the relevant biological pathway.

An extensive knowledge of a biological pathway and its relationship to a specific disease state can provide enough information to select genes for a candidate gene study.[399] The function of specific proteins known to be expressed within the tissue of interest is another means of identifying candidate genes, as are microarray analyses that show differential regulation of genes in relevant tissues and disease states.[400] Candidate genes can also be ascertained through examining phenotypes caused by mutations in model organisms or analysing genes within a previously classified linkage region. Finally, less deleterious variants in genes known to cause extreme phenotypes when mutated can also be used to identify candidate genes. An example of a successful application of this method came with the recent association of the *growth hormone-releasing hormone receptor* gene with normal height variation in humans.[401] Mutations in this gene had been demonstrated to cause isolated growth hormone deficiency, resulting in short stature.

3.2.2 Tag SNPs

Two basic approaches can be used for selecting SNPs to be genotyped in a candidate gene: functional variants or tag SNPs. Functional SNPs have been used extensively as genetic markers for candidate gene studies primarily because they suggest a mechanism for functional change in a protein that could potentially cause disease or alter a trait. Whilst the selection of functional variants is a valid methodology, it does not cover all the genetic variation within a region or gene, thus allowing for the possibility that an unselected or unknown causative variant will be overlooked.[402] A solution to this problem is to employ a tag SNP methodology, which is essentially an indirect approach to finding causal variants that are associated with the disease or trait of interest. The tag SNPs act as genetic markers to detect an association between

a particular genomic region and the disease or trait, whether or not the markers themselves have functional effects (Figure 3.1).

The benefit of the tag SNP approach is that it can detect the majority of variation within a gene by genotyping a minimal number of SNPs.[403-407] The tag SNP methodology takes advantage of the fact that SNPs in close physical proximity to each other tend to be correlated, meaning that the genotype of one SNP reflects the genotype of its correlated SNP. This relationship is described as linkage disequilibrium (LD) and arises from the co-inheritance of alleles within a region of the chromosome (Figure 3.2). As a consequence of LD, there is significant redundancy amongst SNPs found in the same genomic region, a feature that can be exploited for association studies. When individual tag SNPs are used in an analysis, the process is known as pairwise tagging (Figure 3.3A). Another approach is to use haplotypes, which are a combination of any number of alleles on a sequence of chromosome that are inherited together. Whilst pairwise tagging may simplify the design and analysis of a particular study, haplotypes can sometimes identify variation that remains undetected using pairwise tagging (Figure 3.3B).[408, 409]

3.2.3 Selection of central corneal thickness candidate genes

Despite the fact that no genes have been associated with normal CCT variation, there is evidence in the literature that justifies the selection of specific genes as candidates. Based on their structural and functional properties, all the genes selected as candidates in this study met one or more of the following criteria: involvement in corneal structure; function in corneal development pathways; association with a human disease that has abnormal CCT; association with a mouse model that has an

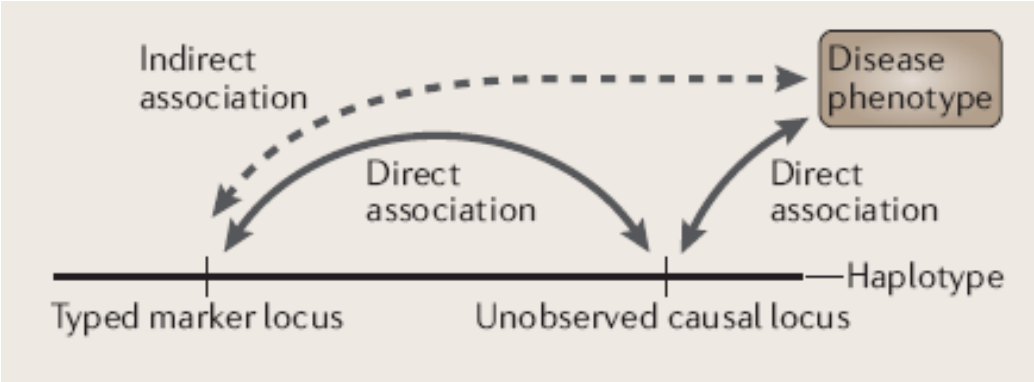

Figure 3.1: Diagram illustrating the concept of using tag SNPs for genetic association studies. The aim of genetic association studies is to find a genomic variant that is correlated with the disease or trait of interest. Whilst the ultimate goal may be to find the actual causal variant, this is not always feasible. In the diagram above, the 'typed marker locus' can be considered a tag SNP. Due to their close physical proximity on the genome and other factors such as linkage disequilibrium, the tag SNP is directly associated with the unobserved causal variant. This therefore implies an indirect interaction between the tag SNP and the disease or trait of interest, which can be detected using a genetic association study. Figure sourced from Balding *et al* 2006.[410]

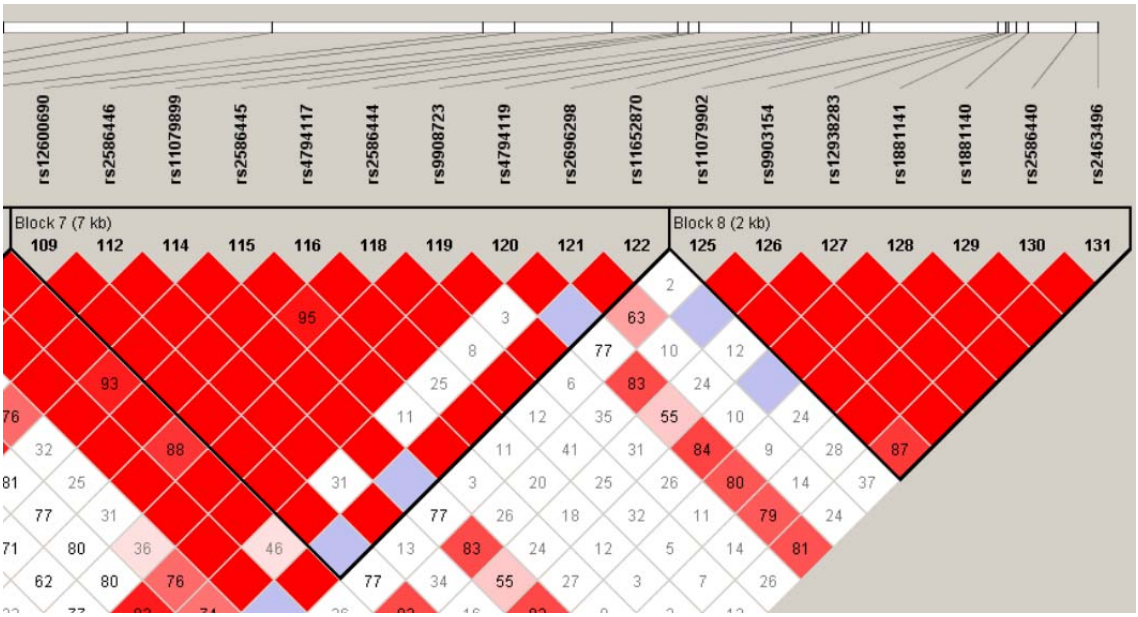

Figure 3.2: Example of LD plot (see next page for legend).

Figure 3.2: Graphical representation of LD. The figure represents an example of an LD plot. The narrow white box at the top of the diagram represents a segment of chromosome, with the connecting lines identifying the SNP located at that point on the chromosome. The coloured squares below the SNP names represent the degree of LD between each SNP. To determine the amount of LD between two specific SNPs, diagonally trace down the column of squares starting beneath each SNP of interest until the intersecting square is found. The colour of this square indicates the amount of LD. The metric used to describe LD on this plot is D', which ranges from -1 to 1. However, on the plot all values are presented as magnitude of D' multiplied by 100 (100*D'). If there is no evidence of recombination between two markers, or they are in complete LD, then D' will equal -1 or 1. The statistical significance of the D' value is represented by a logarithm of odds (LOD) score. If LOD < 2 there is no statistically significant evidence of LD, whilst a LOD ≥ 2 indicates high statistical significance. The colour scheme is as follows:

- *White* diamonds indicate D' values less than 1 with LOD < 2.
- *Light blue* diamonds indicate D' values equal to 1 with LOD < 2.
- *Shades of pink/red* diamonds indicate D' values less than 1 with LOD ≥ 2.
- *Dark red* diamonds indicate D' values equal to 1 with LOD ≥ 2.

The numbers within the boxes are the D' values, but these are only shown if D' is less than 1. The black line that forms a triangle shape around the coloured boxes indicates a LD or haplotype block. On this particular diagram, two LD blocks are illustrated. It can be seen from the diagram that the vast majority of SNPs within a LD block are in strong LD, as indicated the dark red squares. The boundary between these blocks is where recombination occurs more frequently, otherwise known as a 'hot-spot'.

A

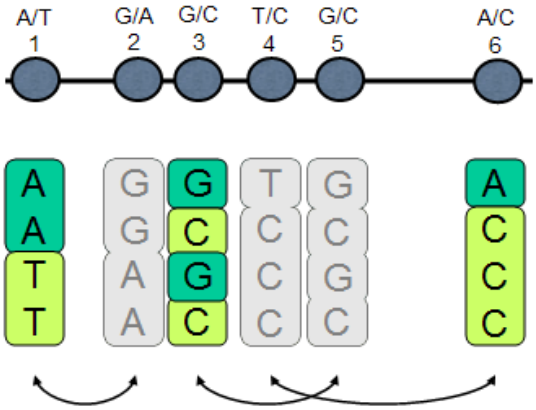

Tags:

SNP 1
SNP 3
SNP 6

3 in total

Test for association:

SNP 1
SNP 3
SNP 6

B

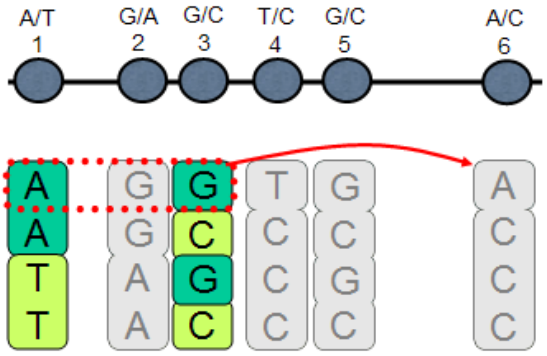

Tags:

SNP 1
SNP 3

2 in total

Test for association:

SNP 1 captures 1+2
SNP 3 captures 3+5
"AG" haplotype captures SNP 4+6

Figure 3.3: Mechanisms of pairwise and haplotype tagging.

(see next page for legend)

Figure 3.3: Mechanisms of pairwise and haplotype tagging. (**A**) Diagram depicting pairwise tagging. Six SNPs are represented along a segment of chromosome, with the respective alleles indicated below. The coloured SNPs (numbers 1, 3 and 6) are tag SNPs that capture the unknown variants indicated by the arrows. The tag SNPs and unknown variants are in high LD as their alleles are correlated. As the diagram illustrates, only three tag SNPs are needed to detect a total of six SNPs in this region of chromosome. (**B**) Example of haplotype tagging. Using pairwise tagging, the tag SNPs 1 and 3 can capture SNPs 2 and 5 respectively. When the tag SNPs are combined, they form a haplotype that can detect the previously undetected SNPs 4 and 6 (red arrow). Not only is the haplotype able to capture the undetected variant but it also reduces the genotyping effort by only requiring two tag SNPs instead of the three needed for pairwise tagging. Figures sourced from the HapMap website (http://hapmap.ncbi.nlm.nih.gov)

altered corneal phenotype; regulation of human pigmentation (Table 3.1). In all, 17 different genes were selected as candidates and in order to detect the majority of genetic variation within these genes, 12 were screened using a tag SNP analysis. For the remaining five genes, only putative functional variants were selected.

3.2.3.1 Structural proteins of the cornea

3.2.3.1.1 Proteoglycans

Proteins that play important roles in the structure and metabolic function of the cornea, such as the small leucine-rich proteoglycans (SLRPs), are suitable candidates for determining CCT. SLRPs are macromolecules composed of a protein core with covalently linked glycosaminoglycan side chains and they constitute a major component of the extracellular matrix, where they form complexes with other matrix proteins such as collagen.[411] The corneal stroma, which accounts for approximately 90% of the total thickness of the cornea, is predominately an extracellular tissue, composed of a highly ordered and uniform array of collagen fibrils, features that are essential for establishing corneal transparency. Corneal SLRPs such as decorin (DCN), keratocan (KERA), lumican (LUM) and osteoglycin (OGN) play a crucial role in assembling this array, which includes regulating the diameter and growth of collagen fibrils, as well as establishing uniform inter-fibrillar spacing.[412] Alterations in the diameter of collagen fibrils could be important in humans, where a narrower collagen fibril diameter has been shown to directly correlate with a reduction in CCT.[255, 413]

Investigation of corneal phenotypes following mutations or knock-outs of the respective genes further supports the potential association of these SLRPs with CCT.

Table 3.1: Criteria for selection of candidate genes

Gene	Structural	Developmental	Disease	Mouse Phenotype	Pigment
COL1A1	✓	-	✓	-	-
COL1A2	✓	-	✓	-	-
COL5A2	✓	-	✓	-	-
DCN	✓	-	✓	-	-
FBN1	✓	-	✓	-	-
PAX6	-	✓	✓	-	-
AQP1	✓	-	-	✓	-
AQP5	✓	-	-	✓	-
KERA	✓	-	-	✓	-
LUM	✓	-	-	✓	-
OGN	✓	-	-	✓	-
*ASIP**	-	-	-	-	✓
MC1R	-	-	-	-	✓
*OCA2**	-	-	-	-	✓
*SLC24A5**	-	-	-	-	✓
*SLC45A2**	-	-	-	-	✓
*TYR**	-	-	-	-	✓

Candidate genes were selected based on evidence that supported their potential association with CCT. This evidence belonged to several criteria that are listed above: involvement in corneal structure; function in corneal development pathways; association with a human disease that has abnormal CCT; association with a mouse model that has an altered corneal phenotype; regulation of human pigmentation. A tick indicates that the gene was chosen based on evidence from that criterion.

* Gene was screened using functional variants and not tag SNPs.

Mutations in *DCN* result in congenital corneal stromal dystrophy, a disorder that presents as corneal opacities that reduce visual acuity.[414] Dysfunction of the DCN protein also results in an abnormally thick cornea, which is likely to stem from disorganisation of the stromal collagen fibrils.[414] Mice with a knock-out of the *KERA* gene have larger and less organised stromal collagen fibrils and a thinner overall corneal stroma.[415] Similarly, *LUM* knock-out mice also have thicker collagen fibrils and a thinner corneal stroma.[416, 417] Mice with a knock-out of the *OGN* gene have also been shown to have thicker collagen fibrils.[418]

3.2.3.1.2 Aquaporins

The aquaporins are another group of proteins that may play a role in CCT determination. Both aquaporin 1 (AQP1) and aquaporin 5 (AQP5) are water channel proteins expressed in the mammalian, including human, cornea.[419-421] *AQP1* is expressed in the corneal endothelium, whilst *AQP5* is found in the epithelium and both play an important role in regulating fluid transport, which is essential for maintaining corneal transparency. In order to further characterise the function of these aquaporins, Thiagarajah *et al.* studied the corneas of mice with *aqp1* and *aqp5* gene knock-outs.[422] It was observed that the *aqp1* null mice had significantly reduced corneal thickness, whilst the *aqp5* mice had significantly increased corneal thickness. Alterations in the water balance of the corneal stroma is the likely mechanism, with dehydration producing a thinner cornea and swelling resulting in a thicker cornea. The hypothesis that minor alterations in the water balance of the cornea caused by polymorphisms in *AQ1* and *AQ5* may account for some of the normal variation in CCT in humans was the basis for including *AQ1* and *AQ5* in the candidate gene study.

3.2.3.2 Genes mutated in diseases with abnormal central corneal thickness

As discussed in Chapter 1, there are several human genetic disorders that present with abnormal CCT as part of their overall phenotype. Given that mutations in the genes responsible for these disorders have a considerable impact on CCT, it was hypothesised that common polymorphisms within these genes could also be associated with normal CCT variation.

3.2.3.2.1 The collagens

Three collagen genes were selected as candidates in this study: *collagen, type I, alpha 1* (*COL1A1*); *collagen, type I, alpha 2* (*COL1A2*); *collagen, type V, alpha 2* (*COL5A2*). The products of both *COL1A1* and *COL1A2* interact to form mature type I collagen, which is the most abundant collagen in the cornea and is primarily localised within the stroma.[6] Type I collagen interacts with type V collagen to form a highly specialised array of fibrils that are crucial in giving the cornea its transparency and strength.[254] A reduction in the diameter of these fibrils has been found in patients with osteogenesis imperfecta,[255, 413] a disease caused by mutations in *COL1A1* and *COL1A2*.[250-252] Along with a reduction in fibril diameter, osteogenesis imperfecta patients also present with abnormally thin CCT measurements,[34, 35] thus directly implicating *COL1A1* and *COL1A2* as potential genetic determinants of this trait. In addition, mutations in *COL1A1* and *COL1A2* have also been identified in some forms of Ehlers-Danlos syndrome,[423-426] another condition characterised by a thin CCT.[29-31]

The other collagen selected as a candidate gene was *COL5A2*, which encodes a collagen precursor alpha chain that interacts with the alpha chain of *COL5A1* to form the mature type V collagen molecule. Type V collagen forms heterotypic fibrils with

type I collagen in the corneal stroma and a reduction in the density of these fibrils caused by haploinsufficiency of *col5a1* in the mouse is correlated with a thinner CCT.[31] Mutations in *COL5A2* have also been identified as a major cause of Ehlers-Danlos syndrome.[253] Due to the high cost of screening *COL5A1*, which requires genotyping of in excess of 70 tag SNPs, it was decided not to include this gene in the study. However, future studies of CCT genetics may choose to investigate this gene as it is also a credible candidate.

3.2.3.2.2 Fibrillin 1

Fibrillin 1 (*FBN1*) is an extracellular glycoprotein that is a constituent of the 8 -10 nm microfibrils that provide structural support to basement membranes and elastic and non-elastic tissues.[427] *FBN1* is widely expressed throughout the body and has been documented in the cornea.[261, 262] Mutations in *FBN1* can cause Marfan syndrome, a connective tissue disorder that results in a range of clinical manifestations, with the principal complications occurring in the ocular, skeletal and cardiovascular systems.[257, 259] Studies have revealed that Marfan syndrome patients also have a thinner CCT.[32, 33]

3.2.3.2.3 PAX6

PAX6 is a transcription factor that plays an integral role in the early development of the ocular, central nervous and endocrine systems.[428, 429] Mutations in *PAX6* have been shown to cause aniridia, a congenital ocular condition that is characterised by abnormalities including iris hypoplasia, corneal opacities, cataracts and foveal and optic nerve hypoplasia.[430, 431] Aniridia has also been associated with a significantly thicker CCT.[243, 244] It has been postulated that mutations in *PAX6* may disrupt the

normal homeostasis of corneal stromal keratocytes, leading to increased stromal extracellular matrix synthesis and subsequent increases in CCT.[244]

3.2.3.3 Pigment genes

Based on the data presented in Chapter 2 that indicated CCT is correlated with pigmentation, genes that show evidence of influencing normal eye, hair or skin colour variation in humans were selected as candidates for this study. Rather than undertake a tag SNP approach, functional variants that have been associated with alterations in pigmentation were genotyped in *ASIP*, *OCA2*, *SLC24A5*, *SLC45A2* and *TYR* (Table 3.2). The only pigment gene that was screened using a tag SNP methodology was *MC1R*.

3.3 METHODS

3.3.1 Ethics statement

Ethics approval for the BMES has been described previously (see Chapter 2.3.1). For the remaining cohorts used in this study, ethics approval was obtained from the human research ethics committees of the following institutions (cohort in parentheses): Flinders University and the Southern Adelaide Health Service (Normal South Australia); Royal Adelaide Hospital (Florey Adelaide Male Ageing Study); University of Tasmania, Royal Victorian Eye and Ear Hospital and Queensland Institute of Medical (Australian twin study); St Thomas' Hospital (UK twin study). As some of the twin recruitment involved participants under the age of 18, informed consent was obtained from parents with the child's assent or from adult participants before testing. Each study adhered to the tenets of the Declaration of Helsinki.

Table 3.2: Functional variants genotyped in the pigment genes

Gene	SNP	Nucleotide Change	DNA/Protein Position	Phenotype	Reference
ASIP	rs6058017	A>G	g.8188	Eye, Hair, Skin	Kanetsky *et al* [340] Bonilla *et al* [342] Norton *et al* [343]
OCA2	rs1800401	C>T	p.Arg305Trp	Eye	Rebbeck *et al* [392]
	rs1800404	A>G	p.Ala355Ala	Skin	Shriver *et al* [432]
	rs1800407	G>A	p.Arg419Gln	Eye	Rebbeck *et al* [392]
	rs1800417	C>T	p.Ile722Thr	*	Lee *et al* [433]
SLC24A5	rs1426654	A>G	p.Thr111Ala	Skin	Lamason *et al* [344]
SLC45A2	rs13289	C>G	c.-1721	Skin	Graf *et al* [434]
	rs6867641	G>A	c.-1169	Skin	Graf *et al* [434]
	rs26722	G>A	p.Glu272Lys	Eye, Hair, Skin	Graf *et al* [435]
	rs16891982	C>G	p.Phe374Leu	Eye, Hair, Skin	Graf *et al* [435] Stokowski *et al* [436] Nan *et al* [437]
TYR	rs4547091	C>T	c. -301	*	Tanita *et al* [438]
	rs1799989	C>A	c. -199	*	Tanita *et al* [438]
	rs1042602	A>C	p.Tyr192Ser	Skin	Shriver *et al* [432] Stokowski *et al* [436]
	rs1126809	G>A	p.Arg402Gln	Skin	Berson *et al* [439] Nan *et al* [437]

Table displays information on all the genotyped functional variants. The DNA/protein position indicates the position of the allele using the cDNA (c), genomic (g) or protein (p) as the reference. The phenotype indicates whether the variant has been associated with pigmentation changes in the eyes, hair or skin. The amino acid change is also given if applicable. * Variation in allele frequency seen in different populations.

3.3.2 Participant recruitment

3.3.2.1 Discovery cohort

3.3.2.1.1 Blue Mountains Eye Study

The recruitment methodology used for the BMES can be found in Chapter 2.3.3.1.1. Genomic DNA was extracted from peripheral blood according to standard methods. Further descriptive details of the BMES can be found in Table 3.3.

3.3.2.2 Replication cohorts

3.3.2.2.1 Normal South Australia

The Normal South Australia (NSA) cohort consisted of healthy elderly controls who were ascertained from the Flinders Eye Centre and residential retirement villages and nursing homes within Adelaide, Australia. As the NSA study was initiated to recruit controls for an OAG study, all participants were required to have no known family history of glaucoma, as well as a normal IOP, optic disc and visual field. As part of the ocular examination, CCT was measured using a Pachmate DGH55 ultrasound pachymeter (DGH-KOI, Inc., PA, USA). The mean CCT of readings from both eyes was used as the participant's measurement. Genomic DNA was extracted from peripheral blood according to standard methods. In total, there were 281 DNA samples from individuals for whom CCT measurements were also taken. Further details of the NSA cohort can be found in Table 3.3.

3.3.2.2.2 Florey Adelaide Male Ageing Study

The Florey Adelaide Male Ageing Study (FAMAS) is a multi-disciplinary population cohort study examining the health and health-related behaviours of 1195 randomly selected men, aged 35–80 years and living in the North West regions of Adelaide, Australia.[440, 441] Participants had a comprehensive assessment of their

general health, which included numerous metabolic and physiological measurements, including CCT. CCT was measured using a Pachmate DGH55 ultrasound pachymeter (DGH Technology, PA, USA). The mean CCT of readings from both eyes was used as the participant's measurement. Genomic DNA was extracted from peripheral blood according to standard methods. In total, there were 269 DNA samples from individuals for whom CCT measurements were also taken. Further details of the FAMAS cohort can be found in Table 3.3.

3.3.2.2.3 Australian and United Kingdom twin studies

Two twin populations that were recruited from Australia (AU) and the United Kingdom (UK) were used to make a further replication cohort. Access to the genotyping data from these cohorts was permitted through collaboration with the Department of Genetics and Population Health, Queensland Institute of Medical Research (QIMR), Brisbane, Australia. The AU twin cohort consisted of two sub-samples, 953 individuals from the Brisbane Adolescent Twin Study and 761 individuals from the Twin Eye Study in Tasmania, comprising a whole cohort of 1714 participants from 786 families. A full description of the AU twin cohorts is given in Mackey et al.[442] Twins from the UK were a sub-sample from the cohorts collected at St Thomas' Hospital in London, with 1759 participants from 1119 families included in this study. Nearly 90% of the UK samples are adult women. Details of the UK twin cohort are given in Healey *et al*.[276] CCT was measured in the twin cohorts using ultrasound pachymetry and recorded for both eyes. Measurements were performed using a Tomey SP 2000 (Tomey Corp., Nagoya, Japan) or a DGH55 Technology (DGH Technology, PA, USA) pachymeter in the Australian and UK twin cohorts respectively. With little evidence for a significant difference between

Table 3.3: Descriptive details of genotyping cohorts

Cohort	Number of Participants	Mean Age (years)	Sex (% male)	Mean CCT ± SD (μm)
BMES	956	73.8	40.1	539.7 ± 32.8
NSA	281	76	43.8	544.1 ± 34.7
FAMAS	269	59.9	100	540.7 ± 32.2
AU twin	1714	21.4	44	544.3 ± 35
UK twin	1759	54	11.1	545.8 ± 34

Characteristics of each cohort used for genotyping in this study are given in the above table. SD = standard deviation.

the left and right eyes (ANOVA *p* value = 0.575), the mean CCT value of both eyes was used throughout as our measurement. Genomic DNA was extracted from peripheral blood according to standard methods.

3.3.3 Study design

The first phase of the study involved genotyping all the selected SNPs in DNA samples from the BMES, which was used as the discovery cohort. In order to undertake a case-control design, the 956 samples that comprise the full BMES cohort were divided into the extreme upper and lower quintiles (above the 80th or below the 20th percentile points) of the normal CCT distribution. In the extreme upper quintile, all participants had a CCT above 567.3 μm, whilst all participants in the extreme lower quintile had a CCT below 510.8 μm. This methodology was used in the initial analysis to enrich for genetic effects contributing to the extremes of CCT variation and has been demonstrated to be a powerful method to detect association for a quantitative trait.[443] It also offers the benefit of significantly reducing costs. Both the upper and lower quintiles contained 188 participants each. Alleles and genotypes were tested for an association with CCT in a case-control design where the thin CCT group represented the cases and the thick CCT represented the controls. Along with the single SNP analysis, haplotypes were also tested for association in the upper and lower CCT quintiles. Haplotypes were primarily constructed based on LD block structure, although a sliding window of sequential SNPs was also evaluated.

The second phase of the study involved screening any significant or nominally significant SNPs or haplotypes from the first phase in the remaining samples from the BMES cohort. Genotyping of the entire cohort allowed for analysis of whether the SNPs or haplotypes were associated with the quantitative trait CCT. Following

screening in the full BMES cohort, any SNPs or haplotypes that showed significant or nominally significant association results were then genotyped in the replication cohorts. Replication was initially performed in the NSA cohort, followed by additional genotyping in samples from the FAMAS. A final replication analysis was undertaken by obtaining data from two large twin cohorts that had undergone prior genotyping as part of a large GWAS.

3.3.4 Selection of SNPs from candidate genes

In order to select tag SNPs for the appropriate candidate genes, genotype data for SNPs around each gene was downloaded from the Centre d'Etude du Polymorphisme Humain from Utah (CEU) population of the HapMap project (http://hapmap.ncbi.nlm.nih.gov).[444] The selection of the tag SNPs was undertaken using the pairwise tagging function in Haploview v4.0 software.[445] Apart from D' (see Figure 3.2), another metric that is used to describe the degree of LD between markers is r^2. Values for r^2 range from 0 to 1, with a value of 1 implying there is no evidence of recombination between the markers and that they provide exactly the same information, or are in complete LD. For the selection of tag SNPs in this study, an r^2 threshold of 0.8 was set and SNPs with a minor allele frequency of less than 0.05 were excluded. Of the 17 candidate genes investigated in this study, 12 were screened using tag SNPs. The number of tag SNPs selected for each gene, with the percentage of total genetic variation covered by the SNPs in parentheses, was as follows: *AQP1* - 10 (97.5)*; AQP5* - 10 (97.6); *COL1A1* – 12 (93.6); *COL1A2* – 25 (89.3); *COL5A2* – 10 (98.5); *DCN* - 10 (98.3); *FBN1* - 8 (94.1); *KERA* - 11 (94); *LUM* - 11 (92.5); *MC1R* – 7 (94.2); *OGN* - 5 (98.4); *PAX6* - 7 (96.3). In the remaining five genes, only functional variants were selected (Table 3.2).

3.3.5 Genotyping methodology

3.3.5.1 Sequenom MassARRAY®

All the BMES and the majority of SNPs in the NSA samples were genotyped using the Sequenom MassARRAY® platform (Sequenom, San Diego, USA). The MassARRAY® platform utilizes the iPLEX GOLD chemistry on a Sequenom Autoflex Mass Spectrometer. This methodology was performed at the Australian Genome Research Facility, Brisbane, Australia. The SNPs not genotyped using this technology in the NSA samples are indicated below.

3.3.5.2 TaqMan® SNP genotyping assay

The *MC1R* SNPs rs2270459 and rs3212346 were genotyped in the FAMAS samples using the TaqMan® SNP Genotyping Assay (Applied Biosystems, Carlsbad, USA). Prior to performing the genotyping assay, all FAMAS samples were subjected to genomic amplification to increase the amount of DNA available for genetic assays. Genomic amplification was undertaken using the Illustra GenomiPhi V2 DNA Amplification Kit according to manufacturer's instructions (GE Healthcare Life Sciences, Uppsala, Sweden). Allele specific probes for rs2270459 and rs3212346 were ordered from Applied Biosystems (Melbourne, Australia) and the TaqMan® reaction procedure was carried out according to manufacturer's instructions. The reaction was performed in an Applied Biosystems StepOnePlus™ Real-Time PCR unit and results analysis undertaken using StepOne v2.1 software.

3.3.5.3 SNaPshot assay

The *TYR* SNP rs1126809 was genotyped in the NSA cohort using the SNaPshot® Multiplex System (Applied Biosystems). The SNaPshot® reaction assay was performed according to manufacturers instructions. Prior to undertaking the assay,

the genomic region containing the SNP was amplified by PCR using 50 ng of genomic DNA, 0.5 U HotStarTaq Plus DNA polymerase (QIAGEN, Valencia, CA), 103 QIAGEN PCR buffer, 2 mM dNTPs, 5 pM of each oligonucleotide primer and water to a total volume of 20 µl. The primer sequences were as follows:

Forward : (5') - GAACTTCAAGGCCTGAAAGAATA

Reverse: (5') - TTCAGCAATTCCTCTGAAAGAA

The amplification conditions involved an initial activation step of 95ºC for 5 minutes, followed by 30 cycles consisting of 30 seconds of denaturation at 94ºC, 30 seconds of annealing at 55ºC and 30 seconds of extension at 72ºC. A final extension step involved 5 minutes at 72ºC. The sequence of the probe used in the SNaPshot® assay was as follows:

(5') - CTTCTGGATAAACTTCTTGAAGAGGACGGTGCCTT

3.3.5.4 Genotyping results from AU and UK twin cohorts

Samples from the AU and UK twin cohorts were utilised in a GWAS designed to identify novel genetic determinants of CCT. For further information on the GWAS methodology refer to Chapter 5. The genotyping and data analysis methods have been validated in the study by Lu *et al* and are described below.[363] AU samples were genotyped by deCODE Genetics (Reykjavik, Iceland) and by the Center for Inherited Disease Research (MD, USA), whilst the UK twin samples were genotyped at the Center for Inherited Disease Research and the Wellcome Trust Sanger Institute (Cambridge, UK). Data analysis was performed by Dr. Stuart Macgregor and Ms. Yi Lu from the Department of Genetics and Population Health at the QIMR and access was only granted to summary statistics from the relevant SNPs. DNA samples from

both cohorts were hybridised to either the Illumina HumanHap 610W Quad arrays or the Illumina HumHap 300K Duo arrays.

A series of quality control criteria were applied to the genotyping data from the AU twins. These included minor allele frequency ≥ 1%, *p* value for Hardy-Weinberg equilibrium test of ≥ 10^{-06}, SNP call rate > 95% or Illumina Beadstudio GenCall score ≥ 0.7. After cleaning, 530,656 SNPs were left for association testing in the AU twin cohort. Slightly different quality control criteria were applied to the UK data compared with the AU twins, including minor allele frequency ≥ 1%, *p* value for Hardy-Weinberg equilibrium test ≥10^{-04} and SNP call rate > 95%, resulting in a complete set of 548,001 SNPs for the association tests. The genotyping data were screened for ancestral outliers using principal components analysis.[446] By comparing AU twin data with 16 global populations sourced from HapMap Phase 3 and Northern European sub-populations from a previous study by McEvoy *et al*,[447] 2% of the samples were excluded for being identified as ancestral outliers, thus giving greater confidence in the homogeneity of the study sample (Appendix 1). UK twin samples were also screened for genetic outliers by comparison with the reference of three main populations from HapMap Phase 2. The Q-Q plot (Appendix 2) clearly shows the homogeneity of the UK panel except for one data point. The discrepancy between the observed and expected statistics for this variant suggests a potential association signal.

Higher density markers on autosomes were also available from imputation. Genotypes were imputed using the software program MACH v1.0 (http://www.sph.umich.edu/csg/abecasis/MACH/index.html) for the AU samples

based on a set of 469,117 SNPs that were common to the six Illumina 610K subsamples at QIMR. The imputation for the UK samples was undertaken with reference to HapMap release 22 CEU using software program IMPUTE v2.0 (https://mathgen.stats.ox.ac.uk/impute/impute.html).[448] Each of the imputed datasets contains up to 2.4 million SNPs.

Both AU and UK twin cohorts in the study consist of either twin pairs or their close relatives (parents, siblings) in the family. Samples within the family are genetically related, sharing the chromosomal regions of identity-by-descent (IBD). In those regions, the related samples will provide the similar genetic information. Failing to estimate the IBD states will result in an increased false-positive rate in the association tests. To avoid this problem, the (–fastassoc) association test was conducted in the software program MERLIN.[449] It incorporated genetic relatedness between the samples by estimating the IBD prior to the association tests. The AU samples were controlled for both age and gender effects, whilst the predominantly female UK samples were only controlled for age effects. The trait distribution of CCT was standardized to increase the inter-sample compatibility as well as robustness to extreme observations.

Results from the AU and UK twins were combined in a meta-analysis, with data obtained for SNPs from the following genes: *COL1A1* (rs1034620, rs2696297); *COL1A2* (rs1034620, rs11764718, rs12668754); *FBN1* (rs10519177, rs17352842); *MC1R* (rs2270459, rs3212346); *PAX6* (rs662702, rs3026398). The data included allele frequencies and significance values for allele association and Hardy-Weinberg equilibrium tests. Not all SNPs were found on the arrays so imputation was used to

determine the allele frequencies. The following SNPs were imputed: rs1034620, rs269629, rs11764718, rs12668754, rs2270459, rs3212346.

3.3.6 Statistical Analysis

All genetic association tests performed in the case-control, full BMES and replication cohorts (except for the twins) were undertaken using the software program PLINK v1.06 (http://pngu.mgh.harvard.edu/purcell/plink/).[450] Haplotypes were constructed from the selected tag SNPs and were generally based on the LD blocks, which were defined using the 'solid spine of LD' function in Haploview. Haplotype associations were tested using HaploStats v1.3.1 software (Mayo Clinic, Rochester, USA). Additive, dominant and recessive models were investigated, with results for the dominant and recessive models shown as they were the most significant . Hardy-Weinberg equilibrium was evaluated for each SNP in every cohort except the twins and a *p* value adjusted for age and sex was also calculated for each SNP in the full BMES, NSA and FAMAS. Both the Hardy-Weinberg and covariate calculations were performed using PLINK. Correction of *p* values for multiple testing was undertaken using the online SNPSpD interface (http://genepi.qimr.edu.au/general/daleN/SNPSpD/).[451, 452] The spectral decomposition correction method implemented in the SNPSpD interface accounts for LD between SNPs and determines the total number of independent tests per gene. The number of independent tests per gene was as follows (number of tests in parentheses): *AQP1* (6)*; AQP5* (7); *ASIP* (1); *COL1A1* (9); *COL1A2* (17.1); *COL5A2* (8); *DCN* (7); *FBN1* (6.1); *KERA* (8); *LUM* (6); *MC1R* (6); *OCA2* (4); *OGN* (98.4); *PAX6* (96.3); *SLC24A5* (1); *SLC45A2* (4); *TYR* (4). Correction for multiple testing of haplotypes was performed using a standard Bonferroni adjustment for the total

number of observed haplotypes. Bonferroni adjustment for the Hardy-Weinberg equilibrium values was performed by correcting for the total number of SNPs screened in the respective gene. Statistical significance was accepted as $p < 0.05$.

3.3.7 Power Calculations

Power calculations were conducted for the case-control analysis using the Genetic Power Calculator (http://pngu.mgh.harvard.edu/~purcell/gpc/).[453] Calculations were performed with risk allele frequencies of 0.2, 0.3 and 0.4. Genotype relative risks for the heterozygous and homozygous genotypes were set at 1.5 and 2.25 respectively (multiplicative model). Linkage disequilibrium between the marker and risk allele was set at D' prime = 1.0. Under these criteria, the cohort had a power of 78.4% at a risk allele frequency of 0.2, 82.9% at 0.3 and 81.6% at 0.4 when calculated for a multiplicative model.

3.4 RESULTS

3.4.1 Case-control analysis in the Blue Mountains Eye Study

The *p* values for both the dominant and recessive inheritance models of all the SNPs typed in the extreme quintiles of the BMES distribution are shown in Tables 3.4 – 3.6. Of the 140 total SNPs that were genotyped, 15 were not in Hardy-Weinberg equilibrium following multiple testing correction and 17 had a very low minor allele frequency and did not yield any significant associations. There were 15 SNPs that had an uncorrected *p* value below the nominal significance threshold of 0.05; rs2696297 and rs1046329 (*COL1A1*); rs1034620 (*COL1A2*); rs12617111 (*COL5A2*); rs17352842 and rs9806323 (*FBN1*); rs11105956 and rs12231819 (*KERA*); rs2270459 and rs3212346 (*MC1R*); rs1800407 (*OCA2*); rs2761678 (*OGN*);

Table 3.4: Results of association tests for the corneal structural genes in the case-control analysis

			p value					*p* value	
Gene	**SNP**	**MAF**	**Dom**	**Rec**	**Gene**	**SNP**	**MAF**	**Dom**	**Rec**
AQ1	rs7788618	0.16	0.49	0.42	*KERA*	rs10745549	0.1	0.23	0.1
	rs1476597*	0.44	0.82	0.6		rs2701166*	0.26	0.7	0.08
	rs2267719	0.06	NR	NR		rs1920773	0.08	0.87	0.24
	rs1004317	0.36	1	0.5		rs11105956	0.06	0.41	**0.04**
	rs17159702	0.24	0.06	0.09		rs2735338	0.05	NR	NR
	rs1049305*	0.39	0.85	0.62		rs11105957	0.18	0.23	0.37
	rs6944844	0.06	NR	NR		rs17018627	0.06	0.98	0.24
	rs13222180	0.24	0.18	0.57		rs10859103	0.2	0.67	0.67
	rs10244884*	0.48	0.16	0.89		rs10859104	0.09	0.67	0.09
AQ5	rs3741559	0.2	0.59	0.93		rs12230223	0.17	0.48	0.53
	rs461872	0.47	0.98	0.35		rs12231819	0.09	0.51	**0.04**
	rs10875989	0.3	0.88	0.42	*LUM*	rs10745551*	0.31	0.55	0.93
	rs2878771	0.2	0.43	0.8		rs10777286*	0.43	0.2	0.42
	rs3759129	0.22	0.77	0.8		rs10777287	0.11	0.19	0.24
	rs296759*	0.36	0.88	0.52		rs10859105	0.25	0.95	0.56
	rs296763	0.23	0.15	0.16		rs11105987	0.12	0.7	0.1
	rs1996315*	0.43	0.35	0.8		rs7976738	0.13	0.29	0.55
	rs2849266	0.08	0.19	0.1		rs11478	0.08	0.53	0.96
	rs10875990	0.06	0.1	0.24		rs2300588	0.04	NR	NR
DCN	rs12819853*	0.3	0.67	0.85		rs2268578	0.11	0.74	0.24
	rs17658598	0.15	0.77	0.32		rs17018765	0.05	NR	NR
	rs17658685	0.04	0.3	0.23	*OGN*	rs7047089	0.33	0.11	0.85
	rs7308752	0.07	NR	NR		rs10761156	0.49	0.46	0.07
	rs3138287	0.0	NR	NR		rs2761678	0.1	0.09	**0.02**
	rs566806	0.25	0.91	1		rs2761680	0.12	0.4	0.54
	rs3138165	0.05	NR	NR					
	rs741212	0.12	0.76	0.42					
	rs10492230	0.16	0.98	0.5					
	rs1718539	0.1	NR	NR					

(see next page for legend)

Table 3.4: Results of association tests for the corneal structural genes in the case-control analysis. Table depicts the results for each tag SNP from the candidate genes that were selected based on their structural and physiological roles in the cornea. The case-control groups consisted of the extreme lower and upper CCT quintiles derived from the 956 normal individuals of the entire BMES cohort. Both the lower and upper quintiles contained 188 subjects each. Significance values are given for both the dominant (Dom) and recessive (Rec) models, with values in bold considered significant at the $p < 0.05$ level (uncorrected). MAF = minor allele frequency. NR = no result. * = SNP not in Hardy-Weinberg equilibrium.

Table 3.5: Results of association tests for genes that are mutated in diseases with abnormal CCT in the case-control analysis

			p value					*p* value	
Gene	**SNP**	**MAF**	**Dom**	**Rec**	**Gene**	**SNP**	**MAF**	**Dom**	**Rec**
COL1A1	rs4459590	0.37	0.084	0.6	*COL1A2*	rs400218	0.32	0.81	0.74
	rs2696297	0.17	0.47	**0.02**		rs10046552	0.1	0.63	0.55
	rs1046329	0.21	0.85	**0.03**		rs6465412	0.22	0.07	0.41
	rs2586488	0.34	0.86	0.54		rs12668754	0.15	0.23	0.38
	rs2075559	0.48	0.64	0.2		rs11764718	0.25	0.33	0.61
	rs2857396	0.15	0.96	0.99		rs1034620	0.31	**0.03**	0.57
	rs2696247	0.16	0.32	0.09	*COL5A2*	rs7424137	0.23	0.93	0.79
	rs2141279	0.13	0.38	1		rs13401377	0.19	0.93	0.91
	rs17639446	0.13	NR	NR		rs12617111	0.09	0.44	**0.02**
	rs2075555	0.13	0.66	0.2		rs7425816	0.14	0.95	0.26
	rs7406586	0.18	0.24	0.3		rs4667266	0.08	0.078	0.99
	rs16970089	0.08	NR	NR		rs6708419	0.32	0.72	0.79
COL1A2	rs3763467	0.1	0.23	0.32		rs10497699	0.16	0.28	0.72
	rs388625	0.38	0.74	0.7		rs11691604	0.29	0.59	0.81
	rs4729131	0.17	0.23	0.96		rs1983318	0.11	0.11	0.16
	rs2299417	0.08	0.81	0.24		rs10166385	0.06	0.74	0.24
	rs420257	0.31	0.51	0.71	*FBN1*	rs17352842	0.2	**0.006**	0.45
	rs3763466	0.36	0.26	0.7		rs10519177	0.25	0.95	0.75
	rs42517	0.27	0.79	0.23		rs9806323	0.14	**0.03**	0.37
	rs2521206	0.2	0.63	0.82		rs683282*	0.32	0.51	0.75
	rs389328	0.11	0.8	0.56		rs12915677	0.17	0.57	0.36
	rs42521	0.35	0.68	0.31		rs17364665	0.05	0.2	0.24
	rs42524	0.24	0.58	0.98		rs591519	0.09	0.09	0.98
	rs10487254	0.17	0.41	0.2		rs11854144	0.12	0.11	0.14
	rs2621213	0.29	0.45	0.43	*PAX6*	rs3026398	0.28	**0.01**	0.15
	rs2521205	0.49	0.35	0.22		rs662702	0.05	0.3	0.24
	rs369982	0.48	0.83	0.47		rs2071754	0.21	0.18	0.3
	rs4266	0.09	0.91	0.24		rs644242	0.04	NR	NR
	rs2472	0.06	NR	NR		rs3026390	0.49	0.24	0.18
	rs42531	0.34	0.92	0.64		rs7942007	0.2	0.86	0.16
	rs441051	0.19	0.85	0.55		rs12286701	0.03	0.28	0.24

(see next page for legend)

Table 3.5: Results of association tests for genes that are mutated in diseases with abnormal CCT in the case-control analysis. Table depicts the results for each tag SNP from the candidate genes that were selected based on their involvement in diseases that have abnormal CCT. The case-control groups consisted of the extreme lower and upper CCT quintiles derived from the 956 normal individuals of the entire BMES cohort. Both the lower and upper quintiles contained 188 subjects each. Significance values are given for both the dominant (Dom) and recessive (Rec) models, with values in bold considered significant at the $p < 0.05$ level (uncorrected). MAF = minor allele frequency. NR = no result. * = SNP not in Hardy-Weinberg equilibrium.

Table 3.6: Results of association tests for human pigment genes in the case-control analysis

			p value					*p* value	
Gene	**SNP**	**MAF**	**Dom**	**Rec**	**Gene**	**SNP**	**MAF**	**Dom**	**Rec**
MC1R	rs8045560*	0.45	0.79	0.83	*ASIP*	rs6058017	0.09	0.39	0.24
	rs2270459	0.1	**0.002**	0.54	*SLC24A5*	rs1426654	0.0	NR	NR
	rs3212346	0.1	**0.02**	0.57	*SLC45A2*	rs13289*	0.39	0.74	0.95
	rs3212363	0.26	0.76	0.76		rs6867641	0.34	0.96	0.77
	rs1805005	0.11	0.4	0.08		rs26722	0.01	NR	NR
	rs1805007	0.09	0.67	0.34		rs16891982*	0.04	0.29	**0.04**
	rs885479	0.04	NR	NR	*TYR*	rs1126809*	0.29	0.49	**0.006**
OCA2	rs1800401	0.04	0.54	0.24		rs1042602*	0.36	0.47	0.4
	rs1800404	0.24	0.34	0.11		rs4547091	0.44	0.53	0.34
	rs1800407	0.07	0.63	**0.04**		rs1799989	0.12	0.57	0.49
	rs1800417	0.0	NR	NR					

Table depicts the results for each tag SNP from the candidate genes that were selected based on their involvement in the regulation of human pigmentation. The case-control groups consisted of the extreme lower and upper CCT quintiles derived from the 956 normal individuals of the entire BMES cohort. Both the lower and upper quintiles contained 188 subjects each. Significance values are given for both the dominant (Dom) and recessive (Rec) models, with values in bold considered significant at the $p < 0.05$ level (uncorrected). In the table, MAF = minor allele frequency. NR = no result. * = SNP not in Hardy-Weinberg equilibrium.

rs3026398 (*PAX6*); rs16891982 (*SLC45A2*); rs1126809 (*TYR*). Of these 15 SNPs, three survived correction for multiple testing (corrected *p* value in parentheses): *FBN1* - rs17352842 (0.037); *MC1R* - rs2270459 (0.013); *TYR* - rs1126809 (0.025). These SNPs were subsequently genotyped in the full BMES cohort. In order to determine if any of the remaining 12 SNPs should be genotyped in the full BMES cohort, haplotype associations were also assessed within the relevant genes. Significant haplotype associations were found within *COL1A2*, *FBN1*, *MC1R* and *PAX6* (Table 3.7). All the SNPs that comprised these significant haplotypes were genotyped in the full BMES cohort.

3.4.2 Genotyping results in the full BMES, NSA and FAMAS cohorts

3.4.2.1 COL1A1

3.4.2.1.1 Single SNP analysis

Following the case-control analysis, two SNPs from *COL1A1* were screened in the full BMES cohort. The SNP rs2696297, found downstream of the 3' end of the gene, was found to be significantly associated with CCT under a recessive model (Table 3.8). Following correction for nine independent tests based on the SNPSpD algorithm, the adjusted *p* value ($p = 0.027$) remained below the significance threshold of 0.05. The neighbouring SNP rs1046329 was slightly over the significance threshold with a corrected *p* value of 0.063. When assessed under the recessive model, the CC genotype of rs2696297 conferred a 20.3 μm reduction in CCT when compared to the mean CCT of both other genotypes combined. Similarly, the GG genotype of rs1046329 resulted in a 15.6 μm reduction in mean CCT values. Replication genotyping was subsequently performed in the NSA cohort, with neither SNP showing any significant association results (Table 3.8). However, a similar

Table 3.7: Significantly associated haplotypes from case-control analysis

Gene	Haplotype Size	Haplotype Frequency	Model	*p* value
COL1A2	3	0.57	Additive	0.012
FBN1	2	0.74	Additive	**0.002**
MC1R	7	0.09	Dominant	**0.003**
PAX6	7	0.24	Dominant	0.039

Data in the table are given for the most associated haplotype from the respective gene following analysis in the case-control cohort. Haplotype size indicates the number of SNPs that comprise the haplotype. Values in bold were considered significant at the $p < 0.05$ level following correction for multiple testing.

Table 3.8: Genotyping results for the *COL1A1* SNPs rs2696297 and rs1046329

Cohort	SNP	Genotype	Frequency	Mean CCT ± SD (µm)	Adjusted *p* value	
					Dominant	Recessive
BMES	rs2696297	T/T	0.69	540.3 ± 31.7	0.97	**0.003**
		T/C	0.29	541.5 ± 32.4		
		C/C	0.02	520 ± 28		
	rs1046329	C/C	0.63	539.9 ± 31.9	0.84	0.007
		C/G	0.33	541.8 ± 33.6		
		G/G	0.03	524.3 ± 30.5		
NSA	rs2696297	T/T	0.68	543.1 ± 33.8	0.73	0.89
		T/C	0.31	544.6 ± 36.6		
		C/C	0.01	537.8 ± 29.2		
	rs1046329	C/C	0.64	544.1 ± 33.9	0.80	0.68
		C/G	0.33	543.7 ± 36.5		
		G/G	0.03	538.4 ± 27.8		

Genotype frequencies and mean CCT values for each genotype of both *COL1A1* SNPs selected for analysis in the full BMES and NSA cohorts based on association results from the case-control analysis. The adjusted *p* values for both the dominant and recessive modes of inheritance are corrected for sex and age. Values in bold were considered significant at the $p < 0.05$ level following multiple testing correction.

trend in the BMES and NSA cohorts was observed, suggesting that these results may replicate given more power from a larger sample size. The SNP rs2696297 was associated with a thinner CCT under a recessive model in the BMES and this finding was reflected in the NSA samples, with the CC genotype conferring a 5.8 μm reduction in CCT. The magnitude of this difference is far less in the NSA samples but the trend is the same, although power calculations confirm that this cohort is under-powered to detect a significant effect.

3.4.2.2 COL1A2

3.4.2.2.1 Single SNP analysis

The only SNP from *COL1A2* to show a significant association result in the case-control analysis was rs1034620, so this SNP was subsequently assessed in the full BMES and NSA cohorts (Table 3.9). Only a nominally significant *p* value ($p = 0.01$) was found under a dominant model in the full BMES, although this failed to survive multiple testing correction.

3.4.2.2.2 Haplotype analysis

A three SNP haplotype consisting of rs1034620 and its neighbouring tag SNPs, rs12668754 and rs11764718, was identified from the case-control analysis as having a significant association with CCT. This haplotype is situated downstream of the 3' end of the gene (Figure 3.4). There was a suggestion that this region may be associated with CCT given the nominally significant *p* values found for rs1034620 in the case-control and full BMES analysis. As a result, these three SNPs were genotyped in the full BMES cohort in order to further assess this haplotype (Table 3.10). Haplotype 1 (GGT with a frequency of 56%, reached significance under the

Table 3.9: Genotyping results for the *COL1A2* SNP rs1034620

Cohort	SNP	Genotype	Frequency	Mean CCT ± SD (µm)	Adjusted *p* value	
					Dominant	Recessive
BMES	rs1034620	T/T	0.44	536.3 ± 32.9	0.01	0.24
		T/C	0.48	541.7 ± 32.7		
		C/C	0.08	543.4 ± 31		
NSA	rs1034620	T/T	0.47	544.6 ± 35.7	0.99	0.68
		T/C	0.43	543.3 ± 33.1		
		C/C	0.1	545.7 ± 38.4		

Genotype frequencies and mean CCT values for each genotype of the *COL1A2* SNP rs1034620 selected for analysis in the full BMES and NSA cohorts based on association results from the case-control analysis. The adjusted *p* values for both the dominant and recessive modes of inheritance are corrected for sex and age. SD = standard deviation.

Figure 3.4: LD plot depicting location of *COL1A2* haplotype

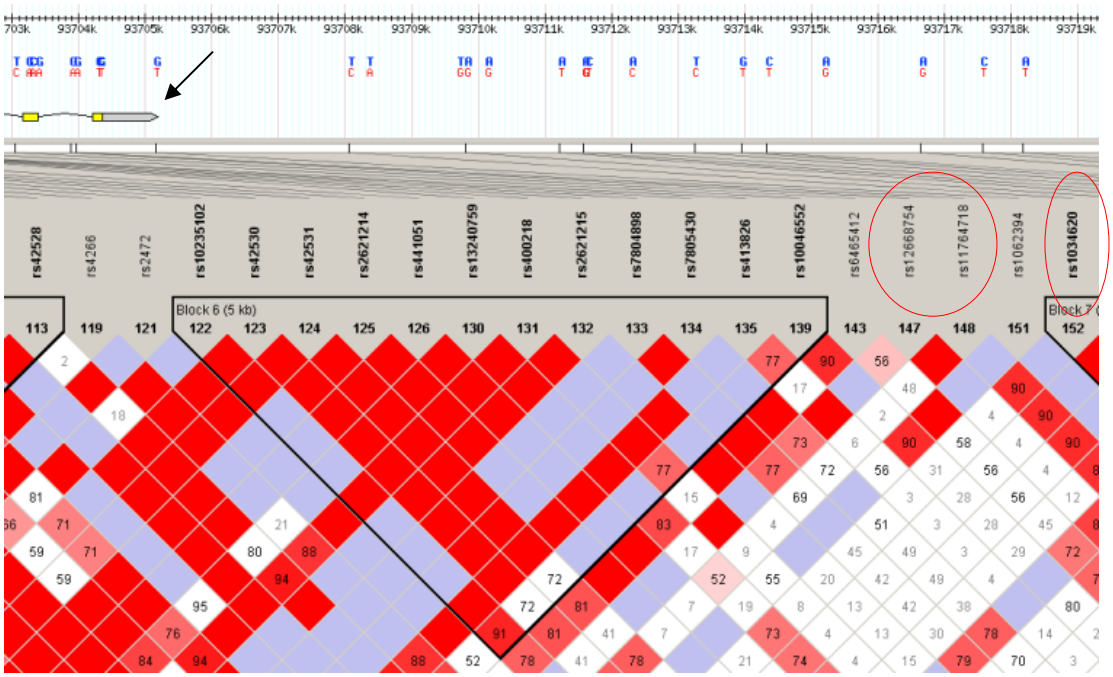

(see next page for legend)

Table 3.10: Results of *COL1A2* haplotype analysis in the full BMES cohort

	SNP				*p* value	
Haplotype	**1**	**2**	**3**	**Frequency**	**Dominant**	**Recessive**
1	G	G	T	0.56	**0.007**	0.67
2	G	A	C	0.24	0.05	0.97
3	A	G	T	0.10	0.79	0.59
4	G	G	C	0.05	0.89	NR
5	A	G	C	0.03	0.13	NR
6	G	A	T	0.01	0.22	NR

(see next page for legend)

Figure 3.4: LD plot depicting location of *COL1A2* haplotype. The LD structure immediately surrounding the three SNPs (circled) that comprise the *COL1A2* haplotype is shown in the diagram. The 3' end of the *COL1A2* gene is indicated by the arrow. The image was generated using Haploview v4.0.

Table 3.10: *COL1A2* haplotype analysis in the full BMES cohort. A three SNP haplotype was constructed from the *COL1A2* SNPs rs12668754 (SNP 1), rs11764718 (SNP 2) and rs1034620 (SNP 3). This haplotype was assessed in 956 subjects from the full BMES cohort and tested for association with CCT as a continuous variable. Both dominant and recessive modes of inheritance were analysed and values in bold were considered significant at the $p < 0.05$ level following multiple testing correction. NR = no result.

dominant model (p = 0.007) and survived Bonferonni correction (corrected p = 0.043) for multiple testing of the six observed haplotypes. Replication genotyping of this haplotype was subsequently performed in the NSA cohort. As with the BMES results, the GGT haplotype was the most common, with a frequency of 58% (Table 3.11). However, this haplotype was not associated with CCT in the dominant model as was seen in the BMES. The only significant association was found with haplotype 5 (AGC), which had a p value of 0.009 under a dominant model but is of borderline significance following correction for multiple testing (corrected p = 0.054).

3.4.2.3 FBN1

3.4.2.3.1 Single SNP analysis

Two SNPs from *FBN1*, rs17352842 and rs9806323, were genotyped in the full BMES cohort following significant association results in the case-control analysis (Table 3.12). A nominally significant p value (p = 0.02) was found under a dominant model for rs17352842, although this did not survive correction for multiple testing. Replication genotyping of rs17352842 in the NSA cohort failed to find any evidence of an association with CCT.

3.4.2.3.2 Haplotype analysis

Results of the *FBN1* haplotype analysis following genotyping in the full BMES cohort can be seen in Table 3.13. A two SNP haplotype was constructed using the SNPs rs17352842 and rs9806323, with rs17352842 located downstream of the 3' end of the gene and rs9806323 found within an intron (Figure 3.5). Both these SNPs are situated within a large LD block that spans the entire *FBN1* gene. This haplotype was investigated following data from the case-control analysis, which showed a p value of 0.002 that survived correction for multiple testing. In the BMES cohort, the CT

Table 3.11: *COL1A2* haplotype analysis in the NSA cohort

	SNP				*p* value	
Haplotype	**1**	**2**	**3**	**Frequency**	**Dominant**	**Recessive**
1	G	G	T	0.58	0.1	0.97
2	G	A	C	0.23	0.75	0.25
3	A	G	T	0.09	0.31	NR
4	G	G	C	0.05	0.7	NR
5	A	G	C	0.04	0.009	NR
6	G	A	T	0.01	0.61	NR

A three SNP haplotype was constructed from the *COL1A2* SNPs rs12668754 (SNP 1), rs11764718 (SNP 2) and rs1034620 (SNP 3). This haplotype was assessed in 281 participants from the NSA replication cohort and tested for association with CCT as a continuous variable. Both dominant and recessive modes of inheritance were analysed. NR = no result.

Table 3.12: Genotyping results for the *FBN1* SNPs rs17352842 and rs9806323

					Adjusted *p* value	
Cohort	**SNP**	**Genotype**	**Frequency**	**Mean CCT ± SD (µm)**	**Dominant**	**Recessive**
BMES	rs17352842	C/C	0.63	541.3 ± 32.4	0.02	0.94
		C/T	0.32	535.9 ± 32.4		
		T/T	0.05	538.2 ± 32		
	rs9806323	T/T	0.70	541.6 ± 33.2	0.11	0.59
		T/A	0.27	536.8 ± 31.8		
		A/A	0.03	543 ± 29.3		
NSA	rs17352842	C/C	0.62	544.6 ± 35.5	0.66	0.77
		C/T	0.35	542.8 ± 32		
		T/T	0.03	548.9 ± 50.3		

Genotype frequencies and mean CCT values for each genotype of *FBN1* SNPs selected for analysis in the full BMES and NSA cohorts based on association results from the case-control analysis. The adjusted *p* values for both the dominant and recessive modes of inheritance were corrected for sex and age. SD = standard deviation.

Figure 3.5: Diagram depicting LD structure surrounding *FBN1* gene

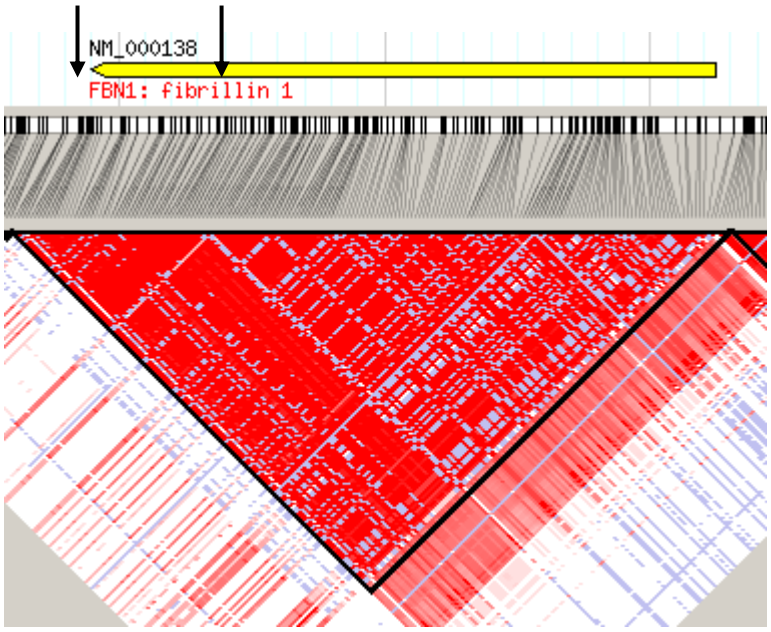

(see next page for legend)

Table 3.13: Results of *FBN1* haplotype analysis in the full BMES cohort

	SNP			*p* value	
Haplotype	**1**	**2**	**Frequency**	**Dominant**	**Recessive**
1	T	A	0.10	0.07	0.53
2	T	T	0.11	0.13	0.81
3	C	A	0.06	0.58	NR
4	C	T	0.73	0.59	**0.01**

(see next page for legend)

Figure 3.5: Diagram depicting LD structure surrounding *FBN1* gene. The entire *FBN1* gene is situated within the one LD block. The two SNPs used to construct the haplotype are both situated within the LD block and the positions are indicated by the black arrows. SNP rs17352842 is located downstream of the 3' end of the gene and rs9806323 is found within an intron. The image was generated using Haploview v4.0.

Table 3.13: Results of *FBN1* haplotype analysis in the full BMES cohort. A two SNP haplotype was constructed from the *FBN1* SNPs rs17352842 (SNP 1) and rs9806323 (SNP 2). This haplotype was assessed in 956 subjects from the full BMES cohort and tested for association with CCT as a continuous variable. Dominant and recessive modes of inheritance were analysed and values in bold were considered significant at the $p < 0.05$ level following multiple testing correction. NR = no result.

haplotype of these two SNPs yielded a significant result under a recessive model that survived Bonferroni correction for the four observed haplotypes (corrected p = 0.048).

3.4.2.4 MC1R

3.4.2.4.1 Single SNP analysis

Following analysis of the results from the case-control design, two SNPs from *MC1R* were screened in the full BMES cohort (Table 3.14). The SNPs, rs2270459 and rs3212346, are both located upstream of the 5' end of the gene. Under a dominant model, rs2270459 was significantly associated with CCT, with a p value of 0.048 following correction for six independent tests. The CA/AA genotypes of rs2270459 conferred a 9.3 μm decrease in CCT when compared to the mean CCT of the CC genotype. However, no significant association results were evident with rs3212346 in the full BMES cohort. Replication genotyping in the NSA cohort revealed similar trends in the magnitude of the CCT difference associated with rs2270459, but none of these results were significant (Table 3.14). The CA/AA genotype of rs2270459 resulted in a 6.3 μm reduction in CCT, which is similar to those seen in the BMES cohort, but the smaller sample size of the NSA group potentially made this replication under-powered.

The FAMAS samples were used as an additional replication cohort for rs2270459. Given the NSA results showed a similar trend to that observed in the BMES, it was decided to increase the power of this replication by incorporating a further 269 DNA samples from the FAMAS. The results from the FAMAS genotyping can be found in Table 3.14. No correlation with CCT was evident under either a dominant or recessive model. In order to further increase the sample size, the NSA and FAMAS

Table 3.14: Genotyping results for the *MC1R* SNPs rs2270459 and rs3212346

Cohort	SNP	Genotype	Frequency	Mean CCT ± SD (µm)	Adjusted *p* value	
					Dominant	Recessive
BMES	rs2270459	C/C	0.81	541.1 ± 33.1	**0.008**	0.33
		C/A	0.18	531.1 ± 30.5		
		A/A	0.01	546.7 ± 25.6		
	rs3212346	G/G	0.79	541.2 ± 33.2	0.08	0.5
		G/A	0.2	533.4 ± 30.8		
		A/A	0.01	546.1 ± 24.3		
NSA	rs2270459	C/C	0.81	545.3 ± 34.2	0.24	0.32
		C/A	0.18	539.8 ± 37.6		
		A/A	0.01	525.7 ± 27.8		
FAMAS	rs2270459	C/C	0.81	541.1 ± 32.1	0.6	0.48
		C/A	0.18	537.8 ± 30.7		
		A/A	0.01	557.2 ± 68		

Genotype frequencies and mean CCT values for each genotype of the *MC1R* SNPs selected for analysis in the full BMES, NSA and FAMAS cohorts based on association results from the case-control analysis. The adjusted *p* values for both the dominant and recessive modes of inheritance were corrected for sex and age. Values in bold were considered significant at the $p < 0.05$ level following correction. SD = standard deviation.

genotyping results were combined to give a total of 550 participants. Despite the larger sample size of the combined cohorts, no association results were found to be significant (Table 3.15). The consistent trend that was apparent between the BMES and NSA samples, with the dominant genotypes causing a reduced CCT, diminished upon addition of the FAMAS samples.

3.4.2.4.2 Haplotype analysis

A haplotype for *MC1R* was constructed using all seven tag SNPs that were genotyped for this gene, as the entire *MC1R* gene was located within a single LD block (Figure 3.6). Evidence from the case-control analysis indicated that this seven SNP haplotype was associated with CCT, so all SNPs were subsequently screened in the full BMES cohort, including the aforementioned rs2270459 and rs3212346. Two haplotypes showed significant results: haplotype 3 under a recessive model and haplotype 5 under a dominant model (Table 3.16). Only the result from haplotype 5 survived the Bonferroni correction for multiple testing, with a *p* value of 0.006 following correction for the six observed haplotypes. This outcome for haplotype 5 is most likely mediated by rs2270459, which demonstrated an association with CCT in the full BMES cohort. This SNP occupies position two in the haplotype and only in haplotype 5 is the 'A' allele present.

3.4.2.5 PAX6

3.4.2.5.1 Single SNP analysis

The only *PAX6* SNP to be screened in the full BMES cohort was rs3026398, which yielded an uncorrected *p* value of 0.02 under a dominant model, a result that did not

Table 3.15: Genotyping results for the *MC1R* SNPs in a combined NSA and FAMAS cohort

Gene	SNP	Genotype	Frequency	Mean CCT ± SD (µm)	Adjusted *p* value	
					Dominant	Recessive
MC1R	rs2270459	C/C	0.81	543.3 ± 33.2	0.24	0.95
		C/A	0.18	538.8 ± 34.2		
		A/A	0.01	541.4 ± 49.6		
	rs3212346	G/G	0.78	543.1 ± 33.6	0.29	0.55
		G/A	0.21	538.6 ± 32		
		A/A	0.01	548.6 ± 41.9		

Genotyping data from the FAMAS and NSA cohorts was combined to give a total sample size of 550 participants. The table depicts the genotype frequencies and mean CCT values for each genotype of the *MC1R* SNPs rs2270459 and rs3212346 in the combined FAMAS and NSA cohorts. The *p* values were calculated for both dominant and recessive modes of inheritance with the adjusted *p* value corrected for sex and age. SD = standard deviation.

Figure 3.6: LD plot depicting location of *MC1R* haplotype

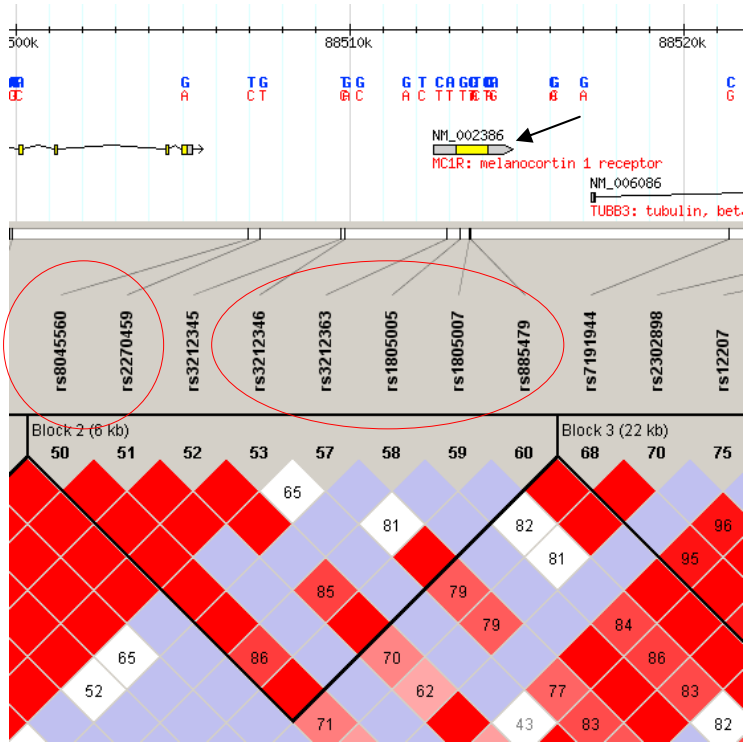

(see next page for legend)

Table 3.16: Results of *MC1R* haplotype analysis in the full BMES cohort

	SNP								*p* value	
Haplotype	**1**	**2**	**3**	**4**	**5**	**6**	**7**	**Frequency**	**Dominant**	**Recessive**
1	T	C	G	A	G	C	G	0.34	0.27	0.61
2	C	C	G	T	G	C	G	0.21	0.85	0.91
3	T	C	G	A	T	C	G	0.12	0.84	0.01
4	T	C	G	A	G	T	G	0.11	0.38	0.39
5	C	A	A	A	G	C	G	0.09	**0.001**	0.54
6	C	C	G	A	G	C	G	0.07	0.42	0.31

(see next page for legend)

Figure 3.6: LD plot depicting location of *MC1R* haplotype. The LD structure immediately surrounding the seven SNPs (circled) that comprise the *MC1R* haplotype is shown in the diagram. All the SNPs are situated within the same LD block. The arrow indicates the position of the *MC1R* gene. The SNP rs7191944, which is located downstream of the *MC1R* gene, was originally included as a tag SNP but failed to genotype. The image was generated using Haploview v4.0.

Table 3.16: Results of *MC1R* haplotype analysis in the full BMES cohort. A seven SNP haplotype was constructed from the *MC1R* SNPs rs8045560 (SNP 1), rs2270459 (SNP 2), rs3212346 (SNP 3), rs3212363 (SNP 4), rs1805005 (SNP 5), rs1805007 (SNP 6) and rs885479 (SNP 7). This haplotype was assessed in 956 subjects from the full BMES cohort and tested for association with CCT as a continuous variable. Dominant and recessive modes of inheritance were analysed and values in bold were considered significant at the $p < 0.05$ level following multiple testing correction.

survive multiple testing correction (Table 3.17). Subsequent genotyping in the NSA cohort failed to find any evidence of a correlation with this SNP and CCT.

3.4.2.5.2 Haplotype analysis

Whilst a seven SNP *PAX6* haplotype was investigated in the case-control analysis, the most significantly associated haplotype in the full BMES cohort was only found to consist of two SNPs, rs3026398 and rs662702. Both these SNPs are located downstream of the 3' end of the gene and are found within the same LD block (Figure 3.7). The strongest result was seen with the GC haplotype under a recessive model, which gave a *p* value of 0.009 following correction for the three observed haplotypes (Table 3.18). The AC haplotype under a dominant model also yielded a *p* value that survived Bonferroni correction for multiple testing ($p = 0.027$).

3.4.2.6 TYR

3.4.2.6.1 Single SNP analysis

The *TYR* SNP rs1126809, which encodes the non-synonymous variant Arg402Gln, was not found to be significantly associated with CCT under a dominant or recessive model in the full BMES cohort (Table 3.19). This was despite a result in the case-control analysis that survived multiple testing correction. A potential explanation could be that rs1126809 was not in Hardy-Weinberg equilibrium in the full BMES cohort. Failure to conform to Hardy-Weinberg equilibrium can sometimes be caused by genotyping errors. Thus, this SNP was screened in the NSA cohort using the SNaPshot® technique rather than the Sequenom MassARRAY®. There was no evidence that rs1126809 is correlated with CCT in the NSA cohort and the SNP was again out of Hardy-Weinberg equilibrium (Table 3.19).

Table 3.17: Genotyping results for the *PAX6* SNP rs3026398

					Adjusted *p* value	
Cohort	**SNP**	**Genotype**	**Frequency**	**Mean CCT ± SD (µm)**	**Dominant**	**Recessive**
BMES	rs3026398	G/G	0.50	536.7 ± 33.3	0.02	0.72
		G/A	0.42	542.1 ± 31.9		
		A/A	0.08	540.2 ± 30.7		
NSA	rs3026398	G/G	0.50	543.6 ± 35	0.76	0.76
		G/A	0.42	544.4 ± 33.8		
		A/A	0.08	546.8 ± 38.1		

Genotype frequencies and mean CCT values for each genotype of the *PAX6* SNP rs3026398 selected for analysis in the full BMES and NSA cohorts based on association results from the case-control analysis. The adjusted *p* values for both the dominant and recessive modes of inheritance were corrected for sex and age. SD = standard deviation.

Figure 3.7: LD plot depicting location of *PAX6* haplotype

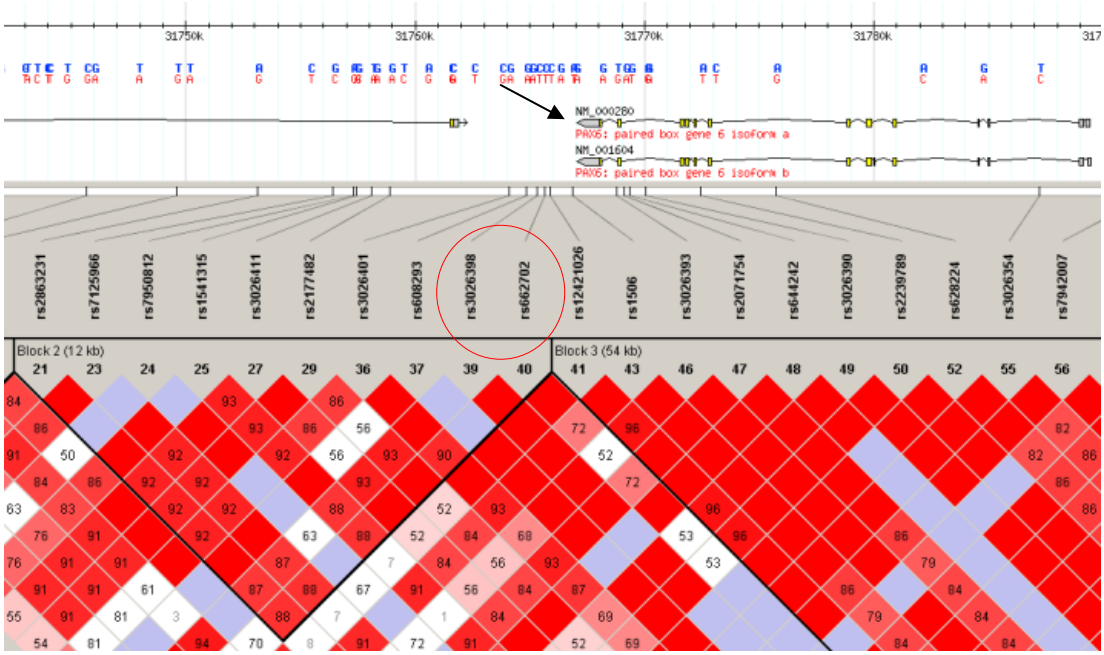

(see next page for legend)

Table 3.18: Results of *PAX6* haplotype analysis in the full BMES cohort

	SNP			*p* value	
Haplotype	**1**	**2**	**Frequency**	**Dominant**	**Recessive**
1	G	C	0.63	0.37	**0.003**
2	G	T	0.06	0.33	0.68
3	A	C	0.31	**0.009**	0.58

(see next page for legend)

Figure 3.7: LD plot depicting location of *PAX6* haplotype. The LD structure immediately surrounding the two SNPs (circled) that comprise the *PAX6* haplotype is shown in the diagram. Both the SNPs are situated within the same LD block that is downstream from the 3' end of the gene. The arrow indicates the position of the *PAX6* gene. The image was generated using Haploview v4.0.

Table 3.18: Results of *PAX6* haplotype analysis in the full BMES cohort. A two SNP haplotype was constructed from the *PAX6* SNPs rs3026398 (SNP 1) and rs662702 (SNP 2). This haplotype was assessed in 956 subjects from the full BMES cohort and tested for association with CCT as a continuous variable. Dominant and recessive modes of inheritance were analysed and values in bold were considered significant at the $p < 0.05$ level following multiple testing correction.

Table 3.19: Genotyping results for the *TYR* SNP rs1126809

					Adjusted *p* value	
Cohort	**SNP**	**Genotype**	**Frequency**	**Mean CCT ± SD (µm)**	**Dominant**	**Recessive**
BMES	rs1126809*	G/G	0.49	537.7 ± 31.4	0.21	0.06
		G/A	0.46	539.4 ± 33		
		A/A	0.05	550.5 ± 27.6		
NSA	rs1126809*	G/G	0.49	549 ± 33	0.06	0.77
		G/A	0.45	540.5 ± 34.2		
		A/A	0.05	541.7 ± 43.5		

Genotype frequencies and mean CCT values for each genotype of the *TYR* SNP rs1126809 selected for analysis in the full BMES cohort based on association results from the case-control analysis. The adjusted *p* values for both the dominant and recessive modes of inheritance are corrected for sex and age. * = SNP not in Hardy-Weinberg equilibrium. SD = standard deviation.

3.4.3 Replication genotyping in the Australian and UK twin cohorts

Genotyping data were also obtained from our research collaborators at the QIMR to investigate if a select number of SNPs were associated with CCT in the AU and UK twin cohorts. As access to this data were limited, the results for each SNP simply reflected allelic associations. It was not possible to investigate dominant and recessive models of inheritance for each SNP and construct haplotypes. The major advantage of obtaining data from the twin cohorts was the substantial increase in power, with a combined total of 3,473 samples. Data were obtained for the following seven SNPs: rs2696297 and rs1046329 (*COL1A1*); rs1034620 (*COL1A2*); rs17352842 (*FBN1*); rs2270459 and rs3212346 (*MC1R*); rs3026398 (*PAX6*) (Table 3.20). These SNPs were selected as the single SNP association data from the BMES, NSA and FAMAS cohorts warranted further investigation. The only SNP to show an association with CCT was rs1046329 from *COL1A1*, with a nominally significant *p* value of 0.047, while rs1034620 was narrowly over the significance threshold with a *p* value of 0.053.

3.5 DISCUSSION AND SUMMARY

The genetic factors involved in the determination of CCT are largely unknown. This is despite several family and twin studies indicating that CCT exhibits a very strong hereditary component.[215-217] Coupled with the ease and accuracy of the measurement methodology and the ability to assemble large cohorts, CCT is an ideal trait for a candidate gene approach. For this study, a total of 17 candidate genes were selected based on the hypothesis that they could be associated with CCT. The selected genes can be divided into three broad groups based on their similarities; structural and

Table 3.20: Allele association results for SNPs genotyped in the twin cohorts

Gene	SNP	Minor Allele	MAF	*p* value
COL1A1	rs2696297	C	0.13	0.141
	rs1046329	G	0.17	**0.047**
COL1A2	rs1034620	C	0.31	0.053
FBN1	rs17352842	T	0.2	0.253
MC1R	rs2270459	A	0.1	0.595
	rs3212346	A	0.11	0.594
PAX6	rs3026398	A	0.27	0.779

Genotyping data for the SNPs shown in the above table was obtained from a genome wide association study of the AU and UK twin cohorts. The combined size of the two twin cohorts was 3,473 samples. The association of each SNP allele with CCT was tested and the corresponding *p* value is represented in the table. Values in bold were considered significant at the $p < 0.05$ level. MAF = minor allele frequency.

physiological proteins of the cornea: *AQP1, AQP5*, *DCN*, *KERA*, *LUM*, *OGN*; genes that cause disease that is characterised by abnormal CCT: *COL1A1, COL1A2, COL5A2, FBN1* and *PAX6*; genes involved in the regulation of human pigment: *ASIP*, *MC1R*, *OCA2*, *SLC24A5*, *SLC45A2* and *TYR*. The hypothesis was that non-pathogenic polymorphisms within these genes could be associated with the normal CCT variation seen within the general population. The approach to find these variants was to select a range of tag SNPs that would cover the majority of genetic variation within these genes.

3.5.1 Structural and physiological proteins of the cornea

There was no conclusive evidence from the single SNP or haplotype analyses that any of the aquaporin or SLRP common variants are associated with CCT. This probably reflects the arbitrary nature of the candidate gene selection process, whereby many genes are selected based on insufficient knowledge of the biological pathways that regulate the phenotype of interest. This is not to say that these genes were not valid candidates for the study and it is possible that future investigations of CCT genetics may find evidence of an association with an aquaporin or SLRP gene.

3.5.2 Pigment genes

Analysis of the six pigment genes in this study was based on the findings from Chapter 2, where it was observed that human and mouse pigmentation appears to influence CCT. In regards to the human data, darker skin was generally correlated with a thinner CCT. Whilst our knowledge of the genetic factors responsible for regulating mouse pigmentation is advanced, relatively little is known about the genetics of normal skin colour variation in humans, which limited the ability to

choose candidate genes. It was therefore determined to select genes that showed any evidence of influencing not only normal skin colour variation, but eye and hair colour as well. In order to limit the total number of SNPs screened, only selected functional variants were chosen from *ASIP*, *OCA2*, *SLC24A5*, *SLC45A2* and *TYR*. These variants were selected as there are published data connecting them with alterations in pigmentation. The tag SNP methodology was used to screen *MC1R*, primarily because in excess of 70 variants that influence skin and hair colour have been identified within this gene.[320, 337]

3.5.2.1 MC1R and TYR

The genotyping results for the pigment genes revealed that only *MC1R* and *TYR* demonstrated any evidence of an association with CCT. Following genotyping in the full BMES cohort, one tag SNPs and a haplotype from *MC1R* displayed strong *p* values that survived multiple testing correction. However, screening of the single SNP in the NSA, FAMAS and twin cohorts failed to replicate these findings, suggesting that the original result was a false positive. The *MC1R* haplotype was not assessed in the replication samples but given the results from the single SNP analysis, it is unlikely that the original haplotype result would also replicate. The *TYR* SNP rs1126809 was found to have a significant *p* value in the case-control analysis, although this result was not evident following genotyping in the full BMES or NSA cohorts. This could be a consequence of rs1126809 not being in Hardy-Weinberg equilibrium in either of these groups. In order to ascertain if genotyping errors were causing the deviations from Hardy-Weinberg equilibrium, two different methodologies, Sequenom MassARRAY® and SNaPshot®, were employed to screen the BMES and NSA samples. Given that rs1126809 was still not in Hardy-

Weinberg equilibrium following the use of two different techniques, it suggests that genotyping error was not the problem. Deviations from Hardy-Weinberg equilibrium can also sometimes be a symptom of a genuine association,[454, 455] although there was no evidence of this in this instance. Given the findings, it is possible that rs1126809 is genuinely out of Hardy-Weinberg equilibrium in the BMES and NSA cohorts.

3.5.2.2 Limitations of the pigment gene analysis

There were several weaknesses with the pigment gene analysis that need to be acknowledged. Firstly, the selection of only functional variants severely limited the chances of detecting an association, as the vast majority of variation in the respective genes was ignored. Therefore, it cannot be concluded from this study that *ASIP*, *OCA2*, *SLC24A5*, *SLC45A2* and *TYR* are not involved in the determination of CCT, merely that the chosen SNPs are not. A further issue was the use of Caucasian cohorts for the genotyping. The correlation between CCT and pigmentation is based on variation in skin colour, an effect that is diminished by only including participants with predominately white skin. If there is genuine genetic interaction between skin pigmentation and CCT, then it can be assumed that the same genetic variants will be involved in the determination of both these traits. In a population with the same skin colour, such as the Caucasian cohorts used in this study, the variants that cause skin colour variation are likely to be missing. This would imply that any genetic variants that are potentially responsible for CCT determination would also be absent.

In order to improve the methodology for a study such as this, it is not just a simple case of including participants with different skin colour. Screening pigment genes in a cohort of participants with varying skin pigmentation will simply result in a

positive association between the SNP of interest and skin colour, thus making it impossible to discern what genetic effect, if any, is acting on CCT. Future researchers looking to investigate the role pigment genes play in the determination of CCT need to take these issues into account and design their study appropriately. This issue may be resolved by experimental procedures that directly test the effect of melanin on developing corneal cells.

3.5.3 Disease genes

Five genes, namely *COL1A1, COL1A2, COL5A2, FBN1* and *PAX6*, were selected as candidates based on their causal involvement with diseases that present with abnormal CCT measurements. Whilst pathogenic mutations within these genes can be directly correlated with alterations in CCT, these same variants of strong effect would contribute little to normal CCT variation. Therefore, the hypothesis was that non-pathogenic polymorphisms could be involved in the more subtle variation in CCT seen in the general population. Following genotyping in the discovery and replication cohorts, the only one of these genes that presented no suggestion of an association with CCT was *COL5A2*, despite good evidence in its selection as a candidate.

3.5.3.1 FBN1 and PAX6

Analysis of the single SNP data from *FBN1* and *PAX6* failed to present any conclusive evidence of an association with CCT. While several SNPs from both these genes were screened in the full BMES cohort following suggestive results in the case-control analysis, all the *p* values weakened following genotyping in the additional samples. The reduction in significance is an interesting observation and

could be the result of several factors. The increased power provided by genotyping the SNPs in an additional 580 samples implies that the initial analysis was under-powered and that the associations seen were possibly type I error. Alternatively, the first phase of genotyping in the upper and lower quintiles could have enriched for variants that are only important in the extreme ends of the CCT spectrum and thus, by introducing the samples from the 'middle' of the distribution, this association was weakened. Genotyping of the *FBN1* and *PAX6* SNPs in the NSA and twin replication cohorts failed to reveal any evidence of a correlation with CCT, which supports the findings from the full BMES cohort.

In contrast to the single SNP data, haplotype analysis conducted on *FBN1* and *PAX6* provided evidence of a potential correlation with CCT, with haplotypes from both genes yielding association results that survived multiple testing correction. Given the relatively strong haplotype data, it is intriguing that single SNP analysis showed a weak or no association. However, studies have demonstrated that examining haplotypes can be superior to single SNP analysis when undertaking a candidate gene study and it is possible that the haplotypes are detecting variation within these genes that cannot be ascertained from investigating single SNPs.[408, 409] The data presented by the single SNP and haplotype analyses of *FBN1* and *PAX6* indicate that further work is needed to assess the potential involvement of these genes with CCT determination. Replication of the haplotype results in other cohorts is required to confirm the findings of this study.

3.5.3.2 COL1A1 and COL1A2

The most conclusive evidence of a role in CCT determination came from the type I collagen genes *COL1A1* and *COL1A2*. For *COL1A1*, SNP rs2696297 conferred a reduction in mean CCT of 20.3 μm in the full BMES cohort and importantly, the test for association survived correction for multiple testing. The neighbouring variant rs1046329 conferred a reduction in CCT of 15.6 μm but was narrowly over the significance threshold. As anticipated, these differences are far more modest than the gross reduction in CCT seen in the osteogenesis imperfecta patients, which can be in the order of 80 μm,[34, 35] but they are consistent with the hypothesis that non-pathogenic changes in these genes lead to more subtle variation. Replication genotyping in the NSA samples revealed similar trends in terms of the reduction in CCT for both these SNPs, although it is likely that this cohort was under-powered to detect a significant effect. In order to overcome this problem, genotyping data were obtained from a meta-analysis of the AU and UK twin studies, which gave a combined cohort size of 3,473 samples. Although only allele association data were available from the twin studies, rs1046329 was found to have a nominally significant *p* value of 0.047. This result is crucial as it demonstrates replication of the data from the BMES in a large, independent cohort. A potential criticism of this finding is that the *p* value for rs1046329 narrowly missed surviving multiple testing correction in the full BMES dataset. However, rs2696297 and rs1046329 are in strong LD with each other as evidenced by a D' of 0.98 ($r^2 = 0.77$) and it is likely that they are both 'tagging' the same unknown causative variant.

In terms of the single SNP analysis from *COL1A2*, only rs1034620 demonstrated any evidence of a correlation with CCT. Data from the BMES samples indicated that rs1034620 conferred a 5.6 μm increase in CCT under a dominant model and also

appeared to exhibit an allele dosage effect, with incremental differences in CCT between each genotype (Table 3.9). This result however, did not survive multiple testing correction and replication genotyping in the NSA samples also failed to confirm an association with CCT. As with *COL1A1*, replication in the NSA samples was probably insufficient and more power was needed to find an effect, so data were obtained from the twin cohorts. The allele association analysis for rs1034620 from the twins yielded a *p* value of 0.053, of borderline statistical significance. This indicated that rs1034620 is possibly having an effect on CCT determination, a view supported by the results of the haplotype analysis. A three SNP haplotype that included rs1034620 was significantly associated with CCT in the full BMES cohort. Interestingly, a different haplotype showed a nominally significant effect in the NSA samples. It is unclear as to why different haplotypes were associated in the BMES and NSA cohorts, although it could be due population differences or a type I error. Further replication of this haplotype in larger studies, such as the twin groups, is required to verify these findings. However, when both the single SNP and haplotype analysis are considered, it appears likely that polymorphisms in *COL1A2* do have an effect on normal CCT variation.

3.5.4 Evaluation of the candidate gene study methodology

Candidate gene studies are well represented in the literature as they offer several advantages over other gene discovery methods. By targeting specific genes, candidate gene studies ensure there is a higher concentration of markers within a given region when compared to an untargeted approach such as a linkage analysis or GWAS, thus increasing the chances of finding a functional variant.[399] Another advantage of the candidate gene approach is that the costs to perform such a study

can be significantly lower than for genome-wide methodology, which makes them available to research groups with limited resources. There are numerous examples of genetic associations that have been identified through this method, including the *ApoE4* allele with sporadic Alzheimer's disease,[456] *PPARγ* gene with type 2 diabetes[457] and *NOD2* with Crohn's disease.[458, 459] However, despite these successful applications, there are several weaknesses to the candidate gene methodology. A major limitation of candidate gene studies lies with the selection of the genes themselves. The success of this approach depends upon the correct choice of genes or pathways to study, which requires an intimate knowledge of the biological function of the relevant proteins. Given the complex nature of the disease or trait phenotypes being studied, this selection criterion is exposed to the risk of arbitrariness.

3.5.5 Summary

Identifying genes involved in normal CCT variation could ultimately lead to an improved understanding of the genetic architecture of OAG, an outcome that would be of enormous clinical value. Of the 17 genes investigated in this candidate gene study, there is strong evidence to support *COL1A1* and *COL1A2* as genes involved in CCT determination, whilst the findings from *FBN1* and *PAX6* also warrant further investigation. This is the first published record of any gene found to influence normal variation of this trait. By utilising a tag SNP methodology, both single SNP and haplotype analyses were able to identify variants within these genes that are associated with CCT, although the actual causative variants remain unknown. This is a relative weakness of the tag SNP approach and further work is required to confirm the causative variants from both genes. Additional genotyping and functional studies

would also verify the findings presented here and improve our understanding of the mechanisms involved.

CHAPTER 4

INVOLVEMENT OF THE TYPE I COLLAGEN GENES IN THE DETERMINATION OF CENTRAL CORNEAL THICKNESS BY STUDYING HUMAN AND MOUSE OSTEOGENESIS IMPERFECTA

Publications arising from this chapter:

Dimasi DP, Chen JY, Hewitt AW, Klebe S, Davey R, Stirling J, Thompson E, Forbes R, Tan TY, Savarirayan R, Mackey DA, Healey PR, Mitchell P, Burdon KP, Craig JE. Novel quantitative trait loci for central corneal thickness identified by candidate gene analysis of osteogenesis imperfecta genes. *Hum Genet.* 2010 Jan; 127(1):33-44.

4.1 HYPOTHESIS AND AIMS

Results from the previous chapter indicated that common polymorphisms in the genes *COL1A1* and *COL1A2* are likely to be associated with normal CCT variation. However, the genetic data are preliminary and additional work is needed to verify the association of these genes with CCT. The known involvement of rare mutations in *COL1A1* and *COL1A2* with the disease osteogenesis imperfecta (OI) provides an avenue for further evaluating the role these genes play in CCT determination. Along with studying human cohorts of OI patients, examination of a mouse model of the disease would offer a unique opportunity to investigate the impact of specific mutations on corneal structure. This chapter will investigate the hypothesis that mutations in type I collagen cause a reduction in CCT and alterations in corneal collagen fibril structure in mice similar to what is observed in humans.

The specific aims investigated in this chapter were:

1. To measure CCT in an Australian cohort of OI patients.
2. To measurement CCT in a mouse model of OI.
3. To examine corneal collagen fibril diameter and density in the OI mouse using electron microscopy.

4.2 OVERVIEW

4.2.1 Osteogenesis imperfecta

OI is a rare, inherited connective tissue disorder characterised by increased bone fragility and low bone mass. It is caused by defects in the structure and synthesis of type I collagen, with approximately 90% of patients having mutations in either the *COL1A1* or *COL1A2* gene.[250-252] OI is a clinically heterogeneous disorder,

characterised by a broad range of signs and symptoms with extreme variation in severity. Whilst some forms of the disease are mild and have no apparent affect on quality of life, others can result in severe physical abnormalities and even perinatal mortality. Apart from its skeletal manifestations, other clinical findings can include hearing loss, dentinogenesis imperfecta, hyperlaxity of the ligaments and skin and blue sclerae. As previously discussed, an abnormally low CCT is another clinical finding associated with OI.[34, 35]

The most widely used classification method for OI was established by Sillence and colleagues and describes four main phenotypes, designated types I-IV, which were based on clinical, radiological and histopathological findings.[460] Recently, four further distinct OI phenotypes have been identified and termed types V-VIII.[461-464] The most common form of the disease is type I, in which patients typically present with a mild phenotype involving blue sclerae and no major bone or teeth deformities. Categorisation of OI patients into specific types can be useful to assess prognosis and evaluate treatment options. However, accurate early diagnosis of OI is often difficult, particularly in the absence of a positive family history or when bone fragility is not associated with obvious skeletal abnormalities. Clinicians often rely on the presence of extra-skeletal manifestations, such as blue sclerae and dentinogenesis imperfecta, to aid in their diagnosis. Whilst not currently considered a part of the diagnostic criteria for OI, CCT is an accurate, objective and clinically relevant measurement that merits further investigation in terms of its association with OI.

4.2.1.1 Mouse model of osteogenesis imperfecta

In order to facilitate investigation into the role of defective type I collagen on connective tissue formation and to potentially offer a means for trialling new therapies, several mouse models representing different forms of OI have been generated.[465] One such model is the *oim* mouse, which results from a single base deletion in *Col1a2* that causes a frameshift in the COOH-terminal portion of the protein.[466] Mice that are homozygous for the *oim* mutation have a complete deficiency of COL1A2 protein and exhibit a moderate to severe phenotype that is characterised by increased susceptibility to fractures, low bone density and skeletal deformities.[466] Heterozygotes exhibit a variable and intermediate phenotype.[467] Whilst the phenotype of the *oim* mouse has been well described, there is no published information available on the structural properties of the cornea.

4.3 METHODS

4.3.1 Ethics statement

Ethics approval for the human component of this study was obtained from the human research ethics committees of Flinders University and the Women's and Children's Hospital, Adelaide, Australia. This research adhered to the tenets of the Declaration of Helsinki and informed consent was obtained from all participants. Ethics approval for the mouse study was obtained from the Animal Welfare Committee of Flinders University.

4.3.2 Participant recruitment

4.3.2.1 Osteogenesis imperfecta cohort

Patients with type I OI were identified and recruited through the databases of the South Australian Clinical Genetics Service and the Flinders Eye Centre, Adelaide, Australia. Written consent was obtained from all participants. Medical histories were performed with particular attention to subtype of OI, symptoms of OI, height and number of fractures sustained. A detailed ocular history and ocular examination was performed on all participants and people who had anterior segment disease or previous refractive surgery were excluded from the study. CCT was measured using an SP-2000 ultrasound pachymeter (Tomey, Nagoya, Japan). Topical anaesthesia was administered as described in previous chapters. An average of 25 consecutive measurements were recorded in each eye, such that each recording had a standard deviation < 5μm. An individuals CCT was calculated as mean of both eye measurements.

4.3.2.2 Blue Mountains Eye Study

Recruitment and CCT measurement methodology for the BMES cohort, which was used as a control population, has been described in Chapter 2 (section 2.3.3.1.1).

4.3.3 Study design

The human studies involved measurement of CCT in a well-characterised cohort of Australian type I OI patients, representing the first analysis of CCT in a group of OI patients from this country. Apart from verifying the previously published results, the focus of this research was to assess the clinical relevance of this trait in the diagnosis and management of OI. In addition to the human study, the corneal properties of the *oim* mouse were also examined. To confirm the findings from human OI patients and

potentially facilitate functional studies, CCT and corneal collagen fibril diameter and density were measured in the *oim* mouse. A mouse model that exhibits a similar corneal phenotype to that seen in humans would allow further study of the factors that influence CCT.

4.3.4 Protocols for the human study

4.3.4.1 Statistical analysis

Comparison of mean CCT values in the OI and BMES cohorts was undertaken using a Mann-Whitney U test in SPSS v18.0 and statistical significance was accepted as $p < 0.05$.

4.3.5 Protocols for the *oim* mouse study

4.3.5.1 Mouse strain

The *oim* mouse strain (B6C3Fe *a/a-Col1a2*^{oim}/J) was sourced from the Jackson Laboratory (Bar Harbor, ME, USA). In order to establish a colony representing all three genotypes, heterozygous breeding pairs were obtained.

4.3.5.2 DNA extraction and genotyping

Genomic DNA was extracted from the tail tips of *oim* mice. Macerated tips were placed in 200 µl of 5% sterile Chelex resin (Biorad, Hercules, USA) supplemented with 10 µl of 10 mg/ml Proteinase K (Sigma-Aldrich, St. Louis, USA). Samples were incubated at 55°C overnight, followed by vortexing, further incubation at 100°C for 8 minutes and a final vortex step. The samples were then centrifuged at 13,000 g for 3 minutes and the supernatant harvested, with this step repeated to obtain the final purified DNA.

The *oim* mutation at position 3983 of *Col1a2* was genotyped in all mice by direct sequencing. PCR was performed using 50 ng of genomic DNA, 0.5 U of HotStarTaq polymerase (Qiagen, Venlo, Netherlands), 1x Qiagen PCR buffer, 0.1mM final concentration of each dNTP, 10 pM of each oligonucleotide primer and water to a total volume of 20 µl. Primers were manufactured by Geneworks (Adelaide, Australia) and sequences were as follows :

Forward: (5')- GCCTTCTGTGGAGTTTCCAG

Reverse: (5')- TCGGAGACACTCAAATCAAAAA

Thermal cycler conditions involved an initial activation step of 95°C for 5 minutes, followed by 35 cycles of 94°C for 30 seconds, 52°C for 30 seconds and 72°C for 30 seconds. Final extension was 72°C for 5 minutes. The PCR products were analysed by electrophoresis on a 1% agarose gel with an expected product size of 367 base pairs. PCR products were purified for sequencing by incubating with 5 U of Shrimp Alkaline Phosphatase and 10 U of Exonuclease I (GE Healthcare Life Sciences, Uppsala, Sweden) at 37°C for 1 hour, followed by heat inactivation at 80°C for 20 minutes. Sequencing was performed on an ABI 3100 Genetic Analyzer (Applied Biosystems, Carlsbad, USA) and the data analysed using Sequence Scanner v1.0 software (Applied Biosystems).

4.3.5.3 Measurement of central corneal thickness

CCT was measured in both male and female *oim* mice at 8 weeks of age, with the researcher blinded to genotype. The protocol has been previously described in detail in Chapter 2.3.4.1.

4.3.5.4 Electron microscopy of the mouse cornea

Eight-week-old male and female *oim* mice, representing both the wild-type and homozygous mutant genotypes, were selected for electron microscopy of the cornea. Mice were sedated with inhaled isofluorane before being euthanased via cervical fracture. One eye from each animal was removed, bisected and fixed overnight (~27 hrs) in 2.5% glutaraldehyde fixative in 0.1 M phosphate buffer, pH 7.4. Subsequently, the specimens were post-fixed in 1% osmium tetroxide in de-ionised water, dehydrated and embedded in epoxy resin using standard techniques.[468]

Samples were initially semithin-sectioned to ensure the cornea was cut transversely and that the central region was included in the plane of section. Subsequently, random representative corneal samples were ultrathin-sectioned and stained with uranyl acetate and lead citrate, again using standard techniques.[468] From each cornea, five random areas in each of the anterior and posterior regions were photographed at a standard magnification of X52,000 to give a total of 10 images. Images were captured on 8.3 by 10.2 cm Kodak 4489 electron microscope film (Eastman Kodak, Rochester, USA). To facilitate image measurements, negatives were scanned, converted to digital images at 600 dpi and printed on plain A4 paper at a final magnification of X104,000. All preparation and imaging procedures were conducted by the Department of Anatomical Pathology, Flinders University, Adelaide, Australia.

Collagen fibril diameter was measured manually on the printed images; each fibril was measured in two opposing planes and the mean diameter calculated. One hundred fibrils were measured in both the anterior and posterior stroma and the mean diameter was calculated for each eye. Collagen fibril density was calculated by

taking the mean of the total number of fibrils in two regions selected randomly on the printed images representing 0.5µm x 0.5µm squares in the original section. Density was measured in both the anterior and posterior stroma and the numbers combined to give a mean for each eye.

4.3.5.5 Statistical Analysis

Association of age, weight and CCT with the mouse genotype was tested using a Kruskal-Wallis test, whilst sex distribution was assessed using a chi-square test. Comparison of collagen fibril diameter and density between the wild-type and mutant strains was undertaken using a Mann-Whitney U test. All statistical analyses were performed in SPSS v18.0, with statistical significance accepted as $p < 0.05$.

4.4 RESULTS

4.4.1 Measurement of central corneal thickness in Australian osteogenesis imperfecta patients

Characteristics of the BMES cohort have been described previously. Briefly, the BMES comprised 956 individuals aged 60 to 95 (mean 73.8) years and 60.1% of participants were female. A total of 28 Australian type I OI patients, ranging from 5 to 59 (mean 34.1) years, were recruited. The mean CCT in the OI group was significantly lower than that in the BMES population (450.7 ± 42.8 µm versus 539.6 ± 32.7 µm [$p < 0.001$]) (Figure 4.1). Extremely thin CCT readings were also more evident in the OI patients, with 23 (82.1%) having readings < 500 µm, four of which were < 400 µm. In contrast, 104 (11%) participants in the BMES cohort had CCT readings < 500 µm and none had a reading < 400 µm.

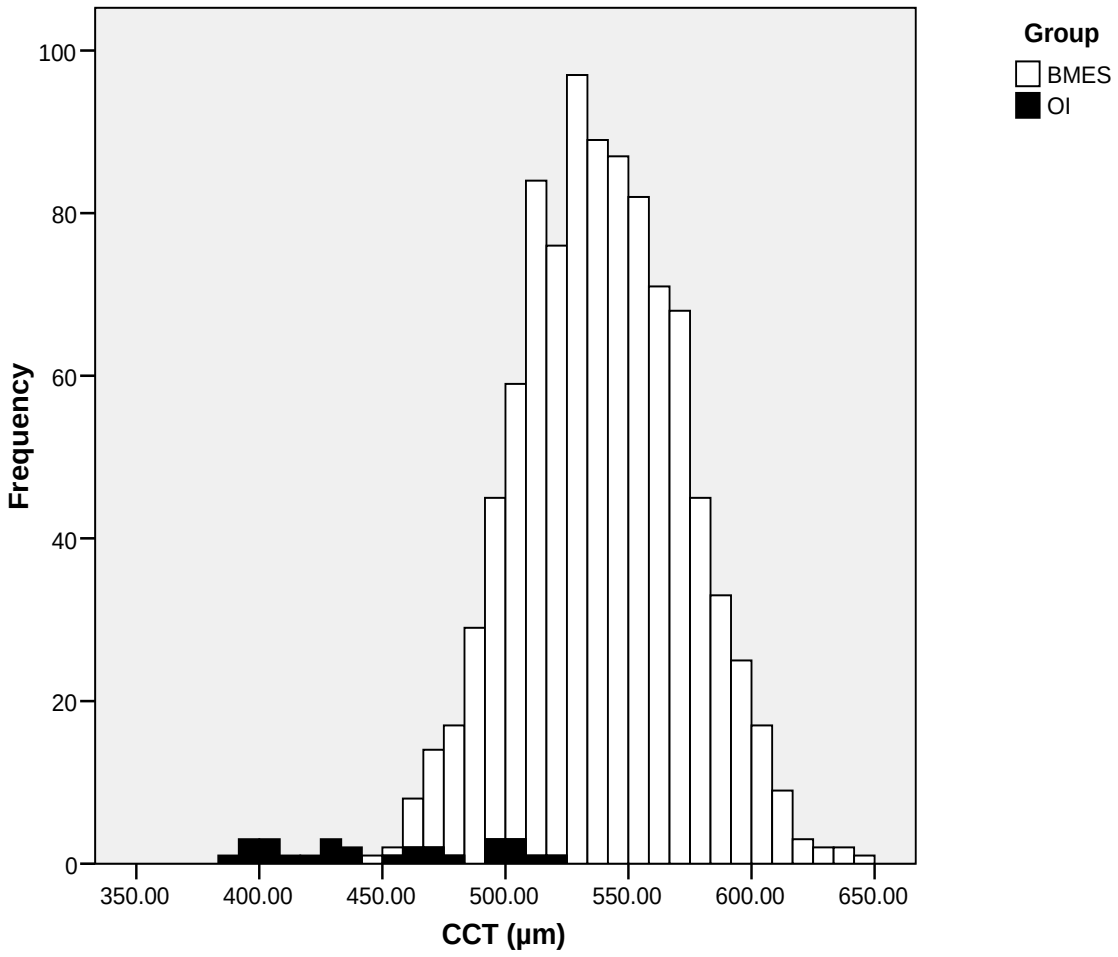

Figure 4.1: Histogram showing distribution of CCT in human cohorts. Type I osteogenesis imperfecta patients (OI) are represented by the black bars while the Blue Mountain's Eye Study (BMES) participants are white. Mean CCT values are as follows: OI = 450.7 ± 42.8 µm; BMES = 539.6 ± 32.8 µm.

4.4.2 Mouse results

4.4.2.1 Measurement of central corneal thickness in the oim mouse

In total, 61 *oim* mice had CCT measurements taken, of which 10 were homozygous mutants (*oim/oim*), 32 were heterozygous (wt/*oim*) and 19 were wild-type (wt/wt) animals (Table 4.1). More males than females were represented in both the wt/wt and wt/*oim* mice but this trend was not significant ($p = 0.249$). Ages were similar across all genotypes ($p = 0.383$). A significant difference was found between the mean weights of the different genotypes ($p = 0.004$) with *oim/oim* mice being significantly lighter than wt/wt litter mates, as has been previously reported.[466]

Mean CCT measurements by genotype are shown in Figure 4.2. Exact values are: wt/wt = 87.7 ± 9.3 μm; wt/*oim* = 80.7 ± 9.4 μm; *oim/oim* = 74.5 ± 7.3 μm. There was a significant association of CCT with genotype ($p = 0.002$). There was an evident allele dosage effect, with each mutant *oim* allele contributing to a reduction in CCT, thereby resulting in the heterozygous mice having an intermediate CCT and the homozygous mice having the thinnest. Addition of each *oim* mutant allele resulted in a 7.8% reduction in CCT. There was no correlation between weight of the mouse and CCT, as calculated by using Pearson's correlation coefficient ($p = 0.676$).

4.4.2.2 Corneal collagen fibril diameter in the oim mouse

Eyes from three wt/wt and four *oim/oim* mice were assessed for collagen fibril diameter by electron microscopy (Figure 4.3A). There was no statistically significant difference in the diameter of collagen fibrils measured in the anterior and posterior segments of the corneal stroma within the wt/wt (anterior = 27.8 ± 3.8 nm; posterior = 27.9 ± 3.9 nm [$p = 0.827$])

Table 4.1: Characteristics of the *oim* mice

Genotype	Total Mice	Females (%)	Males (%)	Mean Age (days)	Mean Weight (grams)
wt/wt	19	8 (42.1)	11 (57.9)	54.6	24.6
wt/*oim*	32	13 (40.6)	19 (59.4)	53.6	23.5
oim/oim	10	5 (50)	5 (50)	55.7	20.1

The sex, age and weight of the *oim* mice from each respective genotype.

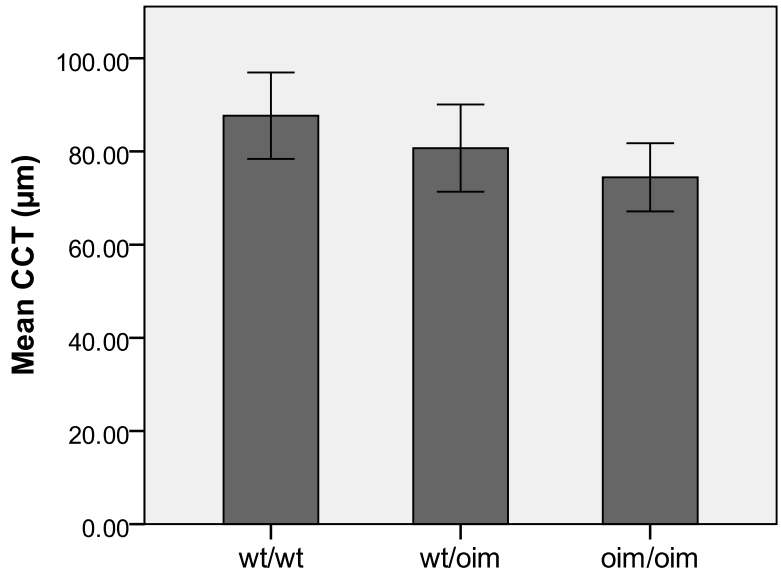

Figure 4.2: Mean CCT values for each genotype of *oim* mouse. The wt/wt mice (n = 19) had the thickest CCT, followed by the wt/*oim* (n = 32) and *oim/oim* mice (n = 10). There was a 13.2 µm difference in mean CCT between the wt/wt and *oim/oim* mice. The difference in CCT between genotypes was significant as assessed by a Kruskal–Wallis test (p = 0.002). Error bars indicate standard deviation.

and *oim/oim* mice (anterior = 23.7 ± 9.8 nm; posterior = 23.5 ± 3.4 nm [p = 1.0]) (Figure 4.3B). Mean collagen fibril diameters for each genotype are shown in Figure 4.3D. Exact values are: wt/wt = 26.8 ± 2.7 nm; *oim/oim* = 22.8 ± 0.7 nm. This represented a significant 14.9% difference in collagen fibril diameter between wt/wt and *oim/oim* mice (p = 0.034).

4.4.2.3 Corneal collagen fibril density in the oim mouse

Collagen fibril density was measured in the anterior and posterior segments of the corneal stroma in the same eyes used for the fibril diameter readings. There was a statistically significant difference in the fibril density between the anterior and posterior segments of the stroma in the wt/wt (anterior = 480.3 ± 20.5 fibrils/μm^2; posterior = 356.7 ± 44.3 fibrils/μm^2 [p = 0.05]) mice but no difference was observed in the *oim/oim* mice (anterior = 521.5 ± 34.7 fibrils/μm^2; posterior = 481.5 ± 33.9 fibrils/μm^2 [p = 0.773]) (Figure 4.3C). Mean collagen fibril density for each genotype is shown in Figure 4.3E. Exact values are: wt/wt = 418.5 ± 34.2 fibrils/μm^2; *oim/oim* = 498.5 ± 53 fibrils/μm^2. There was a significant 19.1% difference in collagen fibril density between wt/wt and *oim/*oim mice (p = 0.034).

4.5 DISCUSSION AND SUMMARY

4.5.1 Assessment of central corneal thickness in human osteogenesis imperfecta

Despite the existence of a well-characterised classification system, diagnosis of OI and categorization of patients into specific groups remains difficult. It is generally recognized that the different OI phenotypes represent a continuum of disease severity, rather than distinct groups, thus classification of patients is often

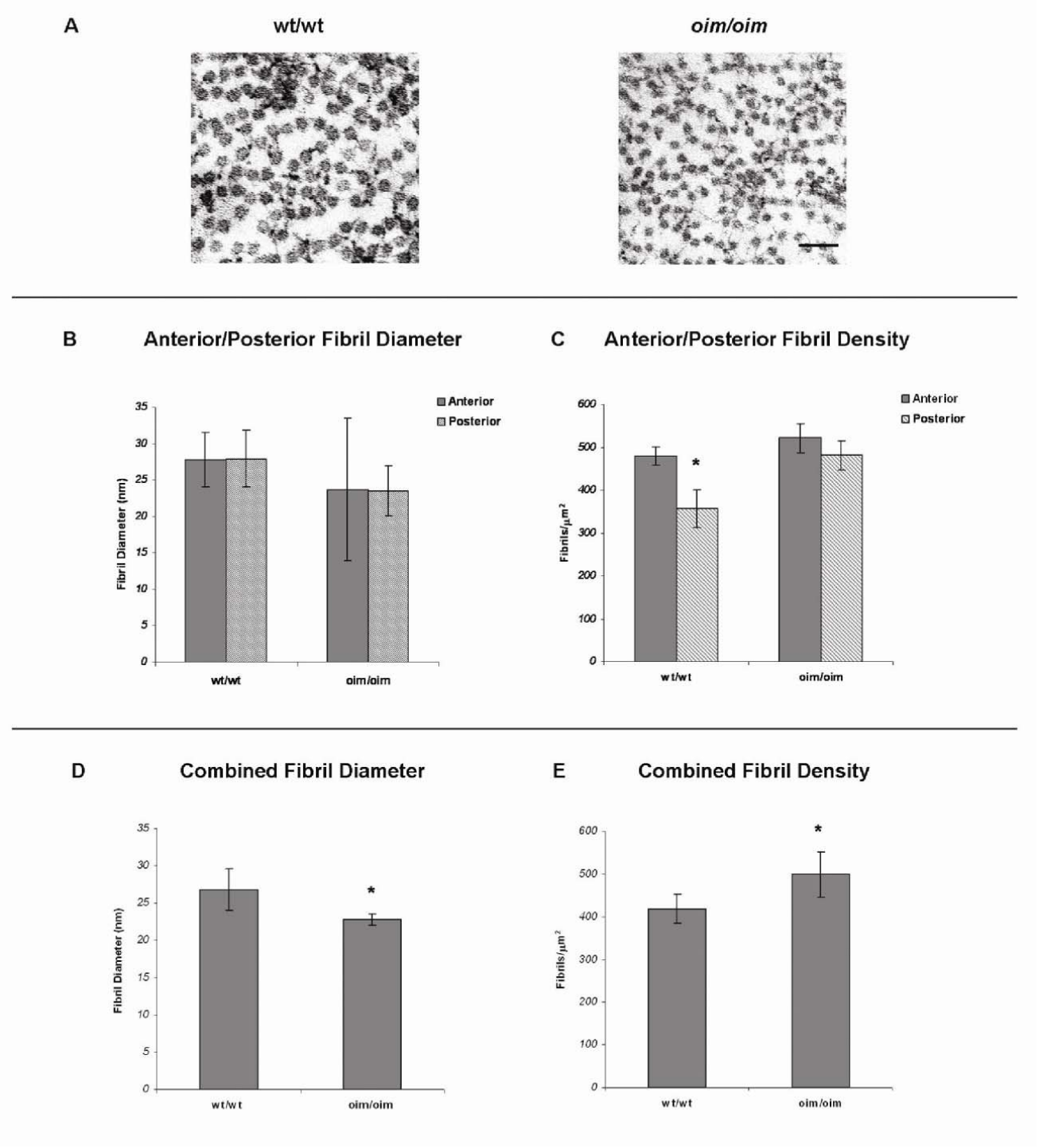

Figure 4.3: Collagen fibril diameter and density in the corneal stroma of *oim* mice. (see next page for legend)

Figure 4.3: Collagen fibril diameter and density in the corneal stroma of *oim* mice. (A) Transmission electron micrographs of collagen fibrils in the corneal stroma of wt/wt and *oim/oim* mice. Bar = 100 nm. **(B)** Mean collagen fibril diameter in the anterior and posterior segments of the corneal stroma as seen in the wt/wt and *oim/oim* mice. **(C)** Mean collagen fibril density in the anterior and posterior segments of the corneal stroma as seen in the wt/wt and *oim/oim* mice. **(D)** Combined anterior and posterior collagen fibril diameter measurements for the wt/wt and *oim/oim* mice. **(E)** Combined anterior and posterior collagen fibril density measurements for the wt/wt and *oim/oim* mice. Error bars indicate standard deviation. * = statistically significant difference between the two groups at the $p < 0.05$ level.

problematic. Whilst our cohort only contained type I OI patients, Evereklioglu *et al* found that CCT was significantly lower in type I OI when compared to type IV, suggesting that CCT may correlate with specific subgroups.[35] There are also several other primary skeletal disorders that can be confused with OI including Bruck syndrome, Osteoporosis-pseudoglioma syndrome, Cole-Carpenter syndrome and idiopathic juvenile osteoporosis.[469] Accurate diagnosis and classification of OI relies on several clinical features and our data have demonstrated that including CCT may enhance the diagnostic criteria, with mean CCT significantly lower by 84.6 μm in OI patients when compared to the normal BMES population cohort. It is likely, however, that this difference is an underestimation, as CCT has been shown to decline slightly with age in the BMES cohort and the mean age of the OI cohort is 39.7 years lower than that of the BMES.[235] These findings are consistent with previous published work but are the first to describe CCT in Australian type I OI patient.[34, 35]

The genetic architecture of OI is complex, with a large spectrum of mutations identified in both *COL1A1* and *COL1A2*. As of September 2010, the online resource termed the 'Database of Collagen Mutations' lists a total of 1067 variants that have been found in the type I collagen genes and associated with OI (http://www.le.ac.uk/genetics/collagen/).[470] Genotype-phenotype correlations have been demonstrated and certain types of mutations have been connected with specific forms of OI, although findings in this area are often unpredictable.[251, 471, 472] Type I OI exhibits autosomal dominant inheritance and is often caused by null mutations in

COL1A1, although missense mutations in either of the type I collagen genes have also been associated with this form of the disease.[251, 471-473] Due to their large size and the extent of genetic heterogeneity, screening *COL1A1* and *COL1A2* is an expensive and time-consuming process and as a consequence, the mutation status of the OI patients assessed in this study is unknown. Therefore, it is uncertain which of the genes is responsible for the reduction in CCT seen in the cohort, although it is clear that alterations in type I collagen have a major effect on this trait.

4.5.2 Structural properties of the cornea in the *oim* mouse

Data from the *oim* mouse support evidence from the genetic and human OI studies that the type I collagen genes are involved in CCT determination. In particular, results from the mouse study directly implicate *Col1a2* as a gene that is integral to the structural properties of the mouse cornea. Both the wt/*oim* and *oim/oim* mice exhibited a significant reduction in CCT when compared to the wt/wt animals, with a notable allele dosage effect resulting in each *oim* allele contributing to an incremental decrease in CCT. The corneal phenotype of the *oim* mouse is consistent with the hypothesis that mutations in type I collagen will cause a reduction in CCT similar to what is observed in human OI patients. This possibly reflects similarities in the genetic architecture, with the *oim* mouse and type I OI typically being caused by frameshift mutations.[473-475]

As the corneal phenotype of the *oim* mouse had not previously been investigated, the stromal collagen fibril diameter and density was analysed in order to determine the structural corneal features associated with this model of OI. Corneal collagen fibril diameter was smaller in the *oim/oim* mice compared to the wt/wt animals. This

reflects other studies that have found corneal stromal collagen fibrils to be 25% narrower in human OI patients compared to controls.[255, 413] In contrast, it was interesting to note that the higher corneal collagen fibril density in the *oim/oim* mice contrasts with the cardiac results of Weis *et al.*, who found that fibril density was 38% lower in the cardiac tissue of *oim/oim* mice compared to wt/wt animals.[476] The increase in fibril density in the *oim/oim* mice compared to the wt/wt animals is an interesting and unexpected outcome. It could be speculated that the cornea compensates for reduced collagen fibril diameter by increasing the total number of fibrils, although this is in disagreement with the findings of Weis *et al*. This discrepancy may be explained by the vastly different nature of cardiac and corneal tissue. The arrangement of collagen fibrils in the cornea is absolutely unique, as this tissue is highly specialised in its requirement for transparency. The corneal stroma has a structure of lamellae consisting of densely packed bundles of collagen fibrils of uniform shape and diameter. Variability in the shape of some of the fibrils seen in Figure 4.3A is most likely due to the fibril not being in the transverse orientation when the section was cut, but other factors such as precursor collagen filament packing or immature collagen fibril cross-linking may also be responsible.

The data from the *oim* mouse are consistent with the hypothesis that this model would exhibit a corneal phenotype similar to that seen in human OI. The advantage of this finding is that there is a known mutation in the *oim* mouse, in contrast to our human cohort. The mouse data confirm that murine CCT is influenced by a mutation in *Col1a2* and the mechanism by which the mutation affects overall CCT is governed by alterations in both collagen fibril diameter and spacing. It also provides us with a mouse model for reduced CCT and the ability to further investigate the ocular

implications of this trait. Preliminary work has begun on utilising the *oim* mouse in a rodent model to examine the response of the retina to light stimuli following acute elevation of IOP. Whilst not a glaucoma model, the acute elevations in IOP are designed to evaluate how the retina and its composite tissues respond to such an insult, which may reflect how chronic increases in IOP can cause visual loss in OAG.[477] In collaboration with Dr. Bang Bui and his laboratory in the Department of Optometry and Vision Sciences at the University of Melbourne, both homozygous wild-type and mutant *oim* mice will be assessed in this model to ascertain whether there is correlation between CCT and the response to acute IOP elevation. If results from this study demonstrate that the mutant *oim* mice have a greater susceptibility to damage induced by elevated IOP, then it would be evidence of a direct biological link between the physical properties of the cornea and retina. Such a conclusion would have implications for the assessment of CCT as a risk factor for OAG.

4.5.3 *COL1A1* and *COL1A2* as open-angle glaucoma susceptibility genes

The type I collagen genes represent plausible susceptibility loci for OAG. Type I collagen is known to be expressed in tissues that are of importantce in the development of OAG, such as the lamina cribrosa and peripapillary sclera.[264] The thickness of the peripapillary sclera and its surrounding posterior scleral tissue have been associated with OAG risk,[266-268] whilst the lamina cribrosa is acknowledged as one of the initial sites of glaucomatous damage.[69-72] The presence of blue sclerae in type I OI is an indication of a thin scleral wall, which could conceivably act as a surrogate for a thin posterior sclera, including the peripapillary tissue adjacent to the optic nerve and the lamina cribrosa. Given that type I OI is caused by mutations in *COL1A1* and *COL1A2*, it is possible that variants in these genes are also involved in

the determination of scleral thickness, thus providing a potential mechanism for an association of these genes with OAG. The planned experiments with the *oim* mouse and the acute IOP challenge model could assist in determining if the type I collagen genes are genuine candidates for increasing OAG susceptibility. Screening of the positive SNPs identified in the candidate gene study in an OAG cohort would also help to establish if *COL1A1* and *COL1A1* are associated with the disease. These experiments would contribute to conclude if CCT is an endophenotype for OAG.

4.5.4 Summary

The results presented in this study demonstrate that CCT is significantly thinner in Australian type I OI patients when compared to normal population controls. Many of the clinical signs of OI, including skeletal abnormalities, can be ambiguous or difficult to detect. Blue sclerae may be a common occurrence in healthy infants and its diagnosis is notoriously subjective, dental abnormalities are present in only 30% of all OI patients and hearing loss is rare in children.[478, 479] Given that CCT is an easily obtainable, safe and objective measurement, incorporating this parameter into existing diagnostic algorithms for OI may aid in accurate diagnosis and possibly subclassification. Additionally, these findings have implications for OAG screening in OI patients. Optometrists and ophthalmologists need to be aware of the association between very low CCT and OI to avoid incorrect measurement of IOP and consequent late glaucoma diagnosis and management in OI patients, which could lead to poor visual outcomes.

The primary purpose of investigating CCT in the human and mouse OI cohorts was to find support for the outcomes of the candidate gene study, where *COL1A1* and

COL1A2 were identified as genetic determinants of normal CCT variation. Results from the human OI study confirm that this disorder is associated with a considerable reduction in CCT and although the exact mutations are not known, defects in the synthesis and organisation of type I collagen are likely to be responsible. Future studies could involve sequencing of OI patients to find if any correlations are evident between specific mutations and corneal thickness. Of perhaps more relevance however, are the findings from the *oim* mouse, where a known mutation in *Col1a2* was demonstrated to have a significant impact on CCT, collagen fibril diameter and collagen fibril density in a way that mimicked the human phenotype. Taken collectively, the data from human OI patients, the *oim* mouse and the genetic studies of normal individuals strongly implicate *COL1A1* and *COL1A2* as important determinants of CCT.

CHAPTER 5

GENOME WIDE ASSOCIATION STUDY TO FIND THE GENETIC DETERMINANTS OF NORMAL CENTRAL CORNEAL THICKNESS VARIATION

Publications arising from this chapter:

Yi Lu, **David P Dimasi**, Pirro G Hysi, Alex W Hewitt, Kathryn P Burdon, Tze'Yo Toh, Jonathon B Ruddle, Yi Ju Li, Paul Mitchell, Paul R Healey, Grant W Montgomery, Narelle Hansell, Timothy D Spector, Nicholas G Martin, Terri L Young, Christopher J Hammond, Stuart Macgregor, Jamie E Craig, David A Mackey. Common Genetic Variants Near the Brittle Cornea Syndrome Locus ZNF469 Influence the Blinding Disease Risk Factor Central Corneal Thickness. *PLoS Genetics.* May 13; 6(5):e1000947

5.1 HYPOTHESIS AND AIMS

Whilst the identification of *COL1A1* and *COL1A2* as CCT genes was a significant finding from the candidate gene study, it is likely that additional genes with perhaps greater effect sizes remain to be characterised. Another approach that can be used to identify genetic loci associated with a disease or trait is the genome-wide association study (GWAS). The research conducted in this chapter was based on the hypothesis that further novel genetic loci associated with normal CCT variation could be identified through a GWAS. The aim was to conduct such a study in local cohorts and meta-analyse GWAS data from multiple cohorts in order to increase the likelihood of finding novel CCT genes.

5.2 OVERVIEW

Population-based association studies currently present an effective approach for finding the genetic determinants of complex traits such as CCT. Several categories of population-based association studies are available, including the candidate gene methodology that was applied in Chapter 3. As evidenced by the results from the candidate gene study, this technique can be hit-or-miss, as selection of specific genes based on biological function can be rather arbitrary. The GWAS is another form of population-based association analysis, which interrogates the entire genome looking for associations of a set of wide-spread genetic markers with the phenotype of interest, rather than just focusing on selected candidate genes. This is a key advantage of the GWAS, in that no *a priori* hypothesis is required about what genes to may be involved and theoretically, any region within the genome could provide a positive signal regardless of what is understood about it function. In recent years, the

GWAS has become a prominent feature of genetics research and in excess of 300 loci associated with common diseases and traits have been identified.[480]

5.2.1 Genome-wide association studies

As with any association study, the basic premise behind a GWAS is to determine the genotypes of markers in a population or cross-sectional cohort and then look for correlations between these marker genotypes and the phenotype of interest, whether it be a disease or quantitative trait. The genetic marker of choice for all recent GWA studies is the SNP, as these are the most common form of variation found within the genome and current technology permits economical genotyping of hundreds of thousands of SNPs in a single experiment. Although some studies have successfully used SNP sets consisting of variants within genes,[481, 482] GWA studies generally aspire to survey all variation within the genome, including non-coding regions. In order to achieve this, genotyping of up to 1 million SNPs can be undertaken, although this is dependent on the technology used.

The concept of LD is fundamental to the application of a GWAS. It enables the majority of variation within the genome to be assessed by genotyping only a subset of the polymorphic loci. This redundancy in the genome is perhaps best illustrated by the fact that within Caucasian populations, genotyping of approximately 500,000 tag SNPs selected from HapMap is sufficient to capture the majority of the 10 million total SNPs.[407] The design of a GWAS can vary according to the number of SNPs chosen and the criteria used for their selection. Some studies select SNPs that are evenly physically spaced,[195, 483, 484] whereas others choose SNPs to maximise the detection of LD based on data from the HapMap project.[485, 486] In order to undertake

the large-scale genotyping required for a GWAS, 'chip'-based technologies are employed, in which arrays of hybridisation assays are embedded on glass slides.

Perhaps one of the most pertinent issues for any GWAS is its power, which depends on the sample size, the effect size of the risk variant and its frequency. Most common diseases and quantitative traits have complex architectures, for which the phenotype is determined by the interactions between multiple genetic and environmental factors.[487] As a consequence, the genetic variants that contribute to the disease or trait are likely to have only small or modest effects on the final phenotype. Therefore, in order to detect theses variants, large sample sizes are crucial. The ability to identify the causal variants is also reliant on the coverage of the genome provided by the genotyped SNPs, with the required sample size increasing proportionately to the degree of LD between the marker SNP and causal SNP.[480] Another factor that must be considered when assessing the power required for a GWAS is correction for multiple testing. Due to the large number of hypotheses being tested, a p value of $< 5x10^{-08}$ is generally accepted as showing genome-wide significance following Bonferroni correction for 1 million SNPs.[194] Achieving such a threshold requires a well-powered study.

5.3 METHODS

5.3.1 Ethics statement

Ethics approval for the BMES (see Chapter 2.3.1), NSA and AU twin and UK twin cohorts (see Chapter 3.3.1) has been described previously. Ethics approval for Flinders Medical Centre CCT cohort was obtained from the human research ethics

committees of Flinders University and the Southern Adelaide Health Service. Each study adhered to the tenets of the Declaration of Helsinki.

5.3.2 Participant recruitment

5.3.2.1 BMES, NSA, AU twin and UK twin cohorts

Recruitment and DNA extraction methodologies for the BMES (see Chapter 2.3.3.1.1 and Chapter 3.3.3.1.1), NSA (see Chapter 3.3.3.2.1) and AU twin and UK twin cohorts (see Chapter 3.3.3.2.3) have been described previously.

5.3.2.2 Flinders Medical Centre CCT cohort

Participants from the NSA cohort with CCT values in the extreme upper and lower quintiles (above the 80th or below the 20th percentile points) were utilised in the creation of another cohort to be screened in the GWAS, termed Flinders Medical Centre CCT (FMC_CCT). In the extreme upper quintile, all participants had a CCT above 568.5 μm, whilst all participants in the extreme lower quintile had a CCT below 511 μm. Additional unrelated Caucasian individuals with CCT measurements that were in the range of these upper and lower quintile limits were recruited from the Flinders Eye Centre, Adelaide, Australia. The measurement methodology for these additional participants was identical to that used for the NSA cohort. Venous blood samples were collected in 9-ml EDTA tubes from all participants in the FMC_CCT cohort and stored at 4ºC until required.

5.3.3 Study design

The initial phase of the GWAS for CCT involved the use of two cohorts, the BMES and FMC_CCT. For the BMES samples, DNA had previously been extracted and was available for use in the GWAS. However, at the time of the study, DNA

extraction had yet to be undertaken on the entire FMC_CCT cohort, although blood samples were accessible. In order to facilitate a case-control design, the BMES and FMC_CCT cohorts were initially divided into the upper and lower quintiles of the CCT distribution, as was performed for the candidate gene analysis. A study by Jawaid *et al* found that segregating a distribution into quintiles was the optimal fraction for mapping of quantitative trait loci in an association study.[488] Rather than perform individual genotyping on each sample, a pooling strategy was utilised. Pooling of DNA samples has been demonstrated to significantly reduce the amount of genotyping required to perform a GWAS, thus making the technique available to laboratories with limited resources.[489, 490] A DNA pooling strategy was utilised with the BMES cohort. The efficacy of extracting DNA from pooled blood samples for use in a GWAS has recently been verified, so this technique was used for the FMC_CCT samples.[491] The results from the BMES and FMC_CCT pooled analyses were then combined in a meta-analysis. To increase the power of the study, the meta-analysed pooling results were then combined with genotyping data from the AU and UK twin cohorts. Both of the twin cohorts had undergone an individually genotyped GWAS, with access to these data permitted through the aforementioned collaboration with the Department of Genetics and Population Health at the QIMR. The top candidate SNPs from both of these meta-analyses were then subjected to individual genotyping in all the BMES and NSA samples. The study protocol is summarised in Figure 5.1.

5.3.4 Construction of DNA pools

Following segregation of the 956 BMES samples into the extreme upper and lower quintiles of the normal CCT distribution, there were 188 samples assigned to each

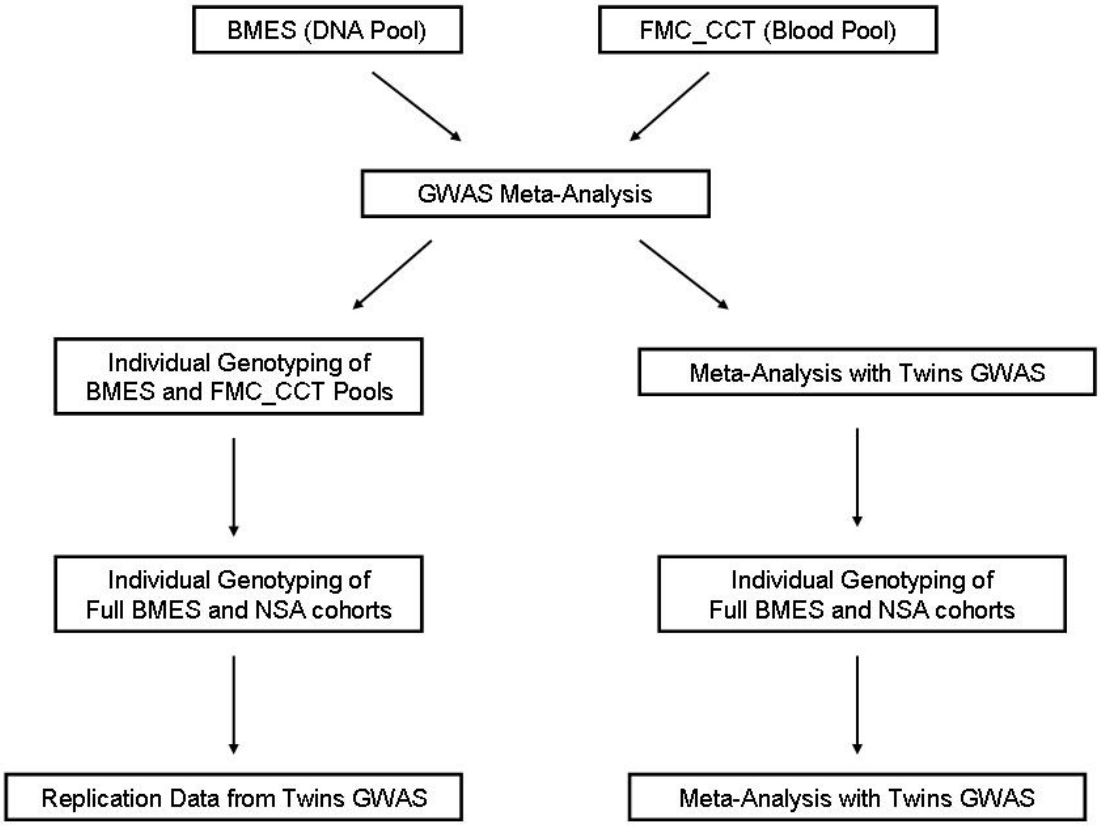

Figure 5.1: Flow-chart of GWAS study design.

group. In practice, sufficient quality DNA was only available for 146 individuals in the upper quintile and 143 individuals in the lower quintile. The drop-out due to insufficient or poor quality DNA was random with respect to phenotype, suggesting the effective sample size of the entire cohort was approximately 737 (145/188*956 = 737). The samples available in the upper and lower quintiles were used in the construction of their respective DNA pools.

The construction of pools from the BMES samples required the addition of equal amounts of DNA from each individual. Therefore, an accurate quantitation of the each individual DNA sample was necessary, which was achieved through the use of the Quant-iT™ PicoGreen® dsDNA reagent (Invitrogen, Carlsbad, USA). The PicoGreen reagent is a fluorochrome that selectively binds double-stranded DNA and has the advantage of producing little background due to the unbound dye having virtually no fluorescence. The Fluoroskan® Ascent microplate fluorometer (ThermoFisher Scientific, Waltham, USA) was used to measure the fluorescence readings from the PicoGreen® assay.

Preparation of a DNA standard for the PicoGreen® assay was undertaken using a stock of 100 ng/µl Lambda DNA (Invitrogen, Carlsbad, USA). The stock DNA was diluted to 1 ng/µl in pH 8.0 TE buffer, which was then serially diluted to the following concentrations: 0.5 ng/µl; 0.25 ng/µl; 0.125 ng/µl; 0.1 ng/µl; 0.05 ng/µl; 0.025 ng/µl; 0.01 ng/µl; 0.005 ng/µl; 0.0025 ng/µl. The standards were all prepared 24 hours prior to the PicoGreen® assay and left at room temperature overnight to promote a homogenous solution.

The genomic DNA samples to be included in the pools were initially quantitated using a spectrophotometer. The DNA was then diluted into a 96 well plate according to its concentration. The dilution procedure is shown below:

< 175 ng/µl = neat (80 µl DNA)

175-300 ng/µl = 1:1 (60 µl DNA + 80 µl TE buffer)

300-600 ng/µl = 1:2 (40 µl DNA + 80 µl TE buffer)

> 600 ng/µl = 1:3 (25 µl DNA + 75 µl TE buffer)

These samples were then further diluted by a factor of 100 in TE buffer into a new 96 well plate. This dilution was also prepared 24 hours prior to the assay. To prepare the DNA for PicoGreen® quantitation, 25 µl of each DNA sample was loaded in duplicate onto a black OptiPlate (PerkinElmer, Waltham, USA), to which a further 25 µl of TE buffer was also added.

Prior to performing the quantitation assay, the PicoGreen® reagent was diluted by a factor of 200 in TE buffer pH 8.0. In order to create a standard curve and calibrate the instrument, the DNA standards were measured first, with 5 µl of each standard and 45 µl of TE buffer added to a black OptiPlate, with blanks also included. Each standard had four replicates. The PicoGreen® reagent reservoir and DNA standards plate were then placed in the Fluoroskan® Ascent microplate fluorometer and measurement was undertaken, with the excitation wavelength set between 475 to 505 nm and the emission wavelength at 520 to 550 nm. Following calibration of the instrument, all the genomic DNA plates were measured.

Based on the calculated concentration each sample was diluted to 75 ng/µl, whilst those with a concentration under 85 ng/µl were left neat. As with the first round of

quantitation, all samples were then diluted by a factor of 100 in TE buffer in a 96 well plate and quantitation measurements repeated. The DNA concentrations obtained following the second PicoGreen® assay were then used to construct the pools.

To create the pools the same amount of total DNA from each sample needs to be included. A minimum of 5 µl of each DNA stock was to be added to the final pool. This was to minimise the impact of pippetting error from using smaller volumes. To achieve this standard, 5 µl of DNA from the sample with the highest concentration was added to the pool. This determined the amount (nmol) of each sample. All samples with lower concentrations required the addition of more than 5 µl to achieve the identical amount of total DNA. Both the upper and lower quintile pools were created in triplicate.

5.3.5 Construction of blood pools

Within the FMC_CCT cohort, there were 105 individuals in the upper quintile group, of which 61 were part of the NSA cohort. The lower quintile consisted of 106 individuals with 49 of these originating from the NSA samples.

The blood samples that were used in the construction of the pools came from two separate sources. Approximately half of the bloods were frozen following cellular lysis as part of the QIAamp DNA blood maxi kit (QIAGEN, Valencia, USA) protocol. The remaining portion of the blood samples were fresh samples that had been stored at 4ºC in EDTA blood collection tubes. In order to create the pools, an equal volume of blood (100 µl) from each sample was combined in a tube and

carried through a DNA extraction protocol using the QIAamp DNA blood maxi kit. The fresh blood samples were taken through this entire process, whilst the frozen samples were added to the pools following the cellular lysis step. Each blood pool was created in duplicate.

5.3.6 Genotyping methodology and analysis

5.3.6.1 DNA and blood pools

Genotyping of the DNA and blood pools and analysis of the data for the GWAS was undertaken by the Department of Genetics and Population Health at the QIMR. These methods have been described in the study by Lu *et al* and are reproduced below.[363] Pooled DNA was genotyped in triplicate on Illumina Human 1M-Duo V3 arrays in the Department of Genetics and Population Health at the QIMR. The output of the raw red and green bead scores from the genotyping stage was available for the pooled data analysis. The same data processing protocol was applied to both cohorts, similar to the method described by Brown *et al*.[492] Before calibrating the raw scores, a number of SNPs with more than 10% negative scores on each array were excluded, as well as the SNPs with the sum of mean red and green scores across each array smaller than 1200. This step was included to ensure that the calibration was done on a pre-cleaned dataset. A normalization/correction factor (corr) was calculated by forcing the mean value of the pooling allele frequency to be 0.5 over all SNPs on each stripe (Illumina Human 1M-Duo V3 array has 6 stripes on a single array). The pooling allele frequency (PAF) was then estimated based on the raw red intensities and the corrected green intensities for all the SNPs [PAF = red/(red+green/corr)]. A final set of autosomal SNPs met the following criteria: more than 5 probes in each pool; with a MAF greater than 1%; without a significant variance difference between

case and control pools (i.e., the log10 transformed *p* values from an F test on the ratio of case control pool variances were smaller than 6), was taken forward to a linear regression model.[493] The total number of SNPs to pass quality control from the BMES DNA pool was 837,061, whilst 784,932 SNPs passed quality control from the FMC_CCT blood pool. The underlying concept was to regress the pooling allele frequency on the case/control status for each SNP and estimate the pooling error across all the SNPs, as described in previous studies.[493, 494] The *p* value from comparing the test statistic described in MacGregor *et al* ($T_{2\text{-}x}$) to $X^2_{(1)}$ distribution was computed to assess the significance of allele frequency difference between the two pools (d).[493]

5.3.6.2 AU and UK twin cohorts

Full description of the genotyping and data analysis methodology for the AU and UK twins can be found in Chapter 3.3.5.4.

5.3.6.3 Individual genotyping of BMES, FMC_CCT and NSA samples

All genotyping in individual BMES, FMC_CCT and NSA samples was performed using the Sequenom MassARRAY® platform (Sequenom, San Diego, USA) as described in Chapter 3.3.5.1.

5.3.7 Comparison of results from different study cohorts

Methods to compare the association results from cohorts with different study designs were conducted by the Department of Genetics and Population Health at the QIMR. These methods have been described in the study by Lu *et al* and are reproduced below.[363] Since the pooling design dichotomizes the quantitative trait of CCT as a

binary trait (case/control status), results from the pooling cohorts are not comparable with those from the twin cohorts. An alternative way of enabling such comparison is to transform the case/control frequency difference (*d*) to be the allelic effect (β), given information on the allele frequency (*p*) and the upper/lower threshold cutting up both tails (T_U/T_L). Following the concepts published by Jawaid *et al*,[488] the expected allele frequencies in the two pools are:

$$E(p_L) = \frac{N[[\Phi(\frac{T_L - \mu_{A1A1}}{\sigma_R})]P(A_1A_1) + \frac{1}{2}[\Phi(\frac{T_L - \mu_{A1A2}}{\sigma_R})]P(A_1A_2)]}{N\sum_G[\Phi(\frac{T_L - \mu_G}{\sigma_R})]P(G)}$$

where N is the sample size; Φ is the density function of standard normal distribution; T_U and T_L are the upper and lower thresholds; P(G) is the genotypic frequency; μ_G stands for the mean trait value for the corresponding genotype; $\sigma_R^2 = 1 - \sigma_Q^2$, assume no dominance effects for the QTL, then $\sigma_R^2 = 1 - 2pq\beta^2$ is the trait variance for each genotype. Thus the case control frequency difference between the two pools is $d = E(p_U) - E(p_L)$. It demonstrates the relation between the case control frequency difference (*d*) in a pooling design and the allelic effect (β) in a conventional design, given the allele frequency (*p*) and the upper/lower threshold (T_U / T_L). Based on the inverse function of *d*, the allelic effect can be obtained from the estimated frequency difference of the case control pools. These statistics were developed and performed by collaborators Dr. Stuart Macgregor and Ms. Yi Lu at the QIMR. As described earlier, the lower threshold in this study is the 20% quintile of the standard normal distribution and the 80% quintile for the upper threshold. The allele frequencies

estimated from the combined AU twin cohort were fitted as the allele frequency parameter, p in this context.

5.3.8 Meta-analysis methodology

By combining the results of two or more cohorts, a meta-analysis will considerably enlarge the overall sample size and increase the power to identify associations. As mentioned above, the mean CCT values were measured and standardized in the same way for all the cohorts. Since the sample size of each cohort was sufficiently large, the distributions of CCT values in all the cohorts were good approximations of CCT distribution for a normal Caucasian population when compared to published data.[109] These compatibilities ensured the comparison of the results from two or more cohorts in a single meta-analysis. The test statistic for the meta-analysis was as follows:

$$T = \frac{(\sum_i \beta_{Si} w_{Si})^2}{\sum_i w_{Si}},$$

with β as the allelic effect from sample Si and the weight w as its inverse variance and is expected to be distributed as a chi-square with 1 degree of freedom. The above test assesses the significance of the weighted effect size with respect to its combined variance and has the advantage of taking into account the direction of the allelic effect. Therefore, the reference alleles from all the samples were required to be coordinated before the meta-analysis. The weighted allele effect was used to calculate the percentage of CCT variance in the population that can be attributed to the variant of interest. This was performed using the following equation:

$$2p*(1-p)*\beta^2$$

where p is the minor allele frequency and β is the weighted allele effect. In this study, a small proportion (<1%) of SNPs with the ambiguous polymorphism types (A/T, C/G) were excluded prior to our main analyses.

5.3.9 Statistical analysis

All genetic association tests performed on individual genotyping in the BMES, FMC_CCT and NSA cohorts were undertaken using the software program PLINK v1.06 (http://pngu.mgh.harvard.edu/purcell/plink/).[450] The output of the PLINK analysis includes five different tests of association between a variant and the trait of interest. These include a basic allelic test (ALLELIC), dominant gene action (DOM), recessive gene action (REC), genotypic or additive test (GENO or ADD) and a Cochran-Armitage trend test (TREND). The Cochran-Armitage trend test is used in categorical data analysis when the aim is to assess for the presence of association between a variable with two categories and a variable with *k* categories. It modifies the chi-square test to incorporate a suspected ordering in the effects of the *k* categories of the second variable. One advantage of the Cochran-Armitage test is that it does not assume Hardy-Weinberg equilibrium, as the individual, not the allele, is the unit of analysis. The genotypic and additive tests provide a general test of association in the 2-by-3 table of trait-by-genotype. Adjustment for the covariates of age and sex was also undertaken using linear regression. Fisher's exact test was used in the calculation of the *p* value for each inheritance model. Any analysis involving the AU and UK twin cohorts was performed by the Department of Genetics and Population Health at the QIMR. Genome-wide statistical significance was accepted

as $p < 5 \times 10^{-08}$, whilst statistical significance in a replication cohort was accepted as $p < 0.05$.

5.4 RESULTS

5.4.1 Outcomes of the GWAS using pooling methodology

5.4.1.1 Meta-analysis of BMES and FMC_CCT pools

The results of the meta-analysis on the BMES and FMC_CCT pools are shown in Figure 5.2, with the top 10 SNPs by *p* value and their respective genes shown in Table 5.1. In total, there were four variants considered to be of genome-wide significance with *p* values below the 5×10^{-08} threshold. The most significant association was with SNP rs4516740, which is located at the 77.63 megabases (Mb) on chromosome 4 (human genome build 36.3) and is located within an intron of the *shroom family member 3* (*SHROOM3*) gene. The *p* value for rs4516740 was stronger in the FMC CCT pool than in the BMES pool.

5.4.1.2 Individual genotyping in pooling cohorts

In order to confirm the association results found in the meta-analysis, individual genotyping of the samples used to construct the pools was undertaken. The top 40 SNPs from the meta-analysis were selected along with a further 49 SNPs that were chosen based on several criteria including being located in cluster of multiple SNPs with *p* values of $<10^{-05}$ and then selecting the SNPs with the smallest *p* values from these regions. Additional SNPs were also selected from genes that are strong CCT candidates (eg *COL5A1*). The full list of selected SNPs and the genetic model giving the smallest *p* value for each is shown in Table 5.2.

Figure 5.2: Manhattan plot for meta-analysis of both pooling cohorts

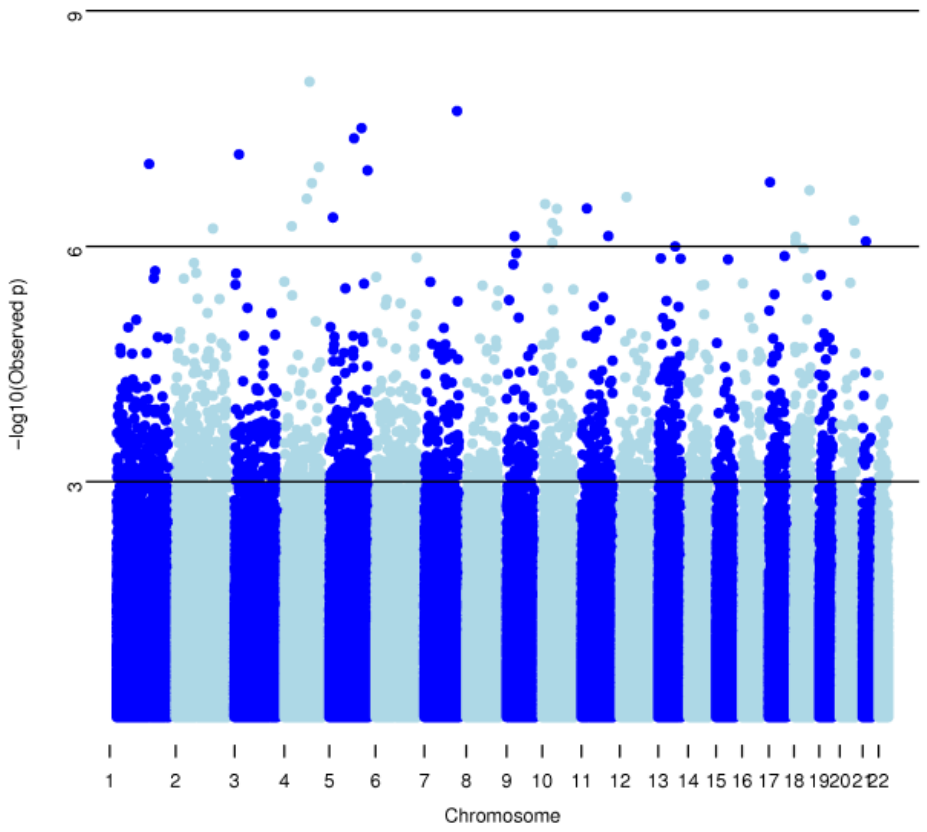

Table 5.1: Top genotyped SNPs from meta-analysis of both pooling cohorts

SNP	Chromosome	Gene	BMES *p* value	FMC_CCT *p* value	Meta-analysis *p* value
rs4516740	4	*SHROOM3*	0.0029	4.09E-07	**7.98E-09**
rs7809581	7	*LOC642663*	6.61E-05	7.29E-05	**1.89E-08**
rs6876787	5	*PRELID2*	4.83E-06	0.0013	**3.11E-08**
rs37369	5	*AGXT2*	0.004058	1.33E-06	**4.21E-08**
rs11928797	3	*UBP1*	6.74E-08	NR	6.74E-08
rs3753194	1	*EDG1*	0.0023	1.03E-05	8.93E-08
rs7679888	4	*DCLK2*	0.0008	3.05E-05	9.77E-08
rs9313984	5	*LOC391844*	0.0008	1.36E-05	1.08E-07
rs11552190	17	*HS3ST3B1*	0.0003	0.0002	1.52E-07
rs4956263	4	*DKK2*	1.57E-07	NR	1.57E-07

(see next page for legend to Figure 5.2 and Table 5.1)

Figure 5.2: Manhattan plot for meta-analysis of both pooling cohorts. The -log10 (observed p) value is plotted against position in the genome. Each chromosome is depicted in alternating colour for clarity. A -log10 (observed p) value >7.3 is considered genome-wide significant.

Table 5.1: Top genotyped SNPs from meta-analysis of both pooling cohorts. Results of allelic association tests for the ten most significant SNPs following meta-analysis of the BMES and FMC_CCT pooling cohorts. Values in bold are considered genome wide significant at the $p < 5 \times 10^{-08}$ level. CHR = chromosome; NR = no result.

Table 5.2: Association results from individual genotyping of the pooling samples. A total of 89 SNPs were selected for genotyping in the individual samples that comprise the BMES and FMC_CCT pooling cohorts based on the meta-analysed GWAS results from these pools. The association results for each cohort as well as a meta-analysis are depicted in the table. Only the model associated with the strongest *p* value for each SNP is shown. Values in bold were considered genome-wide significant at the $p < 5 \times 10^{-08}$ level. CHR = chromosome; DOM = dominant; GENO = genotypic; REC = recessive.

Table 5.2: Association results from individual genotyping of the pooling samples

SNP	CHR	Gene	Model	BMES *p* value	FMC_CCT *p* value	Meta-analysis *p* value
rs2785862	13	*CXXC6P1*	ALLELIC	3.70E-06	1.53E-05	**1.46E-10**
rs2785841	13	*CXXC6P1*	ALLELIC	5.92E-05	2.90E-05	**6.25E-09**
rs4254174	13	*CXXC6P1*	ALLELIC	0.0008	1.87E-05	**4.76E-08**
rs9522400	13	*LOC121727*	DOM	9.90E-05	0.007	2.75E-06
rs1869660	10	*LHPP*	TREND	0.0002	0.0123	6.65E-06
rs4516740	4	*SHROOM3*	TREND	0.0059	0.0005	1.32E-05
rs10764631	10	*APBB1IP*	TREND	0.0076	0.0004	1.36E-05
rs9522433	13	*LOC121727*	DOM	0.0005	0.0109	1.65E-05
rs7703260	5	*FGF1*	DOM	9.44E-05	0.0653	2.19E-05
rs12639868	4	*SHROOM3*	DOM	0.0192	0.0005	3.01E-05
rs7809581	7	*LOC642663*	TREND	0.0041	0.0034	3.69E-05
rs9555836	13	*CXXC6P1*	DOM	0.0018	0.011	4.07E-05
rs173269	17	*KCNJ2*	TREND	0.0102	0.0012	4.17E-05
rs33954	5	*FGF1*	DOM	0.0002	0.0716	5.41E-05
rs10761411	9	*WDR5*	DOM	0.0055	0.0079	8.27E-05
rs37369	5	*AGXT2*	TREND	0.3213	6.20E-06	0.00016
rs17055448	13	*LOC341689*	ALLELIC	0.0032	0.0223	0.0002
rs943051	13	*ATP12A*	TREND	0.0021	0.0323	0.0002
rs17021875	2	*MGAT4A*	DOM	0.1161	0.0003	0.0002
rs11893350	2	*LRRTM1*	TREND	0.0006	0.091	0.0002
rs7228576	18	*APCDD1*	TREND	0.0268	0.0028	0.0002
rs7985340	13	*LOC341689*	GENO	0.0137	0.0038	0.0003
rs296293	7	*LOC392027*	TREND	0.0042	0.0235	0.0003
rs11664141	18	*DLGAP1*	TREND	0.1493	0.0003	0.0004
rs11787841	9	*BRD3*	DOM	0.0148	0.0104	0.0004
rs28480505	19	*MEGF8/CNFN*	TREND	0.1077	0.0009	0.0004
rs1006607	2	*LRRTM1*	TREND	0.0013	0.0857	0.0004
rs1317617	10	*PPIF*	TREND	0.0002	0.3172	0.0005
rs1243977	10	*LOC389935*	ALLELIC	0.0715	0.0027	0.0006
rs7025493	9	*COL5A1*	TREND	0.0208	0.0122	0.0007

(see previous page for legend)

Table 5.2: ***continued***

SNP	CHR	Gene	Model	BMES *p* value	FMC_CCT *p* value	Meta-analysis *p* value
rs2823202	21	*LOC388814*	ALLELIC	0.0129	0.0214	0.0007
rs1243979	10	*LOC389935*	TREND	0.0773	0.0016	0.0008
rs11110622	12	*TMEM16D*	ALLELIC	0.1371	0.0035	0.0016
rs11055391	12	*C12orf36*	TREND	0.0278	0.027	0.0019
rs6772630	3	*SNX4*	TREND	0.0044	0.1423	0.0019
rs1780196	10	*PDSS1*	ALLELIC	0.0263	0.0511	0.0022
rs3765623	18	*MYOM1*	TREND	0.0108	0.0929	0.0025
rs8091028	18	*MYOM1*	TREND	0.019	0.0525	0.0025
rs9393469	6	*NRSN1*	TREND	0.0022	0.264	0.0027
rs17078802	13	*STARD13*	TREND	0.0018	0.3653	0.0027
rs7679888	4	*DCLK2*	TREND	0.1322	0.008	0.0035
rs7115499	11	*NEU3*	DOM	0.0002	1.0	0.0042
rs11186035	10	*LOC119358*	TREND	0.0343	0.0558	0.0044
rs11552190	17	*HS3ST3B1*	DOM	0.1172	0.0133	0.0047
rs9313984	5	*LOC391844*	TREND	0.0909	0.017	0.0048
rs9595630	13	*RP11-298P3.3*	TREND	0.1061	0.0158	0.0049
rs4844815	1	*LOC642587*	TREND	0.0488	0.0504	0.0055
rs11075421	16	*SALL1*	ALLELIC	0.0684	0.0661	0.0057
rs9966933	18	*DLGAP1*	ALLELIC	0.0954	0.042	0.0063
rs3753194	1	*EDG1*	TREND	0.2935	0.0014	0.0078
rs1550322	2	*ACVR2A*	TREND	0.613	0.0014	0.0111
rs6876787	5	*PRELID2*	TREND	0.0505	0.115	0.0124
rs2448111	10	*PDSS1*	TREND	0.0648	0.0974	0.0133
rs11142838	9	*C9orf71*	TREND	0.0803	0.0835	0.0136
rs9491952	6	*PTPRK*	TREND	0.0011	0.9326	0.0139
rs9482890	6	*PTPRK*	TREND	0.0142	0.3681	0.0145
rs16829978	1	*NEK7*	TREND	0.0049	0.4547	0.0162
rs12218866	10	*ZMIZ1*	TREND	0.0292	0.2863	0.0192
rs4420499	15	*PSTPIP1*	REC	0.1224	0.1133	0.0202
rs2788151	1	*LOC391158*	TREND	0.3072	0.0325	0.0252

CHR = chromosome; DOM = dominant; REC = recessive.

Table 5.2: *continued*

SNP	CHR	Gene	Model	BMES *p* value	FMC_CCT *p* value	Meta-analysis *p* value
rs1866131	2	*LOC375295*	TREND	0.2362	0.0456	0.0274
rs10059065	5	*LOC391845*	TREND	0.4797	0.0058	0.0293
rs1874161	5	*LOC345471*	TREND	0.1308	0.1194	0.033
rs6561355	13	*HTR2A*	TREND	0.1843	0.0875	0.033
rs8176257	17	*BRCA1*	DOM	0.8973	0.0042	0.0356
rs4894203	2	*LOC375295*	TREND	0.2994	0.0456	0.0358
rs4956263	4	*DKK2*	TREND	0.0074	0.8906	0.0409
rs11748189	5	*CLINT1*	TREND	0.1119	0.2101	0.0471
rs11661310	18	*KIAA1012*	TREND	0.5552	0.0222	0.0477
rs4148479	13	*ABCC4*	TREND	0.0092	0.9319	0.0536
rs12156626	9	*CYLC2*	TREND	0.0047	0.7631	0.0559
rs7924842	11	*LOC120364*	TREND	0.9636	0.0042	0.0562
rs1305870	13	*DCLK1*	ALLELIC	0.8325	0.0347	0.0588
rs948104	11	*DSCAML1*	TREND	0.4909	0.0515	0.0714
rs1849306	8	*LOC646721*	TREND	0.0021	0.4921	0.0738
rs11215675	11	*LOC283143*	TREND	0.0015	0.2839	0.0775
rs712328	14	*LOC729069*	DOM	0.8922	0.0223	0.0778
rs4987347	1	*SELL*	TREND	0.5581	0.0603	0.0799
rs2039062	13	*USP12*	DOM	0.3937	0.1517	0.0899
rs10515772	5	*EBF1*	TREND	0.1652	0.3164	0.0923
rs10520481	19	*PPP2R1A*	ALLELIC	0.1611	0.4714	0.1021
rs12725073	1	*ATP6V1G3*	TREND	0.3779	0.1646	0.1259
rs6849736	4	*SLC2A9*	TREND	0.7252	0.1017	0.1455
rs13283452	9	*PAPPA*	DOM	0.5268	0.1514	0.1551
rs7265317	20	*PROCR*	DOM	0.0698	0.7132	0.2699
rs34713965	4	*ABCE1*	GENO	0.1724	0.4998	0.3027
rs2561008	19	*ZNF534*	TREND	0.958	0.1127	0.3279
rs6579211	20	*TRPC4AP*	GENO	0.2353	0.5825	0.3416
rs9304376	18	*LOC729881*	GENO	0.4439	0.0092	0.3831

CHR = chromosome; DOM = dominant; GENO = genotypic.

The top three SNPs, which were all of genome-wide significance, were located at 88.19 - 88.22 Mb on chromosome 13. This area of the genome is in the 5' untranslated region of a putative pseudogene *CXXC finger 6 pseudogene 1* (*CXXC6P1*). The fourth SNP on the list, rs9522400, is located approximately 200 kilobases (kb) away from the *CXXC6P1* variants and is found within the 5' region of another pseudogene *peroxisomal biogenesis factor 12 pseudogene* (*LOC121727*). Another two SNPs from these pseudogenes, rs9522433 (*LOC121727*) and rs9555836 (*CXXC6P1*), were found in positions eight and twelve on the table respectively. The prominence of highly significant SNPs in these two adjacent pseudogenes, including three that demonstrated genome-wide significance, was strongly suggestive of a potential association with CCT in this area of the genome.

None of the genome-wide significant SNPs from the initial meta-analysis of the BMES and FMC_CCT pools retained this significance level following individual genotyping, although some did still exhibit strong association results. For example, the top variant following the meta-analysis of the pools, rs4516740 from *SHROOM3*, had the sixth strongest *p* value ($1.32 \times 10^{-05)}$ after individual genotyping. However, no other SNP that was in the top 10 following the meta-analysis remained in this group following the individual genotyping. The inconsistency between the pooling technique and the individual genotyping for some of the results demonstrates the effect that pooling errors can have on the outcomes of this form of analysis. This is well illustrated by the observation that none of the *CXXC6P1* SNPs were found in the top 40 following the meta-analysis of the pools but show clear genome-wide significance on individual typing.

5.4.1.3 Individual genotyping in the full BMES and NSA cohorts

The 43 SNPs with the strongest *p* values from the individual genotyping of the pool samples were then screened in the full BMES and NSA cohorts. Investigation in the full cohorts was able to increase power by yielding a combined sample size of 1,237 participants, as well as allowing for a quantitative analysis rather than a case-control design. Results can be found in Table 5.3. A *p* value adjusted for age and sex is also shown in the table, although in general, the adjustment had minimal impact. Four of the SNPs that were in the top 43 were not able to be genotyped due to not meeting design requirements or through assay failure on the Sequenom MassARRAY® platform and were thus replaced by the SNP with the next smallest *p* value.

As with the individual genotyping from the pool samples, the SNP with the most significant *p* value (1.61×10^{-06}) in the combined BMES and NSA cohorts was rs2785862 from the *CXXC6P1* pseudogene. However, this value did not reach genome-wide significance. The second most significant SNP, rs9522400, is situated near the *LOC121727* pseudogene, which is adjacent to *CXXC6P1* on chromosome 13. For both these variants, the BMES contributed the stronger signal, although this could largely be due to the increased sample size. The four remaining SNPs from these pseudogenes were all situated in the top 10 *p* values for the combined BMES and NSA analysis, thus providing further evidence that a variant(s) in this area of the genome is associated with CCT.

Several other genes of interest were also identified following genotyping in the full BMES and NSA cohorts. Two SNPs from the 141.88 – 141.90 Mb region on chromosome 5, rs33954 and rs7703260, had *p* values of 1.26×10^{-05} and 2.52×10^{-05} respectively, which were both in the top 10 most significant results. Both rs33954

Table 5.3: Results of association tests following individual genotyping in the full BMES and NSA cohorts. A total of 43 SNPs were selected for genotyping in the full BMES and NSA cohorts based on the results of the individual genotyping in the pooling samples. A meta-analysis of the BMES and NSA results was performed and this value was also adjusted for the covariates of age and sex. Only the model associated with the strongest *p* value for each SNP is shown. ADD = additive; CHR = chromosome; DOM = dominant; NR = no result; REC = recessive.

Table 5.3: Association results following individual genotyping in the full BMES and NSA cohorts

SNP	CHR	Gene	Model	BMES *p* value	NSA *p* value	Meta-analysis *p* value	Adjusted *p* value
rs2785862	13	*CXXC6P1*	DOM	6.94E-05	0.0051	1.61E-06	1.38E-06
rs9522400	13	*LOC121727*	DOM	7.42E-05	0.0275	6.50E-06	5.70E-06
rs33954	5	*FGF1*	DOM	4.78E-05	0.1166	1.26E-05	1.77E-05
rs173269	17	*KCNJ2*	ADD	0.0040	0.0002	1.27E-05	1.27E-05
rs9555836	13	*CXXC6P1*	DOM	0.0007	0.0059	1.39E-05	1.37E-05
rs9522433	13	*LOC121727*	DOM	0.0009	0.0037	1.85E-05	1.35E-05
rs7703260	5	*FGF1*	ADD	0.0009	0.0078	2.52E-05	2.31E-05
rs2785841	13	*CXXC6P1*	ADD	0.0006	0.0307	6.25E-05	5.61E-05
rs10764631	10	*APBB1IP*	ADD	0.0015	0.0307	9.38E-05	0.0001
rs4254174	13	*CXXC6P1*	ADD	0.0028	0.0280	0.0003	0.0002
rs1243977	10	*LOC389935*	ADD	0.0509	0.0060	0.0012	0.0011
rs37369	5	*AGXT2*	ADD	0.0972	0.0003	0.0013	0.0009
rs4516740	4	*SHROOM3*	DOM	0.0054	0.1241	0.0014	0.0017
rs11893350	2	*LRRTM1*	ADD	0.0017	0.3643	0.0015	0.0019
rs17078802	13	*STARD13*	ADD	0.0017	0.4139	0.0020	0.0011
rs1869660	10	*LHPP*	ADD	0.0122	0.0623	0.0021	0.0017
rs9393469	6	*NRSN1*	DOM	0.0012	0.5706	0.0022	0.0018
rs9595630	13	*RP11-298P3.3*	ADD	0.0461	0.0105	0.0023	0.0022
rs12639868	4	*SHROOM3*	DOM	0.0104	0.1274	0.0028	0.0033
rs8091028	18	*MYOM1*	ADD	0.0072	0.1929	0.0030	0.0030
rs1006607	2	*LRRTM1*	DOM	0.0028	0.4831	0.0030	0.0040
rs17055448	13	*LOC341689*	REC	0.0022	NR	0.0032	0.0035

(see previous page for legend)

Table 5.3: ***continued***

SNP	CHR	Gene	Model	BMES *p* value	NSA *p* value	Meta-analysis *p* value	Adjusted *p* value
11787841	9	*BRD3*	DOM	0.0011	0.9538	0.0041	0.0055
10761411	9	*WDR5*	DOM	0.0071	0.5775	0.0069	0.0094
28480505	19	*MEGF8/CNFN*	ADD	0.1927	0.0070	0.0075	0.0088
3765623	18	*MYOM1*	ADD	0.0046	0.7356	0.0091	0.0098
1317617	10	*PPIF*	DOM	0.0646	0.0752	0.0095	0.0117
4844815	1	*LOC642587*	DOM	0.0714	0.0376	0.0107	0.0100
7809581	7	*LOC642663*	ADD	0.0350	0.1302	0.0123	0.0099
7228576	18	*APCDD1*	ADD	0.1023	0.0433	0.0152	0.0146
11186035	10	*LOC119358*	ADD	0.0672	0.1292	0.0175	0.0157
7985340	13	*LOC341689*	DOM	0.0214	0.3383	0.0188	0.0123
9313984	5	*LOC391844*	DOM	0.0927	0.1631	0.0198	0.0282
1780196	10	*PDSS1*	ADD	0.0567	0.2410	0.0205	0.0292
11075421	16	*SALL1*	ADD	0.2811	0.0162	0.0247	0.0318
7025493	9	*COL5A1*	ADD	0.1241	0.0698	0.0262	0.0227
12218866	10	*ZMIZ1*	DOM	0.1027	0.2819	0.0507	0.0497
943051	13	*ATP12A*	ADD	0.0636	0.4870	0.0557	0.0497
6772630	3	*SNX4*	ADD	0.1067	0.3432	0.0691	0.0640
7115499	11	*NEU3*	ADD	0.0105	0.4050	0.0752	0.0816
11664141	18	*DLGAP1*	DOM	0.6336	0.0325	0.1397	0.1049
296293	7	*LOC392027*	DOM	0.2525	0.3659	0.1542	0.1500
11110622	12	*TMEM16D*	DOM	0.4387	0.3594	0.2644	0.2270
7679888	4	*DCLK2*	DOM	0.3209	0.6685	0.2724	0.2632

ADD = additive; CHR = chromosome; DOM = dominant.

and rs7703260 are found in the 3' untranslated region of the *fibroblast growth factor 1* (*FGF1*) gene. The SNP with the fourth strongest association, rs173269, is found in the 66.02 Mb region of chromosome 17 and is located within the 3' untranslated sequence of the *potassium inwardly-rectifying channel, subfamily J, member 2* (*KCNJ2*) gene.

5.4.1.4 Replication data from the AU and UK twin cohorts

Given that none of the SNPs from the individual genotyping in the full BMES and NSA cohorts demonstrated genome-wide significance, it would be prudent to conclude that no novel genetic determinants of CCT were identified from this analysis. However, many SNPs showed significance levels that were suggestive of an association, but perhaps through lack of power, could not reach the level of genome-wide significance. In order to investigate whether a genuine association may be evident, genotyping data were obtained from the GWAS of the AU and UK twin cohorts. The results of this examination can be found in Table 5.4. Only three variants from the meta-analysis of the twin cohorts had *p* values below the significance threshold of 0.05. These were rs7703260 from *FGF1*, rs939346 from *neurensin 1* (*NRSN1*) and rs1186035 from *LOC119358*. No SNPs from the *CXXC6P1* or *LOC121727* pseudogenes showed any sign of an association with CCT in the twin data.

5.4.2 Outcomes of the GWAS following meta-analysis of the twin and pooling cohorts

5.4.2.1 Meta-analysis of twin and pooling GWAS data

In order to increase the power of this study, a meta-analysis of the GWA studies performed on the AU and UK twin cohorts and the BMES and FMC_CCT pools was

Table 5.4: Association results in the AU and UK twin cohorts

SNP	Gene	Flinders *p* value	Twins *p* value	SNP	Gene	Flinders *p* value	Twins *p* value
rs2785862	*CXXC6P1*	1.61E-06	0.369	11787841	*BRD3*	0.004	0.153
rs9522400	*LOC121727*	6.50E-06	0.416	10761411	*WDR5*	0.007	0.347
rs33954	*FGF1*	1.26E-05	0.337	28480505	*MEGF8/CNFN*	0.008	NR
rs173269	*KCNJ2*	1.27E-05	NR	3765623	*MYOM1*	0.009	0.559
rs9555836	*CXXC6P1*	1.39E-05	0.866	1317617	*PPIF*	0.01	0.249
rs9522433	*LOC121727*	1.85E-05	0.625	4844815	*LOC642587*	0.011	0.538
rs7703260	*FGF1*	2.52E-05	**0.024**	7809581	*LOC642663*	0.012	0.266
rs2785841	*CXXC6P1*	6.25E-05	0.211	7228576	*APCDD1*	0.015	0.975
rs10764631	*APBB1IP*	9.38E-05	0.498	11186035	*LOC119358*	0.018	**0.046**
rs4254174	*CXXC6P1*	0.0003	0.350	7985340	*LOC341689*	0.019	0.484
rs1243977	*LOC389935*	0.0012	NR	9313984	*LOC391844*	0.02	NR
rs37369	*AGXT2*	0.0013	0.667	1780196	*PDSS1*	0.021	0.759
rs4516740	*SHROOM3*	0.0014	0.109	11075421	*SALL1*	0.025	NR
rs11893350	*LRRTM1*	0.0015	0.248	7025493	*COL5A1*	0.026	0.367
rs17078802	*STARD13*	0.0020	0.344	12218866	*ZMIZ1*	0.051	0.514
rs1869660	*LHPP*	0.0021	0.600	943051	*ATP12A*	0.056	0.965
rs9393469	*NRSN1*	0.0022	**0.050**	6772630	*SNX4*	0.069	NR
rs9595630	*RP11-298P3.3*	0.0023	0.396	7115499	*NEU3*	0.075	0.906
rs12639868	*SHROOM3*	0.0028	0.121	11664141	*DLGAP1*	0.14	0.756
rs8091028	*MYOM1*	0.0030	0.704	296293	*LOC392027*	0.154	NR
rs1006607	*LRRTM1*	0.0030	NR	11110622	*TMEM16D*	0.264	0.270
rs17055448	*LOC341689*	0.0032	0.990	7679888	*DCLK2*	0.272	NR

Table depicts the top candidate SNPs from the pooling analysis and their corresponding *p* value from meta-analysis of the full BMES and NSA data (Flinders *p* value). SNPs are ordered according to their Flinders *p* value. The allelic association *p* value from meta-analysis of the AU and UK twin data is also given (Twins *p* value). Values in bold were considered significant at the $p < 0.05$ threshold. NR = no result (this was a consequence of the SNP not being genotyped on the twin array).

undertaken. The results of the meta-analysis are shown in Figure 5.3, with the top 10 SNPs and their respective genes shown in Table 5.5. In total, there were two SNPs considered to be of genome-wide significance with *p* values below the 5 x 10^{-08} threshold. The most significant association was with SNP rs2755237, which is located at 40.01 Mb on chromosome 13 within the 3' untranslated region of the *forkhead box class O1* (*FOXO1*) gene. The significance level for rs2755237 was almost equivalent in AU and UK twins, although the results in the BMES and FMC_CCT pools did not show clear evidence for replication. The other genome-wide significant SNP was rs12447690, which is located at 86.85 Mb on chromosome 16 and is located approximately 140 kb from the *zinc finger protein 469* (*ZNF469*) gene. A much stronger association was found with this variant in the UK twin cohort when compared to the AU twins and as with rs2755237, the SNP did not reach the 0.05 significance threshold in the BMES and FMC_CCT pools. Another SNP found in the 3' untranslated region of *FOXO1*, rs2721051, had a *p* value that was just below the genome-wide significance level. This SNP is in high LD with rs2755237 (r^2 > 0.8) and the results suggest that these SNPs are tagging a variant or variants within the vicinity of the *FOXO1* gene that is associated with CCT.

5.4.2.2 Individual genotyping of pooling samples

To clarify the results found in the meta-analysis and to eliminate the influence of pooling error, individual genotyping of the pooling samples was undertaken. This analysis was designed to identify SNPs that demonstrated replication of the twins data and should subsequently be screened in the full BMES and NSA cohorts. The SNPs that were selected included those with the top 10 most significant association results from the meta-analysis of the twin and pool GWA studies, as seen in

Figure 5.3: Manhattan plot for meta-analysis of twin and pooling cohorts

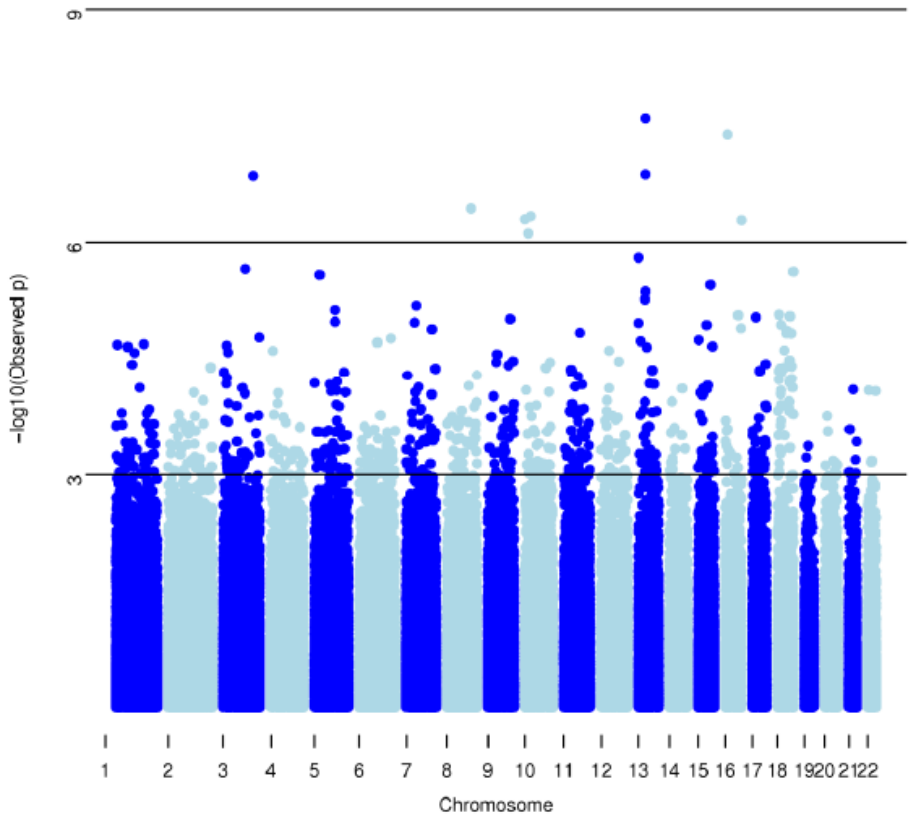

Table 5.5: Top genotyped SNPs from meta-analysis of twin and pooling cohorts

SNP	CHR	Gene	AU twin *p* value	UK twin *p* value	BMES *p* value	FMC_CCT *p* value	Meta-analysis *p* value
rs2755237	13	*FOXO1*	3.2E-04	1.3E-04	0.12	0.23	**2.5E-08**
rs12447690	16	*ZNF469*	3.7E-03	2.9E-08	0.52	0.92	**4.1E-08**
rs2721051	13	*FOXO1*	1.3E-04	9.9E-04	0.16	0.40	1.3E-07
rs7643363	3	*FNDC3B*	1.3E-02	9.7E-06	0.27	0.03	1.4E-07
rs6990252	8	*INDOL1*	5.4E-03	1.6E-05	0.37	0.41	3.7E-07
rs11245330	10	*FAM53B*	2.9E-04	4.0E-05	0.18	0.12	4.6E-07
rs1006368	10	*FAM53B*	2.8E-04	4.2E-05	0.21	0.15	5.0E-07
rs9938149	16	*ZNF469*	2.6E-03	5.3E-06	0.28	0.93	5.2E-07
rs10901827	10	*FAM175B*	7.6E-04	7.1E-05	0.04	0.04	7.7E-07
rs1034200	13	*FTHL7*	4.5E-06	1.5E-01	0.06	NR	1.6E-06

(see next page for legend to Figure 5.3 and Table 5.5)

Figure 5.3: Manhattan plot for meta-analysis of twin and pooling cohorts The -log10 (observed p) value is plotted against position in the genome. Each chromosome is depicted in alternating colour for clarity. A -log10 (observed p) value >7.3 is considered genome-wide significant.

Table 5.5: Top genotyped SNPs from meta-analysis of twin and pooling cohorts. Results of allelic association tests for the ten most significant SNPs following meta-analysis of the twin and pooling data. Values in bold were considered genome-wide significant at the $p < 5 \times 10^{-08}$ level. CHR = chromosome; NR = no result.

Table 5.5. Another 12 SNPs were selected based on several criteria, including strength of association results from the aforementioned meta-analysis and location within an identified candidate gene (eg *ZNF469, COL5A1*). The results can be seen in Table 5.6. The most significant *p* value following combination of the BMES and FMC_CCT data came from the *FGF1* SNP rs7703260, which along with the next four strongest variants (rs1034200, rs2585243, rs1323168, rs7044529) was selected for genotyping in the full BMES and NSA cohorts. Due to the strong evidence for an association with CCT following meta-analysis of the twin and pooling GWAS data, two SNPs from *FOXO1* (rs2755237, rs2721051) and two SNPs from *ZNF469* (rs12447690, rs9938149) were also selected for the next phase of screening.

5.4.2.3 Meta-analysis of individual genotyping data from the twin, BMES and NSA cohorts

To further increase the available sample size, individual genotyping of SNPs of interest was undertaken in the full BMES and NSA cohorts. Apart from increasing sample size, examining the full cohorts allowed for analysis of CCT as a quantitative trait rather than a case-control design, which was consistent with the twins methodology. An additional 594 samples were included from the BMES and 175 from the NSA cohort, yielding overall cohort sizes of 956 and 281 respectively. Meta-analysis of these data with those from the twins was able to further increase the power of the study, with a total cohort size of 4,710 participants, made up of the following: AU twins – 1,714; UK twins – 1759; BMES – 956; NSA – 281. A total of nine SNPs were selected based on the results from the prior genotyping assay. The results can be seen in Table 5.7. Four SNPs showed genome-wide significant results, with rs12447690 from *ZNF469* again having the strongest *p* value of 1.3×10^{-12} and an allele effect size of 0.168. Both the BMES ($p = 2.8 \times 10^{-04}$) and NSA ($p = 0.025$)

Table 5.6: Additional results from individual genotyping of the pooling samples

SNP	CHR	Gene	Model	BMES *p* value	FMC_CCT *p* value	Meta-analysis *p* value
rs7703260	5	*FGF1*	DOM	9.44E-05	0.065	2.19E-05
rs1034200	13	*FTHL7*	REC	0.055	0.052	0.004
rs2585243	15	*LASS3*	DOM	0.032	0.052	0.004
rs1323168	13	*FGF9*	DOM	0.012	0.187	0.005
rs7044529	9	*COL5A1*	GENO	0.194	0.025	0.005
rs746987	18	*VPS4B*	DOM	0.055	0.093	0.008
rs7643363	3	*FNDC3B*	ALLELIC	0.11	0.049	0.01
rs12301696	12	*TMTC2*	DOM	0.068	0.102	0.011
rs2721043	13	*LOC646982*	ALLELIC	0.21	0.084	0.027
rs2721051	13	*FOXO1*	DOM	0.079	0.181	0.0273
rs6990252	8	*INDOL1*	DOM	0.050	0.575	0.057
rs12447690	16	*ZNF469*	DOM	0.041	0.777	0.087
rs7204132	16	*ZNF469*	TREND	0.01	0.765	0.104
rs2755237	13	*FOXO1*	TREND	0.324	0.207	0.105
rs4894535	3	*FNDC3B*	REC	0.329	0.369	0.111
rs1393945	15	*LASS3*	DOM	0.07	0.889	0.132
rs17138064	17	*LOC727853*	TREND	0.304	0.273	0.138
rs9938149	16	*ZNF469*	TREND	0.028	0.777	0.146
rs9965653	18	*hCG_1659830*	TREND	0.196	0.774	0.241
rs10901827	10	*FAM175B*	DOM	0.77	0.328	0.327
rs11245330	10	*FAM53B*	DOM	0.664	0.378	0.369
rs1006368	10	*FAM53B*	TREND	0.568	0.489	0.374

An additional 22 SNPs were selected for individual genotyping in the BMES and FMC_CCT pools samples based on the meta-analysed GWAS results from the twin and pooling cohorts. The association results for each cohort as well as a meta-analysis are depicted in the table. Only the model associated with the strongest *p* value for each SNP is shown. CHR = chromosome; DOM = dominant; GENO = genotypic; REC = recessive.

Table 5.7: Meta-analysis of association results from the twin, BMES and NSA cohorts

			AU twin		UK twin		BMES		NSA		Meta-analysis	
SNP	**CHR**	**Gene**	***p* value**	**Effect (SE)**	***p* value**	**Effect (SE)**	***p* value**	**Effect (SE)**	***p* value**	**Effect (SE)**	***p* value**	**Effect (SE)**
rs12447690	16	*ZNF469*	3.7E-03	0.122 (0.04)	2.9E-08	0.209 (0.04)	2.8E-04	0.183 (0.05)	2.5E-01	0.105 (0.09)	**1.3E-12**	0.168 (0.02)
rs9938149	16	*ZNF469*	2.6E-03	0.125 (0.04)	5.3E-06	0.210 (0.05)	1.1E-03	0.158 (0.05)	2.5E-01	0.105 (0.09)	**2.6E-10**	0.157 (0.02)
rs2721051	13	*FOXO1*	1.3E-04	-0.253 (0.07)	9.9E-04	-0.196 (0.06)	3.5E-03	-0.224 (0.08)	6.5E-01	-0.063 (0.14)	**1.0E-08**	-0.210 (0.04)
rs1034200	13	*FTHL7*	4.5E-06	0.199 (0.04)	1.5E-01	0.070 (0.05)	1.4E-04	0.195 (0.05)	7.7E-01	-0.028 (0.09)	**4.6E-08**	0.142 (0.03)
rs2755237	13	*FOXO1*	3.2E-04	0.200 (0.06)	1.3E-04	0.240 (0.06)	1.3E-01	0.100 (0.07)	3.2E-01	0.109 (0.11)	1.1E-07	0.177 (0.03)
rs7044529	9	*COL5A1*	5.3E-02	-0.107 (0.06)	9.6E-04	-0.168 (0.05)	1.3E-02	-0.169 (0.07)	2.5E-01	-0.148 (0.13)	3.8E-06	-0.147 (0.03)
rs7703260	5	*FGF1*	3.0E-01	0.057 (0.05)	3.6E-02	0.107 (0.05)	5.5E-04	0.210 (0.06)	7.0E-03	0.320 (0.12)	1.6E-05	0.132 (0.03)
rs2585243	15	*LASS3*	8.9E-02	0.073 (0.04)	6.8E-04	0.133 (0.04)	1.3E-01	0.080 (0.05)	1.7E-01	0.128 (0.09)	3.2E-05	0.102 (0.02)
rs1323168	13	*FGF9*	9.3E-03	0.163 (0.06)	9.6E-03	0.147 (0.06)	4.2E-02	0.152 (0.07)	6.6E-01	0.055 (0.13)	3.6E-05	0.146 (0.04)

Genotyping data from the AU and UK twins was combined with that from the full BMES and NSA cohorts for the nine SNPs indicated in the table. Allelic association results for each cohort and the meta-analysis are depicted, as well as the weighted allelic effect (Effect) with the standard error (SE) in parentheses. These results were adjusted for age and sex. Values in bold were considered genome-wide significant at the $p < 5 \times 10^{-08}$ level. CHR = chromosome.

results replicated those from the twins for rs12447690. Another SNP from *ZNF469*, rs9983419, also had a genome-wide significant *p* value of 2.6 x 10^{-10}. The *FOXO1* SNP rs2721051 reached genome-wide significance ($p = 1 \times 10^{-08}$), with a stronger association than that found following meta-analysis of the twin and pooling cohorts. Interestingly, the other *FOXO1* SNP, rs2755237, weakened following genotyping in the full BMES and NSA cohorts to the point where it was no longer genome-wide significant. The fourth genome-wide significant association was found with SNP rs1034200, which is located at the 22.1 Mb position on chromosome 13 and is situated within the 5' untranslated region of the pseudogene *ferritin, heavy polypeptide-like 7* (*FTHL7*). The strongest evidence for association was found in the AU twin and BMES cohorts, with an overall *p* value of 4.6 x 10^{-08}. There is some doubt as to the legitimacy of this result as the allele effect in the NSA group (-0.028) is in the opposite direction to all the other cohorts, which may be an indication of a false positive result. However, the standard error for this allele effect (0.09) is large enough that the actual direction may be the same as in the other cohorts. The mean CCT values of the genome-wide significant variants in the combined BMES and NSA cohort can be seen in Table 5.8.

5.5 DISCUSSION AND SUMMARY

While the results of the candidate gene study conducted in Chapter 3 were successful in identifying two CCT genes, it was hypothesised that much of the genetic architecture of CCT remained unknown. Therefore, in order to discover further novel genes, a GWAS was employed. The GWAS is a powerful method for discovering genetic loci associated with a particular disease or trait and was ideally suited for the study of CCT genetics due to the availability of several large and independent

Table 5.8: Mean CCT associated with genome-wide significant SNPs

Gene	SNP	Genotype	Frequency	Mean CCT ± SD (μm)
FOXO1	rs2721051	G/G	0.82	542.2 ± 32.8
		G/A	0.17	535.8 ± 34.7
		A/A	0.01	533 ± 29.5
FTHL7	rs1034200	G/G	0.53	538.6 ± 32.4
		G/T	0.39	541.8 ± 34
		T/T	0.08	550.1 ± 35.3
ZNF469	rs12447690	T/T	0.41	544.7 ± 33.4
		T/C	0.49	538.6 ± 33
		C/C	0.10	535 ± 31.1
	rs9938149	A/A	0.40	544.1 ± 33.7
		A/C	0.48	539.3 ± 32.9
		C/C	0.12	534.4 ± 31.4

Frequency and mean CCT of each genotype of the genome-wide significant SNPs following analysis in a combined cohort of the BMES and NSA samples.

cohorts. Three study populations were based at Flinders University, the BMES, NSA and FMC_CCT cohorts. Whilst these groups had a combined total of over one-thousand samples, further power for this study was achieved through collaboration with the Department of Genetics and Population Health at QIMR, whereby data from an individually genotyped GWAS on the AU and UK twin cohorts were used to perform a meta-analysis. The twin cohorts comprise a total of 3,473 participants, thus significantly increasing the ability of this study to detect a genetic association. A combination of pooled and individual genotyping strategies were used in an attempt to find additional genetic determinants of CCT.

5.5.1 GWAS methodology

Since the results of the first GWAS were published in 2002,[495] the use of this methodology has increased substantially. As of February 2011, the Catalogue of Genome-Wide Association Studies maintained by the National Human Genome Research Institute cites 796 published GWA studies since November 2008 (www.genome.gov/gwastudies).[496] The technique has had considerable success in identifying novel genetic associations with many diseases and traits, including cancer, diabetes, lipid levels, autoimmune disorders and gastrointestinal disorders to name a few.[497] The recent prominence of GWA studies can largely be credited to advancements in genotyping technology, which have led to significant improvements in data quality and cost and time efficiency.[497] With the advent of genotyping 'chips' developed by companies such Affymetrix and Illumina, it is now feasible to screen up to a million SNPs in large-scale cohorts consisting of thousands of DNA samples. Whilst the affordability of GWA studies has improved considerably, with an approximate 2,000 fold reduction in cost per genotype over the last ten years,[497]

utilisation of this technique is still not practical for all laboratories. For example, a GWAS employing individual genotyping of 2000 cases and 2000 controls would cost approximately US$1.8 million.[491] A potential solution to this problem lies with the use of pooling methodologies.

5.5.1.1 Pooling techniques for GWA studies

The use of pooling techniques for GWA studies were first pioneered with DNA, whereby equal amounts of DNA from multiple individuals were mixed into a single sample for genotyping.[490] The major benefit of conducting a pooled DNA analysis is the significant reduction in price when compared to individual genotyping. Whilst the savings are dependent on the number of samples in the pool, cost reductions of up to 20-fold have been demonstrated.[493] Numerous studies have confirmed the validity of the DNA pooling strategy, with results that are consistent with those obtained from individual genotyping.[493, 498] Recently, a new pooling strategy has been developed that incorporates the use of blood rather than DNA.[491] The blood pooling technique offers significant improvements in time efficiency and an estimated 120-fold reduction in price when compared to individual genotyping.[491] Importantly, blood pooling has been demonstrated to give results that are equivalent to DNA pooling and to replicate the findings of individually genotyped GWA studies.[491] However, pooling techniques are prone to several sources of error that can limit the precision of allele frequency estimation, including inaccuracies in pool construction, bias from poorly amplifying samples and differential allelic amplification. There are also restrictions on analytical methods that can be applied to pooling results, including haplotype construction, SNP imputation and case-control status while adjusting for covariates.[499] Given that the purpose of a pooling design is

to prioritise SNPs for further genotyping, all the aforementioned problems can be alleviated by downstream individual genotyping.

5.5.2 Findings from the GWAS for central corneal thickness

Analysis of the GWAS data was essentially divided into two phases. The first phase involved meta-analysis of the GWAS results from the pooled BMES and FMC_CCT cohorts, with subsequent individual genotyping of prioritised SNPs. Not only was this analysis aimed at identifying genes associated with CCT from the two population groups that were accessible at Flinders University, but it would also demonstrate the effectiveness of the pooling strategy. The second experimental phase involved further meta-analysis of the results from the BMES and FMC_CCT cohorts with GWAS data from the AU and UK twin studies, which was again followed by individual genotyping of prioritised SNPs. The inclusion of the twin cohorts was able to substantially increase the power of this study to find novel quantitative trait loci for CCT. Data from both of these analyses identified several genes or genomic regions of interest, with the most relevant results discussed below.

5.5.2.1 CXXC6P1/ LOC121727

Following individual genotyping of the top candidate SNPs in the BMES and FMC_CCT pool samples, a region of chromosome 13 that contained the pseudogenes *CXXC6P1* and *LOC121727* showed interest in terms of a potential association with CCT. Within a distance of 350,000 bp, a total of six SNPs with *p* values below 10^{-04} were identified, three of which were genome-wide significant (Table 5.2). Analysis of the LD structure of this region of the genome indicated an area of high LD, suggesting that these SNPs may be tagging the same causal variant

or variants (Figure 5.4). Further analysis of these SNPs in the full BMES and NSA cohorts demonstrated a decline in the strength of the association signal, although rs2785862 from *CXXC6P1* and rs9522400 from *LOC121727* still gave the strongest results, with *p* values of 1.61 x 10^{-06} and 6.50 x 10^{-06} respectively (Table 5.3). The results from individual genotyping in the full BMES and NSA cohorts, whilst not genome-wide significant, were consistent and indicated that the previous findings were not merely an artefact of the experimental design with the upper and lower quintiles. However, failure of any of these SNP associations to replicate in either of the twin cohorts suggests that these results could be false positives. Whilst the explanation for this is unclear, replication failure is a common problem with association studies, of which there are several potential causes.[500] One possibility is that a phenomenon known as cryptic population stratification could have caused the inconsistent results seen in the BMES, NSA and twin cohorts.[501] Cryptic population stratification arises from subtle differences in the ancestry of the populations used in the association analysis and whilst all the cohorts used in this study were Caucasian, it is possible that participants from these groups comprised a variety of ethnicities that could have contributed to some spurious associations. Whilst individual genotyping can account for population stratification using principal components analysis, pooling techniques cannot undergo such correction.

5.5.2.2 FTHL7

The *FTHL7* pseudogene was identified as a possible CCT gene following meta-analysis of the individual genotyping results from the BMES, NSA and twin cohorts. The SNP rs1034200 was found to have a genome-wide significant *p* value of 4.6 x 10^{-08}, with an allele effect size of 0.142. There is some doubt as to the validity of this

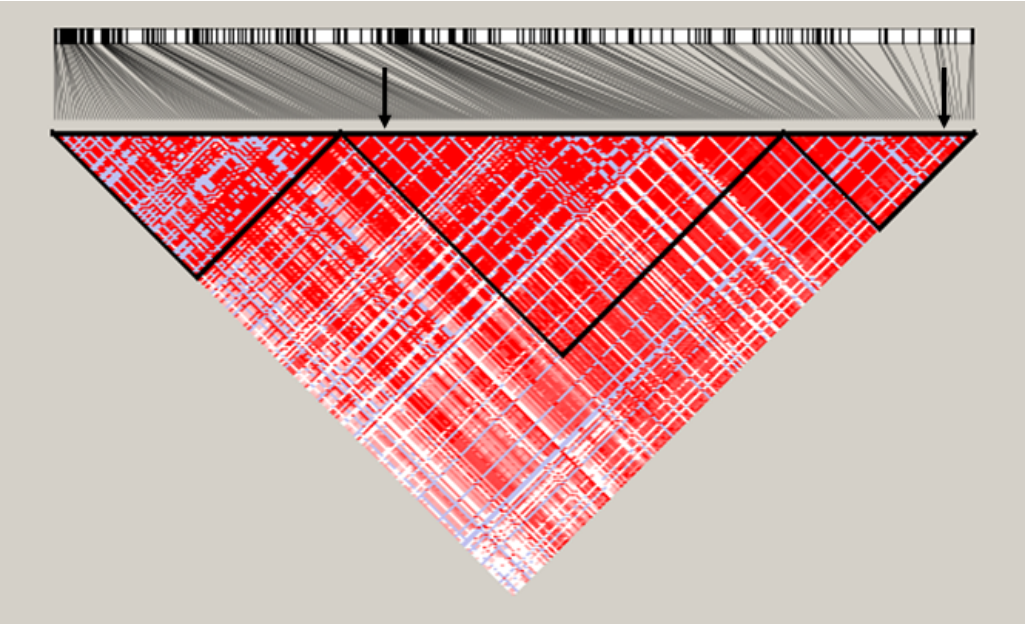

Figure 5.4: LD structure encompassing the *CXXC6P1* and *LOC121727* pseudogenes on chromosme 13. Diagram depicts an area of high LD that includes variants with a potential CCT association. The arrows indicate the positions of SNPs rs4254174 (left arrow) and rs9522433 (right arrow), which are approximately 350 kb apart.

result, as the allele effect in the NSA group is in the opposite direction, indicating this may be a spurious association. However, due to the magnitude of the standard error, it is possible that the allele effect for rs1034200 could actually be in the same direction as the other cohorts. At this stage, more evidence is required to confirm or refute the association of this SNP with CCT. As *FTHL7* is a pseudogene, no functional information is available, which also makes it difficult to predict if this gene could be involved in the determination of CCT.

5.5.2.3 FGF1

Whilst no SNP from *FGF1* reached genome-wide significance in any of the analyses conducted in this chapter, there is evidence to suggest it is a gene of interest in terms of a role in influencing CCT. Across all the cohorts assessed as part of the GWAS, SNPs from *FGF1* were consistently found with strong association signals, albeit at levels that were below the significance threshold. Following meta-analysis of the individually genotyped data from the full BMES and NSA cohorts, the *FGF1* SNPs rs33954 and rs7703260 had the third (p = 1.26 x10^{-05}) and seventh (p = 2.52 x 10^{-05}) strongest association results respectively. Importantly, the rs7703260 result also seemed to replicate in the twins, although when the BMES and NSA data were combined with the results from both the twin cohorts there was only a slight improvement in the p value (1.6 x 10^{-05}). Another *FGF1* SNP of interest was rs11750296, which had a p value of 2.6 x 10^{-06} following meta-analysis of GWAS data from the BMES and FMC_CCT pools with the twin cohorts, thus narrowly missing inclusion in Table 5.5. Unfortunately, this SNP was not individually genotyped in the full BMES and NSA cohorts as it failed the assay design for the Sequenome MassARRAY, therefore limiting further analysis of this variant.

The functional properties of *FGF1* also support the potential role of this gene in CCT determination. The FGF1 protein belongs to the fibroblast growth factor family, the members of which possess broad mitogenic and cell survival activities. During embryonic development, fibroblast growth factors have diverse roles in regulating cell proliferation, migration and differentiation, whilst in adult tissues they function in tissue repair and response to injury.[502, 503] Expression of *FGF1* has been demonstrated in the developing cornea of embryonic rats and a role for fibroblast growth factors in ocular development has been documented.[504, 505] Given its function in embryogenesis and observed expression in the developing cornea, it is plausible that *FGF1* could be involved in the pathways that govern corneal thickness. It is also interesting to note that a SNP from another member of the fibroblast growth factor family, *FGF9*, gave a strong association signal following meta-analysis of the full BMES and NSA cohorts with the twins (Table 5.7). This lends further support to the suggestion that members of the fibroblast growth factor family are potentially involved in a pathway that ultimately influences corneal thickness. Genotyping of *FGF1* SNPs in additional cohorts is required to assess its role further.

5.5.2.4 COL5A1

As acknowledged in previous chapters, the genes that comprise type V collagen are promising candidates for a role in CCT determination due to the intimate involvement of type V collagen in the structure of the corneal stroma. Evidence from patients with Ehlers-Danlos syndrome and a mouse model of the disease also supports the potential association of these genes with CCT.[31] Despite the candidate gene study failing to find any relationship between SNPs in *COL5A2* and CCT, there were no data on *COL5A1* as it was not screened. However, results from the GWAS

indicate that there is a possible association between *COL5A1* and CCT. Following meta-analysis of the genotyping data from the full BMES and NSA cohorts with that of the twins, the *COL5A1* SNP rs7044529 exhibited a moderate *p* value of 3.8 x 10^{-06}. Whilst this value is not genome-wide significant, it is a result that requires further investigation given the evidence that endorses *COL5A1* as a CCT candidate gene. Genotyping in additional cohorts is necessary for any future studies.

5.5.2.5 FOXO1

Results from the GWAS performed in this chapter identified *FOXO1* as a novel CCT gene. Recognition of this gene came primarily from the results of the AU and UK twin cohorts, as investigation of the BMES and FMC_CCT pooling data alone failed to detect any *FOXO1* SNP associations that warranted further investigation (Table 5.1 and 5.2). Following meta-analysis of the twin GWAS data with the BMES and FMC_CCT pooling results, the *FOXO1* SNP rs2755237 presented with a genome-wide significant *p* value of 2.5 x 10^{-08}. Another *FOXO1* variant, rs2721051, was slightly above the genome-wide significance threshold after this analysis. The subsequent individual genotyping of these two SNPs in the full BMES and NSA cohorts and combination of these results with those from the twins confirmed the identification of *FOXO1* as a CCT gene. The SNP rs2721051 was now genome-wide significant, with a *p* value of 1 x 10^{-08} and an allele effect size of -0.210. This variant accounts for 0.78% of the variation in CCT in the normal population. The SNP rs2755237 did not reach genome-wide significance in the final meta-analysis.

FOXO1 is a 111 kb gene that belongs to the forkhead family of transcription factors, which are characterised by a 100-amino acid monomeric DNA-binding motif called

the FOX domain.[506] *In vitro* and *in vivo* studies have shown that the FOXO transcription factors regulate expression of many genes involved in fundamental cellular processes, including cell cycle regulation, cell death, cell differentiation, modulation of inflammation, metabolism, protection from oxidative stress and cell survival.[506-508] Whilst the complete functional repertoire of FOXO1 is not yet understood, it is known to play a role in mesenchymal cell differentiation, including the induction of osteoblast formation.[509] In developing zebrafish embryos, expression of *foxO1* has been demonstrated in the periocular mesenchyme, the tissue that ultimately differentiates into the structures of the anterior segment of the eye, including the cornea.[510] Further evidence that *FOXO1* is involved in ocular development comes from the observation that another member of the forkhead transcription factor family, *FOXC1*, regulates the expression of *FOXO1* by binding to a conserved element in the promoter.[510] *FOXC1* plays a vital role in the development of the anterior segment of the eye and mutations or gene duplications within this gene cause anterior segment dysgenesis phenotypes.[511-513] As part of the anterior segment dysgenesis phenotype, duplication of *FOXC1* also results in a significant increase in CCT.[245] This is of particular interest, as it reveals that *FOXO1* is regulated by a gene that has a direct role in corneal development. In addition, recent studies have demonstrated that *FOXO1* regulates expression of *COL1A1*, a protein that is integral to the structure of the corneal stroma.[514, 515]

Despite the available genetic, expression and functional data, further research is required to elucidate the mechanisms involved in *FOXO1* determination of CCT. In terms of the genetic analysis, investigation in non-Caucasian cohorts would be beneficial to ascertain whether this association is dependent on ethnicity. Functional

studies could initially focus on the spatial and temporal expression of *Foxo1* in a developing mouse embryo, which could provide useful insights into where and when this protein may become involved in corneal development in a mammalian system. Investigation of the corneal phenotype in strains of mice with *Foxo1* mutations could also provide additional information, particularly if the mutation results in alterations in expression patterns of *Foxo1* or any associated genes. Given that the function of FOXO1 has not been completely characterised, a significant amount of research would be required to understand how this protein influences corneal thickness.

5.5.2.6 ZNF469

Along with *FOXO1,* the GWA studies conducted in this chapter identified *ZNF469* as a novel CCT gene. Results from the AU and UK twin cohorts were primarily responsible for the initial recognition of this gene, as investigation of the BMES and FMC_CCT pooling data alone failed to detect any *ZNF469* SNP associations that warranted further investigation. This was illustrated following meta-analysis of twin GWAS data with the BMES and FMC_CCT pooling results, where the *ZNF469* SNP rs12447690 presented with a genome-wide significant *p* value of 4.1×10^{-08}, despite no substantial association in either the BMES or FMC_CCT cohorts. However, subsequent individual genotyping of rs12447690 and another *ZNF469* SNP, rs9938149, in the full BMES and NSA cohorts did find evidence for replication of the twin findings. The combined genotyping results from these four cohorts found genome-wide significant *p* values for both rs12447690 ($1.3 \times 10^{-12)}$ and rs9938149 (2.6×10^{-10}), thus confirming that *ZNF469* is a CCT gene. This was a stronger association than what was found with *FOXO1* and this was reflected by rs12447690 accounting for approximately 1.27% of the variation in CCT in the population.

The function of ZNF469 is largely unknown, although homology modelling has provided some clues as to its potential role. The gene itself is 13 kb in size and is composed of two very large exons that encode a protein of 3925 amino acids. The ZNF469 protein contains three classical zinc-finger domains towards its C-terminal end. Whilst the sequence-specific DNA binding properties of zinc-finger proteins are well documented, these domains also permit interaction with RNA and other proteins.[516] *ZNF469* has been found to share 30% homology with the helical regions of *COL1A1, COL1A2* and *COL4A1,* all of which are highly expressed in the cornea.[517] The type I collagen protein forms fibrils that are an integral structural component of the corneal stroma and the candidate gene study has demonstrated that polymorphisms in these genes can influence CCT. It has been postulated that ZNF469 could act either as a nuclear transcription factor or as an extra-nuclear regulatory molecule involved in the synthesis and/or organization of these collagen fibrils.[517] The potential for ZNF469 to be involved in the structural organisation of components of the corneal stroma is further supported by the documented expression of the gene in human cornea.[517]

Whilst the functional properties of *ZNF469* are consistent with a role in CCT determination, the most compelling evidence for this association comes from studies showing that mutations in *ZNF469* cause a disease known as brittle cornea syndrome.[517, 518] Brittle cornea syndrome is a rare autosomal recessive condition characterised by extreme thinning of the cornea, the consequence of which can be corneal rupture following minor trauma. Other ocular manifestations can include keratoconus, keratoglobus and blue sclera, whilst systemic involvement may cause joint hypermobility, skin hyperelasticity, hearing defects and dental abnormalities.

This disease provides confirmation that *ZNF469* is a CCT gene, although the rare pathogenic mutations that cause brittle cornea syndrome would not be involved in the normal trait distribution. The hypothesis is that less deleterious, functional polymorphisms within *ZNF469* are responsible for contributing to normal CCT variation.

As with *FOXO1*, further work is required to understand the mechanisms involved in the association of *ZNF469* with CCT. It must be acknowledged that rs12447690 is a considerable distance from the *ZNF469* locus and there are four putative genes that are closer to this SNP, although these are poorly characterised with only a hypothetical protein role. However, to verify that *ZNF469* is the CCT gene at this locus, identification of the functional variant(s) could be achieved through sequencing of the surrounding genomic region. The advent of next generation deep sequencing technologies makes this a feasible exercise. Numerous studies to profile the functional properties of ZNF469 could also be performed. A sub-cellular localisation assay would indicate whether the protein is localised to the nucleus, cytoplasm, or both, which would help to ascertain if ZNF469 possesses purely transcription factor capabilities or whether it is also involved in RNA or protein binding. As yet, there are no studies documenting expression of the gene in developing embryos, thus *in situ* hybridisation in a model organism would provide valuable information on its role in development, with a particular emphasis on the cornea. Numerous other experimental procedures could also be undertaken, including establishment of mutant mouse model to further investigate the corneal phenotype or even implementation of techniques designed to find potential protein binding partners, such as phage display or a yeast two-hybrid assay.

5.5.3 Limitations of GWA studies

While this study was successful in identifying two novel CCT genes, it is apparent that both *FOXO1* and *ZNF469* contribute very little to the overall variation in CCT seen in the population, with a combined figure of around 2%. Not only does the minor effect of these genes suggest that the genetic architecture of CCT is complex, but it is also a reflection on the capabilities of the GWAS methodology. Notwithstanding the recent popularity of the GWAS technique, it has become apparent that the common risk variants described in these studies fail to explain the majority of genetic heritability for many complex diseases and traits.[519-521] The underlying rationale for GWA studies is the 'common disease, common variant' hypothesis, which states that common diseases are largely attributable to common genetic variants found in the population.[194, 522] Although the allelic architecture of some conditions, notably age-related macular degeneration[195] and pseudoexfoliation syndrome,[523] reflects the contribution of several common variants of large effect, for the most part, GWA studies have only managed to identify variants that confer relatively minor increases in risk which explain only a small portion of heritability. Recent evidence suggests that many complex diseases and traits may be regulated by combinations of rare variants with moderate effect sizes,[501, 521, 524, 525] the majority of which are undetectable using GWA studies.[526] Whilst GWA studies do have their limitations, they are currently the optimal approach for studying the genetics of highly heritable traits such as CCT, particularly given that this is the first reported instance of such a study.

5.5.4 Summary

The goal of the research conducted in this chapter was to discover novel genetic determinants of CCT using the GWAS methodology, which was achieved through the identification of the *FOXO1* and *ZNF469* genes. Several other genes, notably *COL5A1, FGF1* and *FTHL7*, were also identified as promising candidates and require further research to clarify their role. Aspects of the methodology used in this study were also unique, including the application of blood pooling for the analysis of a quantitative trait and meta-analysis of individually genotyped and pooled GWAS data. The results confirm that these techniques are capable of detecting statistically significant associations. The advent of new deep sequencing technologies also offers the possibility of further expanding on these findings by screening the genomic regions in and around *FOXO1* and *ZNF469* in order to find the functional variants responsible for influencing CCT.

CHAPTER 6

ANALYSIS OF GENETIC VARIANTS ASSOCIATED WITH CENTRAL CORNEAL THICKNESS IN AN OPEN-ANGLE GLAUCOMA COHORT

6.1 HYPOTHESIS AND AIMS

Given that CCT is a well-established risk factor for OAG, it is plausible that a biological interaction exists between pathways involved in the development of the cornea and tissues important in OAG pathogenesis. Therefore, the research in this chapter is based on the hypothesis that genes involved in the determination of CCT can also increase susceptibility to OAG. The aim is to screen genetic variants that have previously been found to be associated with CCT in a large cohort of OAG samples to ascertain if any correlation between these genes and the disease is evident.

6.2 OVERVIEW

Despite a thinner CCT being an established risk factor for OAG,[100, 101, 106, 114] the mechanisms underlying this association are unclear. Factors such as tonometry artefact could potentially be responsible for this relationship, whilst the influence of glaucoma medication on corneal thickness may also play a role. However, it is possible that a genuine biological interaction also exists between the structural properties of the cornea and tissues involved in OAG pathogenesis. By determining what genes govern CCT and whether any of these are involved in the development of OAG, the mechanisms responsible for the relationship between these two traits could be identified. The discovery of novel OAG susceptibility loci is potentially of greater significance. Improving our knowledge of the genetic architecture of OAG will lead to a better understanding of the pathogenesis of the disease, which is vital for developing new methods of treatment. The identification of novel susceptibility

genes will also offer opportunities to ultimately utilise DNA testing to aid in predictive or early diagnosis.

6.3 METHODS

6.3.1 Ethics statement

Ethics approval for the BMES and NSA studies has been described previously (see Chapters 2.3.1 and 3.3.1 respectively). For recruitment of the other cohorts used in this study, ethics approval was obtained from the relevant human research ethics committees of the following institutions (cohort in parentheses): Flinders University and Southern Adelaide Health Service (Australian and New Zealand Registry of Advanced Glaucoma and Glaucoma Flinders Medical Centre); University of Tasmania (Launceston Nursing Home and Glaucoma Inheritance Study in Tasmania). Each study adhered to the tenets of the Declaration of Helsinki.

6.3.2 Participant recruitment

6.3.2.1 Control cohorts

6.3.2.1.1 Blue Mountains Eye Study

The recruitment methodology used for the BMES has been described previously (see Chapter 2.3.3.1.1). The criteria for inclusion as a control sample included a normal optic disc and visual fields. Additional samples were available for this study than what have been employed for the genetic studies as CCT measurements were not required for inclusion. Genomic DNA was extracted from peripheral blood according to standard methods.

6.3.2.1.2 Normal South Australia

The recruitment methodology used for the NSA cohort has been described previously (see Chapter 3.3.3.2.1). Genomic DNA was extracted from peripheral blood according to standard methods.

6.3.2.1.3 Launceston Nursing Home

The Launceston Nursing Home (LNH) cohort consisted of normal elderly controls who were recruited from nursing homes within the Tasmanian city of Launceston, Australia. To qualify for inclusion in the cohort, participants needed to be free of ocular hypertension and have a normal optic disc and visual fields. Genomic DNA was extracted from peripheral blood according to standard methods.

6.3.2.2 Glaucoma cohorts

6.3.2.2.1 Australia and New Zealand Registry of Advanced Glaucoma

The Australia and New Zealand Registry of Advanced Glaucoma (ANZRAG) is based at the Flinders Medical Centre in Adelaide, Australia and aims to recruit cases of advanced glaucoma Australia-wide through ophthalmologist referral. The criteria for inclusion in this cohort are described below. Blood samples from patients who have consented to join the study are sent to the Flinders Medical Centre where DNA is extracted using standard methods. Further information on the ANZRAG can be found at www.anzrag.com.

6.3.2.2.2 Glaucoma Inheritance Study in Tasmania

The Glaucoma Inheritance Study in Tasmania (GIST) is a study that aims to recruit all cases of OAG in Tasmania, an island state of Australia. A full description of the

recruitment methodology has been published in detail previously.[92] Genomic DNA was extracted from peripheral blood according to standard methods.

6.3.2.2.3 Glaucoma Flinders Medical Centre

The Glaucoma Flinders Medical Centre (GFMC) cohort was established through the recruitment of non-advanced OAG cases from the ophthalmology clinic at the Flinders Medical Centre. Subsequent to the initial recruitment, some participants were assessed in follow-up visits and determined to have developed advanced OAG. Genomic DNA was extracted from peripheral blood according to standard methods.

6.3.2.2.4 Blue Mountains Eye Study

As the BMES was a population-based study, participants with OAG were included in the recruitment. The full recruitment methodology has been described in detail previously.[348]

6.3.3 Clinical definition of open-angle glaucoma

Recruitment of all OAG cases was defined by concordant findings of typical glaucomatous visual field defects on the Humphrey 24-2 test, with the Humphrey 30-2 test only used for assessing the BMES participants. Other criteria included optic disc rim thinning with an enlarged cup-disc ratio (≥ 0.7) or cup-disc ratio asymmetry (≥ 0.2) between the two eyes. Clinical exclusion criteria for this cohort were: i) pseudoexfoliation glaucoma, ii) pigmentary glaucoma, iii) angle closure or mixed mechanism glaucoma; iv) secondary glaucoma due to aphakia, rubella, rubeosis or inflammation; v) congenital or infantile glaucoma, vi) glaucoma in the presence of a

known syndrome associated with glaucoma vii) mutation in the *MYOC* gene (all samples were screened by direct sequencing of exon 3).

Enrolment in the ANZRAG was defined by severe visual loss resulting from OAG. This includes best-corrected visual acuity worse than 6/60 due to OAG, or a reliable Humphrey 24-2 Visual Field (Carl Zeiss Meditec, Inc, Dublin, California) with a mean deviation of worse than -22db or at least 2 out of 4 central fixation squares affected with a Pattern Standard Deviation of < 0.5%. The field loss must be due to OAG, and the less severely affected eye was also required to have signs of glaucomatous disc damage. Clinical exclusion criteria were the same as described above.

6.3.4 Study design

The candidate gene and GWA studies outlined in Chapters 3 and 5 respectively identified *COL1A1*, *COL1A2*, *FOXO1* and *ZNF469* as novel CCT genes. In order to ascertain if these and several other genes of interest were also associated with the development of OAG, the relevant SNPs were screened in cohort of combined non-advanced and advanced OAG participants. Genotyping of SNPs from *COL1A1* and *COL1A2* was undertaken at an earlier date than the other genes and as such, a smaller cohort was genotyped. A total of 1172 control samples were used for the collagen genes, consisting of 891 from the BMES and 281 from the NSA study, along with 230 advanced OAG participants from the ANZRAG. The remaining genes to be screened consisted of *FOXO1*, *ZNF469* and an additional 34 SNPs from 24 genes that demonstrated results suggestive of an association with CCT following the GWAS. Genotyping of these genes involved both control and OAG samples that

were not included in the screening of *COL1A1* and *COL1A2*. The control cohort comprised of a total of 1562 participants, made up of samples from the BMES, NSA, and LNH groups, whilst the OAG cohort consisted of 888 participants. For a full description of the samples that comprise the control, non-advanced and advanced cohorts see Table 6.1.

6.3.5 Genotyping Methodology

Genotyping was performed using the Sequenom MassARRAY® platform (Sequenom, San Diego, USA). This technique has been described previously (see Chapter 3.3.5.1).

6.3.6 Statistical Analysis

All single SNP genetic association tests were performed using the software program PLINK v1.06 (http://pngu.mgh.harvard.edu/purcell/plink/).[450] The output of the PLINK analysis includes five different tests of association between a variant and the trait of interest. These include a basic allelic test (ALLELIC), dominant gene action (DOM), recessive gene action (REC), genotypic or additive test (GENO or ADD) and a Cochran-Armitage trend test (TREND). A full description of these tests can be found in Chapter 5.3.8. Fisher's exact test was used in the calculation of the *p* value and multiple testing correction was applied for the number of independent tests per gene as calculated by the SNPSpD interface (http://genepi.qimr.edu.au/general/daleN/SNPSpD/).[451, 452] See Chapter 3.3.6 for further information on the SNPSpD program. For genes with multiple SNPs, the number of independent tests per gene was as follows (number of tests in parentheses): *COL1A1* (1.2); *COL5A1* (2); *CXXC6P1* (2); *FGF1* (1.9)*; FOXO1* (1.4);

Table 6.1: Number of samples in each cohort used in the genotyping study

Controls		OAG	
Cohort	**N**	**Cohort**	**N**
BMES	1180	GIST	499
NSA	282	GFMC	154
LNH	100	ANZRAG	142
-	-	BMES	93
Total	1562	Total	888

N = number of participants.

LOC121727 (1.3); *LOC341689* (2); *SHROOM3* (1); *ZNF469* (1.3). Haplotype associations were tested using HaploStats v1.3.1 software (Mayo Clinic, Rochester, USA). Correction for multiple testing of haplotypes was performed using a standard Bonferroni adjustment for the total number of observed haplotypes. Statistical significance was accepted as $p < 0.05$ following correction.

6.4 RESULTS

Genotyping of the *COL1A1* SNPs rs1046329 and rs2696297 in the case and control cohorts failed to find any association with advanced OAG. The strongest *p* value for rs1046329 was 0.169 under a dominant model, while for rs2696297 it was 0.147 also under a dominant model. Results for the *COL1A2* haplotype analysis can be viewed in Table 6.2. No haplotypes were significantly associated with OAG following correction for multiple testing for the observed number of haplotypes. Genotyping results for all the remaining SNPs screened in the larger OAG cohort can be found in Table 6.3. A total of three SNPs were found to be significantly associated with OAG following correction for multiple testing. The strongest association was found with the *FOXO1* SNP rs2755237, which had a corrected *p* value of 0.033 (odds ratio = 1.74; 95% confidence interval = 1.09 – 2.79) under a recessive model. The second strongest association belonged to the *AGXT2* SNP rs37369, with a corrected *p* value of 0.04 under a genotypic model (no odds ratio could be calculated as the genotypic model takes into account all three possible genotypes). The remaining significant SNP was rs7985340 from the pseudogene *LOC341689*, which had a corrected *p* value of 0.05 (odds ratio = 1.28; 95% confidence interval = 1.03 – 1.59) under a dominant model.

Table 6.2: *COL1A2* haplotype analysis in the OAG and control cohorts

	SNP				*p* value	
Haplotype	**1**	**2**	**3**	**Frequency**	**Dominant**	**Recessive**
1	G	G	T	0.57	0.53	0.91
2	G	A	C	0.23	0.92	0.76
3	A	G	T	0.10	0.11	0.33
4	G	G	C	0.05	0.03	NR
5	A	G	C	0.03	0.74	NR
6	G	A	T	0.01	0.33	NR

A three SNP haplotype was constructed from the *COL1A2* SNPs rs12668754 (SNP 1), rs11764718 (SNP 2) and rs1034620 (SNP 3). This haplotype was tested for an association with OAG by genotyping a total of 1172 control samples and 230 advanced OAG participants from the ANZRAG. Both dominant and recessive modes of inheritance were analysed. NR = no result.

Table 6.3: Results of association tests following genotyping in the control and OAG cohorts

SNP	CHR	Gene	Model	*p* value	SNP	CHR	Gene	Model	*p* value
rs2755237	13	*FOXO1*	REC	**0.024**	rs11186035	10	*LOC119358*	DOM	0.211
rs7985340	13	*LOC341689*	DOM	**0.025**	rs2785862	13	*CXXC6P1*	GENO	0.216
rs37369	5	*AGXT2*	GENO	**0.040**	rs33954	5	*FGF1*	GENO	0.268
rs2721051	13	*FOXO1*	ALLELIC	0.046	rs9393469	6	*NRSN1*	REC	0.283
rs9522400	13	*LOC121727*	DOM	0.054	rs12639868	4	*SHROOM3*	TREND	0.289
rs17078802	13	*STARD13*	ALLELIC	0.055	rs7044529	9	*COL5A1*	REC	0.294
rs11664141	18	*DLGAP1*	GENO	0.069	rs2785841	13	*CXXC6P1*	DOM	0.307
rs173269	17	*KCNJ2*	GENO	0.073	rs17055448	13	*LOC341689*	TREND	0.419
rs12447690	16	*ZNF469*	REC	0.074	rs1317617	10	*PPIF*	DOM	0.433
rs10764631	10	*APBB1IP*	ALLELIC	0.102	rs7703260	5	*FGF1*	TREND	0.439
rs7025493	9	*COL5A1*	DOM	0.152	rs11787841	9	*BRD3*	REC	0.482
rs1323168	13	*FGF9*	ALLELIC	0.153	rs4254174	13	*CXXC6P1*	DOM	0.517
rs9522433	13	*LOC121727*	DOM	0.156	rs1780196	10	*PDSS1*	DOM	0.552
rs9555836	13	*CXXC6P1*	DOM	0.157	rs9938149	16	*ZNF469*	DOM	0.595
rs9313984	5	*LOC391844*	REC	0.170	rs1243977	10	*LOC389935*	DOM	0.685
rs4516740	4	*SHROOM3*	DOM	0.208	rs11893350	2	*LRRTM1*	REC	0.715
rs9595630	13	*RP11-298P3.3*	DOM	0.209	rs8091028	18	*MYOM1*	TREND	0.899

Table depicts the model associated with the strongest uncorrected *p* value for each SNP. Values in bold were considered significant at the $p < 0.05$ threshold following multiple testing correction. DOM = dominant. GENO = genotypic. REC = recessive.

6.5 DISCUSSION AND SUMMARY

The primary goal of the research presented in this thesis was to identify novel susceptibility loci for OAG through ascertaining the genetic determinants of normal CCT variation. Improving our understanding of the genetic factors responsible for the development of OAG offers many potential benefits for both diagnosis and treatment of the disease. Evidence from familial and ethnic studies indicates that OAG has a strong genetic component. For example, the lifetime risk of developing OAG has been shown to be 10 times higher in siblings and offspring of people affected with the condition,[94] whilst ethnic groups such as African-Americans are four to five times more likely to develop the disease than Caucasians.[89] Despite these characteristics, the genetic architecture of OAG remains poorly understood, with the only major gene identified to-date, *MYOC*, accounting for approximately 3% of cases.[158] Given that methodologies such as familial-based linkage and candidate gene analysis have been employed extensively in OAG genetics research with limited success, novel approaches are required. One such approach is to study the genetics of potential endophenotypes, such as CCT.

6.5.1 Central corneal thickness as an endophenotype of open-angle glaucoma

The complex nature of OAG and its broad spectrum of phenotypic heterogeneity ensure that characterising its genetic component is problematic. An essential element of any genetic study aimed at identifying susceptibility loci for a particular disease is a rigid definition of the phenotype, a criterion that is difficult to adhere to with OAG. A potential solution is to break down a complex phenotype into quantifiable intermediate components, also known as endophenotypes. The genetic architecture of the endophenotype can then be studied in order to identify genes associated with the

disease of interest. This approach has been successfully applied in the field of psychiatric genetics[205] and OAG offers a good opportunity to utilise the endophenotype methodology, with quantifiable traits such as IOP, cup-to-disc ratio and CCT all established risk factors. However, a recent study by Charlesworth *et al* that investigated the endophenotypic status of these traits in relation to OAG failed to find any evidence that CCT was an endophenotype for the disease.[206]

In order to classify CCT as an endophenotype of OAG, it must be demonstrated that there is a genetic correlation between the two traits. This was assessed through genotyping a total of 26 different genes, which were selected based on the results of the candidate gene and GWA studies. In essence, only four of these genes showed robust evidence of an association with CCT, namely *COL1A1*, *COL1A2, FOXO1* and *ZNF469*. Therefore, these are the only genes that can legitimately identify CCT as an endophenotype. The remaining genes were selected based on the results of the GWAS, as they showed suggestive evidence of a correlation with CCT, although this was not strong enough to survive multiple testing correction. Nevertheless, if any of these genes were found to be associated with OAG it may identify them as targets of future genetic studies.

6.5.2 Genotyping results in the open-angle glaucoma cohort

Of the 26 genes assessed in this study, a total of three demonstrated evidence of a correlation with OAG, of which *FOXO1* was the only confirmed CCT gene. The remaining two genes, *AGXT2* and *LOC341689*, exhibited weak association data, with nominally significant *p* values close to the 0.05 threshold. This outcome makes it difficult to interpret the significance of these results and further genotyping is

required to support these findings. In regards to the other identified CCT genes, there was no evidence from the genotyping data that *COL1A1* and *COL1A2* are involved in the development of advanced OAG. However, given that these genes were screened in a smaller cohort, it is possible that power may have been an issue and further genotyping could be required to confirm this result. There was also no evidence from that *ZNF469* is a susceptibility gene for OAG. The strongest associated *ZNF469* SNP was rs12447690, which had a *p* value of 0.074 under a recessive model. Whilst it is entirely plausible that these genes have no involvement in the OAG disease process, it may also be difficult to assess such a correlation, given the relatively minor effects that genes such as *COL1A1, COL1A2* and *ZNF469* had on overall CCT variability.

6.5.3 FOXO1 as an open-angle glaucoma gene

The *FOXO1* SNP rs2755237 was found to be the variant most strongly associated with OAG in this study, conferring a 1.74 times increase in the odds of developing the disease. Further support for the association of this gene with OAG came from the other *FOXO1* variant included in the analyses, rs2721051, which had a nominally significant *p* value of 0.046 prior to multiple testing correction. The finding that *FOXO1* potentially increases susceptibility to OAG is significant on several grounds. It supports the hypothesis of a biological link between the CCT and OAG, which could ultimately alter the way in which this trait is perceived in terms of its role as a risk factor. Whilst several studies have indicated that CCT is a risk factor for OAG independent of the influence of IOP,[100, 101, 114] the impact of tonometry artefact on these findings could not be truly separated. The evidence presented here however, indicates that the relationship between CCT and OAG could indeed be independent of IOP and tonometry artefact. This might alter the fundamental rationale for

measuring CCT in terms of OAG diagnosis and treatment and may lead to a different interpretation of the role of this trait in managing the disease.

Another important aspect of these findings is the identification of *FOXO1* as a potential OAG gene. If confirmed, the applications of this result could be substantial and would ultimately lead to a better understanding of OAG pathogenesis, with the possibility of also offering avenues for improved diagnosis through genetic screening. Recognising the genetic factors that contribute to disease is also a promising avenue towards the development of new treatments. Confirmation of this result will require further research, including genetic and molecular studies, although there is evidence to support the role of *FOXO1* in the disease pathogenesis. Apart from its function in ocular development,[510] *FOXO1* is a known mediator of apoptosis[507, 527-529] and has recently been associated with the degeneration of postmitotic neurons,[530] which could have implications for the death of retinal ganglion cells in OAG. *FOXO1* has also shown to regulate endothelial nitric oxide synthase (*eNOS*),[531] a gene that has been linked with OAG.[532-534] In addition, *FOXO1* lies within the *REIG2* locus for Reigers syndrome, a condition that is frequently associated with developmental forms of glaucoma.[535] It must also be acknowledged however, that given that *FOXO1* alone explains less than 2% of the variance in CCT, it's association with OAG maybe due to pleiotropic mechanisms that are independent of CCT.

6.5.4 Summary

In the context of this chapter and the research project as a whole, the identification of *FOXO1* as a gene potentially involved in the development of OAG is a significant

finding, as it supports the hypothesis that the genetic determinants of normal CCT variation are also candidates for increasing susceptibility to OAG. This result strengthens the argument that CCT is an endophenotype for OAG and justifies the use of this methodology to investigate the genetics of this complex disease. It also offers the promise that similar approaches with traits such as IOP and cup-to-disc ratio could lead to the identification of further novel genes. As this is a preliminary study, there is scope for further research in this area. Replication of the *FOXO1* data in additional OAG cohorts is required, particularly given that the association results were only at minor significance levels. Further research will also determine the clinical significance of this finding. The future discovery of new CCT loci will also offer the opportunity to assess their role as candidate OAG genes, thus providing further information on the endophenotypic status of this trait.

CHAPTER 7

FINAL DISCUSSION

7.1 RATIONALE FOR STUDYING CENTRAL CORNEAL THICKNESS GENETICS

The Ocular Hypertension Treatment Study published in 2002 is credited with identifying CCT as a useful prognosticator for progression to OAG independent of IOP.[100] This discovery sparked renewed interest in the properties of this trait, as OAG is a disease of major clinical importance across the world. With subsequent studies verifying the initial findings of the Ocular Hypertension Treatment Study, studying CCT could lead to an improved understanding of OAG. In particular the genetic component of CCT had been poorly characterised. Prior to 2002, only one study had investigated the heritability of CCT,[213] but following publication of the Ocular Hypertension Treatment Study results, a further four studies released data demonstrating that corneal thickness is highly heritable.[206, 215-217] Identifying the genetic factors that govern CCT offers the potential not only to clarify its role as a risk factor but of also discovering new susceptibility loci for OAG and to better understand corneal development. This thesis was undertaken with the aim of characterising the genetic component of this trait.

Prior to this research project commencing, there was no knowledge of the genes involved determining normal CCT variation. Given the paucity of research in this area and the known high heritability of the trait, there was an optimistic view that a well-designed study could successfully identify novel genetic determinants of CCT. It was decided that this research project would employ a multi-faceted approach, with the utilisation of both a human and mouse model. Even though any findings from this study would ultimately have applications in the human population, the use of a mouse model allowed for experimental designs that would not be feasible in

research involving human participants. One of the major strengths of this thesis was the access to large, well-characterised cohorts of human participants, including the BMES, FAMAS, FMC_CCT, NSA and AU and UK twin studies. These cohorts allowed for well-powered genetic studies that were ultimately able to identify several novel CCT genes.

7.2 METHODOLOGICAL APPROACH AND OVERVIEW OF FINDINGS FROM THIS THESIS

7.2.1 Association of pigmentation with central corneal thickness

The discovery that pigmentation appears to influence CCT is perhaps one of the more unique findings arising from this thesis. By pursuing observations from published data on different ethnic groups, an extensive meta-analysis confirmed that human skin pigmentation is associated with CCT. Subsequent analysis in the mouse verified the results from the meta-analysis, with the CCT in pigmented mice significantly thicker than those in their albino counterparts ($p = 0.008$). Utilisation of the mouse model offered several distinct advantages, including the ability to use inbred strains, control environmental conditions and use consistent measurement techniques, thus significantly reducing the sources of variability that can hinder equivalent studies in human populations. The use of mutant mouse strains also provided further insight into the relationship between pigmentation and CCT by identifying *Tyr* and *Slc45a2* as genes potentially involved in the determination of both traits. This methodological approach is a good example of how experiments undertaken in the animal model are able to complement work involving human participants, notably the meta-analysis. Whilst data from the candidate gene and GWA studies failed to confirm that any pigment-related genes were associated with

CCT, further research in this area is warranted, particularly given the results from the human meta-analysis and the mouse model. It is also interesting to note that the DBA/2J inbred mouse strain, which has a mutation in *Tyrp1*, spontaneously develops glaucoma as a result of elevated IOP.[536] Whilst it is postulated that the glaucoma phenotype in this mouse results from inhibiton of aqueous drainage due to the accumulation of toxic by-products of abnormal pigment synthesis in the trabecular meshwork, it is worth noting the association between glaucoma and a pigmentation gene given the discussion surrounding CCT, pigmentation and OAG in this thesis. This could be of potential importance if studying pigmentation genes which influence CCT in an OAG cohort, as a direct link between CCT and OAG must be considered.

7.2.2 Identification of novel genetic determinants of central corneal thickness

Two methodological approaches, a candidate gene study and a GWAS, were employed to identify novel CCT genes in the human population. Following selection of 17 candidate genes, a significant association with CCT was found with both *COL1A1* and *COL1A2*, the products of which interact to form the type I collagen protein. This was the first documentation of any genes found to influence normal CCT variation. A key justification for selecting *COL1A1* and *COL1A2* was their relationship with the connective tissue disorders osteogenesis imperfecta and Ehlers-Danlos syndrome, conditions which present with an abnormally thin CCT.[29-31, 34, 35] Whilst mutations in *COL1A1* and *COL1A2* are known to cause osteogenesis imperfecta, no study, including this one, has demonstrated which variants are correlated with the abnormal corneal phenotype. This problem however, was somewhat overcome with the use of the osteogenesis imperfecta mouse model (*oim*),

which has a single base deletion in *Col1a2*.[466] This mutation was shown to cause a significant reduction in CCT in the *oim* mouse, along with structural alterations in the corneal type I collagen fibrils. These results definitively illustrate the involvement of *Col1a2* in CCT determination and confirm the data from the candidate gene study. These findings demonstrate how the use of a mouse model in this thesis has been able to complement the work performed in humans.

Following implementation of the candidate gene study, the next genetic methodology employed was the GWAS. The use of the DNA and blood pooling techniques for the discovery of quantitative trait loci was a relatively unique strategy, but the utility of these methods had been previously demonstrated within the laboratory.[491] Given its properties, CCT is also an ideal trait for this type of genetic study. Along with CCT being normally distributed in the population, the ease and accuracy with which it can be measured made for efficient recruitment of the several cohorts that were utilised in this study. A collaboration with the Department of Genetics and Population Health at the QIMR was able to provide access to two large twin cohorts and statistical analysis expertise that were crucial to the final outcomes. Not only was this GWAS the first to investigate CCT, but it was also the first to use the blood pooling technique for a quantitative trait and to meta-analyse data from DNA and blood pooling studies with individually genotyped samples. Resources within the laboratory were insufficient to perform costly individual genotyping and due to time constraints, blood pooling was performed as DNA had not been extracted from the required samples. Overall, the pooling strategy, combined with follow-up individual genotyping and meta-analysis with the AU and UK twin cohorts, was successful in identifying novel quantitative trait loci for CCT. Genome-wide significant SNPs

were found within *FOXO1* and *ZNF469*, with both of these genes possessing functions that support their involvement in corneal development. Several other genetic loci of interest were also discovered and further analysis is needed to verify if they are associated with CCT.

7.2.2.1 Comparison of candidate gene study and GWAS methodologies

Both the candidate gene and GWAS methodologies employed in this thesis offer advantages and disadvantages. Candidate gene studies present a more targeted approach if functional pathways for a disease or trait of interest are well-characterised.[399] Given the lower number of tests, they are also less prone to false positives and potentially have a greater ability to find a functional variant within a given region due to a higher concentration of markers.[399] One of the major downfalls of the candidate gene method however, is the arbitrary nature of the gene selection, as an intimate knowledge of the relevant molecular pathways and their proteins is required for effective gene selection. Given the nature of complex diseases and traits, this knowledge is often deficient and illustrates why candidate gene studies often fail.[400] This problem is overcome through the use of a GWAS, which interrogates the entire genome looking for associated loci and requires no *a priori* hypothesis about what genes to test. The ability to screen hundreds to thousands, even millions, of SNPs on a single array ensures that the GWAS yields far more information than a candidate gene study and the cost per genotype is actually lower. Whilst both studies were effective in identifying novel CCT genes, the fact that the GWAS did not detect any significant association signals for *COL1A1* and *COL1A2* suggests that both *FOXO1* and *ZNF469* are stronger determinants of CCT. If the knowledge and resources required to undertake the GWAS were available at the beginning of this

project, it is unlikely that a candidate gene approach would still have been pursued, as the GWAS is a more effective and cost-efficient methodology.

7.2.3 Relationship between central corneal thickness and open-angle glaucoma

The primary goal of this thesis was to identify novel susceptibility genes for OAG on the assumption that CCT is an endophenotype of the disease. In order to achieve this aim, the first objective was to find genes associated with CCT, which was accomplished with the discovery of *COL1A1, COL1A2, FOXO1* and *ZNF469*. Upon screening of these genes in a large cohort of patients with OAG, an association with OAG was found with *FOXO1*. Whilst this result must be viewed cautiously as it needs to be verified through further genotyping, it is a potentially significant finding that would verify the original hypothesis that formed the basis of this project. There are numerous other disorders that may also be influenced more directly by the genes involved in the determination of CCT and it is likely that the genes identified in this study may have other clinical applications. Keratoconus for example, is a disease that results in thinning of the cornea and it is conceivable that CCT genes could be implicated in the disease process. Other ocular diseases such as corneal dystrophies could also be candidates but research is required to confirm any of these associations.

7.3 STRENGTHS AND LIMITATIONS OF THE THESIS

As with any research project, there were strengths and limitations of the work conducted during this thesis. Perhaps one of the major strengths was the access to several large, well-characterised cohorts of human participants with CCT measurements. When the BMES, FAMAS, FMC_CCT, NSA and AU and UK twin

studies were combined, it gave a total cohort size of 5,080 samples. This was a significant resource and was integral in the ability of this project to identify four novel CCT genes. Given the small effect sizes of these genes, it is likely that a smaller study may have been under-powered to detect these associations. In addition, the large cohort of OAG patients utilised for screening of the CCT genes was a considerable asset. The integration of the mouse model was another strength of this project, as the data obtained were able to complement the human results and added significantly to the final outcomes.

Whilst the DNA and blood pooling strategies were an effective and efficient means of conducting the GWAS, they could also be perceived as potential weaknesses. Pooling techniques suffer from several sources of error and are limited in the data analysis that can be performed. Individual genotyping can overcome these issues and provides significantly more information than pooling, although the costs associated with this method are significantly higher. Given the reduced power of the pooling analysis, it is possible that some associated variants may have been overlooked. Another limitation of this thesis was the lack of functional characterisation undertaken on any of the identified CCT genes. Whilst there is considerable information on the function of *COL1A1* and *COL1A2*, relatively little is known about *FOXO1* and *ZNF469*, particularly in relation to their role in corneal development. Furthermore, the functional variants within each gene remain unknown and this could be the focus of future studies.

7.4 SUMMARY

The identification of *FOXO1* as a potential OAG susceptibility gene, coupled with its role in the determination of CCT, is one of the most pertinent findings to arise from this thesis. Not only does it recognise *FOXO1* as a gene worthy of further investigation in terms of its function in the development of OAG, but it could validate the endophenotype methodology that was employed to discover novel genes associated with the disease. It could also enforce the hypothesis that CCT is a risk factor for OAG independent of the influence of IOP. The results obtained from this thesis have also made a considerable contribution to our understanding of the genetic factors responsible for influencing normal CCT variation. One of the primary aims of this research project was to identify novel CCT genes, given that there was no prior knowledge in this area. Through the use of a candidate gene study and a GWAS, *COL1A1*, *COL1A2*, *FOXO1* and *ZNF469* were all found to be significantly associated with CCT, which is the first evidence of any genes found to influence this trait. Another important outcome from this study was the finding that pigmentation is correlated with CCT. An extensive meta-analysis involving published human data and assessment of a range of inbred and mutant mouse strains revealed a significant relationship between skin or coat pigmentation and CCT. This was an extremely novel finding and there was no evidence in the literature demonstrating involvement of the pigmentation pathways in the development of the cornea. Collectively, the data from the pigmentation analysis and the identification of the novel CCT genes have the potential to contribute substantially to our knowledge of corneal biology and development. This could ultimately have important implications for understanding the mechanisms of corneal disease and other ocular disorders such as keratoconus and brittle cornea syndrome.

APPENDIX

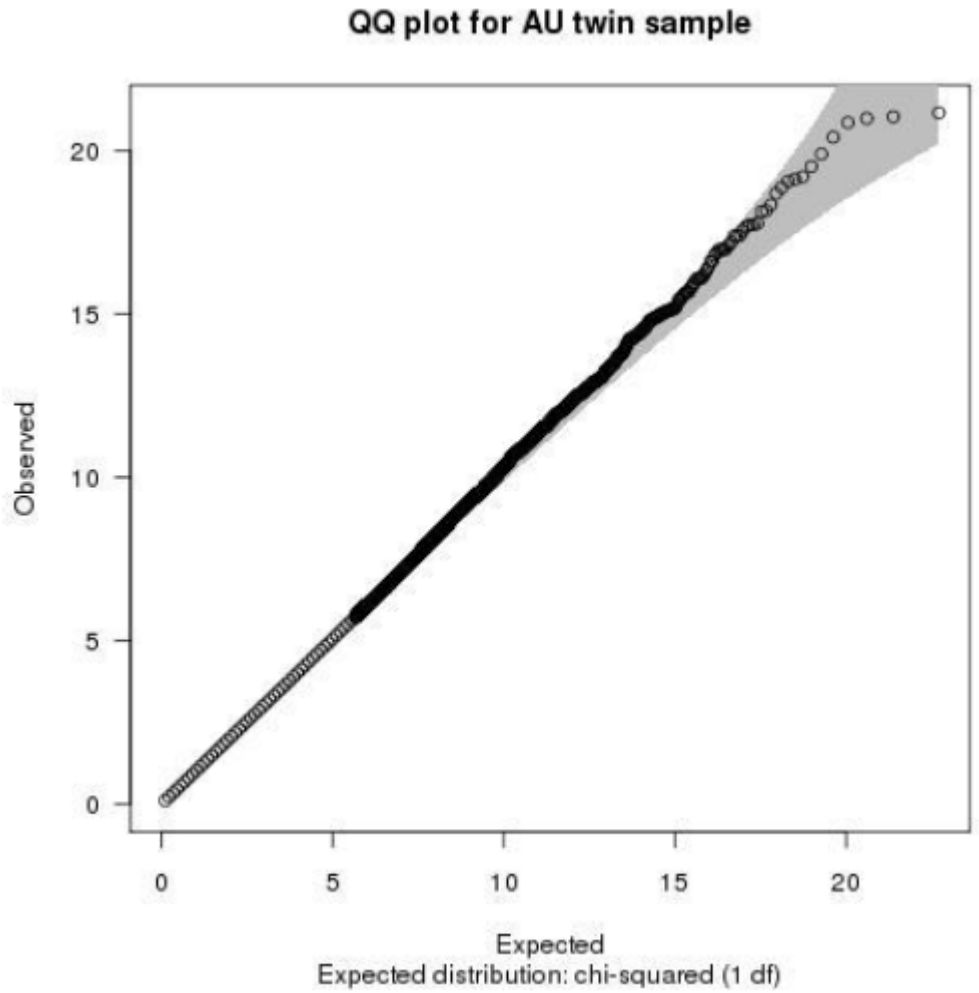

Appendix 1: Q-Q plot for the Australian (AU) twin cohort. The general concordance between the observed and the expected chi-square statistics indicates the homogeneity of the samples. The top data points within the shade zone (confidence interval) shows no evidence for strong association in the AU data alone.

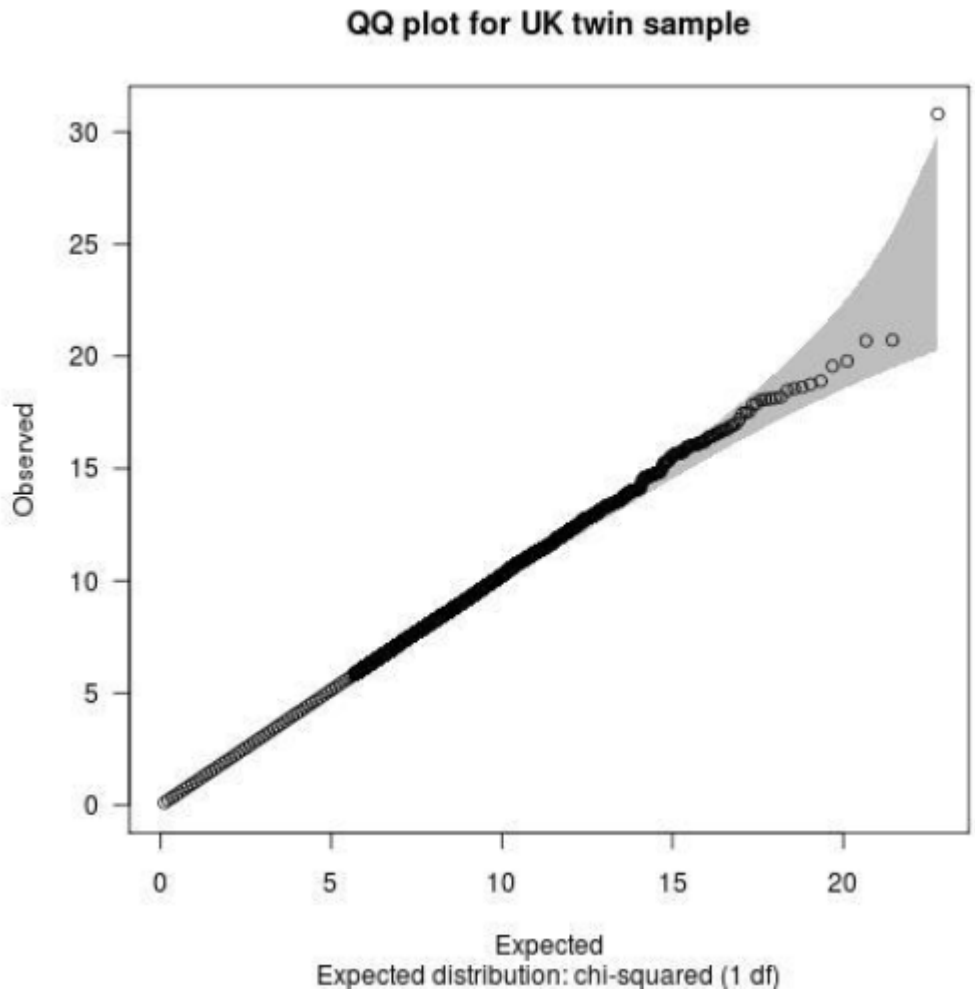

Appendix 2: Q-Q plot for the UK twin study. Almost all the data are within the shade zone (confidence interval) except one data point which suggests a potential strong association signal.

REFERENCES

1. Marieb E. Human Anatomy and Physiology. 4 ed. Menlo Park, California: Benjamin/Cummings Publishing; 1998.
2. Vaughan & Asbury's General Ophthalmology. 16 ed. New York, USA: Lange Medical Books/McGraw-Hill; 2004.
3. Bron AJ, Tripathi RC, Tripathi BJ. Wolff's Anatomy of the Eye and Orbit
Eight Edition. 8 ed. London: Chapman and Hall Medical; 1997.
4. James B, Chew C, Bron A. Lecture Notes on Ophthalmology. 8 ed. Oxford, UK: Blackwell Science; 1997.
5. The Cornea
Scientific Foundations and Clinical Practice. 1 ed. Boston: Little, Brown and Company; 1983.
6. Michelacci YM. Collagens and proteoglycans of the corneal extracellular matrix. Braz J Med Biol Res 2003;36(8):1037-46.
7. Blix M. Oftalmometriska studier. Uppsala Lakareforenings Forhandlingar 1880;15:349 - 420.
8. Gordon A, Boggess EA, Molinari JF. Variability of ultrasonic pachometry. Optom Vis Sci 1990;67(3):162-5.
9. Bovelle R, Kaufman SC, Thompson HW, Hamano H. Corneal thickness measurements with the Topcon SP-2000P specular microscope and an ultrasound pachymeter. Arch Ophthalmol 1999;117(7):868-70.
10. Amano S, Honda N, Amano Y, Yamagami S, Miyai T, Samejima T, Ogata M, Miyata K. Comparison of central corneal thickness measurements by rotating Scheimpflug camera, ultrasonic pachymetry, and scanning-slit corneal topography. Ophthalmology 2006;113(6):937-41.
11. Lackner B, Schmidinger G, Pieh S, Funovics MA, Skorpik C. Repeatability and reproducibility of central corneal thickness measurement with Pentacam, Orbscan, and ultrasound. Optom Vis Sci 2005;82(10):892-9.
12. Marsich MW, Bullimore MA. The repeatability of corneal thickness measures. Cornea 2000;19(6):792-5.
13. Suzuki S, Oshika T, Oki K, Sakabe I, Iwase A, Amano S, Araie M. Corneal thickness measurements: scanning-slit corneal topography and noncontact specular microscopy versus ultrasonic pachymetry. J Cataract Refract Surg 2003;29(7):1313-8.
14. Fishman GR, Pons ME, Seedor JA, Liebmann JM, Ritch R. Assessment of central corneal thickness using optical coherence tomography. J Cataract Refract Surg 2005;31(4):707-11.
15. Doughty MJ, Zaman ML. Human corneal thickness and its impact on intraocular pressure measures: a review and meta-analysis approach. Surv Ophthalmol 2000;44(5):367-408.
16. Foster PJ, Baasanhu J, Alsbirk PH, Munkhbayar D, Uranchimeg D, Johnson GJ. Central corneal thickness and intraocular pressure in a Mongolian population. Ophthalmology 1998;105(6):969-73.
17. Nemesure B, Wu SY, Hennis A, Leske MC. Corneal thickness and intraocular pressure in the Barbados eye studies. Arch Ophthalmol 2003;121(2):240-4.
18. Hahn S, Azen S, Ying-Lai M, Varma R. Central corneal thickness in Latinos. Invest Ophthalmol Vis Sci 2003;44(4):1508-12.
19. Aghaian E, Choe JE, Lin S, Stamper RL. Central corneal thickness of Caucasians, Chinese, Hispanics, Filipinos, African Americans, and Japanese in a glaucoma clinic. Ophthalmology 2004;111(12):2211-9.

20. Suzuki S, Suzuki Y, Iwase A, Araie M. Corneal thickness in an ophthalmologically normal Japanese population. Ophthalmology 2005;112(8):1327-36.
21. Lekskul M, Aimpun P, Nawanopparatskul B, Bumrungsawat S, Trakulmungkijkarn T, Charoenvanichvisit J, Herunpattarawong T, Suksangthong P, Jaiprasat T, Rattananantapat M, Sudprasert T. The correlations between Central Corneal Thickness and age, gender, intraocular pressure and refractive error of aged 12-60 years old in rural Thai community. J Med Assoc Thai 2005;88 Suppl 3:S175-9.
22. Landers JA, Billing KJ, Mills RA, Henderson TR, Craig JE. Central corneal thickness of indigenous Australians within Central Australia. Am J Ophthalmol 2007;143(2):360-2.
23. Eysteinsson T, Jonasson F, Sasaki H, Arnarsson A, Sverrisson T, Sasaki K, Stefansson E. Central corneal thickness, radius of the corneal curvature and intraocular pressure in normal subjects using non-contact techniques: Reykjavik Eye Study. Acta Ophthalmol Scand 2002;80(1):11-5.
24. Shimmyo M, Ross AJ, Moy A, Mostafavi R. Intraocular pressure, Goldmann applanation tension, corneal thickness, and corneal curvature in Caucasians, Asians, Hispanics, and African Americans. Am J Ophthalmol 2003;136(4):603-13.
25. Niederer RLM, Perumal DBH, Sherwin TP, McGhee CNPFF. Age-related differences in the normal human cornea: a laser scanning in vivo confocal microscopy study. Br J Ophthalmol 2007.
26. Zhang H, Xu L, Chen C, Jonas JB. Central corneal thickness in adult Chinese. Association with ocular and general parameters. The Beijing Eye Study. Graefes Arch Clin Exp Ophthalmol 2008;246(4):587-92.
27. Casson RJ, Abraham LM, Newland HS, Muecke J, Sullivan T, Selva D, Aung T. Corneal thickness and intraocular pressure in a nonglaucomatous Burmese population: the Meiktila Eye Study. Arch Ophthalmol 2008;126(7):981-5.
28. Tomidokoro A, Araie M, Iwase A. Corneal thickness and relating factors in a population-based study in Japan: the Tajimi study. Am J Ophthalmol 2007;144(1):152-4.
29. Cameron JA. Corneal abnormalities in Ehlers-Danlos syndrome type VI. Cornea 1993;12(1):54-9.
30. Pesudovs K. Orbscan mapping in Ehlers-Danlos syndrome. J Cataract Refract Surg 2004;30(8):1795-8.
31. Segev F, Heon E, Cole WG, Wenstrup RJ, Young F, Slomovic AR, Rootman DS, Whitaker-Menezes D, Chervoneva I, Birk DE. Structural abnormalities of the cornea and lid resulting from collagen V mutations. Invest Ophthalmol Vis Sci 2006;47(2):565-73.
32. Sultan G, Baudouin C, Auzerie O, De Saint Jean M, Goldschild M, Pisella PJ. Cornea in Marfan disease: Orbscan and in vivo confocal microscopy analysis. Invest Ophthalmol Vis Sci 2002;43(6):1757-64.
33. Heur M, Costin B, Crowe S, Grimm RA, Moran R, Svensson LG, Traboulsi EI. The value of keratometry and central corneal thickness measurements in the clinical diagnosis of Marfan syndrome. Am J Ophthalmol 2008;145(6):997-1001.
34. Pedersen U, Bramsen T. Central corneal thickness in osteogenesis imperfecta and otosclerosis. ORL J Otorhinolaryngol Relat Spec 1984;46(1):38-41.

35. Evereklioglu C, Madenci E, Bayazit YA, Yilmaz K, Balat A, Bekir NA. Central corneal thickness is lower in osteogenesis imperfecta and negatively correlates with the presence of blue sclera. Ophthalmic Physiol Opt 2002;22(6):511-5.
36. Panel AAoOG. Preferred pratice pattern guidelines. Primary open-angle glaucoma. San Francisco, CA; 2010.
37. Quigley HA, Broman AT. The number of people with glaucoma worldwide in 2010 and 2020. Br J Ophthalmol 2006;90(3):262-7.
38. The Glaucoma Laser Trial (GLT) and glaucoma laser trial follow-up study: 7. Results. Glaucoma Laser Trial Research Group. Am J Ophthalmol 1995;120(6):718-31.
39. Comparison of glaucomatous progression between untreated patients with normal-tension glaucoma and patients with therapeutically reduced intraocular pressures. Collaborative Normal-Tension Glaucoma Study Group. Am J Ophthalmol 1998;126(4):487-97.
40. The Advanced Glaucoma Intervention Study (AGIS): 9. Comparison of glaucoma outcomes in black and white patients within treatment groups. Am J Ophthalmol 2001;132(3):311-20.
41. Heijl A, Leske MC, Bengtsson B, Hyman L, Bengtsson B, Hussein M. Reduction of intraocular pressure and glaucoma progression: results from the Early Manifest Glaucoma Trial. Arch Ophthalmol 2002;120(10):1268-79.
42. Kass MA, Heuer DK, Higginbotham EJ, Johnson CA, Keltner JL, Miller JP, Parrish RK, 2nd, Wilson MR, Gordon MO. The Ocular Hypertension Treatment Study: a randomized trial determines that topical ocular hypotensive medication delays or prevents the onset of primary open-angle glaucoma. Arch Ophthalmol 2002;120(6):701-13; discussion 829-30.
43. Kanski J. Clinical Ophthalmology. 5 ed: Butterworth Heinemann; 2003.
44. Quigley HA. Open-angle glaucoma. N Engl J Med 1993;328(15):1097-106.
45. Coleman AL. Glaucoma. Lancet 1999;354(9192):1803-10.
46. Weinreb RN, Khaw PT. Primary open-angle glaucoma. Lancet 2004;363(9422):1711-20.
47. Quigley HA, Katz J, Derick RJ, Gilbert D, Sommer A. An evaluation of optic disc and nerve fiber layer examinations in monitoring progression of early glaucoma damage. Ophthalmology 1992;99(1):19-28.
48. Glynn RJ, Seddon JM, Krug JH, Jr., Sahagian CR, Chiavelli ME, Campion EW. Falls in elderly patients with glaucoma. Arch Ophthalmol 1991;109(2):205-10.
49. Ivers RQ, Cumming RG, Mitchell P, Attebo K. Visual impairment and falls in older adults: the Blue Mountains Eye Study. J Am Geriatr Soc 1998;46(1):58-64.
50. Nelson P, Aspinall P, O'Brien C. Patients' perception of visual impairment in glaucoma: a pilot study. Br J Ophthalmol 1999;83(5):546-52.
51. Turano KA, Rubin GS, Quigley HA. Mobility performance in glaucoma. Invest Ophthalmol Vis Sci 1999;40(12):2803-9.
52. Haymes SA, Leblanc RP, Nicolela MT, Chiasson LA, Chauhan BC. Risk of falls and motor vehicle collisions in glaucoma. Invest Ophthalmol Vis Sci 2007;48(3):1149-55.
53. Lamoureux EL, Chong E, Wang JJ, Saw SM, Aung T, Mitchell P, Wong TY. Visual impairment, causes of vision loss, and falls: the singapore malay eye study. Invest Ophthalmol Vis Sci 2008;49(2):528-33.

54. Bramley T, Peeples P, Walt JG, Juhasz M, Hansen JE. Impact of vision loss on costs and outcomes in medicare beneficiaries with glaucoma. Arch Ophthalmol 2008;126(6):849-56.
55. Owsley C, McGwin G, Jr., Ball K. Vision impairment, eye disease, and injurious motor vehicle crashes in the elderly. Ophthalmic Epidemiol 1998;5(2):101-13.
56. Gilhotra JS, Mitchell P, Ivers R, Cumming RG. Impaired vision and other factors associated with driving cessation in the elderly: the Blue Mountains Eye Study. Clin Experiment Ophthalmol 2001;29(3):104-7.
57. McGwin G, Jr., Xie A, Mays A, Joiner W, DeCarlo DK, Hall TA, Owsley C. Visual field defects and the risk of motor vehicle collisions among patients with glaucoma. Invest Ophthalmol Vis Sci 2005;46(12):4437-41.
58. Altangerel U, Spaeth GL, Steinmann WC. Assessment of function related to vision (AFREV). Ophthalmic Epidemiol 2006;13(1):67-80.
59. Gutierrez P, Wilson MR, Johnson C, Gordon M, Cioffi GA, Ritch R, Sherwood M, Meng K, Mangione CM. Influence of glaucomatous visual field loss on health-related quality of life. Arch Ophthalmol 1997;115(6):777-84.
60. Parrish RK, 2nd, Gedde SJ, Scott IU, Feuer WJ, Schiffman JC, Mangione CM, Montenegro-Piniella A. Visual function and quality of life among patients with glaucoma. Arch Ophthalmol 1997;115(11):1447-55.
61. Sherwood MB, Garcia-Siekavizza A, Meltzer MI, Hebert A, Burns AF, McGorray S. Glaucoma's impact on quality of life and its relation to clinical indicators. A pilot study. Ophthalmology 1998;105(3):561-6.
62. Alm A, Nilsson SF. Uveoscleral outflow--a review. Exp Eye Res 2009;88(4):760-8.
63. Kwon YH, Fingert JH, Kuehn MH, Alward WL. Primary open-angle glaucoma. N Engl J Med 2009;360(11):1113-24.
64. Gabelt BT, Kaufman PL. Changes in aqueous humor dynamics with age and glaucoma. Prog Retin Eye Res 2005;24(5):612-37.
65. Burgoyne CF, Downs JC, Bellezza AJ, Suh JK, Hart RT. The optic nerve head as a biomechanical structure: a new paradigm for understanding the role of IOP-related stress and strain in the pathophysiology of glaucomatous optic nerve head damage. Prog Retin Eye Res 2005;24(1):39-73.
66. Kuehn MH, Fingert JH, Kwon YH. Retinal ganglion cell death in glaucoma: mechanisms and neuroprotective strategies. Ophthalmol Clin North Am 2005;18(3):383-95, vi.
67. Jonas JB, Budde WM. Optic nerve head appearance in juvenile-onset chronic high-pressure glaucoma and normal-pressure glaucoma. Ophthalmology 2000;107(4):704-11.
68. Mok KH, Lee VW, So KF. Retinal nerve fiber loss in high- and normal-tension glaucoma by optical coherence tomography. Optom Vis Sci 2004;81(5):369-72.
69. Quigley HA, Hohman RM, Addicks EM, Massof RW, Green WR. Morphologic changes in the lamina cribrosa correlated with neural loss in open-angle glaucoma. Am J Ophthalmol 1983;95(5):673-91.
70. Yan DB, Coloma FM, Metheetrairut A, Trope GE, Heathcote JG, Ethier CR. Deformation of the lamina cribrosa by elevated intraocular pressure. Br J Ophthalmol 1994;78(8):643-8.

71. Bellezza AJ, Rintalan CJ, Thompson HW, Downs JC, Hart RT, Burgoyne CF. Deformation of the lamina cribrosa and anterior scleral canal wall in early experimental glaucoma. Invest Ophthalmol Vis Sci 2003;44(2):623-37.
72. Howell GR, Libby RT, Jakobs TC, Smith RS, Phalan FC, Barter JW, Barbay JM, Marchant JK, Mahesh N, Porciatti V, Whitmore AV, Masland RH, John SW. Axons of retinal ganglion cells are insulted in the optic nerve early in DBA/2J glaucoma. J Cell Biol 2007;179(7):1523-37.
73. Yang H, Downs JC, Girkin C, Sakata L, Bellezza A, Thompson H, Burgoyne CF. 3-d histomorphometry of the normal and early glaucomatous monkey optic nerve head: lamina cribrosa and peripapillary scleral position and thickness. Invest Ophthalmol Vis Sci 2007;48(10):4597-607.
74. Fechtner RD, Weinreb RN. Mechanisms of optic nerve damage in primary open angle glaucoma. Surv Ophthalmol 1994;39(1):23-42.
75. Kidd MN, O'Connor M. Progression of field loss after trabeculectomy: a five-year follow-up. Br J Ophthalmol 1985;69(11):827-31.
76. Popovic V, Sjostrand J. Long-term outcome following trabeculectomy: II Visual field survival. Acta Ophthalmol (Copenh) 1991;69(3):305-9.
77. Tezel G, Siegmund KD, Trinkaus K, Wax MB, Kass MA, Kolker AE. Clinical factors associated with progression of glaucomatous optic disc damage in treated patients. Arch Ophthalmol 2001;119(6):813-8.
78. Quigley HA, Nickells RW, Kerrigan LA, Pease ME, Thibault DJ, Zack DJ. Retinal ganglion cell death in experimental glaucoma and after axotomy occurs by apoptosis. Invest Ophthalmol Vis Sci 1995;36(5):774-86.
79. Levin LA. Pathophysiology of the progressive optic neuropathy of glaucoma. Ophthalmol Clin North Am 2005;18(3):355-64, v.
80. Jonas JB, Gusek GC, Naumann GO. Optic disc, cup and neuroretinal rim size, configuration and correlations in normal eyes. Invest Ophthalmol Vis Sci 1988;29(7):1151-8.
81. Healey PR, Mitchell P, Smith W, Wang JJ. Optic disc hemorrhages in a population with and without signs of glaucoma. Ophthalmology 1998;105(2):216-23.
82. Siegner SW, Netland PA. Optic disc hemorrhages and progression of glaucoma. Ophthalmology 1996;103(7):1014-24.
83. Ishida K, Yamamoto T, Sugiyama K, Kitazawa Y. Disk hemorrhage is a significantly negative prognostic factor in normal-tension glaucoma. Am J Ophthalmol 2000;129(6):707-14.
84. Lee DA, Higginbotham EJ. Glaucoma and its treatment: a review. Am J Health Syst Pharm 2005;62(7):691-9.
85. McKinnon SJ, Goldberg LD, Peeples P, Walt JG, Bramley TJ. Current management of glaucoma and the need for complete therapy. Am J Manag Care 2008;14(1 Suppl):S20-7.
86. Bean GW, Camras CB. Commercially available prostaglandin analogs for the reduction of intraocular pressure: similarities and differences. Surv Ophthalmol 2008;53 Suppl1:S69-84.
87. Boland MV, Quigley HA. Risk factors and open-angle glaucoma: classification and application. J Glaucoma 2007;16(4):406-18.
88. Rudnicka AR, Mt-Isa S, Owen CG, Cook DG, Ashby D. Variations in primary open-angle glaucoma prevalence by age, gender, and race: a Bayesian meta-analysis. Invest Ophthalmol Vis Sci 2006;47(10):4254-61.

89. Tielsch JM, Sommer A, Katz J, Royall RM, Quigley HA, Javitt J. Racial variations in the prevalence of primary open-angle glaucoma. The Baltimore Eye Survey. Jama 1991;266(3):369-74.
90. Leske MC, Connell AM, Schachat AP, Hyman L. The Barbados Eye Study. Prevalence of open angle glaucoma. Arch Ophthalmol 1994;112(6):821-9.
91. Varma R, Ying-Lai M, Francis BA, Nguyen BB, Deneen J, Wilson MR, Azen SP. Prevalence of open-angle glaucoma and ocular hypertension in Latinos: the Los Angeles Latino Eye Study. Ophthalmology 2004;111(8):1439-48.
92. Green CM, Kearns LS, Wu J, Barbour JM, Wilkinson RM, Ring MA, Craig JE, Wong TL, Hewitt AW, Mackey DA. How significant is a family history of glaucoma? Experience from the Glaucoma Inheritance Study in Tasmania. Clin Experiment Ophthalmol 2007;35(9):793-9.
93. Tielsch JM, Katz J, Sommer A, Quigley HA, Javitt JC. Family history and risk of primary open angle glaucoma. The Baltimore Eye Survey. Arch Ophthalmol 1994;112(1):69-73.
94. Wolfs RC, Klaver CC, Ramrattan RS, van Duijn CM, Hofman A, de Jong PT. Genetic risk of primary open-angle glaucoma. Population-based familial aggregation study. Arch Ophthalmol 1998;116(12):1640-5.
95. Colton T, Ederer F. The distribution of intraocular pressures in the general population. Surv Ophthalmol 1980;25(3):123-9.
96. Nemesure B, Honkanen R, Hennis A, Wu SY, Leske MC. Incident open-angle glaucoma and intraocular pressure. Ophthalmology 2007;114(10):1810-5.
97. Cartwright MJ, Anderson DR. Correlation of asymmetric damage with asymmetric intraocular pressure in normal-tension glaucoma (low-tension glaucoma). Arch Ophthalmol 1988;106(7):898-900.
98. Iwase A, Suzuki Y, Araie M, Yamamoto T, Abe H, Shirato S, Kuwayama Y, Mishima HK, Shimizu H, Tomita G, Inoue Y, Kitazawa Y. The prevalence of primary open-angle glaucoma in Japanese: the Tajimi Study. Ophthalmology 2004;111(9):1641-8.
99. Shields MB. Normal-tension glaucoma: is it different from primary open-angle glaucoma? Curr Opin Ophthalmol 2008;19(2):85-8.
100. Gordon MO, Beiser JA, Brandt JD, Heuer DK, Higginbotham EJ, Johnson CA, Keltner JL, Miller JP, Parrish RK, 2nd, Wilson MR, Kass MA. The Ocular Hypertension Treatment Study: baseline factors that predict the onset of primary open-angle glaucoma. Arch Ophthalmol 2002;120(6):714-20; discussion 829-30.
101. Miglior S, Pfeiffer N, Torri V, Zeyen T, Cunha-Vaz J, Adamsons I. Predictive factors for open-angle glaucoma among patients with ocular hypertension in the European Glaucoma Prevention Study. Ophthalmology 2007;114(1):3-9.
102. Medeiros FA, Sample PA, Weinreb RN. Corneal thickness measurements and visual function abnormalities in ocular hypertensive patients. Am J Ophthalmol 2003;135(2):131-7.
103. Zeppieri M, Brusini P, Miglior S. Corneal thickness and functional damage in patients with ocular hypertension. Eur J Ophthalmol 2005;15(2):196-201.
104. Bhatt N, Bhojwani R, Morrison A, Kwartz J, Laiquzzaman M, Shah S. A 10-year follow up of ocular hypertensive patients within the Bolton Corneal

Thickness Study. Can measured factors predict prognostic outcomes? Cont Lens Anterior Eye 2008;31(3):147-53.

105. Konstas AG, Irkec MT, Teus MA, Cvenkel B, Astakhov YS, Sharpe ED, Hollo G, Mylopoulos N, Bozkurt B, Pizzamiglio C, Potyomkin VV, Alemu AM, Nasser QJ, Stewart JA, Stewart WC. Mean intraocular pressure and progression based on corneal thickness in patients with ocular hypertension. Eye (Lond) 2009;23(1):73-8.
106. Dueker DK, Singh K, Lin SC, Fechtner RD, Minckler DS, Samples JR, Schuman JS. Corneal thickness measurement in the management of primary open-angle glaucoma: a report by the American Academy of Ophthalmology. Ophthalmology 2007;114(9):1779-87.
107. Leske MC, Wu SY, Hennis A, Honkanen R, Nemesure B. Risk factors for incident open-angle glaucoma: the Barbados Eye Studies. Ophthalmology 2008;115(1):85-93.
108. Sullivan-Mee M, Halverson KD, Saxon GB, Saxon MC, Shafer KM, Sterling JA, Sterling MJ, Qualls C. The relationship between central corneal thickness-adjusted intraocular pressure and glaucomatous visual-field loss. Optometry 2005;76(4):228-38.
109. Wolfs RC, Klaver CC, Vingerling JR, Grobbee DE, Hofman A, de Jong PT. Distribution of central corneal thickness and its association with intraocular pressure: The Rotterdam Study. Am J Ophthalmol 1997;123(6):767-72.
110. Jonas JB, Stroux A, Velten I, Juenemann A, Martus P, Budde WM. Central corneal thickness correlated with glaucoma damage and rate of progression. Invest Ophthalmol Vis Sci 2005;46(4):1269-74.
111. Sullivan-Mee M, Halverson KD, Saxon MC, Saxon GB, Qualls C. Central corneal thickness and normal tension glaucoma: a cross-sectional study. Optometry 2006;77(3):134-40.
112. Francis BA, Varma R, Chopra V, Lai MY, Shtir C, Azen SP. Intraocular pressure, central corneal thickness, and prevalence of open-angle glaucoma: the Los Angeles Latino Eye Study. Am J Ophthalmol 2008;146(5):741-6.
113. Vijaya L, George R, Paul PG, Baskaran M, Arvind H, Raju P, Ramesh SV, Kumaramanickavel G, McCarty C. Prevalence of open-angle glaucoma in a rural south Indian population. Invest Ophthalmol Vis Sci 2005;46(12):4461-7.
114. Leske MC, Heijl A, Hyman L, Bengtsson B, Dong L, Yang Z. Predictors of long-term progression in the early manifest glaucoma trial. Ophthalmology 2007;114(11):1965-72.
115. Medeiros FA, Sample PA, Zangwill LM, Bowd C, Aihara M, Weinreb RN. Corneal thickness as a risk factor for visual field loss in patients with preperimetric glaucomatous optic neuropathy. Am J Ophthalmol 2003;136(5):805-13.
116. Kim JW, Chen PP. Central corneal pachymetry and visual field progression in patients with open-angle glaucoma. Ophthalmology 2004;111(11):2126-32.
117. Congdon NG, Broman AT, Bandeen-Roche K, Grover D, Quigley HA. Central corneal thickness and corneal hysteresis associated with glaucoma damage. Am J Ophthalmol 2006;141(5):868-75.
118. Herndon LW, Weizer JS, Stinnett SS. Central corneal thickness as a risk factor for advanced glaucoma damage. Arch Ophthalmol 2004;122(1):17-21.

119. Hewitt AW, Cooper RL. Relationship between corneal thickness and optic disc damage in glaucoma. Clin Experiment Ophthalmol 2005;33(2):158-63.
120. Kurtz S, Haber I, Kesler A. Corneal thickness measurements in normal-tension glaucoma workups: is it worth the effort? J Glaucoma 2010;19(1):58-60.
121. Wessels IF, Oh Y. Tonometer utilization, accuracy, and calibration under field conditions. Arch Ophthalmol 1990;108(12):1709-12.
122. Goldmann H, Schmidt T. [Applanation tonometry.]. Ophthalmologica 1957;134(4):221-42.
123. Ehlers N, Bramsen T, Sperling S. Applanation tonometry and central corneal thickness. Acta Ophthalmol (Copenh) 1975;53(1):34-43.
124. Kniestedt C, Lin S, Choe J, Bostrom A, Nee M, Stamper RL. Clinical comparison of contour and applanation tonometry and their relationship to pachymetry. Arch Ophthalmol 2005;123(11):1532-7.
125. Tonnu PA, Ho T, Newson T, El Sheikh A, Sharma K, White E, Bunce C, Garway-Heath D. The influence of central corneal thickness and age on intraocular pressure measured by pneumotonometry, non-contact tonometry, the Tono-Pen XL, and Goldmann applanation tonometry. Br J Ophthalmol 2005;89(7):851-4.
126. Orssengo GJ, Pye DC. Determination of the true intraocular pressure and modulus of elasticity of the human cornea in vivo. Bull Math Biol 1999;61(3):551-72.
127. Gunvant P, O'Leary DJ, Baskaran M, Broadway DC, Watkins RJ, Vijaya L. Evaluation of tonometric correction factors. J Glaucoma 2005;14(5):337-43.
128. Brubaker RF. Tonometry and corneal thickness. Arch Ophthalmol 1999;117(1):104-5.
129. Brandt JD. CJO Lecture 2007: Central corneal thickness, tonometry, and glaucoma risk - a guide for the perplexed. Can J Ophthalmol 2007;42(4):562-6.
130. Tonnu PA, Ho T, Sharma K, White E, Bunce C, Garway-Heath D. A comparison of four methods of tonometry: method agreement and interobserver variability. Br J Ophthalmol 2005;89(7):847-50.
131. Lass JH, Eriksson GL, Osterling L, Simpson CV. Comparison of the corneal effects of latanoprost, fixed combination latanoprost-timolol, and timolol: A double-masked, randomized, one-year study. Ophthalmology 2001;108(2):264-71.
132. Harasymowycz PJ, Papamatheakis DG, Ennis M, Brady M, Gordon KD. Relationship between travoprost and central corneal thickness in ocular hypertension and open-angle glaucoma. Cornea 2007;26(1):34-41.
133. Arcieri ES, Pierre Filho PT, Wakamatsu TH, Costa VP. The effects of prostaglandin analogues on the blood aqueous barrier and corneal thickness of phakic patients with primary open-angle glaucoma and ocular hypertension. Eye (Lond) 2008;22(2):179-83.
134. Sen E, Nalcacioglu P, Yazici A, Aksakal FN, Altinok A, Tuna T, Koklu G. Comparison of the effects of latanoprost and bimatoprost on central corneal thickness. J Glaucoma 2008;17(5):398-402.
135. Hatanaka M, Vessani RM, Elias IR, Morita C, Susanna R, Jr. The effect of prostaglandin analogs and prostamide on central corneal thickness. J Ocul Pharmacol Ther 2009;25(1):51-3.

136. Schlote T, Tzamalis A, Kynigopoulos M. Central corneal thickness during treatment with travoprost 0.004% in glaucoma patients. J Ocul Pharmacol Ther 2009;25(5):459-62.
137. Bafa M, Georgopoulos G, Mihas C, Stavrakas P, Papaconstantinou D, Vergados I. The effect of prostaglandin analogues on central corneal thickness of patients with chronic open-angle glaucoma: a 2-year study on 129 eyes. Acta Ophthalmol 2009.
138. Mitchell P, Smith W, Attebo K, Healey PR. Prevalence of open-angle glaucoma in Australia. The Blue Mountains Eye Study. Ophthalmology 1996;103(10):1661-9.
139. Wensor MD, McCarty CA, Stanislavsky YL, Livingston PM, Taylor HR. The prevalence of glaucoma in the Melbourne Visual Impairment Project. Ophthalmology 1998;105(4):733-9.
140. Rochtchina E, Mitchell P. Projected number of Australians with glaucoma in 2000 and 2030. Clin Experiment Ophthalmol 2000;28(3):146-8.
141. Tunnel Vision - The Economic Impact of Primary Open Angle Glaucoma. Melbourne: Centre for Eye Research Australia and Access Economics; 2008.
142. Klein BE, Klein R, Sponsel WE, Franke T, Cantor LB, Martone J, Menage MJ. Prevalence of glaucoma. The Beaver Dam Eye Study. Ophthalmology 1992;99(10):1499-504.
143. Coffey M, Reidy A, Wormald R, Xian WX, Wright L, Courtney P. Prevalence of glaucoma in the west of Ireland. Br J Ophthalmol 1993;77(1):17-21.
144. Dielemans I, Vingerling JR, Wolfs RC, Hofman A, Grobbee DE, de Jong PT. The prevalence of primary open-angle glaucoma in a population-based study in The Netherlands. The Rotterdam Study. Ophthalmology 1994;101(11):1851-5.
145. Tielsch JM, Katz J, Singh K, Quigley HA, Gottsch JD, Javitt J, Sommer A. A population-based evaluation of glaucoma screening: the Baltimore Eye Survey. Am J Epidemiol 1991;134(10):1102-10.
146. Quigley HA, West SK, Rodriguez J, Munoz B, Klein R, Snyder R. The prevalence of glaucoma in a population-based study of Hispanic subjects: Proyecto VER. Arch Ophthalmol 2001;119(12):1819-26.
147. Shiose Y, Kitazawa Y, Tsukahara S, Akamatsu T, Mizokami K, Futa R, Katsushima H, Kosaki H. Epidemiology of glaucoma in Japan--a nationwide glaucoma survey. Jpn J Ophthalmol 1991;35(2):133-55.
148. He M, Foster PJ, Ge J, Huang W, Zheng Y, Friedman DS, Lee PS, Khaw PT. Prevalence and clinical characteristics of glaucoma in adult Chinese: a population-based study in Liwan District, Guangzhou. Invest Ophthalmol Vis Sci 2006;47(7):2782-8.
149. Ramakrishnan R, Nirmalan PK, Krishnadas R, Thulasiraj RD, Tielsch JM, Katz J, Friedman DS, Robin AL. Glaucoma in a rural population of southern India: the Aravind comprehensive eye survey. Ophthalmology 2003;110(8):1484-90.
150. Bourne RR, Sukudom P, Foster PJ, Tantisevi V, Jitapunkul S, Lee PS, Johnson GJ, Rojanapongpun P. Prevalence of glaucoma in Thailand: a population based survey in Rom Klao District, Bangkok. Br J Ophthalmol 2003;87(9):1069-74.

151. Rahman MM, Rahman N, Foster PJ, Haque Z, Zaman AU, Dineen B, Johnson GJ. The prevalence of glaucoma in Bangladesh: a population based survey in Dhaka division. Br J Ophthalmol 2004;88(12):1493-7.
152. Teikari JM. Genetic factors in open-angle (simple and capsular) glaucoma. A population-based twin study. Acta Ophthalmol (Copenh) 1987;65(6):715-20.
153. Ofner S, Samples JR. Low-tension glaucoma in identical twins. Am J Ophthalmol 1992;114(6):764-5.
154. Gottfredsdottir MS, Sverrisson T, Musch DC, Stefansson E. Chronic open-angle glaucoma and associated ophthalmic findings in monozygotic twins and their spouses in Iceland. J Glaucoma 1999;8(2):134-9.
155. Fan BJ, Wang DY, Lam DS, Pang CP. Gene mapping for primary open angle glaucoma. Clin Biochem 2006;39(3):249-58.
156. Sheffield VC, Stone EM, Alward WL, Drack AV, Johnson AT, Streb LM, Nichols BE. Genetic linkage of familial open angle glaucoma to chromosome 1q21-q31. Nat Genet 1993;4(1):47-50.
157. Stone EM, Fingert JH, Alward WL, Nguyen TD, Polansky JR, Sunden SL, Nishimura D, Clark AF, Nystuen A, Nichols BE, Mackey DA, Ritch R, Kalenak JW, Craven ER, Sheffield VC. Identification of a gene that causes primary open angle glaucoma. Science 1997;275(5300):668-70.
158. Fingert JH, Heon E, Liebmann JM, Yamamoto T, Craig JE, Rait J, Kawase K, Hoh ST, Buys YM, Dickinson J, Hockey RR, Williams-Lyn D, Trope G, Kitazawa Y, Ritch R, Mackey DA, Alward WL, Sheffield VC, Stone EM. Analysis of myocilin mutations in 1703 glaucoma patients from five different populations. Hum Mol Genet 1999;8(5):899-905.
159. Hogewind BF, Gaplovska-Kysela K, Theelen T, Cremers FP, Yam GH, Hoyng CB, Mukhopadhyay A. Identification and functional characterization of a novel MYOC mutation in two primary open angle glaucoma families from The Netherlands. Mol Vis 2007;13:1793-801.
160. Fingert JH, Ying L, Swiderski RE, Nystuen AM, Arbour NC, Alward WL, Sheffield VC, Stone EM. Characterization and comparison of the human and mouse GLC1A glaucoma genes. Genome Res 1998;8(4):377-84.
161. Tamm ER. Myocilin and glaucoma: facts and ideas. Prog Retin Eye Res 2002;21(4):395-428.
162. Jacobson N, Andrews M, Shepard AR, Nishimura D, Searby C, Fingert JH, Hageman G, Mullins R, Davidson BL, Kwon YH, Alward WL, Stone EM, Clark AF, Sheffield VC. Non-secretion of mutant proteins of the glaucoma gene myocilin in cultured trabecular meshwork cells and in aqueous humor. Hum Mol Genet 2001;10(2):117-25.
163. Sarfarazi M, Child A, Stoilova D, Brice G, Desai T, Trifan OC, Poinoosawmy D, Crick RP. Localization of the fourth locus (GLC1E) for adult-onset primary open-angle glaucoma to the 10p15-p14 region. Am J Hum Genet 1998;62(3):641-52.
164. Rezaie T, Child A, Hitchings R, Brice G, Miller L, Coca-Prados M, Heon E, Krupin T, Ritch R, Kreutzer D, Crick RP, Sarfarazi M. Adult-onset primary open-angle glaucoma caused by mutations in optineurin. Science 2002;295(5557):1077-9.
165. Aung T, Ebenezer ND, Brice G, Child AH, Prescott Q, Lehmann OJ, Hitchings RA, Bhattacharya SS. Prevalence of optineurin sequence variants in adult primary open angle glaucoma: implications for diagnostic testing. J Med Genet 2003;40(8):e101.

166. Alward WL, Kwon YH, Kawase K, Craig JE, Hayreh SS, Johnson AT, Khanna CL, Yamamoto T, Mackey DA, Roos BR, Affatigato LM, Sheffield VC, Stone EM. Evaluation of optineurin sequence variations in 1,048 patients with open-angle glaucoma. Am J Ophthalmol 2003;136(5):904-10.
167. Aung T, Rezaie T, Okada K, Viswanathan AC, Child AH, Brice G, Bhattacharya SS, Lehmann OJ, Sarfarazi M, Hitchings RA. Clinical features and course of patients with glaucoma with the E50K mutation in the optineurin gene. Invest Ophthalmol Vis Sci 2005;46(8):2816-22.
168. Hauser MA, Sena DF, Flor J, Walter J, Auguste J, Larocque-Abramson K, Graham F, Delbono E, Haines JL, Pericak-Vance MA, Rand Allingham R, Wiggs JL. Distribution of optineurin sequence variations in an ethnically diverse population of low-tension glaucoma patients from the United States. J Glaucoma 2006;15(5):358-63.
169. Craig JE, Hewitt AW, Dimasi DP, Howell N, Toomes C, Cohn AC, Mackey DA. The role of the Met98Lys optineurin variant in inherited optic nerve diseases. Br J Ophthalmol 2006;90(11):1420-4.
170. Wajant H, Pfizenmaier K, Scheurich P. Tumor necrosis factor signaling. Cell Death Differ 2003;10(1):45-65.
171. Zhu G, Wu CJ, Zhao Y, Ashwell JD. Optineurin negatively regulates TNFalpha- induced NF-kappaB activation by competing with NEMO for ubiquitinated RIP. Curr Biol 2007;17(16):1438-43.
172. Sudhakar C, Nagabhushana A, Jain N, Swarup G. NF-kappaB mediates tumor necrosis factor alpha-induced expression of optineurin, a negative regulator of NF-kappaB. PLoS One 2009;4(4):e5114.
173. Maruyama H, Morino H, Ito H, Izumi Y, Kato H, Watanabe Y, Kinoshita Y, Kamada M, Nodera H, Suzuki H, Komure O, Matsuura S, Kobatake K, Morimoto N, Abe K, Suzuki N, Aoki M, Kawata A, Hirai T, Kato T, Ogasawara K, Hirano A, Takumi T, Kusaka H, Hagiwara K, Kaji R, Kawakami H. Mutations of optineurin in amyotrophic lateral sclerosis. Nature 2010;465(7295):223-6.
174. Chalasani ML, Radha V, Gupta V, Agarwal N, Balasubramanian D, Swarup G. A glaucoma-associated mutant of optineurin selectively induces death of retinal ganglion cells which is inhibited by antioxidants. Invest Ophthalmol Vis Sci 2007;48(4):1607-14.
175. Chi ZL, Akahori M, Obazawa M, Minami M, Noda T, Nakaya N, Tomarev S, Kawase K, Yamamoto T, Noda S, Sasaoka M, Shimazaki A, Takada Y, Iwata T. Overexpression of optineurin E50K disrupts Rab8 interaction and leads to a progressive retinal degeneration in mice. Hum Mol Genet 2010;19(13):2606-15.
176. Monemi S, Spaeth G, DaSilva A, Popinchalk S, Ilitchev E, Liebmann J, Ritch R, Heon E, Crick RP, Child A, Sarfarazi M. Identification of a novel adult-onset primary open-angle glaucoma (POAG) gene on 5q22.1. Hum Mol Genet 2005;14(6):725-33.
177. Hewitt AW, Dimasi DP, Mackey DA, Craig JE. A Glaucoma Case-control Study of the WDR36 Gene D658G sequence variant. Am J Ophthalmol 2006;142(2):324-5.
178. Fingert JH, Alward WL, Kwon YH, Shankar SP, Andorf JL, Mackey DA, Sheffield VC, Stone EM. No association between variations in the WDR36 gene and primary open-angle glaucoma. Arch Ophthalmol 2007;125(3):434-6.

179. Weisschuh N, Wolf C, Wissinger B, Gramer E. Variations in the WDR36 gene in German patients with normal tension glaucoma. Mol Vis 2007;13:724-9.
180. Pasutto F, Mardin CY, Michels-Rautenstrauss K, Weber BH, Sticht H, Chavarria-Soley G, Rautenstrauss B, Kruse F, Reis A. Profiling of WDR36 Missense Variants in German Patients with Glaucoma. Invest Ophthalmol Vis Sci 2008;49(1):270-4.
181. Miyazawa A, Fuse N, Mengkegale M, Ryu M, Seimiya M, Wada Y, Nishida K. Association between primary open-angle glaucoma and WDR36 DNA sequence variants in Japanese. Mol Vis 2007;13:1912-9.
182. Chi ZL, Yasumoto F, Sergeev Y, Minami M, Obazawa M, Kimura I, Takada Y, Iwata T. Mutant WDR36 directly affects axon growth of retinal ganglion cells leading to progressive retinal degeneration in mice. Hum Mol Genet 2010.
183. Hewitt AW, Craig JE, Mackey DA. Complex genetics of complex traits: the case of primary open-angle glaucoma. Clin Experiment Ophthalmol 2006;34(5):472-84.
184. Fuse N. Genetic bases for glaucoma. Tohoku J Exp Med 2010;221(1):1-10.
185. Sommer A, Katz J, Quigley HA, Miller NR, Robin AL, Richter RC, Witt KA. Clinically detectable nerve fiber atrophy precedes the onset of glaucomatous field loss. Arch Ophthalmol 1991;109(1):77-83.
186. McKendrick AM. Recent developments in perimetry: test stimuli and procedures. Clin Exp Optom 2005;88(2):73-80.
187. Burr JM, Mowatt G, Hernandez R, Siddiqui MA, Cook J, Lourenco T, Ramsay C, Vale L, Fraser C, Azuara-Blanco A, Deeks J, Cairns J, Wormald R, McPherson S, Rabindranath K, Grant A. The clinical effectiveness and cost-effectiveness of screening for open angle glaucoma: a systematic review and economic evaluation. Health Technol Assess 2007;11(41):iii-iv, ix-x, 1-190.
188. Craig JE, Baird PN, Healey DL, McNaught AI, McCartney PJ, Rait JL, Dickinson JL, Roe L, Fingert JH, Stone EM, Mackey DA. Evidence for genetic heterogeneity within eight glaucoma families, with the GLC1A Gln368STOP mutation being an important phenotypic modifier. Ophthalmology 2001;108(9):1607-20.
189. Mackey DA, Healey DL, Fingert JH, Coote MA, Wong TL, Wilkinson CH, McCartney PJ, Rait JL, de Graaf AP, Stone EM, Craig JE. Glaucoma phenotype in pedigrees with the myocilin Thr377Met mutation. Arch Ophthalmol 2003;121(8):1172-80.
190. Hewitt AW, Bennett SL, Richards JE, Dimasi DP, Booth AP, Inglehearn C, Anwar R, Yamamoto T, Fingert JH, Heon E, Craig JE, Mackey DA. Myocilin Gly252Arg mutation and glaucoma of intermediate severity in Caucasian individuals. Arch Ophthalmol 2007;125(1):98-104.
191. Fingert JH, Stone EM, Sheffield VC, Alward WL. Myocilin glaucoma. Surv Ophthalmol 2002;47(6):547-61.
192. Healey DL, Craig JE, Wilkinson CH, Stone EM, Mackey DA. Attitudes to predictive DNA testing for myocilin glaucoma: experience with a large Australian family. J Glaucoma 2004;13(4):304-11.
193. Allingham RR, Liu Y, Rhee DJ. The genetics of primary open-angle glaucoma: a review. Exp Eye Res 2009;88(4):837-44.

194. Risch N, Merikangas K. The future of genetic studies of complex human diseases. Science 1996;273(5281):1516-7.
195. Klein RJ, Zeiss C, Chew EY, Tsai JY, Sackler RS, Haynes C, Henning AK, SanGiovanni JP, Mane SM, Mayne ST, Bracken MB, Ferris FL, Ott J, Barnstable C, Hoh J. Complement factor H polymorphism in age-related macular degeneration. Science 2005;308(5720):385-9.
196. Edwards AO, Ritter R, 3rd, Abel KJ, Manning A, Panhuysen C, Farrer LA. Complement factor H polymorphism and age-related macular degeneration. Science 2005;308(5720):421-4.
197. Consortium WTCC. Genome-wide association study of 14,000 cases of seven common diseases and 3,000 shared controls. Nature 2007;447(7145):661-78.
198. Voight BF, Scott LJ, Steinthorsdottir V, Morris AP, Dina C, Welch RP, Zeggini E, Huth C, Aulchenko YS, Thorleifsson G, McCulloch LJ, Ferreira T, Grallert H, Amin N, Wu G, Willer CJ, Raychaudhuri S, McCarroll SA, Langenberg C, Hofmann OM, Dupuis J, Qi L, Segre AV, van Hoek M, Navarro P, Ardlie K, Balkau B, Benediktsson R, Bennett AJ, Blagieva R, Boerwinkle E, Bonnycastle LL, Bengtsson Bostrom K, Bravenboer B, Bumpstead S, Burtt NP, Charpentier G, Chines PS, Cornelis M, Couper DJ, Crawford G, Doney AS, Elliott KS, Elliott AL, Erdos MR, Fox CS, Franklin CS, Ganser M, Gieger C, Grarup N, Green T, Griffin S, Groves CJ, Guiducci C, Hadjadj S, Hassanali N, Herder C, Isomaa B, Jackson AU, Johnson PR, Jorgensen T, Kao WH, Klopp N, Kong A, Kraft P, Kuusisto J, Lauritzen T, Li M, Lieverse A, Lindgren CM, Lyssenko V, Marre M, Meitinger T, Midthjell K, Morken MA, Narisu N, Nilsson P, Owen KR, Payne F, Perry JR, Petersen AK, Platou C, Proenca C, Prokopenko I, Rathmann W, Rayner NW, Robertson NR, Rocheleau G, Roden M, Sampson MJ, Saxena R, Shields BM, Shrader P, Sigurdsson G, Sparso T, Strassburger K, Stringham HM, Sun Q, Swift AJ, Thorand B, Tichet J, Tuomi T, van Dam RM, van Haeften TW, van Herpt T, van Vliet-Ostaptchouk JV, Bragi Walters G, Weedon MN, Wijmenga C, Witteman J, Bergman RN, Cauchi S, Collins FS, Gloyn AL, Gyllensten U, Hansen T, Hide WA, Hitman GA, Hofman A, Hunter DJ, Hveem K, Laakso M, Mohlke KL, Morris AD, Palmer CN, Pramstaller PP, Rudan I, Sijbrands E, Stein LD, Tuomilehto J, Uitterlinden A, Walker M, Wareham NJ, Watanabe RM, Abecasis GR, Boehm BO, Campbell H, Daly MJ, Hattersley AT, Hu FB, Meigs JB, Pankow JS, Pedersen O, Wichmann HE, Barroso I, Florez JC, Frayling TM, Groop L, Sladek R, Thorsteinsdottir U, Wilson JF, Illig T, Froguel P, van Duijn CM, Stefansson K, Altshuler D, Boehnke M, McCarthy MI. Twelve type 2 diabetes susceptibility loci identified through large-scale association analysis. Nat Genet 2010;42(7):579-89.
199. Mathew CG. New links to the pathogenesis of Crohn disease provided by genome-wide association scans. Nat Rev Genet 2008;9(1):9-14.
200. Lettre G, Rioux JD. Autoimmune diseases: insights from genome-wide association studies. Hum Mol Genet 2008;17(R2):R116-21.
201. Ishibashi T, Takagi Y, Mori K, Naruse S, Nishino H, Yue BY, Kinoshita S. cDNA microarray analysis of gene expression changes induced by dexamethasone in cultured human trabecular meshwork cells. Invest Ophthalmol Vis Sci 2002;43(12):3691-7.
202. Borras T. Gene expression in the trabecular meshwork and the influence of intraocular pressure. Prog Retin Eye Res 2003;22(4):435-63.

203. Steely HT, Jr., English-Wright SL, Clark AF. The similarity of protein expression in trabecular meshwork and lamina cribrosa: implications for glaucoma. Exp Eye Res 2000;70(1):17-30.
204. Levkovitch-Verbin H. Animal models of optic nerve diseases. Eye 2004;18(11):1066-74.
205. Gottesman, II, Gould TD. The endophenotype concept in psychiatry: etymology and strategic intentions. Am J Psychiatry 2003;160(4):636-45.
206. Charlesworth J, Kramer PL, Dyer T, Diego V, Samples JR, Craig JE, Mackey DA, Hewitt AW, Blangero J, Wirtz MK. The path to open angle glaucoma gene discovery: Endophenotypic status of intraocular pressure, cup-to-disc ratio and central corneal thickness. Invest Ophthalmol Vis Sci 2010.
207. Chen P, Jou YS, Fann CS, Chen JW, Chung CM, Lin CY, Wu SY, Kang MJ, Chen YC, Jong YS, Lo HM, Kang CS, Chen CC, Chang HC, Huang NK, Wu YL, Pan WH. Lipoprotein lipase variants associated with an endophenotype of hypertension: hypertension combined with elevated triglycerides. Hum Mutat 2009;30(1):49-55.
208. Hodgkinson CA, Enoch MA, Srivastava V, Cummins-Oman JS, Ferrier C, Iarikova P, Sankararaman S, Yamini G, Yuan Q, Zhou Z, Albaugh B, White KV, Shen PH, Goldman D. Genome-wide association identifies candidate genes that influence the human electroencephalogram. Proc Natl Acad Sci U S A 2010;107(19):8695-700.
209. Sacco R, Papaleo V, Hager J, Rousseau F, Moessner R, Militerni R, Bravaccio C, Trillo S, Schneider C, Melmed R, Elia M, Curatolo P, Manzi B, Pascucci T, Puglisi-Allegra S, Reichelt KL, Persico AM. Case-control and family-based association studies of candidate genes in autistic disorder and its endophenotypes: TPH2 and GLO1. BMC Med Genet 2007;8:11.
210. Watanabe A, Toyota T, Owada Y, Hayashi T, Iwayama Y, Matsumata M, Ishitsuka Y, Nakaya A, Maekawa M, Ohnishi T, Arai R, Sakurai K, Yamada K, Kondo H, Hashimoto K, Osumi N, Yoshikawa T. Fabp7 maps to a quantitative trait locus for a schizophrenia endophenotype. PLoS Biol 2007;5(11):e297.
211. Rommelse NN, Arias-Vasquez A, Altink ME, Buschgens CJ, Fliers E, Asherson P, Faraone SV, Buitelaar JK, Sergeant JA, Oosterlaan J, Franke B. Neuropsychological endophenotype approach to genome-wide linkage analysis identifies susceptibility loci for ADHD on 2q21.1 and 13q12.11. Am J Hum Genet 2008;83(1):99-105.
212. Zhou X, Tang W, Greenwood TA, Guo S, He L, Geyer MA, Kelsoe JR. Transcription factor SP4 is a susceptibility gene for bipolar disorder. PLoS One 2009;4(4):e5196.
213. Alsbirk PH. Corneal thickness. II. Environmental and genetic factors. Acta Ophthalmol (Copenh) 1978;56(1):105-13.
214. Vijaya L, George R, Baskaran M, Arvind H, Raju P, Ramesh SV, Kumaramanickavel G, McCarty C. Prevalence of primary open-angle glaucoma in an urban south Indian population and comparison with a rural population. The Chennai Glaucoma Study. Ophthalmology 2008;115(4):648-54 e1.
215. Toh T, Liew SH, MacKinnon JR, Hewitt AW, Poulsen JL, Spector TD, Gilbert CE, Craig JE, Hammond CJ, Mackey DA. Central corneal thickness is highly heritable: the twin eye studies. Invest Ophthalmol Vis Sci 2005;46(10):3718-22.

216. Zheng Y, Ge J, Huang G, Zhang J, Liu B, Hur YM, He M. Heritability of central corneal thickness in Chinese: the Guangzhou Twin Eye Study. Invest Ophthalmol Vis Sci 2008;49(10):4303-7.
217. Landers JA, Hewitt AW, Dimasi DP, Charlesworth JC, Straga T, Mills RA, Savarirayan R, Mackey DA, Burdon KP, Craig JE. Heritability of central corneal thickness in nuclear families. Invest Ophthalmol Vis Sci 2009;50(9):4087-90.
218. Spence MA, Westlake J, Lange K. Estimation of the variance components for dermal ridge count. Ann Hum Genet 1977;41(1):111-5.
219. Martin NG, Eaves LJ, Loesch DZ. A genetical analysis of covariation between finger ridge counts. Ann Hum Biol 1982;9(6):539-52.
220. Loesch DZ, Huggins RM. Fixed and random effects in the variation of the finger ridge count: a study of fragile-X families. Am J Hum Genet 1992;50(5):1067-76.
221. Herndon LW, Choudhri SA, Cox T, Damji KF, Shields MB, Allingham RR. Central corneal thickness in normal, glaucomatous, and ocular hypertensive eyes. Arch Ophthalmol 1997;115(9):1137-41.
222. Copt RP, Thomas R, Mermoud A. Corneal thickness in ocular hypertension, primary open-angle glaucoma, and normal tension glaucoma. Arch Ophthalmol 1999;117(1):14-6.
223. Emara BY, Tingey DP, Probst LE, Motolko MA. Central corneal thickness in low-tension glaucoma. Can J Ophthalmol 1999;34(6):319-24.
224. Su DH, Wong TY, Wong WL, Saw SM, Tan DT, Shen SY, Loon SC, Foster PJ, Aung T. Diabetes, hyperglycemia, and central corneal thickness: the Singapore Malay Eye Study. Ophthalmology 2008;115(6):964-8 e1.
225. Nissen J, Hjortdal JO, Ehlers N, Frost-Larsen K, Sorensen T. A clinical comparison of optical and ultrasonic pachometry. Acta Ophthalmol (Copenh) 1991;69(5):659-63.
226. Giasson C, Forthomme D. Comparison of central corneal thickness measurements between optical and ultrasound pachometers. Optom Vis Sci 1992;69(3):236-41.
227. Salz JJ, Azen SP, Berstein J, Caroline P, Villasenor RA, Schanzlin DJ. Evaluation and comparison of sources of variability in the measurement of corneal thickness with ultrasonic and optical pachymeters. Ophthalmic Surg 1983;14(9):750-4.
228. Bechmann M, Thiel MJ, Neubauer AS, Ullrich S, Ludwig K, Kenyon KR, Ulbig MW. Central corneal thickness measurement with a retinal optical coherence tomography device versus standard ultrasonic pachymetry. Cornea 2001;20(1):50-4.
229. Wong AC, Wong CC, Yuen NS, Hui SP. Correlational study of central corneal thickness measurements on Hong Kong Chinese using optical coherence tomography, Orbscan and ultrasound pachymetry. Eye 2002;16(6):715-21.
230. Leung DY, Lam DK, Yeung BY, Lam DS. Comparison between central corneal thickness measurements by ultrasound pachymetry and optical coherence tomography. Clin Experiment Ophthalmol 2006;34(8):751-4.
231. Zhao PS, Wong TY, Wong WL, Saw SM, Aung T. Comparison of central corneal thickness measurements by visante anterior segment optical coherence tomography with ultrasound pachymetry. Am J Ophthalmol 2007;143(6):1047-9.

232. Barkana Y, Gerber Y, Elbaz U, Schwartz S, Ken-Dror G, Avni I, Zadok D. Central corneal thickness measurement with the Pentacam Scheimpflug system, optical low-coherence reflectometry pachymeter, and ultrasound pachymetry. J Cataract Refract Surg 2005;31(9):1729-35.
233. Modis L, Jr., Langenbucher A, Seitz B. Corneal thickness measurements with contact and noncontact specular microscopic and ultrasonic pachymetry. Am J Ophthalmol 2001;132(4):517-21.
234. Zhao MH, Zou J, Wang WQ, Li J. Comparison of central corneal thickness as measured by non-contact specular microscopy and ultrasound pachymetry before and post LASIK. Clin Experiment Ophthalmol 2007;35(9):818-23.
235. Healey P, Mitchell P, Rochtchina E, Lee AJ, Chia E, Wang JJ. Distribution and associations of central corneal thickness in an Australian population. In: Annual Scientific Congress of the Royal Australian and New Zealand College of Ophthalmologists. Hobart, Tasmania, Australia; 2005.
236. Alsbirk PH. Corneal thickness. I. Age variation, sex difference and oculometric correlations. Acta Ophthalmol (Copenh) 1978;56(1):95-104.
237. Wu LL, Suzuki Y, Ideta R, Araie M. Central corneal thickness of normal tension glaucoma patients in Japan. Jpn J Ophthalmol 2000;44(6):643-7.
238. Dohadwala AA, Munger R, Damji KF. Positive correlation between Tono-Pen intraocular pressure and central corneal thickness. Ophthalmology 1998;105(10):1849-54.
239. La Rosa FA, Gross RL, Orengo-Nania S. Central corneal thickness of Caucasians and African Americans in glaucomatous and nonglaucomatous populations. Arch Ophthalmol 2001;119(1):23-7.
240. Torres RJ, Jones E, Edmunds B, Becker T, Cioffi GA, Mansberger SL. Central Corneal Thickness in Northwestern American Indians/Alaskan Natives and Comparison with White and African-American Persons. Am J Ophthalmol 2008.
241. Durkin SR, Tan EW, Casson RJ, Selva D, Newland HS. Central corneal thickness among Aboriginal people attending eye clinics in remote South Australia. Clin Experiment Ophthalmol 2007;35(8):728-32.
242. Lifshitz T, Levy J, Rosen S, Belfair N, Levinger S. Central corneal thickness and its relationship to the patient's origin. Eye 2006;20(4):460-5.
243. Brandt JD, Casuso LA, Budenz DL. Markedly increased central corneal thickness: an unrecognized finding in congenital aniridia. Am J Ophthalmol 2004;137(2):348-50.
244. Whitson JT, Liang C, Godfrey DG, Petroll WM, Cavanagh HD, Patel D, Fellman RL, Starita RJ. Central corneal thickness in patients with congenital aniridia. Eye Contact Lens 2005;31(5):221-4.
245. Lehmann OJ, Tuft S, Brice G, Smith R, Blixt A, Bell R, Johansson B, Jordan T, Hitchings RA, Khaw PT, John SW, Carlsson P, Bhattacharya SS. Novel anterior segment phenotypes resulting from forkhead gene alterations: evidence for cross-species conservation of function. Invest Ophthalmol Vis Sci 2003;44(6):2627-33.
246. Asai-Coakwell M, Backhouse C, Casey RJ, Gage PJ, Lehmann OJ. Reduced human and murine corneal thickness in an Axenfeld-Rieger syndrome subtype. Invest Ophthalmol Vis Sci 2006;47(11):4905-9.
247. Evereklioglu C, Er H. Increased corneal thickness in active Behcet's disease. Eur J Ophthalmol 2002;12(1):24-9.

248. Evereklioglu C, Yilmaz K, Bekir NA. Decreased central corneal thickness in children with Down syndrome. J Pediatr Ophthalmol Strabismus 2002;39(5):274-7.
249. Razeghinejad MR, Safavian H. Central corneal thickness in patients with Weill-Marchesani syndrome. Am J Ophthalmol 2006;142(3):507-8.
250. Sykes B, Ogilvie D, Wordsworth P, Wallis G, Mathew C, Beighton P, Nicholls A, Pope FM, Thompson E, Tsipouras P, et al. Consistent linkage of dominantly inherited osteogenesis imperfecta to the type I collagen loci: COL1A1 and COL1A2. Am J Hum Genet 1990;46(2):293-307.
251. Gajko-Galicka A. Mutations in type I collagen genes resulting in osteogenesis imperfecta in humans. Acta Biochim Pol 2002;49(2):433-41.
252. Pollitt R, McMahon R, Nunn J, Bamford R, Afifi A, Bishop N, Dalton A. Mutation analysis of COL1A1 and COL1A2 in patients diagnosed with osteogenesis imperfecta type I-IV. Hum Mutat 2006;27(7):716.
253. Malfait F, Coucke P, Symoens S, Loeys B, Nuytinck L, De Paepe A. The molecular basis of classic Ehlers-Danlos syndrome: a comprehensive study of biochemical and molecular findings in 48 unrelated patients. Hum Mutat 2005;25(1):28-37.
254. Birk DE, Fitch JM, Babiarz JP, Linsenmayer TF. Collagen type I and type V are present in the same fibril in the avian corneal stroma. J Cell Biol 1988;106(3):999-1008.
255. Mietz H, Kasner L, Green WR. Histopathologic and electron-microscopic features of corneal and scleral collagen fibers in osteogenesis imperfecta type III. Graefes Arch Clin Exp Ophthalmol 1997;235(7):405-10.
256. Lee B, Godfrey M, Vitale E, Hori H, Mattei MG, Sarfarazi M, Tsipouras P, Ramirez F, Hollister DW. Linkage of Marfan syndrome and a phenotypically related disorder to two different fibrillin genes. Nature 1991;352(6333):330-4.
257. Dietz HC, Cutting GR, Pyeritz RE, Maslen CL, Sakai LY, Corson GM, Puffenberger EG, Hamosh A, Nanthakumar EJ, Curristin SM, et al. Marfan syndrome caused by a recurrent de novo missense mutation in the fibrillin gene. Nature 1991;352(6333):337-9.
258. Tsipouras P, Del Mastro R, Sarfarazi M, Lee B, Vitale E, Child AH, Godfrey M, Devereux RB, Hewett D, Steinmann B, et al. Genetic linkage of the Marfan syndrome, ectopia lentis, and congenital contractural arachnodactyly to the fibrillin genes on chromosomes 15 and 5. The International Marfan Syndrome Collaborative Study. N Engl J Med 1992;326(14):905-9.
259. Dietz HC, Pyeritz RE, Puffenberger EG, Kendzior RJ, Jr., Corson GM, Maslen CL, Sakai LY, Francomano CA, Cutting GR. Marfan phenotype variability in a family segregating a missense mutation in the epidermal growth factor-like motif of the fibrillin gene. J Clin Invest 1992;89(5):1674-80.
260. Faivre L, Gorlin RJ, Wirtz MK, Godfrey M, Dagoneau N, Samples JR, Le Merrer M, Collod-Beroud G, Boileau C, Munnich A, Cormier-Daire V. In frame fibrillin-1 gene deletion in autosomal dominant Weill-Marchesani syndrome. J Med Genet 2003;40(1):34-6.
261. Zaidi TS, Hasan A, Baum J, Panjwani N. Localization of fibrillin in normal human and bovine corneas (ARVO Abstract). Invest Ophthalmol Vis Sci 1991;32(4).

262. Wheatley HM, Traboulsi EI, Flowers BE, Maumenee IH, Azar D, Pyeritz RE, Whittum-Hudson JA. Immunohistochemical localization of fibrillin in human ocular tissues. Relevance to the Marfan syndrome. Arch Ophthalmol 1995;113(1):103-9.
263. Gage PJ, Rhoades W, Prucka SK, Hjalt T. Fate maps of neural crest and mesoderm in the mammalian eye. Invest Ophthalmol Vis Sci 2005;46(11):4200-8.
264. Rehnberg M, Ammitzboll T, Tengroth B. Collagen distribution in the lamina cribrosa and the trabecular meshwork of the human eye. Br J Ophthalmol 1987;71(12):886-92.
265. Watson PG, Young RD. Scleral structure, organisation and disease. A review. Exp Eye Res 2004;78(3):609-23.
266. Sigal IA, Flanagan JG, Ethier CR. Factors influencing optic nerve head biomechanics. Invest Ophthalmol Vis Sci 2005;46(11):4189-99.
267. Norman RE, Flanagan JG, Rausch SM, Sigal IA, Tertinegg I, Eilaghi A, Portnoy S, Sled JG, Ethier CR. Dimensions of the human sclera: Thickness measurement and regional changes with axial length. Exp Eye Res 2010;90(2):277-84.
268. Downs JC, Ensor ME, Bellezza AJ, Thompson HW, Hart RT, Burgoyne CF. Posterior scleral thickness in perfusion-fixed normal and early-glaucoma monkey eyes. Invest Ophthalmol Vis Sci 2001;42(13):3202-8.
269. Albekioni Z, Joson P, Tello C, Liebmann JM, Ritch R. Correlation between Central Corneal Thickness and Scleral Thickness. Invest Ophthalmol Vis Sci 2003;44:E-Abstract 103.
270. Mohamed-Noor J, Bochmann F, Siddiqui MA, Atta HR, Leslie T, Maharajan P, Wong YM, Azuara-Blanco A. Correlation between corneal and scleral thickness in glaucoma. J Glaucoma 2009;18(1):32-6.
271. Yoo C, Eom YS, Suh YW, Kim YY. Central Corneal Thickness and Anterior Scleral Thickness in Korean Patients With Open-angle Glaucoma: An Anterior Segment Optical Coherence Tomography Study. J Glaucoma 2010.
272. Jonas JB, Holbach L. Central corneal thickness and thickness of the lamina cribrosa in human eyes. Invest Ophthalmol Vis Sci 2005;46(4):1275-9.
273. Ren R, Wang N, Li B, Li L, Gao F, Xu X, Jonas JB. Lamina cribrosa and peripapillary sclera histomorphometry in normal and advanced glaucomatous Chinese eyes with various axial length. Invest Ophthalmol Vis Sci 2009;50(5):2175-84.
274. Jonas JB, Hayreh SS, Tao Y. Central corneal thickness and thickness of the lamina cribrosa and peripapillary sclera in monkeys. Arch Ophthalmol 2009;127(10):1395-6.
275. van Koolwijk LM, Despriet DD, van Duijn CM, Pardo Cortes LM, Vingerling JR, Aulchenko YS, Oostra BA, Klaver CC, Lemij HG. Genetic contributions to glaucoma: heritability of intraocular pressure, retinal nerve fiber layer thickness, and optic disc morphology. Invest Ophthalmol Vis Sci 2007;48(8):3669-76.
276. Healey P, Carbonaro F, Taylor B, Spector TD, Mitchell P, Hammond CJ. The heritability of optic disc parameters: a classic twin study. Invest Ophthalmol Vis Sci 2008;49(1):77-80.
277. He M, Liu B, Huang W, Zhang J, Yin Q, Zheng Y, Wang D, Ge J. Heritability of optic disc and cup measured by the Heidelberg Retinal

Tomography in Chinese: the Guangzhou twin eye study. Invest Ophthalmol Vis Sci 2008;49(4):1350-5.

278. Pakravan M, Parsa A, Sanagou M, Parsa CF. Central corneal thickness and correlation to optic disc size: a potential link for susceptibility to glaucoma. Br J Ophthalmol 2007;91(1):26-8.
279. Cankaya AB, Elgin U, Batman A, Acaroglu G. Relationship between central corneal thickness and parameters of optic nerve head topography in healthy subjects. Eur J Ophthalmol 2008;18(1):32-8.
280. Terai N, Spoerl E, Pillunat LE, Kuhlisch E, Schmidt E, Boehm AG. The relationship between central corneal thickness and optic disc size in patients with primary open-angle glaucoma in a hospital-based population. Acta Ophthalmol 2009.
281. Insull E, Nicholas S, Ang GS, Poostchi A, Chan K, Wells A. Optic disc area and correlation with central corneal thickness, corneal hysteresis and ocular pulse amplitude in glaucoma patients and controls. Clin Experiment Ophthalmol 2010.
282. Healey PR, Mitchell P. Optic disk size in open-angle glaucoma: the Blue Mountains Eye Study. Am J Ophthalmol 1999;128(4):515-7.
283. Tezel G, Trinkaus K, Wax MB. Alterations in the morphology of lamina cribrosa pores in glaucomatous eyes. Br J Ophthalmol 2004;88(2):251-6.
284. Hawker MJ, Edmunds MR, Vernon SA, Hillman JG, Macnab HK. The relationship between central corneal thickness and the optic disc in an elderly population: the Bridlington Eye Assessment Project. Eye 2007.
285. Gunvant P, Porsia L, Watkins RJ, Bayliss-Brown H, Broadway DC. Relationships between central corneal thickness and optic disc topography in eyes with glaucoma, suspicion of glaucoma, or ocular hypertension. Clin Ophthalmol 2008;2(3):591-9.
286. Tomais G, Georgopoulos G, Koutsandrea C, Moschos M. Correlation of central corneal thickness and axial length to the optic disc and peripapillary atrophy among healthy individuals, glaucoma and ocular hypertension patients. Clin Ophthalmol 2008;2(4):981-8.
287. Lesk MR, Hafez AS, Descovich D. Relationship between central corneal thickness and changes of optic nerve head topography and blood flow after intraocular pressure reduction in open-angle glaucoma and ocular hypertension. Arch Ophthalmol 2006;124(11):1568-72.
288. Nicolela MT, Soares AS, Carrillo MM, Chauhan BC, LeBlanc RP, Artes PH. Effect of moderate intraocular pressure changes on topographic measurements with confocal scanning laser tomography in patients with glaucoma. Arch Ophthalmol 2006;124(5):633-40.
289. Wells AP, Garway-Heath DF, Poostchi A, Wong T, Chan KC, Sachdev N. Corneal hysteresis but not corneal thickness correlates with optic nerve surface compliance in glaucoma patients. Invest Ophthalmol Vis Sci 2008;49(8):3262-8.
290. Wyatt D, Taheri S, Triana M, Abdrabou W, Desronvil T, Delbono E, Olivier M, Wiggs JL. Distribution of DNA Sequence Variants in COL8A1 and COL8A2 in Glaucoma Patients With Thin CCT. In: ARVO. Fort Lauderdale, Florida, United States; 2009.
291. Johansson A, Marroni F, Hayward C, Franklin CS, Kirichenko AV, Jonasson I, Hicks AA, Vitart V, Isaacs A, Axenovich T, Campbell S, Dunlop MG, Floyd J, Hastie N, Hofman A, Knott S, Kolcic I, Pichler I, Polasek O,

Rivadeneira F, Tenesa A, Uitterlinden AG, Wild SH, Zorkoltseva IV, Meitinger T, Wilson JF, Rudan I, Campbell H, Pattaro C, Pramstaller P, Oostra BA, Wright AF, van Duijn CM, Aulchenko YS, Gyllensten U. Common variants in the JAZF1 gene associated with height identified by linkage and genome-wide association analysis. Hum Mol Genet 2009;18(2):373-80.

292. Lei SF, Yang TL, Tan LJ, Chen XD, Guo Y, Guo YF, Zhang L, Liu XG, Yan H, Pan F, Zhang ZX, Peng YM, Zhou Q, He LN, Zhu XZ, Cheng J, Liu YZ, Papasian CJ, Deng HW. Genome-wide association scan for stature in Chinese: evidence for ethnic specific loci. Hum Genet 2009;125(1):1-9.

293. Thorleifsson G, Walters GB, Gudbjartsson DF, Steinthorsdottir V, Sulem P, Helgadottir A, Styrkarsdottir U, Gretarsdottir S, Thorlacius S, Jonsdottir I, Jonsdottir T, Olafsdottir EJ, Olafsdottir GH, Jonsson T, Jonsson F, Borch-Johnsen K, Hansen T, Andersen G, Jorgensen T, Lauritzen T, Aben KK, Verbeek AL, Roeleveld N, Kampman E, Yanek LR, Becker LC, Tryggvadottir L, Rafnar T, Becker DM, Gulcher J, Kiemeney LA, Pedersen O, Kong A, Thorsteinsdottir U, Stefansson K. Genome-wide association yields new sequence variants at seven loci that associate with measures of obesity. Nat Genet 2009;41(1):18-24.

294. Willer CJ, Speliotes EK, Loos RJ, Li S, Lindgren CM, Heid IM, Berndt SI, Elliott AL, Jackson AU, Lamina C, Lettre G, Lim N, Lyon HN, McCarroll SA, Papadakis K, Qi L, Randall JC, Roccasecca RM, Sanna S, Scheet P, Weedon MN, Wheeler E, Zhao JH, Jacobs LC, Prokopenko I, Soranzo N, Tanaka T, Timpson NJ, Almgren P, Bennett A, Bergman RN, Bingham SA, Bonnycastle LL, Brown M, Burtt NP, Chines P, Coin L, Collins FS, Connell JM, Cooper C, Smith GD, Dennison EM, Deodhar P, Elliott P, Erdos MR, Estrada K, Evans DM, Gianniny L, Gieger C, Gillson CJ, Guiducci C, Hackett R, Hadley D, Hall AS, Havulinna AS, Hebebrand J, Hofman A, Isomaa B, Jacobs KB, Johnson T, Jousilahti P, Jovanovic Z, Khaw KT, Kraft P, Kuokkanen M, Kuusisto J, Laitinen J, Lakatta EG, Luan J, Luben RN, Mangino M, McArdle WL, Meitinger T, Mulas A, Munroe PB, Narisu N, Ness AR, Northstone K, O'Rahilly S, Purmann C, Rees MG, Ridderstrale M, Ring SM, Rivadeneira F, Ruokonen A, Sandhu MS, Saramies J, Scott LJ, Scuteri A, Silander K, Sims MA, Song K, Stephens J, Stevens S, Stringham HM, Tung YC, Valle TT, Van Duijn CM, Vimaleswaran KS, Vollenweider P, Waeber G, Wallace C, Watanabe RM, Waterworth DM, Watkins N, Witteman JC, Zeggini E, Zhai G, Zillikens MC, Altshuler D, Caulfield MJ, Chanock SJ, Farooqi IS, Ferrucci L, Guralnik JM, Hattersley AT, Hu FB, Jarvelin MR, Laakso M, Mooser V, Ong KK, Ouwehand WH, Salomaa V, Samani NJ, Spector TD, Tuomi T, Tuomilehto J, Uda M, Uitterlinden AG, Wareham NJ, Deloukas P, Frayling TM, Groop LC, Hayes RB, Hunter DJ, Mohlke KL, Peltonen L, Schlessinger D, Strachan DP, Wichmann HE, McCarthy MI, Boehnke M, Barroso I, Abecasis GR, Hirschhorn JN. Six new loci associated with body mass index highlight a neuronal influence on body weight regulation. Nat Genet 2009;41(1):25-34.

295. Richards JB, Rivadeneira F, Inouye M, Pastinen TM, Soranzo N, Wilson SG, Andrew T, Falchi M, Gwilliam R, Ahmadi KR, Valdes AM, Arp P, Whittaker P, Verlaan DJ, Jhamai M, Kumanduri V, Moorhouse M, van Meurs JB, Hofman A, Pols HA, Hart D, Zhai G, Kato BS, Mullin BH, Zhang F, Deloukas P, Uitterlinden AG, Spector TD. Bone mineral density,

osteoporosis, and osteoporotic fractures: a genome-wide association study. Lancet 2008;371(9623):1505-12.

296. Styrkarsdottir U, Halldorsson BV, Gretarsdottir S, Gudbjartsson DF, Walters GB, Ingvarsson T, Jonsdottir T, Saemundsdottir J, Center JR, Nguyen TV, Bagger Y, Gulcher JR, Eisman JA, Christiansen C, Sigurdsson G, Kong A, Thorsteinsdottir U, Stefansson K. Multiple genetic loci for bone mineral density and fractures. N Engl J Med 2008;358(22):2355-65.
297. Aulchenko YS, Ripatti S, Lindqvist I, Boomsma D, Heid IM, Pramstaller PP, Penninx BW, Janssens AC, Wilson JF, Spector T, Martin NG, Pedersen NL, Kyvik KO, Kaprio J, Hofman A, Freimer NB, Jarvelin MR, Gyllensten U, Campbell H, Rudan I, Johansson A, Marroni F, Hayward C, Vitart V, Jonasson I, Pattaro C, Wright A, Hastie N, Pichler I, Hicks AA, Falchi M, Willemsen G, Hottenga JJ, de Geus EJ, Montgomery GW, Whitfield J, Magnusson P, Saharinen J, Perola M, Silander K, Isaacs A, Sijbrands EJ, Uitterlinden AG, Witteman JC, Oostra BA, Elliott P, Ruokonen A, Sabatti C, Gieger C, Meitinger T, Kronenberg F, Doring A, Wichmann HE, Smit JH, McCarthy MI, van Duijn CM, Peltonen L. Loci influencing lipid levels and coronary heart disease risk in 16 European population cohorts. Nat Genet 2009;41(1):47-55.
298. Racette L, Liebmann JM, Girkin CA, Zangwill LM, Jain S, Becerra LM, Medeiros FA, Bowd C, Weinreb RN, Boden C, Sample PA. African Descent and Glaucoma Evaluation Study (ADAGES): III. Ancestry differences in visual function in healthy eyes. Arch Ophthalmol 2010;128(5):551-9.
299. Nangia V, Jonas JB, Sinha A, Matin A, Kulkarni M. Central corneal thickness and its association with ocular and general parameters in Indians: the Central India Eye and Medical Study. Ophthalmology 2010;117(4):705-10.
300. Barsh GS. What controls variation in human skin color? PLoS Biol 2003;1(1):E27.
301. Slominski A, Wortsman J, Plonka PM, Schallreuter KU, Paus R, Tobin DJ. Hair follicle pigmentation. J Invest Dermatol 2005;124(1):13-21.
302. Yamaguchi Y, Brenner M, Hearing VJ. The regulation of skin pigmentation. J Biol Chem 2007;282(38):27557-61.
303. Sturm RA, Larsson M. Genetics of human iris colour and patterns. Pigment Cell Melanoma Res 2009;22(5):544-62.
304. Land EJ, Riley PA. Spontaneous redox reactions of dopaquinone and the balance between the eumelanic and phaeomelanic pathways. Pigment Cell Res 2000;13(4):273-7.
305. Costin GE, Hearing VJ. Human skin pigmentation: melanocytes modulate skin color in response to stress. Faseb J 2007;21(4):976-94.
306. Lin JY, Fisher DE. Melanocyte biology and skin pigmentation. Nature 2007;445(7130):843-50.
307. Kobayashi T, Imokawa G, Bennett DC, Hearing VJ. Tyrosinase stabilization by Tyrp1 (the brown locus protein). J Biol Chem 1998;273(48):31801-5.
308. Manga P, Sato K, Ye L, Beermann F, Lamoreux ML, Orlow SJ. Mutational analysis of the modulation of tyrosinase by tyrosinase-related proteins 1 and 2 in vitro. Pigment Cell Res 2000;13(5):364-74.
309. Kobayashi T, Hearing VJ. Direct interaction of tyrosinase with Tyrp1 to form heterodimeric complexes in vivo. J Cell Sci 2007;120(Pt 24):4261-8.

310. Ito S, Wakamatsu K. Chemistry of mixed melanogenesis--pivotal roles of dopaquinone. Photochem Photobiol 2008;84(3):582-92.
311. Van Den Bossche K, Naeyaert JM, Lambert J. The quest for the mechanism of melanin transfer. Traffic 2006;7(7):769-78.
312. Fukuda M, Kuroda TS, Mikoshiba K. Slac2-a/melanophilin, the missing link between Rab27 and myosin Va: implications of a tripartite protein complex for melanosome transport. J Biol Chem 2002;277(14):12432-6.
313. Kuroda TS, Ariga H, Fukuda M. The actin-binding domain of Slac2-a/melanophilin is required for melanosome distribution in melanocytes. Mol Cell Biol 2003;23(15):5245-55.
314. Tadokoro T, Yamaguchi Y, Batzer J, Coelho SG, Zmudzka BZ, Miller SA, Wolber R, Beer JZ, Hearing VJ. Mechanisms of skin tanning in different racial/ethnic groups in response to ultraviolet radiation. J Invest Dermatol 2005;124(6):1326-32.
315. Wakamatsu K, Kavanagh R, Kadekaro AL, Terzieva S, Sturm RA, Leachman S, Abdel-Malek Z, Ito S. Diversity of pigmentation in cultured human melanocytes is due to differences in the type as well as quantity of melanin. Pigment Cell Res 2006;19(2):154-62.
316. Szabo G, Gerald AB, Pathak MA, Fitzpatrick TB. Racial differences in the fate of melanosomes in human epidermis. Nature 1969;222(5198):1081-2.
317. Rees JL. The melanocortin 1 receptor (MC1R): more than just red hair. Pigment Cell Res 2000;13(3):135-40.
318. Cone RD, Lu D, Koppula S, Vage DI, Klungland H, Boston B, Chen W, Orth DN, Pouton C, Kesterson RA. The melanocortin receptors: agonists, antagonists, and the hormonal control of pigmentation. Recent Prog Horm Res 1996;51:287-317; discussion 8.
319. Busca R, Ballotti R. Cyclic AMP a key messenger in the regulation of skin pigmentation. Pigment Cell Res 2000;13(2):60-9.
320. Garcia-Borron JC, Sanchez-Laorden BL, Jimenez-Cervantes C. Melanocortin-1 receptor structure and functional regulation. Pigment Cell Res 2005;18(6):393-410.
321. Levy C, Khaled M, Fisher DE. MITF: master regulator of melanocyte development and melanoma oncogene. Trends Mol Med 2006;12(9):406-14.
322. Furumura M, Sakai C, Abdel-Malek Z, Barsh GS, Hearing VJ. The interaction of agouti signal protein and melanocyte stimulating hormone to regulate melanin formation in mammals. Pigment Cell Res 1996;9(4):191-203.
323. Suzuki I, Tada A, Ollmann MM, Barsh GS, Im S, Lamoreux ML, Hearing VJ, Nordlund JJ, Abdel-Malek ZA. Agouti signaling protein inhibits melanogenesis and the response of human melanocytes to alpha-melanotropin. J Invest Dermatol 1997;108(6):838-42.
324. Clark P, Stark AE, Walsh RJ, Jardine R, Martin NG. A twin study of skin reflectance. Ann Hum Biol 1981;8(6):529-41.
325. Eller MS, Gilchrest BA. Tanning as part of the eukaryotic SOS response. Pigment Cell Res 2000;13 Suppl 8:94-7.
326. Miyamura Y, Coelho SG, Wolber R, Miller SA, Wakamatsu K, Zmudzka BZ, Ito S, Smuda C, Passeron T, Choi W, Batzer J, Yamaguchi Y, Beer JZ, Hearing VJ. Regulation of human skin pigmentation and responses to ultraviolet radiation. Pigment Cell Res 2007;20(1):2-13.

327. Colour Genes. European Society for Pigment Cell Research, 2010. (Accessed July, 2010, at http://www.espcr.org/micemut.)
328. Sturm RA. Molecular genetics of human pigmentation diversity. Hum Mol Genet 2009;18(R1):R9-17.
329. Wasmeier C, Hume AN, Bolasco G, Seabra MC. Melanosomes at a glance. J Cell Sci 2008;121(Pt 24):3995-9.
330. Oetting WS, King RA. Molecular basis of albinism: mutations and polymorphisms of pigmentation genes associated with albinism. Hum Mutat 1999;13(2):99-115.
331. Gronskov K, Ek J, Brondum-Nielsen K. Oculocutaneous albinism. Orphanet J Rare Dis 2007;2:43.
332. Brilliant MH. The mouse p (pink-eyed dilution) and human P genes, oculocutaneous albinism type 2 (OCA2), and melanosomal pH. Pigment Cell Res 2001;14(2):86-93.
333. Puri N, Gardner JM, Brilliant MH. Aberrant pH of melanosomes in pink-eyed dilution (p) mutant melanocytes. J Invest Dermatol 2000;115(4):607-13.
334. Manga P, Boissy RE, Pifko-Hirst S, Zhou BK, Orlow SJ. Mislocalization of melanosomal proteins in melanocytes from mice with oculocutaneous albinism type 2. Exp Eye Res 2001;72(6):695-710.
335. Chen K, Manga P, Orlow SJ. Pink-eyed dilution protein controls the processing of tyrosinase. Mol Biol Cell 2002;13(6):1953-64.
336. Costin GE, Valencia JC, Vieira WD, Lamoreux ML, Hearing VJ. Tyrosinase processing and intracellular trafficking is disrupted in mouse primary melanocytes carrying the underwhite (uw) mutation. A model for oculocutaneous albinism (OCA) type 4. J Cell Sci 2003;116(Pt 15):3203-12.
337. Wong TH, Rees JL. The relation between melanocortin 1 receptor (MC1R) variation and the generation of phenotypic diversity in the cutaneous response to ultraviolet radiation. Peptides 2005;26(10):1965-71.
338. Rees JL. The genetics of sun sensitivity in humans. Am J Hum Genet 2004;75(5):739-51.
339. Abdel-Malek ZA, Knittel J, Kadekaro AL, Swope VB, Starner R. The melanocortin 1 receptor and the UV response of human melanocytes--a shift in paradigm. Photochem Photobiol 2008;84(2):501-8.
340. Kanetsky PA, Swoyer J, Panossian S, Holmes R, Guerry D, Rebbeck TR. A polymorphism in the agouti signaling protein gene is associated with human pigmentation. Am J Hum Genet 2002;70(3):770-5.
341. Frudakis T, Thomas M, Gaskin Z, Venkateswarlu K, Chandra KS, Ginjupalli S, Gunturi S, Natrajan S, Ponnuswamy VK, Ponnuswamy KN. Sequences associated with human iris pigmentation. Genetics 2003;165(4):2071-83.
342. Bonilla C, Boxill LA, Donald SA, Williams T, Sylvester N, Parra EJ, Dios S, Norton HL, Shriver MD, Kittles RA. The 8818G allele of the agouti signaling protein (ASIP) gene is ancestral and is associated with darker skin color in African Americans. Hum Genet 2005;116(5):402-6.
343. Norton HL, Kittles RA, Parra E, McKeigue P, Mao X, Cheng K, Canfield VA, Bradley DG, McEvoy B, Shriver MD. Genetic evidence for the convergent evolution of light skin in Europeans and East Asians. Mol Biol Evol 2007;24(3):710-22.
344. Lamason RL, Mohideen MA, Mest JR, Wong AC, Norton HL, Aros MC, Jurynec MJ, Mao X, Humphreville VR, Humbert JE, Sinha S, Moore JL, Jagadeeswaran P, Zhao W, Ning G, Makalowska I, McKeigue PM,

O'Donnell D, Kittles R, Parra EJ, Mangini NJ, Grunwald DJ, Shriver MD, Canfield VA, Cheng KC. SLC24A5, a putative cation exchanger, affects pigmentation in zebrafish and humans. Science 2005;310(5755):1782-6.

345. Ginger RS, Askew SE, Ogborne RM, Wilson S, Ferdinando D, Dadd T, Smith AM, Kazi S, Szerencsei RT, Winkfein RJ, Schnetkamp PP, Green MR. SLC24A5 encodes a trans-Golgi network protein with potassium-dependent sodium-calcium exchange activity that regulates human epidermal melanogenesis. J Biol Chem 2008;283(9):5486-95.
346. Myles S, Somel M, Tang K, Kelso J, Stoneking M. Identifying genes underlying skin pigmentation differences among human populations. Hum Genet 2007;120(5):613-21.
347. Vinyard CJ, Payseur BA. Of ‘‘mice’’ and mammals: utilizing classical inbred mice to study the genetic architecture of function and performance in mammals. Integrative and Comparative Biology 2008;48(3):324-37.
348. Mitchell P, Smith W, Attebo K, Wang JJ. Prevalence of age-related maculopathy in Australia. The Blue Mountains Eye Study. Ophthalmology 1995;102(10):1450-60.
349. Airiani S, Trokel SL, Lee SM, Braunstein RE. Evaluating central corneal thickness measurements with noncontact optical low-coherence reflectometry and contact ultrasound pachymetry. Am J Ophthalmol 2006;142(1):164-5.
350. Graeber CP, Torres MB, Shields MB. Central corneal thickness in a Puerto Rican population. J Glaucoma 2008;17(5):356-60.
351. Semes L, Shaikh A, McGwin G, Bartlett JD. The relationship among race, iris color, central corneal thickness, and intraocular pressure. Optom Vis Sci 2006;83(7):512-5.
352. Yo C, Ariyasu RG. Racial differences in central corneal thickness and refraction among refractive surgery candidates. J Refract Surg 2005;21(2):194-7.
353. Eballe AO, Koki G, Ellong A, Owono D, Epee E, Bella LA, Mvogo CE, Kouam JM. Central corneal thickness and intraocular pressure in the Cameroonian nonglaucomatous population. Clin Ophthalmol 2010;4:717-24.
354. Gelaw Y, Kollmann M, Irungu NM, Ilako DR. The Influence of Central Corneal Thickness on Intraocular Pressure Measured by Goldmann Applanation Tonometry Among Selected Ethiopian Communities. J Glaucoma 2010.
355. Kim HY, Budenz DL, Lee PS, Feuer WJ, Barton K. Comparison of central corneal thickness using anterior segment optical coherence tomography vs ultrasound pachymetry. Am J Ophthalmol 2008;145(2):228-32.
356. Iyamu E, Ituah I. The relationship between central corneal thickness and intraocular pressure: a comparative study of normals and glaucoma subjects. Afr J Med Med Sci 2008;37(4):345-53.
357. Mercieca K, Odogu V, Fiebai B, Arowolo O, Chukwuka F. Comparing central corneal thickness in a sub-Saharan cohort to African Americans and Afro-Caribbeans. Cornea 2007;26(5):557-60.
358. Vitart V, Bencic G, Hayward C, Herman JS, Huffman J, Campbell S, Bucan K, Zgaga L, Kolcic I, Polasek O, Campbell H, Wright A, Vatavuk Z, Rudan I. Heritabilities of ocular biometrical traits in two croatian isolates with extended pedigrees. Invest Ophthalmol Vis Sci 2010;51(2):737-43.
359. Vitart V, Bencic G, Hayward C, Herman JS, Huffman J, Campbell S, Bucan K, Navarro P, Gunjaca G, Marin J, Zgaga L, Kolcic I, Polasek O, Kirin M,

Hastie ND, Wilson JF, Rudan I, Campbell H, Vatavuk Z, Fleck B, Wright A. New loci associated with central cornea thickness include COL5A1, AKAP13 and AVGR8. Hum Mol Genet 2010.

360. Kitsos G, Gartzios C, Asproudis I, Bagli E. Central corneal thickness in subjects with glaucoma and in normal individuals (with or without pseudoexfoliation syndrome). Clin Ophthalmol 2009;3:537-42.
361. Schneider M, Borgulya G, Seres A, Nagy Z, Nemeth J. Central corneal thickness measurements with optical coherence tomography and ultrasound pachymetry in healthy subjects and in patients after photorefractive keratectomy. Eur J Ophthalmol 2009;19(2):180-7.
362. Sanchis-Gimeno JA, Lleo-Perez A, Alonso L, Rahhal MS. Caucasian emmetropic aged subjects have reduced corneal thickness values: emmetropia, CCT and age. Int Ophthalmol 2004;25(4):243-6.
363. Lu Y, Dimasi DP, Hysi PG, Hewitt AW, Burdon KP, Toh T, Ruddle JB, Li YJ, Mitchell P, Healey PR, Montgomery GW, Hansell N, Spector TD, Martin NG, Young TL, Hammond CJ, Macgregor S, Craig JE, Mackey DA. Common genetic variants near the Brittle Cornea Syndrome locus ZNF469 influence the blinding disease risk factor central corneal thickness. PLoS Genet 2010;6(5):e1000947.
364. Phillips LJ, Cakanac CJ, Eger MW, Lilly ME. Central corneal thickness and measured IOP: a clinical study. Optometry 2003;74(4):218-25.
365. Realini T, Weinreb RN, Hobbs G. Correlation of intraocular pressure measured with goldmann and dynamic contour tonometry in normal and glaucomatous eyes. J Glaucoma 2009;18(2):119-23.
366. Li P, Hu Y, Xu Q, Zhang G, Mai C. Central corneal thickness in adult Chinese. J Huazhong Univ Sci Technolog Med Sci 2006;26(1):141-4.
367. Cho P, Lam C. Factors affecting the central corneal thickness of Hong Kong-Chinese. Curr Eye Res 1999;18(5):368-74.
368. Lam AK, Douthwaite WA. The corneal-thickness profile in Hong Kong Chinese. Cornea 1998;17(4):384-8.
369. Lam A, Chen D, Chiu R, Chui WS. Comparison of IOP measurements between ORA and GAT in normal Chinese. Optom Vis Sci 2007;84(9):909-14.
370. Kim JM, Park KH, Kim SH, Kang JH, Cho SW. The relationship between the cornea and the optic disc. Eye (Lond) 2010.
371. Lee ES, Kim CY, Ha SJ, Seong GJ, Hong YJ. Central corneal thickness of Korean patients with glaucoma. Ophthalmology 2007;114(5):927-30.
372. Chen MJ, Liu YT, Tsai CC, Chen YC, Chou CK, Lee SM. Relationship between central corneal thickness, refractive error, corneal curvature, anterior chamber depth and axial length. J Chin Med Assoc 2009;72(3):133-7.
373. Ko YC, Liu CJ, Hsu WM. Varying effects of corneal thickness on intraocular pressure measurements with different tonometers. Eye (Lond) 2005;19(3):327-32.
374. Pekmezci M, Vo B, Lim AK, Hirabayashi DR, Tanaka GH, Weinreb RN, Lin SC. The characteristics of glaucoma in Japanese Americans. Arch Ophthalmol 2009;127(2):167-71.
375. Erickson DH, Goodwin D, Anderson C, Hayes JR. Ocular pulse amplitude and associated glaucomatous risk factors in a healthy Hispanic population. Optometry 2010;81(8):408-13.

376. Kohli PG, Randhawa BK, Singh KD, Randhawa GS, Kohli AK. Relation between central corneal thickness and intraocular pressure in Punjabi population. J Med Eng Technol 2010;34(1):1-6.
377. Kunert KS, Bhartiya P, Tandon R, Dada T, Christian H, Vajpayee RB. Central corneal thickness in Indian patients undergoing LASIK for myopia. J Refract Surg 2003;19(3):378-9.
378. Ladi JS, Shah NA. Comparison of central corneal thickness measurements with the Galilei dual Scheimpflug analyzer and ultrasound pachymetry. Indian J Ophthalmol 2010;58(5):385-8.
379. Channa R, Mir F, Shah MN, Ali A, Ahmad K. Central corneal thickness of Pakistani adults. J Pak Med Assoc 2009;59(4):225-8.
380. Chaidaroon W. The comparison of corneal thickness measurement: ultrasound versus optical methods. J Med Assoc Thai 2003;86(5):462-6.
381. Biasutti R. Le Razze e i Popoli Della Terra. Torino: Unione Tipografico 1941.
382. Schulz D, Iliev ME, Frueh BE, Goldblum D. In vivo pachymetry in normal eyes of rats, mice and rabbits with the optical low coherence reflectometer. Vision Res 2003;43(6):723-8.
383. Voisey J, van Daal A. Agouti: from mouse to man, from skin to fat. Pigment Cell Res 2002;15(1):10-8.
384. Mercer JA, Seperack PK, Strobel MC, Copeland NG, Jenkins NA. Novel myosin heavy chain encoded by murine dilute coat colour locus. Nature 1991;349(6311):709-13.
385. Jackson IJ, Bennett DC. Identification of the albino mutation of mouse tyrosinase by analysis of an in vitro revertant. Proc Natl Acad Sci U S A 1990;87(18):7010-4.
386. Zdarsky E, Favor J, Jackson IJ. The molecular basis of brown, an old mouse mutation, and of an induced revertant to wild type. Genetics 1990;126(2):443-9.
387. Mackey DA. Central corneal thickness and glaucoma in the Australian Aboriginal population. Clin Experiment Ophthalmol 2007;35(8):691-2.
388. Tomita Y, Takeda A, Okinaga S, Tagami H, Shibahara S. Human oculocutaneous albinism caused by single base insertion in the tyrosinase gene. Biochem Biophys Res Commun 1989;164(3):990-6.
389. Lively GD, Jiang B, Hedberg-Buenz A, Chang B, Petersen GE, Wang K, Kuehn MH, Anderson M. Genetic Dependence of Central Corneal Thickness among Inbred Strains of Mice. Invest Ophthalmol Vis Sci 2009.
390. Henriksson JT, McDermott AM, Bergmanson JP. Dimensions and morphology of the cornea in three strains of mice. Invest Ophthalmol Vis Sci 2009;50(8):3648-54.
391. Lively GD, Koehn D, Hedberg-Buenz A, Wang K, Anderson MG. Quantitative trait loci associated with murine central corneal thickness. Physiol Genomics 2010;42(2):281-6.
392. Rebbeck TR, Kanetsky PA, Walker AH, Holmes R, Halpern AC, Schuchter LM, Elder DE, Guerry D. P gene as an inherited biomarker of human eye color. Cancer Epidemiol Biomarkers Prev 2002;11(8):782-4.
393. Zhu G, Evans DM, Duffy DL, Montgomery GW, Medland SE, Gillespie NA, Ewen KR, Jewell M, Liew YW, Hayward NK, Sturm RA, Trent JM, Martin NG. A genome scan for eye color in 502 twin families: most variation is due to a QTL on chromosome 15q. Twin Res 2004;7(2):197-210.

394. Jannot AS, Meziani R, Bertrand G, Gerard B, Descamps V, Archimbaud A, Picard C, Ollivaud L, Basset-Seguin N, Kerob D, Lanternier G, Lebbe C, Saiag P, Crickx B, Clerget-Darpoux F, Grandchamp B, Soufir N, Melan C. Allele variations in the OCA2 gene (pink-eyed-dilution locus) are associated with genetic susceptibility to melanoma. Eur J Hum Genet 2005;13(8):913-20.
395. Duffy DL, Montgomery GW, Chen W, Zhao ZZ, Le L, James MR, Hayward NK, Martin NG, Sturm RA. A three-single-nucleotide polymorphism haplotype in intron 1 of OCA2 explains most human eye-color variation. Am J Hum Genet 2007;80(2):241-52.
396. Higa K, Shimmura S, Miyashita H, Shimazaki J, Tsubota K. Melanocytes in the corneal limbus interact with K19-positive basal epithelial cells. Exp Eye Res 2005;81(2):218-23.
397. Campbell S. Melanogenesis of avian neural crest cells in vitro is influenced by external cues in the periorbital mesenchyme. Development 1989;106(4):717-26.
398. Libby RT, Smith RS, Savinova OV, Zabaleta A, Martin JE, Gonzalez FJ, John SW. Modification of ocular defects in mouse developmental glaucoma models by tyrosinase. Science 2003;299(5612):1578-81.
399. Jorgensen TJ, Ruczinski I, Kessing B, Smith MW, Shugart YY, Alberg AJ. Hypothesis-driven candidate gene association studies: practical design and analytical considerations. Am J Epidemiol 2009;170(8):986-93.
400. Tabor HK, Risch NJ, Myers RM. Candidate-gene approaches for studying complex genetic traits: practical considerations. Nat Rev Genet 2002;3(5):391-7.
401. Johansson A, Jonasson I, Gyllensten U. Extended haplotypes in the growth hormone releasing hormone receptor gene (GHRHR) are associated with normal variation in height. PLoS One 2009;4(2):e4464.
402. Risch NJ. Searching for genetic determinants in the new millennium. Nature 2000;405(6788):847-56.
403. Daly MJ, Rioux JD, Schaffner SF, Hudson TJ, Lander ES. High-resolution haplotype structure in the human genome. Nat Genet 2001;29(2):229-32.
404. Johnson GC, Esposito L, Barratt BJ, Smith AN, Heward J, Di Genova G, Ueda H, Cordell HJ, Eaves IA, Dudbridge F, Twells RC, Payne F, Hughes W, Nutland S, Stevens H, Carr P, Tuomilehto-Wolf E, Tuomilehto J, Gough SC, Clayton DG, Todd JA. Haplotype tagging for the identification of common disease genes. Nat Genet 2001;29(2):233-7.
405. Carlson CS, Eberle MA, Rieder MJ, Yi Q, Kruglyak L, Nickerson DA. Selecting a maximally informative set of single-nucleotide polymorphisms for association analyses using linkage disequilibrium. Am J Hum Genet 2004;74(1):106-20.
406. Stram DO. Tag SNP selection for association studies. Genet Epidemiol 2004;27(4):365-74.
407. Frazer KA, Ballinger DG, Cox DR, Hinds DA, Stuve LL, Gibbs RA, Belmont JW, Boudreau A, Hardenbol P, Leal SM, Pasternak S, Wheeler DA, Willis TD, Yu F, Yang H, Zeng C, Gao Y, Hu H, Hu W, Li C, Lin W, Liu S, Pan H, Tang X, Wang J, Wang W, Yu J, Zhang B, Zhang Q, Zhao H, Zhao H, Zhou J, Gabriel SB, Barry R, Blumenstiel B, Camargo A, Defelice M, Faggart M, Goyette M, Gupta S, Moore J, Nguyen H, Onofrio RC, Parkin M, Roy J, Stahl E, Winchester E, Ziaugra L, Altshuler D, Shen Y, Yao Z, Huang

W, Chu X, He Y, Jin L, Liu Y, Shen Y, Sun W, Wang H, Wang Y, Wang Y, Xiong X, Xu L, Waye MM, Tsui SK, Xue H, Wong JT, Galver LM, Fan JB, Gunderson K, Murray SS, Oliphant AR, Chee MS, Montpetit A, Chagnon F, Ferretti V, Leboeuf M, Olivier JF, Phillips MS, Roumy S, Sallee C, Verner A, Hudson TJ, Kwok PY, Cai D, Koboldt DC, Miller RD, Pawlikowska L, Taillon-Miller P, Xiao M, Tsui LC, Mak W, Song YQ, Tam PK, Nakamura Y, Kawaguchi T, Kitamoto T, Morizono T, Nagashima A, Ohnishi Y, Sekine A, Tanaka T, Tsunoda T, Deloukas P, Bird CP, Delgado M, Dermitzakis ET, Gwilliam R, Hunt S, Morrison J, Powell D, Stranger BE, Whittaker P, Bentley DR, Daly MJ, de Bakker PI, Barrett J, Chretien YR, Maller J, McCarroll S, Patterson N, Pe'er I, Price A, Purcell S, Richter DJ, Sabeti P, Saxena R, Schaffner SF, Sham PC, Varilly P, Altshuler D, Stein LD, Krishnan L, Smith AV, Tello-Ruiz MK, Thorisson GA, Chakravarti A, Chen PE, Cutler DJ, Kashuk CS, Lin S, Abecasis GR, Guan W, Li Y, Munro HM, Qin ZS, Thomas DJ, McVean G, Auton A, Bottolo L, Cardin N, Eyheramendy S, Freeman C, Marchini J, Myers S, Spencer C, Stephens M, Donnelly P, Cardon LR, Clarke G, Evans DM, Morris AP, Weir BS, Tsunoda T, Mullikin JC, Sherry ST, Feolo M, Skol A, Zhang H, Zeng C, Zhao H, Matsuda I, Fukushima Y, Macer DR, Suda E, Rotimi CN, Adebamowo CA, Ajayi I, Aniagwu T, Marshall PA, Nkwodimmah C, Royal CD, Leppert MF, Dixon M, Peiffer A, Qiu R, Kent A, Kato K, Niikawa N, Adewole IF, Knoppers BM, Foster MW, Clayton EW, Watkin J, Gibbs RA, Belmont JW, Muzny D, Nazareth L, Sodergren E, Weinstock GM, Wheeler DA, Yakub I, Gabriel SB, Onofrio RC, Richter DJ, Ziaugra L, Birren BW, Daly MJ, Altshuler D, Wilson RK, Fulton LL, Rogers J, Burton J, Carter NP, Clee CM, Griffiths M, Jones MC, McLay K, Plumb RW, Ross MT, Sims SK, Willey DL, Chen Z, Han H, Kang L, Godbout M, Wallenburg JC, L'Archeveque P, Bellemare G, Saeki K, Wang H, An D, Fu H, Li Q, Wang Z, Wang R, Holden AL, Brooks LD, McEwen JE, Guyer MS, Wang VO, Peterson JL, Shi M, Spiegel J, Sung LM, Zacharia LF, Collins FS, Kennedy K, Jamieson R, Stewart J. A second generation human haplotype map of over 3.1 million SNPs. Nature 2007;449(7164):851-61.

408. Clark AG. The role of haplotypes in candidate gene studies. Genet Epidemiol 2004;27(4):321-33.
409. de Bakker PI, Yelensky R, Pe'er I, Gabriel SB, Daly MJ, Altshuler D. Efficiency and power in genetic association studies. Nat Genet 2005;37(11):1217-23.
410. Balding DJ. A tutorial on statistical methods for population association studies. Nat Rev Genet 2006;7(10):781-91.
411. Iozzo RV, Murdoch AD. Proteoglycans of the extracellular environment: clues from the gene and protein side offer novel perspectives in molecular diversity and function. Faseb J 1996;10(5):598-614.
412. Quantock AJ, Young RD. Development of the corneal stroma, and the collagen-proteoglycan associations that help define its structure and function. Dev Dyn 2008;237(10):2607-21.
413. Chan CC, Green WR, de la Cruz ZC, Hillis A. Ocular findings in osteogenesis imperfecta congenita. Arch Ophthalmol 1982;100(9):1458-63.
414. Bredrup C, Knappskog PM, Majewski J, Rodahl E, Boman H. Congenital stromal dystrophy of the cornea caused by a mutation in the decorin gene. Invest Ophthalmol Vis Sci 2005;46(2):420-6.

415. Liu CY, Birk DE, Hassell JR, Kane B, Kao WW. Keratocan-deficient mice display alterations in corneal structure. J Biol Chem 2003;278(24):21672-7.
416. Chakravarti S, Petroll WM, Hassell JR, Jester JV, Lass JH, Paul J, Birk DE. Corneal opacity in lumican-null mice: defects in collagen fibril structure and packing in the posterior stroma. Invest Ophthalmol Vis Sci 2000;41(11):3365-73.
417. Chakravarti S, Zhang G, Chervoneva I, Roberts L, Birk DE. Collagen fibril assembly during postnatal development and dysfunctional regulation in the lumican-deficient murine cornea. Dev Dyn 2006;235(9):2493-506.
418. Tasheva ES, Koester A, Paulsen AQ, Garrett AS, Boyle DL, Davidson HJ, Song M, Fox N, Conrad GW. Mimecan/osteoglycin-deficient mice have collagen fibril abnormalities. Mol Vis 2002;8:407-15.
419. Hamann S, Zeuthen T, La Cour M, Nagelhus EA, Ottersen OP, Agre P, Nielsen S. Aquaporins in complex tissues: distribution of aquaporins 1-5 in human and rat eye. Am J Physiol 1998;274(5 Pt 1):C1332-45.
420. Macnamara E, Sams GW, Smith K, Ambati J, Singh N, Ambati BK. Aquaporin-1 expression is decreased in human and mouse corneal endothelial dysfunction. Mol Vis 2004;10:51-6.
421. Garfias Y, Navas A, Perez-Cano HJ, Quevedo J, Villalvazo L, Zenteno JC. Comparative expression analysis of aquaporin-5 (AQP5) in keratoconic and healthy corneas. Mol Vis 2008;14:756-61.
422. Thiagarajah JR, Verkman AS. Aquaporin deletion in mice reduces corneal water permeability and delays restoration of transparency after swelling. J Biol Chem 2002;277(21):19139-44.
423. Watson RB, Wallis GA, Holmes DF, Viljoen D, Byers PH, Kadler KE. Ehlers Danlos syndrome type VIIB. Incomplete cleavage of abnormal type I procollagen by N-proteinase in vitro results in the formation of copolymers of collagen and partially cleaved pNcollagen that are near circular in cross-section. J Biol Chem 1992;267(13):9093-100.
424. Byers PH, Duvic M, Atkinson M, Robinow M, Smith LT, Krane SM, Greally MT, Ludman M, Matalon R, Pauker S, Quanbeck D, Schwarze U. Ehlers-Danlos syndrome type VIIA and VIIB result from splice-junction mutations or genomic deletions that involve exon 6 in the COL1A1 and COL1A2 genes of type I collagen. Am J Med Genet 1997;72(1):94-105.
425. Nuytinck L, Freund M, Lagae L, Pierard GE, Hermanns-Le T, De Paepe A. Classical Ehlers-Danlos syndrome caused by a mutation in type I collagen. Am J Hum Genet 2000;66(4):1398-402.
426. Giunta C, Chambaz C, Pedemonte M, Scapolan S, Steinmann B. The arthrochalasia type of Ehlers-Danlos syndrome (EDS VIIA and VIIB): the diagnostic value of collagen fibril ultrastructure. Am J Med Genet A 2008;146A(10):1341-6.
427. Sakai LY, Keene DR, Engvall E. Fibrillin, a new 350-kD glycoprotein, is a component of extracellular microfibrils. J Cell Biol 1986;103(6 Pt 1):2499-509.
428. Ton CC, Hirvonen H, Miwa H, Weil MM, Monaghan P, Jordan T, van Heyningen V, Hastie ND, Meijers-Heijboer H, Drechsler M, et al. Positional cloning and characterization of a paired box- and homeobox-containing gene from the aniridia region. Cell 1991;67(6):1059-74.
429. Simpson TI, Price DJ. Pax6; a pleiotropic player in development. Bioessays 2002;24(11):1041-51.

430. Jordan T, Hanson I, Zaletayev D, Hodgson S, Prosser J, Seawright A, Hastie N, van Heyningen V. The human PAX6 gene is mutated in two patients with aniridia. Nat Genet 1992;1(5):328-32.
431. Glaser T, Walton DS, Maas RL. Genomic structure, evolutionary conservation and aniridia mutations in the human PAX6 gene. Nat Genet 1992;2(3):232-9.
432. Shriver MD, Parra EJ, Dios S, Bonilla C, Norton H, Jovel C, Pfaff C, Jones C, Massac A, Cameron N, Baron A, Jackson T, Argyropoulos G, Jin L, Hoggart CJ, McKeigue PM, Kittles RA. Skin pigmentation, biogeographical ancestry and admixture mapping. Hum Genet 2003;112(4):387-99.
433. Lee ST, Nicholls RD, Jong MT, Fukai K, Spritz RA. Organization and sequence of the human P gene and identification of a new family of transport proteins. Genomics 1995;26(2):354-63.
434. Graf J, Voisey J, Hughes I, van Daal A. Promoter polymorphisms in the MATP (SLC45A2) gene are associated with normal human skin color variation. Hum Mutat 2007.
435. Graf J, Hodgson R, van Daal A. Single nucleotide polymorphisms in the MATP gene are associated with normal human pigmentation variation. Hum Mutat 2005;25(3):278-84.
436. Stokowski RP, Pant PV, Dadd T, Fereday A, Hinds DA, Jarman C, Filsell W, Ginger RS, Green MR, van der Ouderaa FJ, Cox DR. A genomewide association study of skin pigmentation in a South Asian population. Am J Hum Genet 2007;81(6):1119-32.
437. Nan H, Kraft P, Hunter DJ, Han J. Genetic variants in pigmentation genes, pigmentary phenotypes, and risk of skin cancer in Caucasians. Int J Cancer 2009;125(4):909-17.
438. Tanita M, Matsunaga J, Miyamura Y, Dakeishi M, Nakamura E, Kono M, Shimizu H, Tagami H, Tomita Y. Polymorphic sequences of the tyrosinase gene: allele analysis on 16 OCA1 patients in Japan indicate that three polymorphic sequences in the tyrosinase gene promoter could be powerful markers for indirect gene diagnosis. J Hum Genet 2002;47(1):1-6.
439. Berson JF, Frank DW, Calvo PA, Bieler BM, Marks MS. A common temperature-sensitive allelic form of human tyrosinase is retained in the endoplasmic reticulum at the nonpermissive temperature. J Biol Chem 2000;275(16):12281-9.
440. Martin S, Haren M, Taylor A, Middleton S, Wittert G. Cohort profile: the Florey Adelaide Male Ageing Study (FAMAS). Int J Epidemiol 2007;36(2):302-6.
441. Martin SA, Haren MT, Middleton SM, Wittert GA. The Florey Adelaide Male Ageing Study (FAMAS): design, procedures & participants. BMC Public Health 2007;7:126.
442. Mackey DA, Mackinnon JR, Brown SA, Kearns LS, Ruddle JB, Sanfilippo PG, Sun C, Hammond CJ, Young TL, Martin NG, Hewitt AW. Twins eye study in Tasmania (TEST): rationale and methodology to recruit and examine twins. Twin Res Hum Genet 2009;12(5):441-54.
443. Van Gestel S, Houwing-Duistermaat JJ, Adolfsson R, van Duijn CM, Van Broeckhoven C. Power of selective genotyping in genetic association analyses of quantitative traits. Behav Genet 2000;30(2):141-6.
444. A haplotype map of the human genome. Nature 2005;437(7063):1299-320.

445. Barrett JC, Fry B, Maller J, Daly MJ. Haploview: analysis and visualization of LD and haplotype maps. Bioinformatics 2005;21(2):263-5.
446. Price AL, Patterson NJ, Plenge RM, Weinblatt ME, Shadick NA, Reich D. Principal components analysis corrects for stratification in genome-wide association studies. Nat Genet 2006;38(8):904-9.
447. McEvoy BP, Montgomery GW, McRae AF, Ripatti S, Perola M, Spector TD, Cherkas L, Ahmadi KR, Boomsma D, Willemsen G, Hottenga JJ, Pedersen NL, Magnusson PK, Kyvik KO, Christensen K, Kaprio J, Heikkila K, Palotie A, Widen E, Muilu J, Syvanen AC, Liljedahl U, Hardiman O, Cronin S, Peltonen L, Martin NG, Visscher PM. Geographical structure and differential natural selection among North European populations. Genome Res 2009;19(5):804-14.
448. Howie BN, Donnelly P, Marchini J. A flexible and accurate genotype imputation method for the next generation of genome-wide association studies. PLoS Genet 2009;5(6):e1000529.
449. Abecasis GR, Cherny SS, Cookson WO, Cardon LR. Merlin--rapid analysis of dense genetic maps using sparse gene flow trees. Nat Genet 2002;30(1):97-101.
450. Purcell S, Neale B, Todd-Brown K, Thomas L, Ferreira MA, Bender D, Maller J, Sklar P, de Bakker PI, Daly MJ, Sham PC. PLINK: a tool set for whole-genome association and population-based linkage analyses. Am J Hum Genet 2007;81(3):559-75.
451. Nyholt DR. A simple correction for multiple testing for single-nucleotide polymorphisms in linkage disequilibrium with each other. Am J Hum Genet 2004;74(4):765-9.
452. Li J, Ji L. Adjusting multiple testing in multilocus analyses using the eigenvalues of a correlation matrix. Heredity 2005;95(3):221-7.
453. Purcell S, Cherny SS, Sham PC. Genetic Power Calculator: design of linkage and association genetic mapping studies of complex traits. Bioinformatics 2003;19(1):149-50.
454. Nielsen DM, Ehm MG, Weir BS. Detecting marker-disease association by testing for Hardy-Weinberg disequilibrium at a marker locus. Am J Hum Genet 1998;63(5):1531-40.
455. Wittke-Thompson JK, Pluzhnikov A, Cox NJ. Rational inferences about departures from Hardy-Weinberg equilibrium. Am J Hum Genet 2005;76(6):967-86.
456. Saunders AM, Strittmatter WJ, Schmechel D, George-Hyslop PH, Pericak-Vance MA, Joo SH, Rosi BL, Gusella JF, Crapper-MacLachlan DR, Alberts MJ, et al. Association of apolipoprotein E allele epsilon 4 with late-onset familial and sporadic Alzheimer's disease. Neurology 1993;43(8):1467-72.
457. Altshuler D, Hirschhorn JN, Klannemark M, Lindgren CM, Vohl MC, Nemesh J, Lane CR, Schaffner SF, Bolk S, Brewer C, Tuomi T, Gaudet D, Hudson TJ, Daly M, Groop L, Lander ES. The common PPARgamma Pro12Ala polymorphism is associated with decreased risk of type 2 diabetes. Nat Genet 2000;26(1):76-80.
458. Hugot JP, Chamaillard M, Zouali H, Lesage S, Cezard JP, Belaiche J, Almer S, Tysk C, O'Morain CA, Gassull M, Binder V, Finkel Y, Cortot A, Modigliani R, Laurent-Puig P, Gower-Rousseau C, Macry J, Colombel JF, Sahbatou M, Thomas G. Association of NOD2 leucine-rich repeat variants with susceptibility to Crohn's disease. Nature 2001;411(6837):599-603.

459. Ogura Y, Bonen DK, Inohara N, Nicolae DL, Chen FF, Ramos R, Britton H, Moran T, Karaliuskas R, Duerr RH, Achkar JP, Brant SR, Bayless TM, Kirschner BS, Hanauer SB, Nunez G, Cho JH. A frameshift mutation in NOD2 associated with susceptibility to Crohn's disease. Nature 2001;411(6837):603-6.
460. Sillence DO, Senn A, Danks DM. Genetic heterogeneity in osteogenesis imperfecta. J Med Genet 1979;16(2):101-16.
461. Glorieux FH, Rauch F, Plotkin H, Ward L, Travers R, Roughley P, Lalic L, Glorieux DF, Fassier F, Bishop NJ. Type V osteogenesis imperfecta: a new form of brittle bone disease. J Bone Miner Res 2000;15(9):1650-8.
462. Glorieux FH, Ward LM, Rauch F, Lalic L, Roughley PJ, Travers R. Osteogenesis imperfecta type VI: a form of brittle bone disease with a mineralization defect. J Bone Miner Res 2002;17(1):30-8.
463. Ward LM, Rauch F, Travers R, Chabot G, Azouz EM, Lalic L, Roughley PJ, Glorieux FH. Osteogenesis imperfecta type VII: an autosomal recessive form of brittle bone disease. Bone 2002;31(1):12-8.
464. Cabral WA, Chang W, Barnes AM, Weis M, Scott MA, Leikin S, Makareeva E, Kuznetsova NV, Rosenbaum KN, Tifft CJ, Bulas DI, Kozma C, Smith PA, Eyre DR, Marini JC. Prolyl 3-hydroxylase 1 deficiency causes a recessive metabolic bone disorder resembling lethal/severe osteogenesis imperfecta. Nat Genet 2007;39(3):359-65.
465. Kamoun-Goldrat AS, Le Merrer MF. Animal models of osteogenesis imperfecta and related syndromes. J Bone Miner Metab 2007;25(4):211-8.
466. Chipman SD, Sweet HO, McBride DJ, Jr., Davisson MT, Marks SC, Jr., Shuldiner AR, Wenstrup RJ, Rowe DW, Shapiro JR. Defective pro alpha 2(I) collagen synthesis in a recessive mutation in mice: a model of human osteogenesis imperfecta. Proc Natl Acad Sci U S A 1993;90(5):1701-5.
467. Camacho NP, Dow D, Toledano TR, Buckmeyer JK, Gertner JM, Brayton CF, Raggio CL, Root L, Boskey AL. Identification of the oim mutation by dye terminator chemistry combined with automated direct DNA sequencing. J Orthop Res 1998;16(1):38-42.
468. Woods A, Stirling JW. Electron Microscopy. In: Bancroft JD, Gamble, eds. Theory and Practice of Histological Techniques. 6 ed. London: Churchill Livingstone; 2008:601-40.
469. Rauch F, Glorieux FH. Osteogenesis imperfecta. Lancet 2004;363(9418):1377-85.
470. Dalgleish R. The human type I collagen mutation database. Nucleic Acids Res 1997;25(1):181-7.
471. Roughley PJ, Rauch F, Glorieux FH. Osteogenesis imperfecta--clinical and molecular diversity. Eur Cell Mater 2003;5:41-7; discussion 7.
472. Marini JC, Forlino A, Cabral WA, Barnes AM, San Antonio JD, Milgrom S, Hyland JC, Korkko J, Prockop DJ, De Paepe A, Coucke P, Symoens S, Glorieux FH, Roughley PJ, Lund AM, Kuurila-Svahn K, Hartikka H, Cohn DH, Krakow D, Mottes M, Schwarze U, Chen D, Yang K, Kuslich C, Troendle J, Dalgleish R, Byers PH. Consortium for osteogenesis imperfecta mutations in the helical domain of type I collagen: regions rich in lethal mutations align with collagen binding sites for integrins and proteoglycans. Hum Mutat 2007;28(3):209-21.
473. Willing MC, Deschenes SP, Scott DA, Byers PH, Slayton RL, Pitts SH, Arikat H, Roberts EJ. Osteogenesis imperfecta type I: molecular

heterogeneity for COL1A1 null alleles of type I collagen. Am J Hum Genet 1994;55(4):638-47.

474. Korkko J, Ala-Kokko L, De Paepe A, Nuytinck L, Earley J, Prockop DJ. Analysis of the COL1A1 and COL1A2 genes by PCR amplification and scanning by conformation-sensitive gel electrophoresis identifies only COL1A1 mutations in 15 patients with osteogenesis imperfecta type I: identification of common sequences of null-allele mutations. Am J Hum Genet 1998;62(1):98-110.
475. Ries-Levavi L, Ish-Shalom T, Frydman M, Lev D, Cohen S, Barkai G, Goldman B, Byers P, Friedman E. Genetic and biochemical analyses of Israeli osteogenesis imperfecta patients. Hum Mutat 2004;23(4):399-400.
476. Weis SM, Emery JL, Becker KD, McBride DJ, Jr., Omens JH, McCulloch AD. Myocardial mechanics and collagen structure in the osteogenesis imperfecta murine (oim). Circ Res 2000;87(8):663-9.
477. Bui BV, Edmunds B, Cioffi GA, Fortune B. The gradient of retinal functional changes during acute intraocular pressure elevation. Invest Ophthalmol Vis Sci 2005;46(1):202-13.
478. Lund AM, Jensen BL, Nielsen LA, Skovby F. Dental manifestations of osteogenesis imperfecta and abnormalities of collagen I metabolism. J Craniofac Genet Dev Biol 1998;18(1):30-7.
479. Kuurila K, Grenman R, Johansson R, Kaitila I. Hearing loss in children with osteogenesis imperfecta. Eur J Pediatr 2000;159(7):515-9.
480. Spencer CC, Su Z, Donnelly P, Marchini J. Designing genome-wide association studies: sample size, power, imputation, and the choice of genotyping chip. PLoS Genet 2009;5(5):e1000477.
481. Hampe J, Franke A, Rosenstiel P, Till A, Teuber M, Huse K, Albrecht M, Mayr G, De La Vega FM, Briggs J, Gunther S, Prescott NJ, Onnie CM, Hasler R, Sipos B, Folsch UR, Lengauer T, Platzer M, Mathew CG, Krawczak M, Schreiber S. A genome-wide association scan of nonsynonymous SNPs identifies a susceptibility variant for Crohn disease in ATG16L1. Nat Genet 2007;39(2):207-11.
482. Kubo M, Hata J, Ninomiya T, Matsuda K, Yonemoto K, Nakano T, Matsushita T, Yamazaki K, Ohnishi Y, Saito S, Kitazono T, Ibayashi S, Sueishi K, Iida M, Nakamura Y, Kiyohara Y. A nonsynonymous SNP in PRKCH (protein kinase C eta) increases the risk of cerebral infarction. Nat Genet 2007;39(2):212-7.
483. Maraganore DM, de Andrade M, Lesnick TG, Strain KJ, Farrer MJ, Rocca WA, Pant PV, Frazer KA, Cox DR, Ballinger DG. High-resolution whole-genome association study of Parkinson disease. Am J Hum Genet 2005;77(5):685-93.
484. Dewan A, Liu M, Hartman S, Zhang SS, Liu DT, Zhao C, Tam PO, Chan WM, Lam DS, Snyder M, Barnstable C, Pang CP, Hoh J. HTRA1 promoter polymorphism in wet age-related macular degeneration. Science 2006;314(5801):989-92.
485. Duerr RH, Taylor KD, Brant SR, Rioux JD, Silverberg MS, Daly MJ, Steinhart AH, Abraham C, Regueiro M, Griffiths A, Dassopoulos T, Bitton A, Yang H, Targan S, Datta LW, Kistner EO, Schumm LP, Lee AT, Gregersen PK, Barmada MM, Rotter JI, Nicolae DL, Cho JH. A genome-wide association study identifies IL23R as an inflammatory bowel disease gene. Science 2006;314(5804):1461-3.

486. Sladek R, Rocheleau G, Rung J, Dina C, Shen L, Serre D, Boutin P, Vincent D, Belisle A, Hadjadj S, Balkau B, Heude B, Charpentier G, Hudson TJ, Montpetit A, Pshezhetsky AV, Prentki M, Posner BI, Balding DJ, Meyre D, Polychronakos C, Froguel P. A genome-wide association study identifies novel risk loci for type 2 diabetes. Nature 2007;445(7130):881-5.
487. Wang WY, Barratt BJ, Clayton DG, Todd JA. Genome-wide association studies: theoretical and practical concerns. Nat Rev Genet 2005;6(2):109-18.
488. Jawaid A, Bader JS, Purcell S, Cherny SS, Sham P. Optimal selection strategies for QTL mapping using pooled DNA samples. Eur J Hum Genet 2002;10(2):125-32.
489. Barratt BJ, Payne F, Rance HE, Nutland S, Todd JA, Clayton DG. Identification of the sources of error in allele frequency estimations from pooled DNA indicates an optimal experimental design. Ann Hum Genet 2002;66(Pt 5-6):393-405.
490. Sham P, Bader JS, Craig I, O'Donovan M, Owen M. DNA Pooling: a tool for large-scale association studies. Nat Rev Genet 2002;3(11):862-71.
491. Craig JE, Hewitt AW, McMellon AE, Henders AK, Ma L, Wallace L, Sharma S, Burdon KP, Visscher PM, Montgomery GW, MacGregor S. Rapid inexpensive genome-wide association using pooled whole blood. Genome Res 2009;19(11):2075-80.
492. Brown KM, Macgregor S, Montgomery GW, Craig DW, Zhao ZZ, Iyadurai K, Henders AK, Homer N, Campbell MJ, Stark M, Thomas S, Schmid H, Holland EA, Gillanders EM, Duffy DL, Maskiell JA, Jetann J, Ferguson M, Stephan DA, Cust AE, Whiteman D, Green A, Olsson H, Puig S, Ghiorzo P, Hansson J, Demenais F, Goldstein AM, Gruis NA, Elder DE, Bishop JN, Kefford RF, Giles GG, Armstrong BK, Aitken JF, Hopper JL, Martin NG, Trent JM, Mann GJ, Hayward NK. Common sequence variants on 20q11.22 confer melanoma susceptibility. Nat Genet 2008;40(7):838-40.
493. Macgregor S, Zhao ZZ, Henders A, Nicholas MG, Montgomery GW, Visscher PM. Highly cost-efficient genome-wide association studies using DNA pools and dense SNP arrays. Nucleic Acids Res 2008;36(6):e35.
494. Macgregor S, Visscher PM, Montgomery G. Analysis of pooled DNA samples on high density arrays without prior knowledge of differential hybridization rates. Nucleic Acids Res 2006;34(7):e55.
495. Ozaki K, Ohnishi Y, Iida A, Sekine A, Yamada R, Tsunoda T, Sato H, Sato H, Hori M, Nakamura Y, Tanaka T. Functional SNPs in the lymphotoxin-alpha gene that are associated with susceptibility to myocardial infarction. Nat Genet 2002;32(4):650-4.
496. Hindorff L, Junkins H, Hall P, Mehta J, Manolio T. A Catalog of Published Genome-Wide Association Studies (Available at: www.genome.gov/gwastudies). November 2010.
497. Cichon S, Craddock N, Daly M, Faraone SV, Gejman PV, Kelsoe J, Lehner T, Levinson DF, Moran A, Sklar P, Sullivan PF. Genomewide association studies: history, rationale, and prospects for psychiatric disorders. Am J Psychiatry 2009;166(5):540-56.
498. Pearson JV, Huentelman MJ, Halperin RF, Tembe WD, Melquist S, Homer N, Brun M, Szelinger S, Coon KD, Zismann VL, Webster JA, Beach T, Sando SB, Aasly JO, Heun R, Jessen F, Kolsch H, Tsolaki M, Daniilidou M, Reiman EM, Papassotiropoulos A, Hutton ML, Stephan DA, Craig DW. Identification of the genetic basis for complex disorders by use of pooling-

based genomewide single-nucleotide-polymorphism association studies. Am J Hum Genet 2007;80(1):126-39.
499. Jawaid A, Sham P. Impact and quantification of the sources of error in DNA pooling designs. Ann Hum Genet 2009;73(1):118-24.
500. Hirschhorn JN, Lohmueller K, Byrne E, Hirschhorn K. A comprehensive review of genetic association studies. Genet Med 2002;4(2):45-61.
501. McClellan J, King MC. Genetic heterogeneity in human disease. Cell 2010;141(2):210-7.
502. Thomas KA. Fibroblast growth factors. Faseb J 1987;1(6):434-40.
503. Ornitz DM, Itoh N. Fibroblast growth factors. Genome Biol 2001;2(3):REVIEWS3005.
504. Lovicu FJ, de Iongh RU, McAvoy JW. Expression of FGF-1 and FGF-2 mRNA during lens morphogenesis, differentiation and growth. Curr Eye Res 1997;16(3):222-30.
505. Lovicu FJ, Overbeek PA. Overlapping effects of different members of the FGF family on lens fiber differentiation in transgenic mice. Development 1998;125(17):3365-77.
506. Carlsson P, Mahlapuu M. Forkhead transcription factors: key players in development and metabolism. Dev Biol 2002;250(1):1-23.
507. Lam EW, Francis RE, Petkovic M. FOXO transcription factors: key regulators of cell fate. Biochem Soc Trans 2006;34(Pt 5):722-6.
508. van der Horst A, Burgering BM. Stressing the role of FoxO proteins in lifespan and disease. Nat Rev Mol Cell Biol 2007;8(6):440-50.
509. Teixeira CC, Liu Y, Thant LM, Pang J, Palmer G, Alikhani M. Foxo1, a novel regulator of osteoblast differentiation and skeletogenesis. J Biol Chem 2010;285(40):31055-65.
510. Berry FB, Skarie JM, Mirzayans F, Fortin Y, Hudson TJ, Raymond V, Link BA, Walter MA. FOXC1 is required for cell viability and resistance to oxidative stress in the eye through the transcriptional regulation of FOXO1A. Hum Mol Genet 2008;17(4):490-505.
511. Mears AJ, Jordan T, Mirzayans F, Dubois S, Kume T, Parlee M, Ritch R, Koop B, Kuo WL, Collins C, Marshall J, Gould DB, Pearce W, Carlsson P, Enerback S, Morissette J, Bhattacharya S, Hogan B, Raymond V, Walter MA. Mutations of the forkhead/winged-helix gene, FKHL7, in patients with Axenfeld-Rieger anomaly. Am J Hum Genet 1998;63(5):1316-28.
512. Lehmann OJ, Ebenezer ND, Jordan T, Fox M, Ocaka L, Payne A, Leroy BP, Clark BJ, Hitchings RA, Povey S, Khaw PT, Bhattacharya SS. Chromosomal duplication involving the forkhead transcription factor gene FOXC1 causes iris hypoplasia and glaucoma. Am J Hum Genet 2000;67(5):1129-35.
513. Lehmann OJ, Ebenezer ND, Ekong R, Ocaka L, Mungall AJ, Fraser S, McGill JI, Hitchings RA, Khaw PT, Sowden JC, Povey S, Walter MA, Bhattacharya SS, Jordan T. Ocular developmental abnormalities and glaucoma associated with interstitial 6p25 duplications and deletions. Invest Ophthalmol Vis Sci 2002;43(6):1843-9.
514. Tanaka H, Murakami Y, Ishii I, Nakata S. Involvement of a forkhead transcription factor, FOXO1A, in UV-induced changes of collagen metabolism. J Investig Dermatol Symp Proc 2009;14(1):60-2.
515. Poulsen RC, Carr AJ, Hulley PA. Protection against glucocorticoid-induced damage in human tenocytes by modulation of ERK, Akt, and forkhead signaling. Endocrinology 2011;152(2):503-14.

516. Laity JH, Lee BM, Wright PE. Zinc finger proteins: new insights into structural and functional diversity. Curr Opin Struct Biol 2001;11(1):39-46.
517. Abu A, Frydman M, Marek D, Pras E, Nir U, Reznik-Wolf H, Pras E. Deleterious mutations in the Zinc-Finger 469 gene cause brittle cornea syndrome. Am J Hum Genet 2008;82(5):1217-22.
518. Christensen AE, Knappskog PM, Midtbo M, Gjesdal CG, Mengel-From J, Morling N, Rodahl E, Boman H. Brittle cornea syndrome associated with a missense mutation in the zinc-finger 469 gene. Invest Ophthalmol Vis Sci 2009.
519. Maher B. Personal genomes: The case of the missing heritability. Nature 2008;456(7218):18-21.
520. Goldstein DB. Common genetic variation and human traits. N Engl J Med 2009;360(17):1696-8.
521. Manolio TA, Collins FS, Cox NJ, Goldstein DB, Hindorff LA, Hunter DJ, McCarthy MI, Ramos EM, Cardon LR, Chakravarti A, Cho JH, Guttmacher AE, Kong A, Kruglyak L, Mardis E, Rotimi CN, Slatkin M, Valle D, Whittemore AS, Boehnke M, Clark AG, Eichler EE, Gibson G, Haines JL, Mackay TF, McCarroll SA, Visscher PM. Finding the missing heritability of complex diseases. Nature 2009;461(7265):747-53.
522. Collins FS, Guyer MS, Charkravarti A. Variations on a theme: cataloging human DNA sequence variation. Science 1997;278(5343):1580-1.
523. Thorleifsson G, Magnusson KP, Sulem P, Walters GB, Gudbjartsson DF, Stefansson H, Jonsson T, Jonasdottir A, Jonasdottir A, Stefansdottir G, Masson G, Hardarson GA, Petursson H, Arnarsson A, Motallebipour M, Wallerman O, Wadelius C, Gulcher JR, Thorsteinsdottir U, Kong A, Jonasson F, Stefansson K. Common sequence variants in the LOXL1 gene confer susceptibility to exfoliation glaucoma. Science 2007;317(5843):1397-400.
524. Pritchard JK. Are rare variants responsible for susceptibility to complex diseases? Am J Hum Genet 2001;69(1):124-37.
525. Cirulli ET, Goldstein DB. Uncovering the roles of rare variants in common disease through whole-genome sequencing. Nat Rev Genet 2010;11(6):415-25.
526. Zeggini E, Rayner W, Morris AP, Hattersley AT, Walker M, Hitman GA, Deloukas P, Cardon LR, McCarthy MI. An evaluation of HapMap sample size and tagging SNP performance in large-scale empirical and simulated data sets. Nat Genet 2005;37(12):1320-2.
527. Burgering BM, Kops GJ. Cell cycle and death control: long live Forkheads. Trends Biochem Sci 2002;27(7):352-60.
528. Alikhani M, Alikhani Z, Graves DT. FOXO1 functions as a master switch that regulates gene expression necessary for tumor necrosis factor-induced fibroblast apoptosis. J Biol Chem 2005;280(13):12096-102.
529. Huang H, Tindall DJ. Dynamic FoxO transcription factors. J Cell Sci 2007;120(Pt 15):2479-87.
530. Yuan Z, Becker EB, Merlo P, Yamada T, DiBacco S, Konishi Y, Schaefer EM, Bonni A. Activation of FOXO1 by Cdk1 in cycling cells and postmitotic neurons. Science 2008;319(5870):1665-8.
531. Potente M, Urbich C, Sasaki K, Hofmann WK, Heeschen C, Aicher A, Kollipara R, DePinho RA, Zeiher AM, Dimmeler S. Involvement of Foxo

transcription factors in angiogenesis and postnatal neovascularization. J Clin Invest 2005;115(9):2382-92.

532. Toda N, Nakanishi-Toda M. Nitric oxide: ocular blood flow, glaucoma, and diabetic retinopathy. Prog Retin Eye Res 2007;26(3):205-38.
533. Ayub H, Khan MI, Micheal S, Akhtar F, Ajmal M, Shafique S, Ali SH, den Hollander AI, Ahmed A, Qamar R. Association of eNOS and HSP70 gene polymorphisms with glaucoma in Pakistani cohorts. Mol Vis 2010;16:18-25.
534. Liao Q, Wang DH, Sun HJ. Association of genetic polymorphisms of eNOS with glaucoma. Mol Vis 2011;17:153-8.
535. Phillips JC, del Bono EA, Haines JL, Pralea AM, Cohen JS, Greff LJ, Wiggs JL. A second locus for Rieger syndrome maps to chromosome 13q14. Am J Hum Genet 1996;59(3):613-9.
536. Anderson MG, Smith RS, Hawes NL, Zabaleta A, Chang B, Wiggs JL, John SW. Mutations in genes encoding melanosomal proteins cause pigmentary glaucoma in DBA/2J mice. Nat Genet 2002;30(1):81-5.